

The Pennsylvania State University

The Graduate School

College of Engineering

**Design and Optimization of UVGI
Air Disinfection Systems**

A Thesis in
Architectural Engineering
by
Wladyslaw Jan Kowalski

Submitted in Partial Fulfillment
of the Requirements
for the Degree of

Doctor of Philosophy

August 2001

We approve the thesis of W. J. Kowalski

Date of Signature

William P. Bahnfleth
Associate Professor of Architectural Engineering
Thesis Adviser
Chair of Committee

Thomas S. Whittam
Professor of Biology

Richard G. Mistrick
Associate Professor of Architectural Engineering

Stanley A. Mumma
Professor of Architectural Engineering

Richard A. Behr
Professor of Architectural Engineering
Head of the Architectural Engineering Department

ABSTRACT

Mathematical models of the response of populations of microorganisms exposed to ultraviolet germicidal irradiation (UVGI) are developed that include two-stage response curves and shoulder effects. Models are used to develop a C++ computer program that is capable of predicting the performance of UVGI air disinfection systems. The algorithms are based on models for 1) the intensity field of UVGI lamps, 2) the intensity field due to UVGI reflective enclosures, and 3) the kill rate of microorganisms to UVGI exposure as they pass through the modeled intensity field. The validity of the UVGI lamp model is established by comparison with lamp photosensor data. The validity of the overall predictive model is established by comparison of predictions with laboratory bioassays for two species of airborne pathogens – *Serratia marcescens* and *Bacillus subtilis*. First stage rate constants, second stage rate constants, and the defining shoulder parameters are determined for *Aspergillus niger* and *Rhizopus nigricans* based on bioassay data, and it is shown how predictions using only single stage rate constants can deviate significantly from predictions using the complete survival curve. A dimensional analysis of UVGI systems identifies nine dimensionless parameters responsible for determining the effectiveness of any rectangular UVGI system. A factorial analysis of the dimensionless parameters based on data output by the program identifies the most critical parameters and the inter-relationships that determine UVGI system effectiveness. Response surfaces are generated using program output to illustrate the inter-relationships of the dimensionless parameters. The optimum values of the dimensionless parameters are summarized that result in optimized performance. Economic optimization is demonstrated by a series of examples that calculate life cycle costs, and principles of economic optimization are summarized. Conclusions are presented that will produce more energy-efficient and effective designs and a proposed model for improved UVGI systems is presented.

TABLE OF CONTENTS

LIST OF FIGURES	vii
LIST OF TABLES	ix
Acknowledgements	x
Chapter 1. Introduction.....	1
Chapter 2. Literature Review.....	3
2.1. History of UVGI	3
2.2. UVGI Systems Today	4
2.3. Airborne Pathogens	6
2.4. UVGI Rate Constant Studies	7
2.5. Relative Humidity Effects.....	7
2.6. Air Temperature Effects.....	8
2.7. Shoulder Effects	8
2.8. Second Stage Rate Constant.....	9
2.9. Radiation View Factors	9
2.10. Ventilation Systems.....	10
2.11. Design Guidelines and Criteria for Air Disinfection	10
2.12. New Technologies and Materials	10
Chapter 3. Objectives and Scope.....	12
3.1. Objectives	12
3.2. Scope... ..	12
Chapter 4. Mathematical Modeling of UVGI.....	14
4.1. Lamp Intensity Field.....	14
4.2. Reflected Intensity Field	17
4.3. Inter-Reflected Intensity Field.....	20
Chapter 5. Mathematical Modeling of Microbial Response.....	24
5.1. Modeling Microbial Decay.....	24
5.2. Two-Stage Survival Curves	26
5.3. The Shoulder.....	28
5.4. The Complete Microbial Decay Model.....	33
Chapter 6. The UVX Computer Program.....	35
6.1. Description of the Program	35
6.2. Operation of the Program.....	36
6.2. Program Input and Output.....	44
Chapter 7. Model Validation	45

7.1. Lamp Model Validation.....	45
7.2. Bioassays for <i>Serratia Marcescens</i>	47
7.3. Bioassays for <i>Bacillus subtilis</i>	49
7.4. Shoulder and Second Stage Model Validation	50
7.4.1 Bioassays for <i>Aspergillus niger</i>	52
7.4.2 Bioassays for <i>Rhizopus nigricans</i>	56
Chapter 8. Dimensional Analysis of UVGI Systems.....	60
Chapter 9. Factorial Analysis of UVGI Systems	66
9.1. The 2k Factorial Screening Analysis.....	66
9.2. RSM Analysis of the Central Composite Design	69
Chapter 10. Optimization of Performance and Economics	74
10.1. Performance Optimization.....	74
10.2. Economic Optimization	81
10.2.1. Life Cycle Cost of UVGI Systems	81
10.2.2. Basic Cost Relationships of UVGI System Components	84
10.2.3. Annual Costs of UVGI Systems.....	86
10.2.4. Economic Optimization of UVGI Systems	90
10.2.5. Economic Optimization UVGI Recirculation Systems	94
10.2.5. Performance of Multiple Lamp and Axial Configurations	103
Chapter 11. Summary and Conclusions.....	106
REFERENCES	111
Appendix A: Airborne Pathogen Database.....	119
Appendix B: UVGI Rate Constants	124
Appendix C: UVGI Units of Intensity and Dose.....	125
Appendix D: UVGI Lamp Database.....	126
Appendix E: Material Reflectivity Database.....	128
Appendix F. Program Microbe Rate Constant Database.....	129
Appendix G. UVX Program Listing	130
Appendix H. Program Input File	186
Appendix I: Program Output File.....	187
Appendix J: Bioassay test results and Analysis.....	188
Appendix K: Dimensionless Parameters and Variables for CCD Analysis	189
Appendix L. Response Surfaces for Dimensionless Parameters	194
Appendix M. Minitab Output – General Linear Model for lnK	208
Appendix N: Minitab Output – Regression Analysis -- lnK	212
Appendix O. Input Data for Cost Optimization	214

Appendix P: First Costs for Economic Optimization	227
Appendix Q. Energy & Maintenance for Cost Optmization.....	240

LIST OF FIGURES

Figure 2.1: Facilities Where UVGI Systems Are Installed.....	5
Figure 2.2: Breakdown of Types of UVGI Systems	6
Figure 4.1: Illustration of Geometry for View Factor Model.....	16
Figure 4.2: Three-Dimensional Intensity Field for a UV Lamp	17
Figure 4.3 Illustration of View Factor Geometry for a Differential Element Parallel	18
Figure 4.4 Subdivision of a Rectangular Surface	19
Figure 4.5 Illustration of a UVGI System.....	19
Figure 4.6: Comparison of Direct and Reflected Components.....	23
Figure 5.1: Two-Stage Decay Curve with Shoulder	24
Figure 5.2: Survival Curve of <i>Streptococcus pyogenes</i>	26
Figure 5.3: Survival Curve for <i>Adenovirus</i>	27
Figure 5.4: Survival Curve of <i>Staphylococcus aureus</i>	29
Figure 5.5: Development of Shoulder Curve	29
Figure 5.6: Illustration of Generic Shoulder Model Response to Intensity	33
Figure 6.1: Grid For a 10x10x20 Matrix and Coordinate System	36
Figure 6.2: Flow Chart for Calculation of Overall Intensity Field	37
Figure 6.3: Illustration of the Two Bounding Conditions.....	38
Figure 6.4: Kill Zones for the Unmixed Air Condition	39
Figure 6.5: Simplified Flow Chart For Program Operation	40
Figure 6.6: Direct Intensity Algorithm Flowchart	41
Figure 6.7: Flowchart For Reflected Intensity Algorithm.....	42
Figure 6.8: Flowchart for Inter-reflection Algorithm	43
Figure 6.9: Program Window Showing Results.....	44
Figure 7.1: Comparison of View factor Model With Photosensor Data.....	45
Figure 7.2: Comparison of View Factor Model with Photosensor Data	46
Figure 7.3: Comparison of View Factor Model Along Lamp Length.....	47
Figure 7.4: Bioassay Results for <i>Serratia marcescens</i>	48
Figure 7.5: Bioassay Results for <i>Bacillus subtilis</i>	49
Figure 7.6: The Complete Survival Curve	51
Figure 7.7: Results of Three Tests for <i>Aspergillus niger</i>	54
Figure 7.8: Comparison of Complete Survival Curve of <i>A. niger</i>	55
Figure 7.9: Predicted Survival Curves of <i>Rhizopus nigricans</i>	55
Figure 7.10: Results for Two Tests of <i>Rhizopus nigricans</i>	57
Figure 7.11: Comparison of the Complete Survival Curve for <i>R. nigricans</i>	57

Figure 7.12: Predicted Survival Curve of <i>R. nigricans</i>	58
Figure 7.13: Time to Obtain Sterilization of <i>R. nigricans</i>	59
Figure 8.1: The Three Geometric Ratios	65
Figure 9.1: Normal Probability Plot for 2k Factorial Analysis of lnK	69
Figure 9.2: Predictive Scatter Plot for Regression Model	72
Figure 10.1: RSM for % Kill Rate of Specific Dose vs. Duct Aspect Ratio	74
Figure 10.2: RSM for % Kill Rate of Reflectivity vs. Duct Aspect Ratio	75
Figure 10.3: RSM for % Kill Rate of Lamp Aspect Ratio vs. Y Ratio	76
Figure 10.4: RSM for % Kill Rate of X Ratio vs. Y Ratio	77
Figure 10.5: RSM for % Kill Rate of Z Ratio vs. Specific Dose	78
Figure 10.6: Optimum Values of Dimensionless Parameters	80
Figure 10.7: Variation of Cost with Increasing UV Power	84
Figure 10.8: Cost of Reflective Materials	85
Figure 10.9: Kill Rates of <i>Serratia marcescens</i> vs. Annual Cost	91
Figure 10.10: Cost Breakdown for Typical System	91
Figure 10.11: Cost Breakdown for Energy-Efficient Design	92
Figure 10.12: UVGI Cost Efficiency of Typical Systems	93
Figure 10.13: Response Surface for Cost Efficiency (CE) for Length vs. Power	95
Figure 10.14: Response Surface for CE for Reflectivity vs. Power	96
Figure 10.15: Response Surface for CE for Reflectivity vs. Length	96
Figure 10.16: Response Surface for CE for Airflow vs. Power	97
Figure 10.17: Response Surface for CE for Airflow vs. Length	98
Figure 10.18: Response Surface for CE for Airflow vs. Reflectivity	98
Figure 10.19: Response Surface for CE for Power vs. Width	99
Figure 10.20: Response Surface for CE for Length vs. Width	99
Figure 10.21: Response Surface for CE for Width vs. Airflow	100
Figure 10.22: Response Surface for CE for Width vs. Reflectivity	100
Figure 10.23: CE for Square Duct of Constant Area, 75% Reflectivity	101
Figure 10.24: CE for Square Duct of Constant Area, 93% Reflectivity	101
Figure 10.25: UVGI System Optimized for Different Geographic Locations	103
Figure 10.26: Comparison of Multiple Lamp Configurations	105
Figure 11.1: Proposed Configuration of an Optimized UVGI System	109

LIST OF TABLES

Table 5.1: Two Stage Parameters	28
Table 5.2: Shoulder Parameters	34
Table 7.1: Test Results & Derived Constants for <i>Aspergillus niger</i>	53
Table 7.2: Test Results & Derived Constants for <i>Rhizopus nigricans</i>	56
Table 8.1: Physical Parameters Relevant to UVGI Systems	60
Table 8.2: Minimum Set of Parameters for UVGI Model	61
Table 8.3: Array of Units for UVGI System Minimum Parameters	61
Table 8.4: Dimensionless Groups	62
Table 8.5: Ranges for Dimensionless Parameters	65
Table 9.1: Variable Minimum and Maximum Values	67
Table 9.2: Limits of Dimensionless Parameters	68
Table 9.3: Star Points and Center Points for Parameters	70
Table 9.4: Model Sum of Square Error % Contributions	71
Table 10.1: Optimum Values for Parameters	78
Table 10.2: Life Cycle Cost of Typical UVGI Systems	83
Table 10.3: Range of Variables for CE Evaluation	95
Table 11.1: Optimum Values for Dimensionless Parameters	107

Acknowledgments

I thank all my family and friends for their encouragement and assistance. I especially thank my father, Stanislaw J. Kowalski, for his patience and understanding of my mid-career return to academia, and I hope that my achievements have made both of our sacrifices and efforts worthwhile.

I thank my thesis advisor and committee, Dr. William Bahnfleth, Dr. Thomas Whittam, Dr. Richard Mistrick, and Dr. Stanley Mumma, for their guidance and steadfast support.

Thanks are due to Dave Witham of Ultraviolet Devices, Inc. (UVDI) of Valencia, CA for financial and technical support for much of this research.

Thanks to all those who provided technical support and encouragement: Charley Dunn of Commercial Lighting Design, John Brockman and Bill Perkins of Air Refinement Systems, John Buettner of Donaldson, Michael Ivanovich of HPAC Engineering, Jack Kulp, and the people at American Ultraviolet, Inc., Abatement Technologies, Inc., Indoor Purifiers, Steril-Aire, Robert Key of Applied Research Labs, Larry Kilham of Ecosensors, Hollingsworth & Vose, Scott Moore of Airguard, Daniel Price of Interface Research, and the American Society of Heating, Refrigeration, and Air Conditioning Engineers.

Special thanks to Laraine and Jack Beiter for the scholarship that got me through my final semester, and thanks to the people of the Kissinger Fellowship for supporting my doctorate.

Thanks to Dr. James Rosenberger for his careful assistance in the statistical evaluations.

Thanks to Dr. Michael Modest for his patient support for my studies of thermal radiation.

And thanks to all the other professors and graduate students at Penn State and elsewhere who assisted or encouraged me throughout this research, including, Dr. Philip Mohr, Dr. Gita Talmage, Dr. Gretchen Kuldau, Dr. Gren Yuill, Dr. Robert Gannon, Dr. Richard Behr, Dr. Kevin Parfitt, Dr. Heinsohn, Dr. Geschwindner, Brad Striebig, Dr. Hasson Tavossi, Richard Hermans, Paul Ninomura, Jing Song, Eric Peyer, Paul Bowers, Jack Futrick, Nancy Smith and the rest of the AE Department staff, Robert Arance, Tom Bowles, Dr. John Mahaffy, Shashikala Kumari Ranasinghe, Dr. J. Cimbala, Dr. Philip Mohr, Jeremy Snyder, Amy Musser and Matt Vande, Brian Lee, Helen Lee, Alison Bell, Ed Clements, Rebecca and David Upham, Dr. Mark Hernandez, George Walton, James Johnson, and everyone else I forgot to mention.

And thanks to all the great men and women in the history of Science and the Arts who, by their selfless dedication to making the world a better place, inspired me to seek excellence and achievement in a field that may contribute to helping the people of the world.

Chapter 1. Introduction

Air disinfection with ultraviolet germicidal irradiation (UVGI) has often been highly effective when tested under laboratory conditions but has suffered from unpredictability and occasional failure in applications. The problem has been a lack of knowledge about the fundamental design principles of UVGI systems and an absence of analytical tools available to designers. These problems are addressed here by a comprehensive evaluation of all aspects of the UVGI air disinfection process.

The mathematical basis for microbial disinfection is elucidated and a complete model of microbial decay is presented. A mathematical model for UV lamp intensity is developed along with a model for the reflected intensity inside a rectangular UVGI enclosure. These models are coded in a computer program that produces a three-dimensional matrix of the total intensity field. The dose received by any microbe passing through this field can then be computed and the disinfection rate of an airborne population of microbes passing through this field is then evaluated.

The factors that are included in the predictive model are lamp dimensions, enclosure dimensions, lamp location and orientation within the enclosure, microbial species, air velocity, surface reflectivity, and the conditions of mixed or unmixed flow.

Some factors are not included in the model due to various reasons. Air temperature has an almost negligible impact (Rentschler et al 1941). The effect of Relative Humidity has an unknown impact due to null or contradictory published results (Riley and Kaufman 1972, Lidwell and Lowbury 1950, Rentschler and Nagy 1942). The performance of individual lamp models under varying airflow is not addressed although cooling effects were incorporated in the evaluation of bioassay results.

The predictive accuracy of the computer model allows for study of the parameters to determine which factors are critical to the design of effective systems and how these factors are inter-related. This program is used to generate thousands of data sets that are, in turn, analyzed to assess these parameters. The result is new insight into what factors lead to the design of more effective UVGI systems.

The ability to accurately predict the performance of UVGI systems creates new possibilities and options for engineers and scientists working in the health care industry or in the field of indoor air quality (IAQ). It also allows for reducing costs of systems since over-designing systems as a means of hedging poor performance becomes unnecessary. The implications of these new design methods include lower energy consumption and more affordable systems that may be within easier reach of those who need them most.

Given the principles of design and the ability to model systems on a computer as a means of augmenting laboratory tests, UVGI equipment can be produced at lower costs. Previous inefficiencies that resulted from unfounded design habits and conventions can now be

eliminated. Guidelines can now be established to assist in the design and evaluation of UVGI systems and their performance.

In addition to being useful to engineers, the methods developed here for the analysis of the three dimensional intensity field of a UVGI enclosure provide microbiologists with a means of determining rate constants for airborne pathogens more accurately and easily than has previously been possible. These methods are also applicable to studies of the effects of Relative Humidity on airborne rate constants.

Chapter 2. Literature Review

A considerable body of literature exists that spans the relevant fields of study. These include the areas of airborne pathogens, air disinfection technology, experimental studies on microbial response to UVGI, and radiation heat transfer.

2.1 History of UVGI

Ultraviolet light has been successfully applied to the disinfection of water and equipment since the late 1800s. Applications to airstream disinfection began in the 1930s but had varying degrees of success. Up until the present, the design of UVGI air disinfection systems has remained an art in search of a science. The problem has been a lack of focused research and analysis of sufficient detail to establish the fundamental mathematical relationships between UVGI lamps, reflective enclosures, and microbial response to passage through an intensity field.

Currently available design information has not guaranteed predictable performance for UVGI air disinfection systems. Some of today's design practices can overdesign systems leading to prohibitive costs and high-energy consumption. Other design practices lead to undersized and ineffective systems. Design practices have not changed in decades and it is worthwhile to review the history of UVGI applications to discover how this situation has come to be.

Although the first UVGI water disinfection system was implemented in 1909 (AWWA 1971) the first UVGI systems designed for airstream disinfection weren't implemented until the 1930s (Sharp 1940). Based on limited laboratory data and using newly available UVGI lamps, these systems were sized without the benefit of pre-existing criteria. Tests, either air sampling or epidemiological, were used to determine their efficacy. Some of these systems were highly successful; such as those used to control measles in schools, and one used by Riley to eliminate TB bacilli from hospital ward exhaust air (Riley and O'Grady 1961).

Other designs appeared to be ineffective, apparently as the result of cloning of designs and the resulting degradation of performance that came with inattention to detail and specifics of different applications, as well as a lack of available design information. The result was that the initial glowing reviews of this technology became tempered. Guidelines were issued that sanctioned the use of UVGI only in combination with HEPA filters. No studies were ever undertaken to determine the root cause for any UVGI system failures. Apart from improvements in lamp designs, applications technology for airstream disinfection has remained almost stagnant for decades.

The first design guidelines for UVGI airstream disinfection systems were developed in the 1940s (Luckiesh and Holladay 1942a, Luckiesh 1946). Versions appeared in catalogs that continue to be reproduced and used today (Philips 1985). These guidelines offer procedures,

charts, and tables to size lamps and reflective surfaces so as to obtain a desired disinfection rate. These sizing methods, though admirably detailed for the period, suffer from a number of deficiencies:

- ❖ They fail to define the intensity field, instead merely using the lamp rating or else relying on photometric data for lamp midpoints.
- ❖ Lamps are specified without regard to lamp location or type.
- ❖ The correction factor for rectangular ducts ignores the intensity field variations due to surface reflectivity.
- ❖ These methods are based on a rate constant for *E. coli* from plate studies only.
- ❖ The relative humidity correction relies on limited studies for *E. coli* only, ignoring other studies.
- ❖ The correction factors for reflectivity ignore duct dimensions and lengths.
- ❖ The temperature correction chart is based on a single model of lamp and does not apply to other manufacturer's lamps.

Other manufacturers size systems by rules of thumb, such as filling the available cross-section with an array of lamps, or base designs on proprietary testing. A number of sources refer to the Inverse Square Law (ISL) as defining the intensity field of UVGI lamps but this model may be insufficiently accurate for system design and can result in systems that are under-designed or over-designed. Over-designed systems, although conservative, may have prohibitive economics, or, if installed, may waste energy. No current literature provides any rigorous methodology for designing and predicting the airstream disinfection rate of UVGI systems.

The net result of the various inaccuracies detailed above would, in general, result in over-sized systems for most applications. However, ignoring the placement of lamps could result in systems that are both over-sized (in terms of total wattage) and less effective than they could be. Energy savings could be achieved through improvement of these design methodologies, as well as lowered first costs.

2.2 UVGI Systems Today

Air disinfection systems are commonly used today in the health care industry and sectors with similar requirements such as prisons and homeless shelters. Some limited use of UVGI for air disinfection occurs in schools and in domestic households. Figure 2-1 shows a breakdown of where UVGI systems are currently being installed. The largest market is hospitals, with an almost even distribution of the rest among prisons, shelters, and clinics.

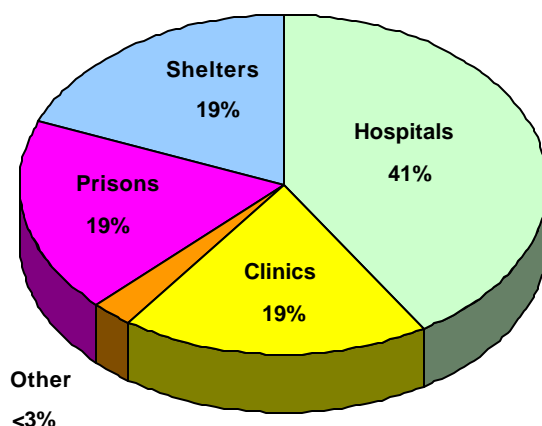


Figure 2-1: Facilities where UVGI systems are installed.

The types of UVGI systems that are currently being installed are shown in the breakdown in Figure 2-2. A developing market involves the use of UVGI to control microbial growth in ductwork, on filters, cooling coils, and other air handling unit components.

Microbial growth control has been undergoing much study recently and has enjoyed success in field applications (Shaughnessy et al 1999, Scheir et al 1996). In Europe, the control of microbial growth on cooling coils has been practiced since at least 1985 in breweries, where the wrong fungus can cause spoilage problems. One manufacturer recommends placing a 15 W lamp 1 meter from the surface of cooling coils or walls where condensation may occur (Phillips 1985).

Microbial growth on surfaces may be comprised of fungi, bacteria, or even algae, but not viruses, which are intracellular parasites. Continuous direct UVGI exposure can sterilize any surface given enough time. Theoretically, low intensity UVGI could be used for surface microbial growth since the exposure time is extended. In practical applications, however, microbial growth can occur in crevices, shadowed areas like insulation, and stagnant water where UVGI may not penetrate.

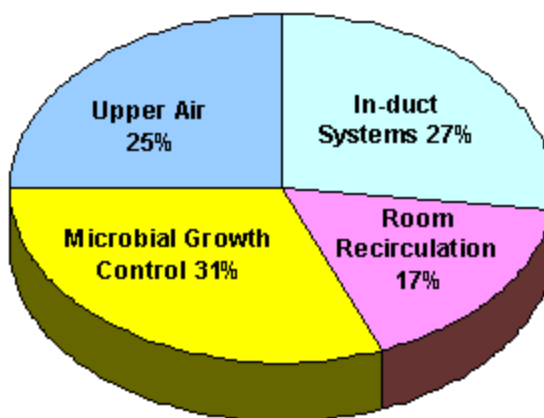


Figure 2.2: Breakdown of types of UVGI air and surface disinfection systems currently being installed

UVGI air disinfection systems rarely function in isolation but are normally associated with air filtration and building ventilation systems. The effect of filtration combined with UVGI is not additive but complementary, since filtration tends to remove large microbes from the airstream that are often resistant to UVGI. A model for the filtration of microorganisms has been developed independently and can be used in conjunction with the UVGI model to predict the effects of combination systems (Kowalski et al 1999, Kowalski and Bahnfleth 2000b). The filter model is, however, beyond the scope of the current work and is not addressed here.

Likewise, methods exist for the evaluation of building purge air systems and these effects tend to be additive or complementary (on a species basis) when combined with UVGI. Again, this technology is addressed elsewhere and is beyond the scope of the current work (Kowalski 1997).

2.3 Airborne Pathogens

An airborne pathogen database has been assembled and is summarized in Appendix A. This list includes approximately one hundred viruses, bacteria, and fungal spores that may pose health hazards in indoor environments. Few of these pathogens have known UVGI rate constants but they are included for completeness and in the hope that investigators will ultimately resolve all the unknown airborne rate constants.

The types of microbes that may be encountered by a UVGI system are essentially unpredictable, but depend to some degree on the type of facility and geographic location. All viruses and almost all bacteria (excluding spores) are vulnerable to moderate levels of UVGI exposure. Viruses are primarily contagious pathogens that come from human sources, and therefore, will be found in occupied buildings. Bacteria can be contagious or opportunistic, with

many found indoors but some that are environmental. Certain facilities, like agricultural buildings, may disseminate unique types of bacteria such as the spore-forming actinomycetes (lacey and Crook 1988).

Spores, which are larger and more resistant to UVGI than most bacteria, can be effectively controlled through the use of high efficiency or HEPA filters. The coupling of filters with UVGI is the recommended practice in any health care setting (ASHRAE 1991) and for UVGI applications in general.

2.4 UVGI Rate Constant Studies

Experimental studies on microbial response to UVGI exposure have been numerous but often limited either to pathogens of primary concern or to benchmark test microbes. As a result much redundancy, and concomitant contradiction, exists in the literature. The results of all complete studies have been summarized in Appendix 2, which shows the rate constants determined in various test media (i.e. air, water, or plates). Additional UVGI studies, from which rate constants could not be determined, are listed in the References.

Finally, UVGI rate constants, mostly plate or water based, are known for only some twenty out of one hundred airborne pathogens and future research is needed to resolve rate constants for the remaining microbes, but this is beyond the scope of the current work. The program developed here, however, can greatly facilitate research into rate constants by virtue of the fact that it resolves the three dimensional intensity field, thereby allowing accurate interpretation of experimental results without complicated test apparatus.

The rate constant is also impacted by the relative humidity, and only aerosolization experiments can resolve the effects of relative humidity. The program developed here also provides a means of interpreting relative humidity experiments, in the same way that the rate constants can be resolved.

2.5 Relative Humidity Effects

Numerous sources state that increased Relative Humidity (RH) decreases the decay rate under UVGI exposure (Riley and Kaufman 1972, Philips 1985) but this position is, at best, a selective conclusion. Lidwell and Lowbury (1950) showed the rate constant for *Serratia marcescens* decreasing with increasing RH. Rentschler and Nagy (1942) showed the rate constant for *Streptococcus pyogenes* increasing with increasing RH.

Taken as a whole, these results suggest that the relationship between RH and UVGI susceptibility is at least species-dependent and therefore no definitive general relationship can be established. Furthermore, no RH study can be performed without aerosolizing microorganisms

and this requires more detailed treatment of the 3D intensity field than has previously been accomplished. A need exists for additional experimental data on airborne disinfection to resolve the issue of relative humidity. The new models and analytical tools presented here will facilitate the interpretation of such experimental results.

2.6 Air Temperature Effects

Within normal ranges of ventilation system design, air temperature has a negligible impact on microbial susceptibility to UVGI (Rentschler et al 1941). Temperature can, however, impact the power output of UVGI lamps if either the temperature or the air velocity exceeds design parameters.

Operating a UVGI system at air velocities above design will degrade its effectiveness due to the cooling effect of the air on the lamp surface, which in turn cools the plasma inside the lamp. UV output is a function of plasma temperature when power input is constant.

Not all UVGI lamps have the same response to cooling effects. Some lamps have different plasma mixtures, overdriven power supplies that respond to plasma temperature, or UV-transparent, infrared-blocking shielding that limits cooling effects. Data from the manufacturer should be consulted to determine the cooling effects or the limiting design air velocities and temperatures within which the lamps can be efficiently operated.

2.7 Shoulder Effects

In addition to the first stage rate constant, a shoulder in the decay curve defines microbial response. This is a delay in the response to UVGI exposure and this effect has not previously been quantified mathematically in any usable form.

For most cases the effect of the shoulder is likely insignificant, but it can become significant when the exposure time is too short or the intensity too low (i.e. when the dose is too low). This can be a concern for systems that are designed poorly, since it will overpredict kill rates.

Insufficient data is currently available that would facilitate determination of shoulder constants for most microbial species. In order to develop the constants necessary to define the shoulder, data is required on kill rates at different intensities. Although some data exist to indicate the presence of a shoulder (Jensen 1964, Hill et al 1970, Sharp 1939, Gates 1929, Abshire and Dunton 1981), no data set exists that allows the prediction of shoulder effects as a function of intensity, except that which was taken as part of this research (UVDI 2001).

2.8 Second Stage Rate Constant

In addition to the first stage rate constant and the shoulder, a third factor, the second stage rate constant, can influence the kill rates when exposure times are long. A fraction of any microbial population will remain more resistant to UVGI exposure, and behaves essentially like a second microbial population with a distinctive rate constant.

Some data are currently available to establish second stage rate constants for a few of the microbes in the database (Jensen 1964, Hill et al 1970, Rainbow and Mak 1973, Lidwell and Lowbury 1950). However, these results are limited and not always detailed enough to draw statistically significant conclusions. Two microbes were studied as part of this research and data were developed into second stage rate constants.

2.9 Thermal Radiation View Factors

Of critical importance to the present work is the body of literature related to the determination of lamp intensity fields and reflected intensity fields. This literature comes primarily from the field of Radiation Heat Transfer but also from the field of Illumination Engineering. The core models of lamp intensity and reflected intensity are based on radiation view factors (Modest 1993, Howell 1982) and it is these view factors that have allowed detailed models of the net intensity field of any UVGI enclosure to be resolved.

2.10 Ventilation Systems

Several types of ventilation systems are used today, including recirculation systems, 100% outside air systems, and VAV systems. In general, UVGI systems are design for constant air velocity, although some types of UVGI lamps are able to adjust output for variable airflow and air temperature. The design of any UVGI system must take into account the specific operating characteristics of the ventilation system that it is being added to, including air velocity, air temperature, and Relative Humidity, although the latter is a factor with a mostly unknown impact on performance.

Outside air may contain mainly spores, while recirculated air may contain airborne microbes from human or other sources. The location of the UVGI system, whether in a return duct, an outside air duct, or in a mixing plenum, can affect the performance and economics.

The presence or absence of filtration is also a consideration. Many buildings use only prefilters for controlling dust. UVGI systems typically include higher efficiency filters and these have an effect in controlling spores, which are more resistant to UVGI than other microbes. In certain facilities, such as hospitals, high efficiency filters are already present and may not need to be added to a UVGI system that is being retrofitted to the ventilation system.

One new type of ventilation systems design, Dedicated Outside Air Systems (DOAS), uses minimum quantities of outside air and may dehumidify or humidify the air as necessary (Mumma 2001). Although the effects of humidity on microbial UVGI rate constants is unknown at present, it could be speculated that, if low humidity increases microbial susceptibility to UVGI, then placement upstream of humidifiers, or downstream of dehumidifiers, may improve performance. The reverse situation could also be the case, and may even be species specific.

2.11 Design Guidelines and Criteria for Air Disinfection

No specific design criteria exists for airborne concentrations of pathogens. Some suggested guidelines have been assembled (Kowalski and Bahnfleth 1998), but the benefits from the use of UVGI systems cannot easily be quantified at present. The costs, in terms of illness, lost work time, and health care are certainly great on a nationwide basis and so there are clearly huge benefits from developing technology that will contribute to reducing the spread of disease, however, without detailed data on infection rates, airborne concentrations, and sources of infections, it is difficult to assess the benefits of air disinfection systems other than to speculate that some level of investment in such systems could offer considerable benefits.

2.12 New Technologies and Materials

Several related developments may contribute to modern UVGI research, including new reflective materials, new types of UVGI lamps, and improvements in filtration technology.

Two materials are currently available that have unusually high reflectivities, Spectralon (trademark Labsphere, Inc.) and expanded polytetrafluoroethylene, or ePTFE, (Hannon et al 1997, Lash 1999). Spectralon can produce reflectivities as high as 99% across a broad spectrum of light that extends into the UV. However, Spectralon is a thick, solid material that is expensive to fabricate and difficult to install in UVGI systems.

The material ePTFE has a reflectivity of approximately 98-99% across a spectrum that extends into the UV range (Lash 2000, Hannon et al 1997). This material can be applied as a coating on metallic surfaces and although the costs are not presently known, it is likely to prove economic in comparison with polished aluminum sheet for UVGI system applications.

The same material, ePTFE, is also currently being developed as a filter fiber media (Folmsbee and Ganatra 1996). Because of the material's ability to be organized into microscopic fibrous patterns, it promises high performance and design flexibility. Although filtration is not the subject of this thesis, the value of filtration is as a complementary technology to UVGI, since it

removes most of the microbes (i.e. spores) that are resistant to UVGI, and also is necessary to maintain lamp cleanliness.

The use of pulsed UV light to disinfect surfaces has shown promise in terms of the high disinfection rates obtainable (Wekhof 2000), although the costs associated with this technology limit it to specialized applications. One unique application of pulsed UV light is in the operating room – pulsed UVA light can be used to disinfect surfaces such as open wounds, without causing harm to the patients or medical personnel. Although the technology is outside the scope of this research, it may still be possible to adapt the methods described in this dissertation to predicting pulsed UV disinfection rates, possibly through the addition of a ‘pulsed heating’ model.

Other new technologies are currently under research in projects such as the DARPA Immune Building project, in which systems are being designed and tested for the detection of airborne pathogens and the protection of buildings against the use of biological weapons. Obviously, any system that was capable of defending a building against the deliberate spread of airborne pathogens could be applied to the normal spread of diseases in indoor environments, and may lead to immune building technologies that can be used in schools, commercial buildings, and residential buildings. UVGI, with its excellent potential for high performance and low cost, may prove to be a key component in the development of immune building technology.

Chapter 3. Objectives and Scope

3.1 Objectives

The objective of this work was to develop a comprehensive method for designing UVGI systems capable of predicting UVGI system performance so as to establish optimized designs. This method consists of a computer program and the results of analysis that have led to general guidelines for the design of effective UVGI systems and methods for reducing energy consumption and thereby improving economic performance.

3.2 Scope

The scope of this research includes the following steps:

- ❖ Development of a mathematical model describing the UVGI intensity field in reflective rectangular enclosures
- ❖ Development of a mathematical model for microbial response
- ❖ Development of a software package incorporating the mathematical models
- ❖ Validation of models and program results
- ❖ Dimensional analysis of UVGI systems
- ❖ Parametric study of the dimensionless parameters and interactions
- ❖ Energy and economic analysis
- ❖ Optimization of UVGI systems

Development of the mathematical model of UVGI systems included development of individual algorithms for the following aspects:

- ❖ UV lamp direct intensity field
- ❖ First reflection intensity field for a rectangular enclosure
- ❖ Inter-reflected intensity field for a rectangular enclosure
- ❖ A model for the mixed and unmixed airflow conditions.

All the models above were coded as part of a software package written in the C++ programming language. The program was used to analyze several thousand systems that represented the full range of design parameters.

A formal dimensional analysis of program results produced a set of eight dimensionless parameters that define any UVGI system. A statistical analysis of the program results based on these dimensionless parameters produced a linear regression model that incorporated the dimensionless parameters in various mathematical functions. These methods allowed for quantification of the relationships and influence of each parameter on the final kill rates.

The linear regression model, which includes non-linear terms, facilitated the study of UVGI system economics. This was evaluated for a standard recirculation system such as are currently available for various applications. Costs and energy consumption information for the equipment and materials were quantified and used in an optimization study.

In addition to program development and the analysis of program results, the mathematical models of the shoulder and second stage were evaluated against laboratory data for two microbial species that were provided by an independent source (UVDI 2001). This data allowed the development of critical shoulder and second stage constants for two fungal species. These data are not included in the program but provide the basis for both program enhancement and further research.

Chapter 4. Mathematical Modeling of UVGI Systems

A typical UVGI system consists of one or more UVGI lamps located inside a rectangular duct. This duct may be reflective or include reflective panels. Three distinct components must be evaluated to determine the total three dimensional (3D) intensity field – the direct intensity of the lamp, the intensity due to the first reflection, and the intensity due to all subsequent inter-reflections. Once the total intensity field is determined, the dose received by any passing airborne microbe can be computed.

4.1 The Lamp Intensity Field

The dose received by any airborne microorganism is dependent on the lamp intensity field through which it passes. Computation of the intensity field is essential for the sizing of any system. If the entire intensity field can be established and reduced to a single value for average intensity then the sizing will be greatly simplified.

The Inverse Square Law is often used to compute the intensity of light at any distance from a lamp. This is adequate for lighting purposes but is inaccurate in the near field where much of the germicidal effect occurs. In water based systems the ISL can be effective, but the attenuation of UVGI by water plays a larger part than the lamp geometry (Qualls and Johnson 1983 & 1985, Severin et al 1983). In air, where there is negligible attenuation of UVGI, the ISL fails to account for the lamp diameter and is at best an approximation. Even numerical integration of the ISL to create a line source fails to result in agreement with photosensor data. A more accurate approach, and one that fully accounts for lamp geometry, is to use radiation view factors.

The radiation view factor represents the fraction of diffuse radiative energy emitted by one surface that is absorbed by another surface. It defines the geometric relationship between the emitting and the receiving surface. If the emitting surface is at a constant intensity and the receiving surface is a differential element, then the view factor can be used to determine the intensity at the location of the differential element. If the receiving surface is a finite area or the emitting surface is not uniform then the relationship can be integrated over the respective surfaces to find the total radiation absorbed.

The intensity at an arbitrary point outside a UVGI lamp can be computed using the radiation view factor from a differential planar element to a finite cylinder when the element is perpendicular to the cylinder axis and located axially at one end of the cylinder (Modest 1993):

$$F_{d1-2}(x, l, r) = \frac{L}{pH} \left[\frac{1}{L} ATAN \left(\frac{L}{\sqrt{H^2 - 1}} \right) - ATAN \left(\sqrt{\frac{H-1}{H+1}} \right) + \frac{X - 2H}{\sqrt{XY}} ATAN \left(\sqrt{\frac{X(H-1)}{Y(H+1)}} \right) \right] \quad (4-1)$$

The parameters in the above equation are defined as follows:

$$H = x / r$$

$$L = l / r$$

$$X = (1 + H)^2 + L^2$$

$$Y = (1 - H)^2 + L^2$$

where x = distance from the lamp, cm
 l = length of the lamp segment, cm
 r = radius of the lamp, cm

To compute the view factor along the axis of the lamp at any radial distance from the axis, the lamp must be divided into two segments of lengths l_1 and $l_g - l_1$. The sum of these will be the total lamp length l_g as shown in Figure 4.1. This process is known as view factor algebra. The total view factor at any point will be:

$$F_{tot}(x, l_1, l_g, r) = F_{d1-2}(x, l_1, r) + F_{d1-2}(x, l_g - l_1, r) \quad (4-2)$$

To compute the view factor for a point beyond the ends of the lamp an imaginary lamp must be constructed from the real portion of length l_g and a "ghost" portion of some length equivalent to the distance beyond, or before, the end of the lamp l_b . The view factor of the ghost portion is then subtracted from the total as follows:

$$F_{tot}(x, l_b + l_g, l_g, r) = F_{d1-2}(x, l_b + l_g, r) + F_{d1-2}(x, l_b, r) \quad (4-3)$$

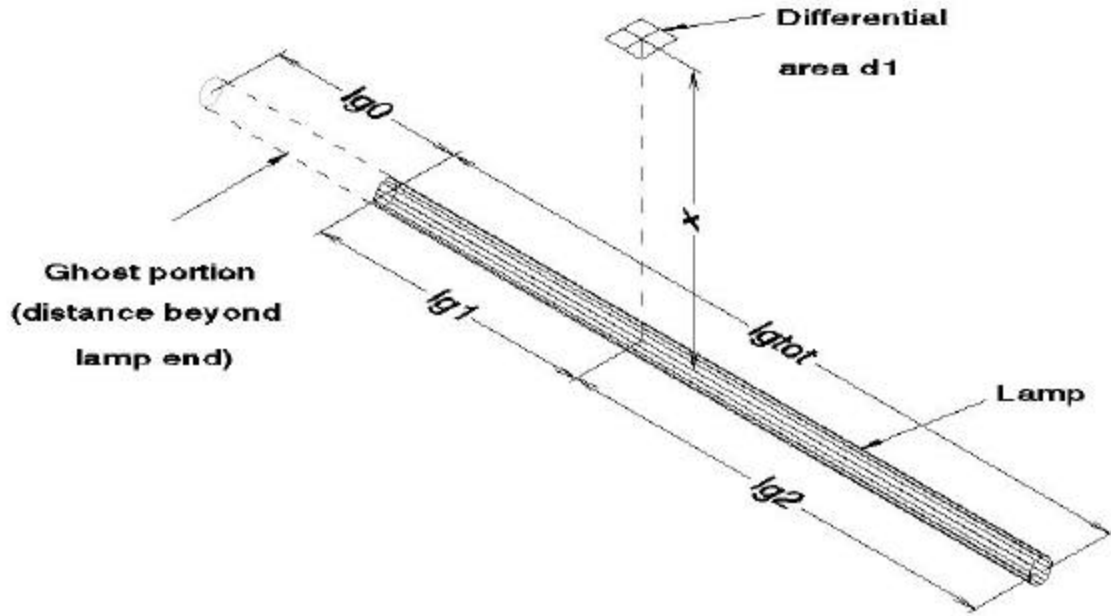


Figure 4.1: Illustration of Geometry for the View Factor Model of a Lamp.

The intensity at any point will be the product of the surface intensity I_s and the total view factor. The lamp surface intensity equals the UV power output divided by the lamp surface area. The intensity field at any coordinates x , y , and z will be described by:

$$I_s = \frac{E_{uv} F_{tot}}{2\pi r l} \quad (4-4)$$

where I_s = UV intensity at any (x,y,z) point, $\mu\text{W}/\text{cm}^2$

E_{uv} = UV power output of lamp, μW

Equations (4-1) through (4-4) are used to create a 3D matrix defining the intensity field around a lamp in any enclosure. This matrix can then be used to determine the dose received by a passing airborne microorganism, either by averaging the field intensity for mixed air or by integrating the dose along airflow streamlines for unmixed air.

Figure 4.2 illustrates the intensity field around a UVGI lamp at the midpoint in the absence of reflective surfaces. The field was computed using equation (4-1) for a Philips model G25T8 UV lamp. Similar fields could be generated for the ends of the lamp or any point beyond the ends of the lamp using equations (4-2) and (4-3), respectively.

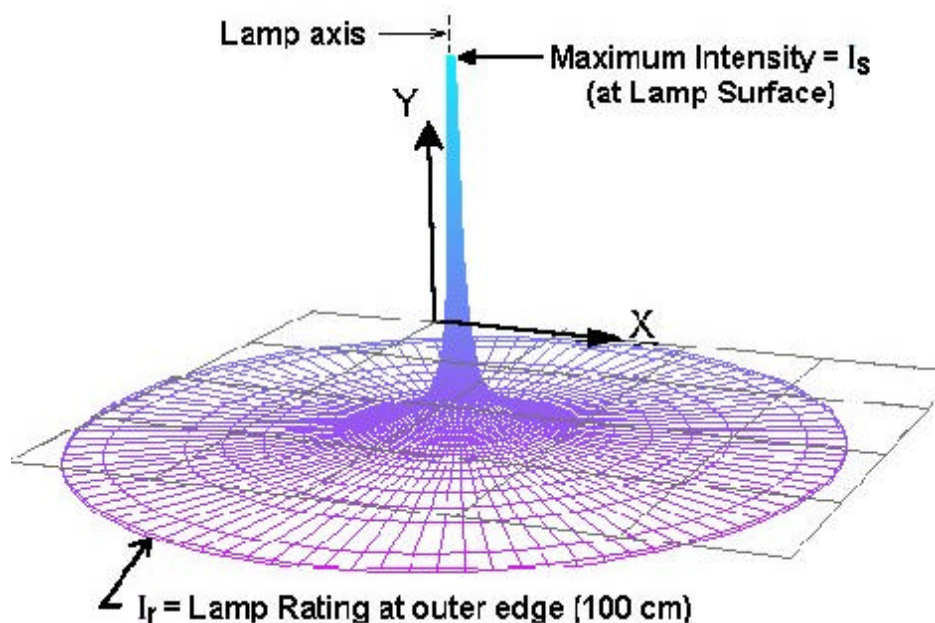


Figure 4.2: Three-Dimensional Intensity Field of a UV Lamp in a vertical (y axis) orientation, measured at the lamp midpoint

4.2 The Reflected Intensity Field

Reflective materials such as aluminum or magnesium oxide can boost the intensity field both from direct reflections and from inter-reflections. The intensity field due to reflectivity depends on surface geometry and the field of the lamp. Some lamps include fixtures that are themselves reflective surfaces. Although the model developed here is considered to be a naked lamp in a rectangular enclosure, the same principles apply to the reflective surfaces of the fixtures.

The assumption is made that the surfaces are purely diffuse reflectors. This is a reasonable assumption for specular surfaces because the same total reflectance is accounted for and, since complete mixing is assumed, the average intensity should be approximately the same. Also, in most situations, the lamp tends to be located centrally inside a long duct and in this situation specular surfaces will tend to contain more of the light intensity, rendering the assumption conservative. Furthermore, most specular surfaces of interest in UVGI, such as galvanized steel or unpolished aluminum, have a large diffuse reflectivity component. The reflective surface of greatest current interest, ePTFE, is, in fact, purely diffuse, and diffuse view factor should be perfectly applicable in this case. At present, however, it is difficult to test the diffuse reflectivity assumption, but it is reasonable to assume that it will cause no major discrepancies.

The direct intensity at each surface is determined with equation (4-4). Averaging the surface intensity to simplify computations may be possible provided the intensity distribution on

the wall is relatively even. Otherwise the surface must be subdivided into elements over which the assumption of uniform intensity is valid. The reflected intensity I_{Rn} for each of n surfaces is:

$$I_{Rn} = I_{Dn} \rho \quad (4-5)$$

where I_{Dn} = direct intensity incident on surface n and ρ is the diffuse global spectral reflectivity in the UVGI range

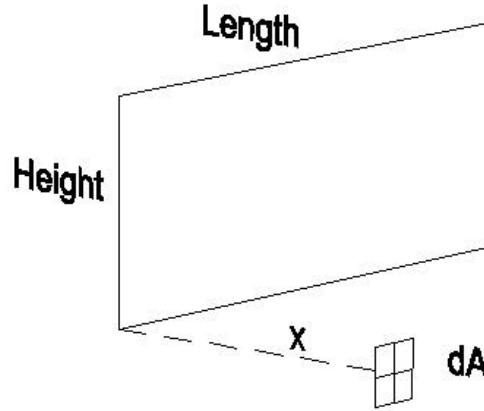


Figure 4.3: Illustration of View Factor Geometry for a Differential Element Parallel to a Rectangular Plane and Perpendicular to the Corner

The view factor from a differential element to a rectangular surface, through the corner and located perpendicular to the surface, as illustrated in Figure 4.2, is (Modest 1993):

$$F_{d1-2} = \frac{1}{2p} \left[\frac{X}{\sqrt{1+X^2}} \text{ATAN} \left(\frac{Y}{\sqrt{1+X^2}} \right) + \frac{Y}{\sqrt{1+Y^2}} \text{ATAN} \left(\frac{X}{\sqrt{1+Y^2}} \right) \right] \quad (4-6)$$

where $X = \text{Height} / x$

$Y = \text{Length} / x$

$x = \text{distance to the corner, perpendicular to the surface.}$

To account for surfaces with non-homogeneous intensity contours, the surfaces can be subdivided into an array of smaller elements. In this application the surfaces are divided into 200 blocks – 10 for the Height or Width and 20 for the Length. The contribution of each smaller rectangle is individually determined by considering the entire surface measured from the corner and then subtracting all the contributions except the small rectangle under evaluation. In effect, the other rectangles are ghost rectangles as illustrated in Figure 4.4, and they are assumed to be

at the same intensity as the smaller rectangle of interest. The process of subdividing the surface into smaller blocks and computing each block's contribution is repeated for each and every one of the 200 block rectangles. The references may be consulted for more details on view factor algebra (Modest 1993, Howell 1982, Seigel and Howell 1981).

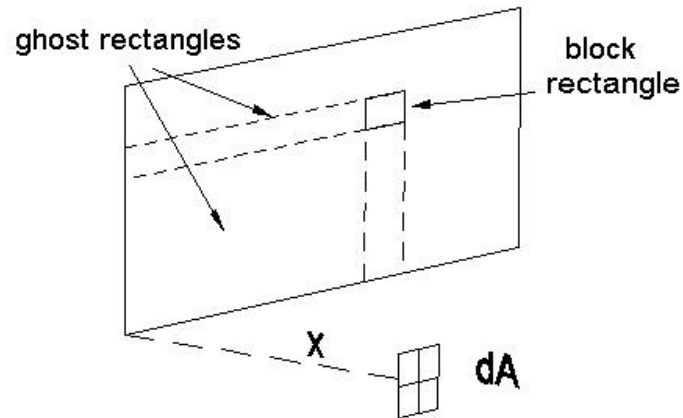


Figure 4.4: Subdivision of Rectangular Surface into smaller blocks to account for non-homogeneous intensity contours

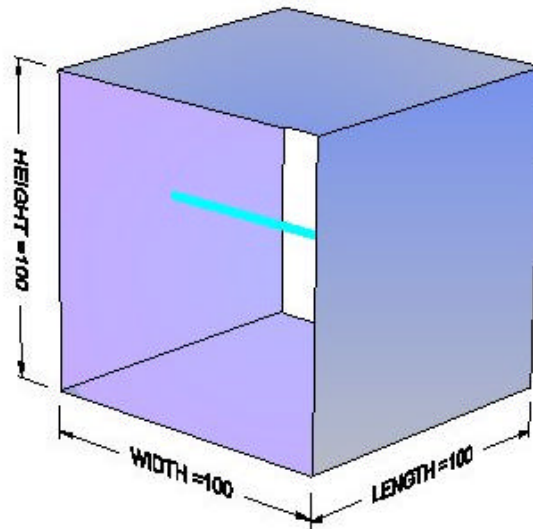


Figure 4.5: Illustration of a UVGI System with the lamp in a crossflow arrangement showing coordinate convention

Equation (4-6) can be used to compute a 3D matrix defining the intensity field due to the first reflections. This matrix can then be used to compute both the average and integrated dose as described later.

For a rectangular duct such as shown in Figure 4.5, there will be four surfaces (top, bottom, left, & right) but the model can be generalized to any number of surfaces. For example, a round duct could be approximated by a polygon with a sufficiently large number of sides. The reflected intensity I_R seen by a microbe at any (x, y, z) point will be the algebraic sum of those from all surfaces:

$$I_R = \sum_{i=1}^n I_{Rn} F_{d1-2,n} \quad (4-7)$$

where F_{d1-2} = view factor to n facing walls (up to 4).

No account has been taken in the above model of reflected radiation that is re-absorbed by the lamp itself, but this will generally be negligible provided the lamp occupies a small fraction of the total enclosure volume. The above procedure also assumes reflectivity is diffuse. More commonly, reflective surfaces are specular, or mirror-like. Analysis of specular reflections can be complex and although some methods exist like ray tracing techniques (Glassner 1989, Kowalski and Bahnfleth 2000a), the assumption of diffuse surfaces should produce results that approach those of specular modeling provided lamps are spaced, not concentrated, and specular surfaces do not create focal points, and also for all the previously stated reasons.

4.3 The Inter-reflected Intensity Field

When reflectivity is high (e.g. 75-85% for polished aluminum) and the reflective surfaces enclose most of the chamber area, the subsequent reflections may contribute significant to the total field. These reflections will bounce between the surfaces and are called inter-reflections. The intensity due to the inter-reflections will achieve steady state at the speed of light, converging to a finite value that depends on geometry and reflectivity. The physical process of inter-reflections can be simulated by using a computer model and performing a sufficient number of iterations. In this application, only three iterations are performed and the rest are handled with a geometric series.

Given that the surface intensities of the first reflections are known for all four surfaces from the preceding equations, each surface will then absorb some amount of energy from each of the other three surfaces. The amount of energy absorbed from the opposite parallel surface is determined from equation (4-6). For surfaces that are adjacent and perpendicular to each other, the following view factor can be used:

$$F_{d1-2} = \frac{1}{2p} \left[\tan^{-1} \left(\frac{1}{Y} \right) - \frac{Y}{\sqrt{X^2 + Y^2}} \tan^{-1} \left(\frac{1}{\sqrt{X^2 + Y^2}} \right) \right] \quad (4-8)$$

The parameters in the above equation are defined as follows:

$$X = a / b$$

$$Y = c / b$$

where a = height, b = length, c = perpendicular distance to surface.

Equations (4-6) and (4-8) can be used on each of the four surfaces in turn to determine the intensity received by each of the other three surfaces. The sum of the three contributions defines the incident energy on the surface. The amount actually reflected would be this total multiplied by the reflectivity, as in the first reflection case. The surface intensities computed represent the first inter-reflection.

For accurate predictions with this method it is necessary to subdivide the surfaces into smaller elements and compute the view factors and intensity contributions individually. This integrated sum will account for the variations in intensity across the surfaces.

The new surface intensities computed from the first inter-reflection can then be used to determine the next inter-reflection in an iterative fashion, simply by repeating this computational process. These computations should be performed for some ten or more reflections, at which point there will be little energy left to exchange. However, once the first two or three inter-reflections have been computed, the remaining inter-reflections can be computed by summing the resulting geometric series.

Consider the ideal case where the surface intensity from the first inter-reflection is uniform everywhere. The second inter-reflection intensity, I_{R2} , will be the product of the reflectivity, the total view factor, and the first inter-reflection surface intensity, I_{R1} , as follows:

$$I_{R2} = I_{R1}(\mathbf{r}F_{tot}) \quad (4-9)$$

The third inter-reflection intensity, I_{R3} , will be the reflectivity times the view factor times the second inter-reflection as follows:

$$I_{R3} = I_{R2}(\mathbf{r}F_{tot}) = I_{R1}(\mathbf{r}F_{tot})^2 \quad (4-10)$$

Obviously, each subsequent inter-reflection will be the product of the reflectivity times the view factor, multiplied by the previous inter-reflection, in an infinite series. The total intensity I_{Rtot} for all subsequent inter-reflections can be summed as:

$$I_{Rtot} = I_{R1}(\mathbf{r}F_{tot}) + I_{R1}(\mathbf{r}F_{tot})^2 + I_{R1}(\mathbf{r}F_{tot})^3 + \dots \quad (4-11)$$

This geometric series for the inter-reflected intensity sums to:

$$I_{Rtot} = I_{R1} \frac{rF_{tot}}{1 - rF_{tot}} \quad (4-12)$$

However, because the intensity field is not uniform for the first inter-reflection, equation (4-12) cannot be used to compute the first or the second inter-reflection accurately. In fact, the first three inter-reflections need to be computed to determine the ratio between them before equation (4-12) can be applied, after which it will give the total reflected intensity from the fourth reflection onwards. This approach works when the ratio becomes constant due to the fact that the diffuse reflections become approximately homogenous and the view factors and reflectivity remain constant.

The reason the geometric series approach works after three inter-reflections is because the effect of inter-reflection between surfaces is to average out the intensities and produce even intensity contours. In the example shown in Figure 4.4, the first three inter-reflections were used to compute the geometric series total for all the subsequent inter-reflections. The difference between these approaches was found to be only 0.05% of the total after computing 30 inter-reflections between rectangular surfaces, each of which was subdivided into 10x20 elements.

A convenient way of computing the factor of reflectivity times the view factor in equation (4-12) is to divide the third inter-reflection intensity by the second. This produces the following version of equation (4-12) in which the total inter-reflection intensity is computed for reflections 3 through infinity:

$$\sum_{i=3}^{\infty} I_R = I_{R3} \frac{\frac{I_{R3}}{I_{R2}}}{1 - \frac{I_{R3}}{I_{R2}}} = \frac{(I_{R3})^2}{I_{R2} - I_{R3}} \quad (4-13)$$

The total for all inter-reflections then becomes:

$$I_{Rtot} = I_{R1} + I_{R2} + I_{R3} + \frac{(I_{R3})^2}{I_{R2} - I_{R3}} \quad (4-14)$$

The above methods can be used to compute the matrix of values defining the inter-reflection intensity field, which is then added (point-by-point) to the direct intensity field matrix and the first reflection intensity field matrix. Figure 4-6 shows the results of a detailed computation of the direct, reflected, and inter-reflections for a particular test case.

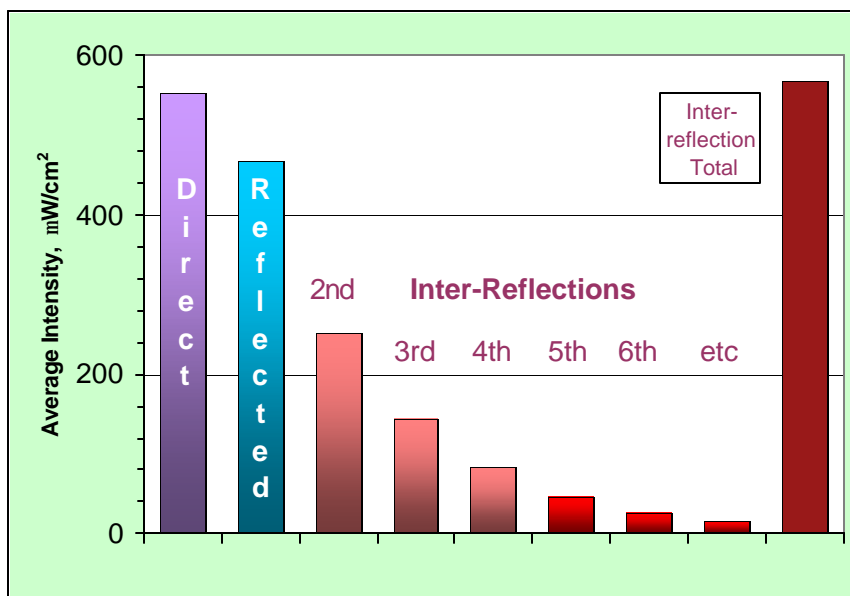


Figure 4.6: Comparison of Direct and Reflected Components computed with model

Chapter 5: Mathematical Modeling of Microbial Response

Microbial response to UVGI exposure can be modeled as a single stage exponential decay or a two-stage exponential decay, and the response may include a shoulder. Figure 5.1 illustrates the complete microbial decay curve. The mathematics for each of these components and a complete combined model are presented here.

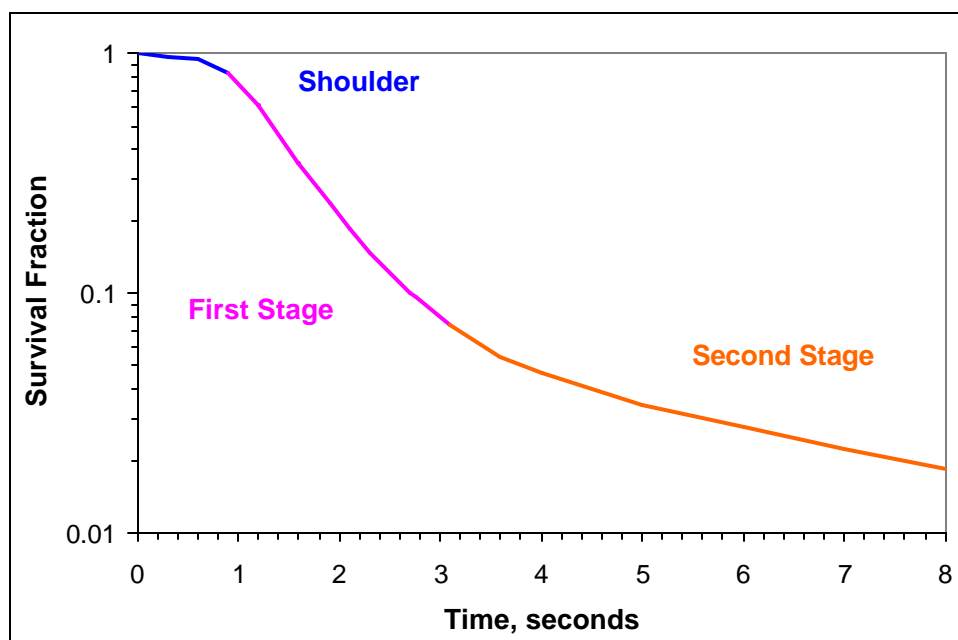


Figure 5.1: Two-stage Decay Curve with Shoulder for *Staphylococcus aureus*. Based on data from Sharp (1939).

5.1. Single Stage Microbial Decay

The classical exponential decay curve models microbial population survival under the influence of any biocidal factor (Chick 1908, Watson 1908). The refinements presented here, the two-stage model and the shoulder model, extend its accuracy. Alternative models, such as the multi-hit model (Severin and Roessler 1998), may also be able to account for the shoulder and two stages of inactivation. The choice of which model to use is somewhat arbitrary, but because of its simplicity and familiarity to most researchers the classical model is treated here explicitly.

Microorganisms exposed to UVGI experience an exponential decrease in population similar to other methods of disinfection such as heating, ozonation, and exposure to ionizing radiation (Hollaender 1943, Riley and Nardell 1989, Whiting 1991). The exact reasons that microbial populations decay exponentially when subject to biocidal factors has been dealt with at length by various researchers (i.e. Koch 1966) and is not readdressed here except as it is relevant to UVGI.

Ultraviolet rays are capable of breaking the molecular bonds of DNA and other cellular components (Jagger 1967, Casarett 1968, Coggle 1971, Eisenstark 1989). The ultraviolet radiation produced by UV lamps, specifically in the range of 2250-3020 Angstroms, happens to be sufficiently close, although not in exact correspondence (Kuluncsics et al 1999), to the wavelengths that define the bonding energy of some of the molecular bonds in DNA that it can dissociate these bonds. When a sufficient number of these bonds are broken, DNA self-repair becomes impossible and the microorganism may become incapable of normal functions such as growth and reproduction, or may even be destroyed as a result of the total absorbed dose.

What determines whether an individual microbe survives UV irradiation may be beyond current analytical means, but it is known empirically that populations will decrease exponentially under UVGI exposure and there is a high probability that the exponential decay process will be consistently obeyed for any sufficiently large microbial population. This is especially true considering that the density of photons produced by UVGI guarantees a large number of hits on any airborne microbe. It is likely that the probability of a sufficient number of these hits disrupting molecular bonds forms the primary determinant of whether a microbe succumbs, but, as stated, this may be beyond current analytical technology and we can only make accurate survival predictions based on macroscopic conditions and whole microbial populations.

The single stage exponential decay equation for microbial populations exposed to UV irradiation is as follows:

$$S = e^{-kIt} \quad (5-1)$$

where S = surviving fraction of initial microbial population

k = standard rate constant, $\text{cm}^2/\mu\text{W}\cdot\text{s}$

I = Intensity of UVGI irradiation, $\mu\text{W}/\text{cm}^2$

t = time of exposure, seconds

The rate constant defines the sensitivity of a microorganism to UVGI intensity and is unique to each microbial species (Hollaender 1943, Rauth 1965, Jensen 1964). Most published test results provide an overall rate constant that applies only at the test intensity. The rate constant k in equation (5-1) is the equivalent rate constant at an intensity of $1 \mu\text{W}/\text{cm}^2$ and is termed the standard rate constant to distinguish it from the overall rate constant. The standard rate constant is found by dividing the overall rate constant by the test intensity. Appendix B lists all published test results from which rate constants of respiratory pathogens could be extracted. Appendix C provides conversion factors for intensity and dose units.

If the average intensity is constant or can be calculated then the standard rate constant can be computed as

$$k = \frac{-\ln S}{It} \quad (5-2)$$

5.2 Two-Stage Survival Curves

In general, a small fraction of any microbial population is resistant to UVGI or other bactericidal factors (Cerf 1977, Fujikawa and Itoh 1996, Whiting 1991). Typically, over 99% of the microbial population will succumb to initial exposure but a remaining fraction will survive, sometimes for prolonged periods (Smerage 1993, Qualls and Johnson 1983). This effect may be due to clumping (Moats et al 1971, Davidovich and Kishchenko 1991), dormancy (Koch 1995), or other factors.

The two-stage survival curve can be represented mathematically as the summed response of two separate microbial populations that have respective rate constants k_1 and k_2 . If we define f as the fraction of the total initial population with rate constant k_2 , then $(1-f)$ is the fraction of the total initial population with rate constant k_1 . The total survival $S(t)$ will then be:

$$S(t) = (1-f)S(t) + fS(t) \quad (5-3)$$

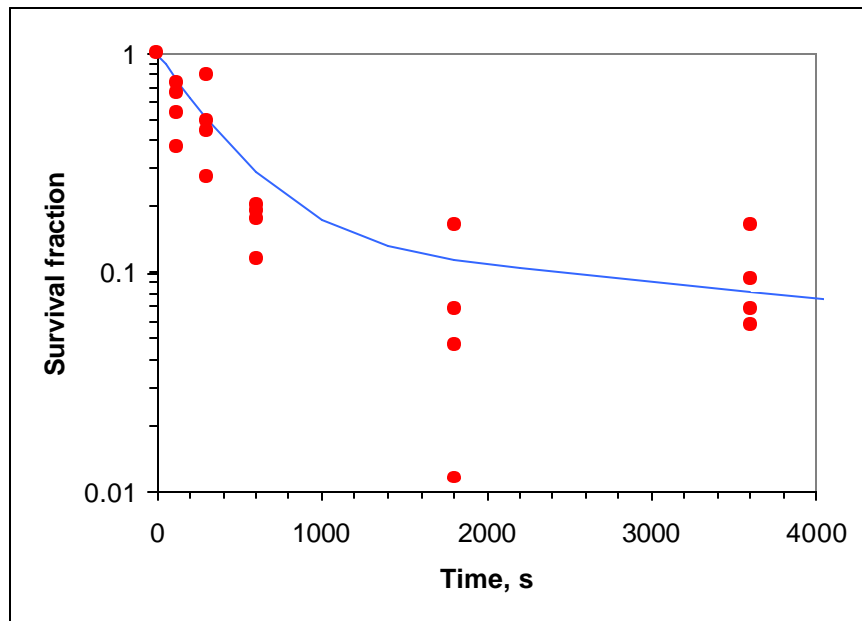


Figure 5.2: Survival Curve of *Streptococcus pyogenes* showing Two Stages, based on data from Lidwell and Lowbury (1950).

For UVGI irradiation, the total survival curve is therefore the sum of the rapid decay curve (the vulnerable majority with rate constant k_1) and the slow decay curve (the resistant minority with rate constant k_2), and the complete equation is:

$$S(t) = (1 - f)e^{-k_f It} + fe^{-k_s It} \quad (5-4)$$

where k_f = rate constant for fast decay population, $\text{cm}^2/\mu\text{W}\cdot\text{s}$

k_s = rate constant for slow decay population, $\text{cm}^2/\mu\text{W}\cdot\text{s}$

f = fraction of the total initial population subject to slow decay

Figure 5.2 shows data for *Streptococcus pyogenes* that exhibits a two-stage curve. The resistant fraction of most microbial populations may be about 0.01% but some studies suggest it can be as high as 30% or more for certain species (Riley and Kaufman 1972, Gates 1929, UVDI 2001).

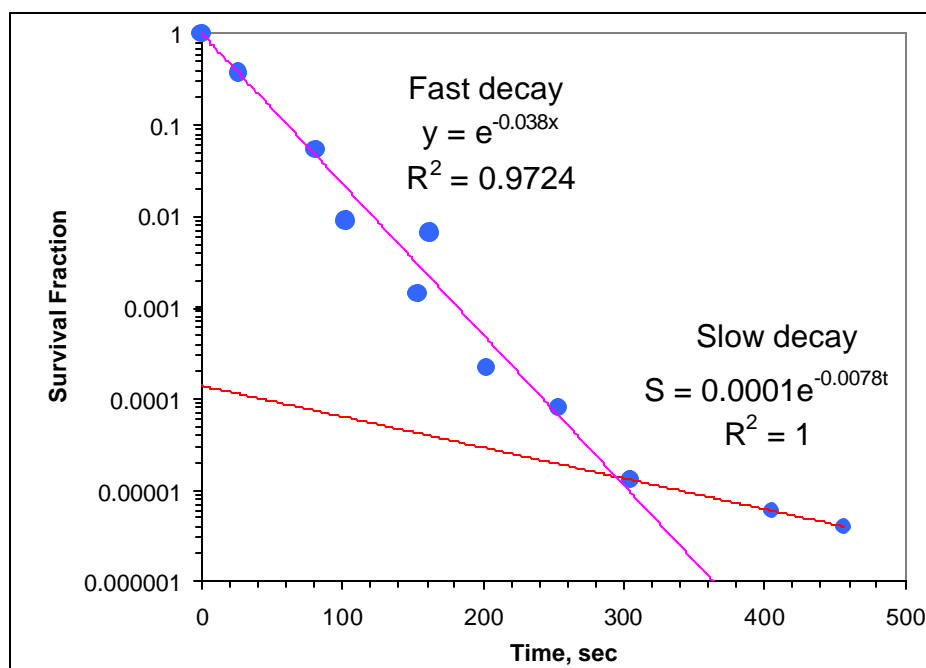


Figure 5.3: Survival curve for *Adenovirus* showing two stages. Based on data from Rainbow and Mak (1973).

Figure 5.3 shows data for Adenovirus in which the two stages are separated into their component equations. Since the second stage has an intercept at approximately 0.00013, implying the resistant fraction is 0.013 %. Following the second stage to the intercept is the primary means of extracting the fraction $(1-f)$, and requires separation of the data set into its two components.

Values of the two stage rate constants are summarized in Table 5-1 for the few microbes for which second stage data has been published. These parameters are a re-interpretation of the original published results by the indicated researchers and results in an improved curve-fit in all cases. The two-stage rate constants k_{of} and k_{os} listed in Table 5-1 are overall rate constants that apply only at the intensity shown, which is the intensity of the original test.

TABLE 5-1: Two Stage Parameters (based on re-evaluation of original data)

Airborne Microorganism	Reference	k original cm ² /μW-s	Two Stage Curve			
			k ₁ cm ² /μW-s	Pop. f	k ₂ cm ² /μW-s	Pop. (1-f)
Adenovirus Type 2	Rainbow 1973	0.000047	0.00005	0.99986	0.00778	0.00014
Coxsackievirus B-1	Hill 1970	0.000202	0.000248	0.9807	8.81E-05	0.0193
Coxsackievirus A-9	Hill 1970	0.000159	0.00016	0.7378	0.000125	0.2622
Staphylococcus aureus	Sharp 1939	0.000886	0.01702	0.914	0.0091	0.086
Streptococcus pyogenes	Lidwell 1950	0.000616	0.00287	0.8516	0.000167	0.1484
E. coli (Reference only)	Sharp 1939	0.000927	0.008098	0.9174	0.003947	0.0826
Serratia marcescens	Riley 1972	0.049900	0.0757	0.712	0.0292	0.288

5.3 The Shoulder

The initiation of exponential decay in response to UVGI exposure, or any other biocidal factor, is often delayed for a period of time (Cerf 1977, Munakata et al 1991, Pruitt and Kamau 1993).

Figure 5.4 shows the survival curve for *Staphylococcus aureus*, in which a shoulder is evident from the fact that the regression line intercepts the y-axis above unity. Shoulder curves typically start out horizontally before developing into full exponential decay. This region of transition is referred to as a shoulder.

As shown in Figure 5.5, the initial part of the decay curve has zero slope at time $t=0$ and exponential decay is not fully manifested until time t_d . The intersection of the horizontal line $S=1$ (100% Survival) at t_c with the extension of the decay curve is known as the "quasi-threshold" in the field of radiation biology (Casarett 1968). The point t_d is tangent to both curves and provides for the mathematical solution following.

The lag in response to the stimulus implies that either a threshold dose is necessary before measurable effects occur or that that repair mechanisms actively deal with low-level damage (Casarett 1968). The effect is species and intensity dependent. In many cases it can be neglected, however, for some species and sometimes for low intensity exposure, the shoulder can become significant and prolonged.

Different mathematical models have been proposed to account for the shoulder including variations of the multi-hit model, recovery models, split-dose recovery models, and empirical models (Russell 1982, Alper 1979, Harm 1980, Casarett 1968). The various limitations of these models render them difficult to use for predictive purposes. Further hampering the use of these

equations is a lack of published empirical data detailed enough to resolve the shoulders under differing irradiation doses.

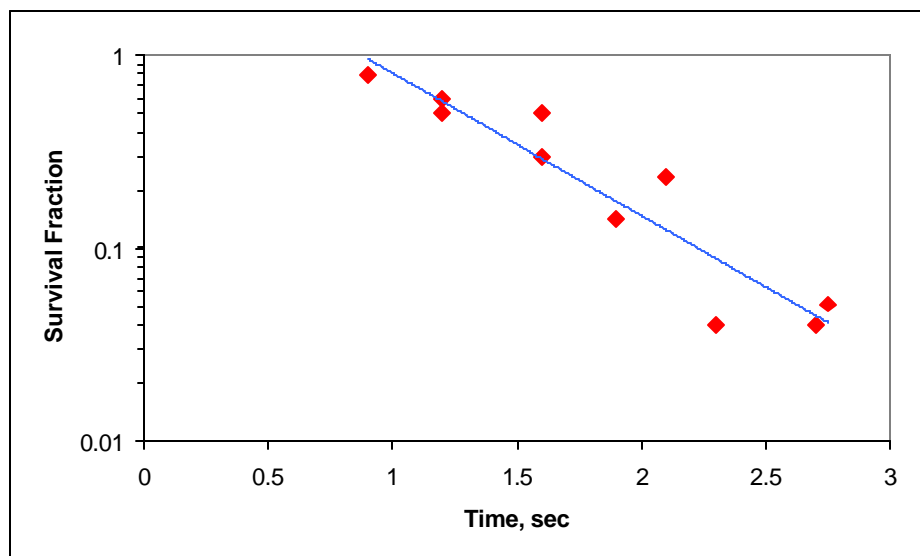


Figure 5.4: Survival Curve of *Staphylococcus aureus* showing evidence of shoulder. Based on data from Sharp 1939.

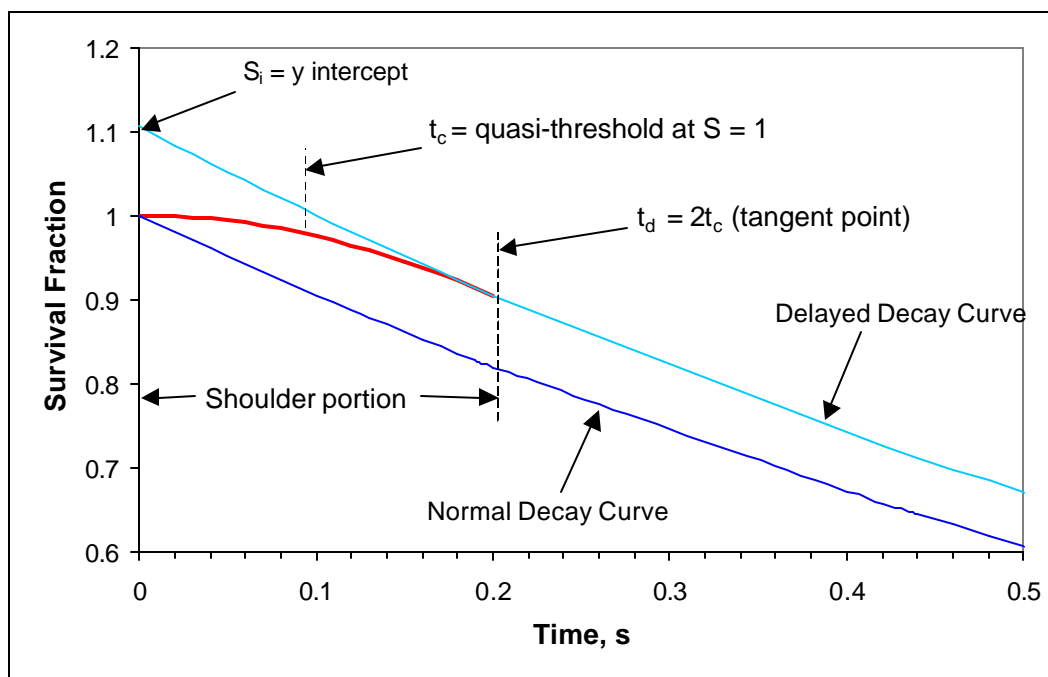


Figure 5.5: Development of Shoulder Curve, showing the effect of the time delay t_c and relation to the tangent point d .

To create a workable mathematical model of the complete decay curve a simple and general model is derived from fundamentals. This model recognizes that any exponential decay curve that exhibits a shoulder will have an intercept with the y-axis (the survival axis) that is a function of the species rate constant, the intensity, and the quasi-threshold.

Recovery due to growth during irradiation is assumed negligible and to be encompassed by the model -- this must be true if the parameters are based on a broad range of empirical data. If recovery factors are not minor, then they will at least be additive and the model can be easily adjusted at such time as data becomes available. Recovery of spores, although not well understood, is recognized as a process associated with germination (Russell 1982). The recovery of spores is, therefore, a self-limiting factor since a germinated spore invariably becomes less resistant to UVGI irradiation (Harm 1980). This process, induced germination, can even be used to control spores (Kowalski and Bahnfleth 2000a, Sakuma and Abe 1996).

An exponential decay curve with a shoulder will have an intercept greater than unity when the first stage rate constant is extrapolated to the y-axis. It is naturally assumed that a shoulder exhibited in the data is statistically significant and not an artifact of measurement uncertainty. With respect to a decay curve that has an intercept of unity, the shouldered curve is shifted ahead by a time interval t_c , the quasi-threshold. The equation for the delayed single stage survival curve, when $t \geq t_d$ is:

$$\ln S(t) = -kI(t - t_c) \quad (5-5)$$

The shoulder occurs during the time interval $0 < t < t_d$. It is apparent that the shoulder portion is a non-linear function of $\ln S$ (see Figure 5.3). Insufficient data exists to precisely define the form of the relationship but $\ln S$ cannot be simpler than a polynomial function of second order.

In fact, the error resulting from any mathematical relationship assumed for the shoulder will be small as long as it provides a smooth transition between the horizontal and the delayed decay curve. In other words, a parabolic curve will result in less error than the sharp transition from the horizontal to the decay curve that would result from a purely linear model.

Assuming a second order polynomial relationship between the dose (intensity times time) and $\ln S$, we have:

$$\ln S(t) = -p(It)^2 \quad (5-6)$$

where $0 < t < t_d$

$p = \text{a constant}$

The constant p can be evaluated by requiring continuity through the first derivative between equations (5-5) and (5-6) at the tangent point $t = t_d$. For any constant intensity I , the

slope of the exponential portion of the survival curve may be obtained by straightforward time differentiation of the right hand side of equation (5-5):

$$\frac{d}{dt}(\ln S) = -kI \quad (5-7)$$

Similarly, the slope of the shoulder curve is obtained by differentiation of the right hand side of equation (5-6):

$$\frac{d}{dt}(\ln S) = -2pIt \quad (5-8)$$

The constant p is determined by equating (5-7) and (5-8) at time t_d :

$$p = \frac{k}{2It_d} \quad (5-9)$$

Substitution of this expression for p into equation (5-6) and equating (5-5) and (5-6) at $t=t_d$ yields the relation:

$$t_d = 2t_c \quad (5-10)$$

Equation (5-10) is, in fact, a version of the result Appolonius of Perga arrived at in the 3rd century BC through lengthy geometry for the special case of ellipses, which are also described by second order polynomials (Elmer 1989). The term p is now discarded, after substituting for equations (5-9) and (5-10), and equation (5-6) can be written in the form:

$$\ln S = -\frac{kI}{4t_c} t^2 \quad (5-11)$$

In general, any data set describing single stage microbial decay can be easily fit to a single stage exponential decay curve. Normally, the y-intercept is fixed at $S=1$ when fitting data to a curve. If a shoulder is suspected, the constraint on the y-intercept should be removed and the coefficient of the exponential will then have some value greater than 1. This assumes, of course, that the shoulder is real and not a result of measurement uncertainty.

The term S_i denotes the y-intercept of the shifted exponential portion of a survival curve with a shoulder, as shown in Figure 5.5. If S_i is known, the value of t_c can be determined by evaluating equation (5-5) at $t=0$:

$$t_c = \frac{\ln(S_i)}{kI} \quad (5-12)$$

The threshold t_c is assumed to be manifest as a function of the first stage rate constant. The complete single stage survival curve for each stage of a population with two stages can then be defined as the piecewise continuous function:

$$\ln S(t) = \begin{cases} -\frac{kI}{4t_c} t^2 & t \leq 2t_c \\ -kI(t - t_c) & t \geq 2t_c \end{cases} \quad (5-13)$$

The period of time, t_c , may approach zero at high intensities and it may be negligible for long exposures. However, if the exposure time is brief the shoulder may be a significant fraction of the total and the impact should be given consideration. For $t_c=0$ equation (5-13) reduces to equation (5-1).

The threshold t_c will decrease as the intensity increases for constant exposure. No studies exist that define the relationship, but data from Riley and Kaufman (1972) suggest that a linear relation exists between intensity and the logarithm of the y-intercept S_i . A theoretical basis can be found for the same relationship in the Arrhenius rate equation, which describes the influence of temperature or radiation on process rates as being that of simple exponential decay (Rohsenow and Hartnett 1973). Assuming, therefore, that the threshold t_c is an exponential function of intensity I we can write:

$$t_c = Ae^{-BI} \quad (5-14)$$

where A = a constant defining the intercept at $I=0$

B = a constant defining the slope of the plotted line of $\ln(t_c)$ vs. I

Given any two sets of data for t_c and I , equation (5-14) can be used to determine the values of A and B . Prediction of t_c for any arbitrary value of intensity I then becomes possible. Figure 5.6 shows hypothetical survival curves of spores subject to various intensities. Research is needed to empirically verify the form of the shoulder equation, since data in the literature are scant, but preliminary studies by the authors suggest this model is robust over a wide range of intensities.

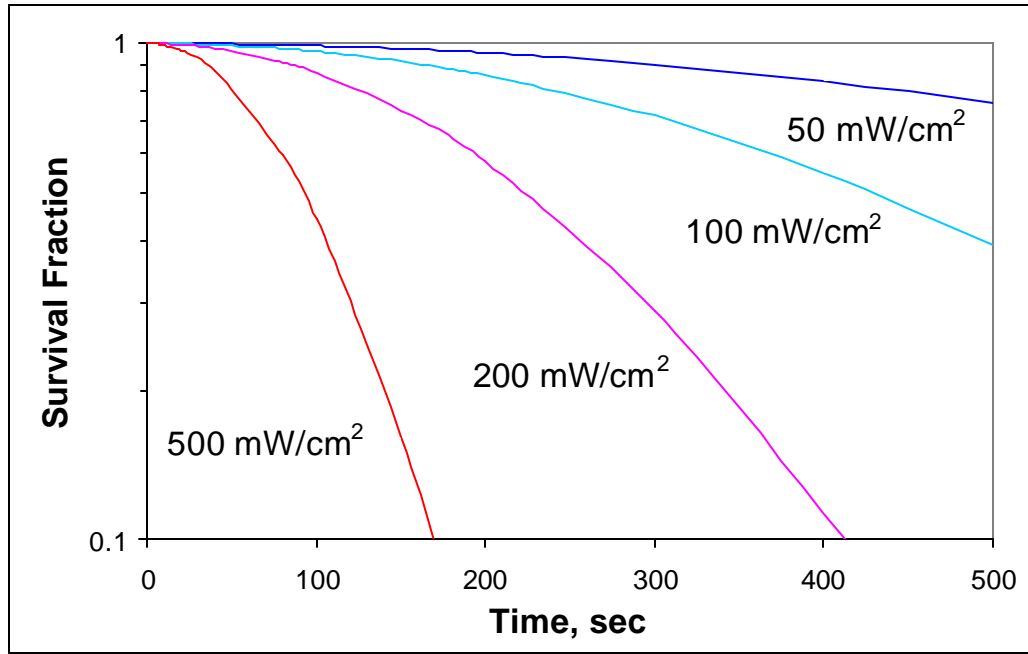


Figure 5.6: Illustration of Generic Shoulder Model Response to Intensity

5.4 The Complete Microbial Decay Model

The complete model for microbial decay, including both the second stage and the shoulder, can be written by combining equation (5-4) and equation (5-13), and adding the two stages together as separate populations (with the threshold conservatively assumed identical in each case):

$$S(t) = \begin{cases} fe^{-\frac{k_f I}{4t_c} t^2} + (1-f)e^{-\frac{k_s I}{4t_c} t^2} & t \leq 2t_d \\ fe^{-k_f I(t-t_c)} + (1-f)e^{-k_s I(t-t_c)} & t \geq 2t_d \end{cases} \quad (5-15)$$

If the fraction f is relatively small compared with $(1-f)$, then equation (5-15) may be simplified by ignoring the second stage terms in the shoulder.

Parameters defining the shoulder characteristics of various microbes are summarized in Table 5.2. These were obtained by re-interpreting the original published results and in all cases an improved curve-fit resulted. The parameters “A” and “B” defining the relationship between the threshold t_c and the intensity I could not be established due to the insufficient data in the literature for different intensities. Data taken by UVDI (2001) is addressed in Chapter 7, Model Validation.

TABLE 5.2: Shoulder Parameters

Airborne Microorganism (see Table 1 for References)	Reference	k original cm ² /μW-s	Time Delay Shoulder		
			Intensity μW/cm ²	Intercept S _i	Threshold t _c
Coxsackievirus A-9	Hill 1970	0.000202	83	1.1484	0.4801
Reovirus Type 1	Hill 1970	0.000132	1160	1.7237	3.1202
Staphylococcus aureus	Sharp 1939	0.000886	10	4.4246	87.38
	Gate 1929	0.001184	110	1.225	1.8432
Mycobacterium tuberculosis	David 1973	0.000987	400	2.6336	4.176
	Riley 1961	0.004720	85	1.7863	3
Mycobacterium kansasii	David 1973	0.000364	400	6	4.254
Mycobacterium avium-intra.	David 1973	0.000406	400	5.62	9.227
Haemophilus influenzae	Mongold 1992	0.000599	50	1.0902	2.5703
Pseudomonas aeruginosa	Abshire 1981	0.000640	100	1.3858	9.6818
Legionella pneumophila	Antopol 1979	0.002503	50	1.288	96.69
Serratia marcescens	Rentschler 1941	0.001225	1	2.0824	190.5
Bacillus anthracis	Sharp 1939	0.000509	1	2.0806	109.8

Occasionally in the literature the first stage intercept proves to be less than 1, which is probably due to experimental error and limited data sets. In all cases when shoulder parameters are evaluated, an uncertainty analysis should be performed to verify that the results defining the shoulder and second stage are significant.

The complete mathematical model of microbial decay, in contrast with the single stage model, makes it more mathematically obvious that the second stage could produce resistant survivors when the delivered dose is less than that required for sterilization. It has been observed by many previous researchers that insufficient disinfection may lead to the generation of resistant microbial populations. This is just as true with UVGI systems, say, in a building ventilation system, as it is with bacterial infections inadequately treated with antibiotics. It is hoped that once second stage and shoulder data become available for a wide array of microbes that the complete microbial decay model will come into common use to help assure that such resistant strains of airborne pathogens do not, in fact, develop in indoor environments as the result of insufficiently designed systems.

Chapter 6. The UVX Computer Program

The mathematical models described in Chapters 4 and 5 have been coded into a C++ program called by the acronym UVD, for UV Design. Two main versions of this program were developed, including a user-friendly version with dialog-style data input windows developed for UVDI, but the version presented here includes only the fundamental computational algorithms. The latter version has been used to provide output in the form necessary to run the factorial analysis (see Chapter 8) and is called the UVX program. Appendix G lists the C++ source code for the computational algorithms and the global and local variables. The compiler used was Microsoft Visual C++ 6.0, but the C++ routines can be compiled on virtually any C++ compiler.

6.1 Description of the Program

The UVX program takes input parameters describing a rectangular UVGI system in terms of its geometry, lamp characteristics, lamp placement, lamp orientation, and surface reflectivity. The program requires the following input parameters (either entered or implicit) for each analysis:

- ❖ Height, Width, and Length of enclosure, in cm.
- ❖ Lamp wattage (W), lamp length (arc length) and lamp radius, in cm.
- ❖ Lamp end coordinates (x1, y1, z1, x2, y2, z2, in cm).
- ❖ Reflectivity of enclosure, in %.
- ❖ Airflow, in cu.m./min.
- ❖ Microbe rate constant, in $\text{cm}^2/\mu\text{W}\cdot\text{s}$.

A three dimensional matrix of Width = 50, Height = 50, and Length = 100 is scaled to match the actual system dimensions. This primary matrix is used to determine the direct intensity field due to the lamp alone. A smaller matrix sized 10x10x20 is used for the computations of the first reflections and the inter-reflections, and is illustrated in Figure 6.1.

The smaller 10x10x20 matrix is necessary due to the large number of calculations required to compute the radiative intensity exchanged between each block of the 10x20 wall matrix and each other block on the three opposite walls. This approach is justified by the fact that each reflection from the walls has a more diffuse intensity contour and doesn't need as much resolution as the direct intensity field. In fact, inspection of the wall contours shows that essentially all detail is lost after two or three inter-reflections. This latter fact allows for the mathematical shortcut of equation (4-17) in Chapter 4 and greatly simplifies the computations as well as improving accuracy of the model.

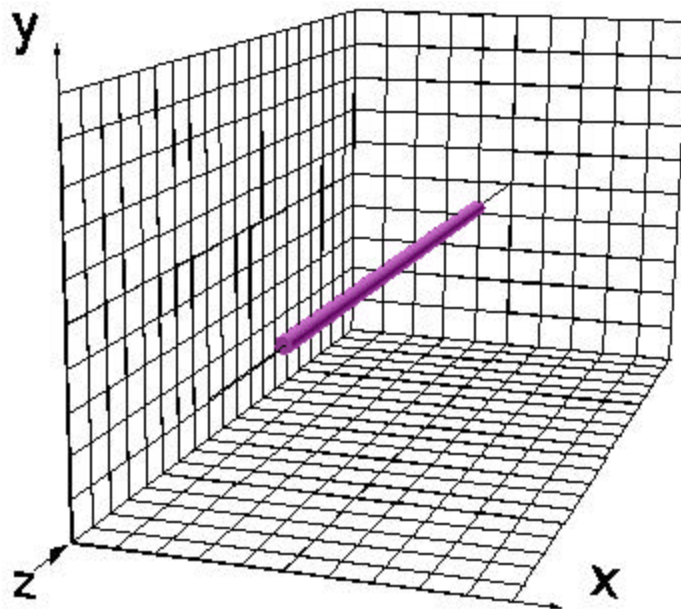


Figure 6.1: Grid for a 10x10x20 Matrix and Coordinate System, shown with a lamp in an axial configuration.

6.2 Operation of the Program

The program takes the input data from an input text file, performs the analysis and outputs results in a text file. Intermediate results can be extracted and graphed in spreadsheets.

Input data requires definition of the coordinate system. The lamp coordinates are based on the lower left front corner of the matrix being at (0, 0, 0). The indices for both the large and small matrices are also based on this (0, 0, 0) point.

Using the input the enclosure intensity field is determined by evaluating the direct intensity field of the lamp, the first reflection intensity field, and the total inter-reflected intensity field. These are summed to produce the total intensity field of the enclosure. This process is shown by the flow chart in Figure 6.2.

As mentioned previously, the inter-reflections are only computed for three iterations, after which the total bulk average intensity is determined mathematically for the remaining inter-reflections. Each of the first three inter-reflection calculations involves computing the exchange of radiative energy from each of the blocks on the other three sides, for all four walls. The summed result produces the wall intensity contours for the next set of inter-reflection calculations. This is the most calculation-intensive portion of the program and takes up the most operating time. In comparison, the direct and first reflection calculations proceed relatively rapidly.

Because two different size matrices are used for the computations, it is necessary to scale up the smaller matrix to match the size of the larger matrix prior to adding them. This is

done by performing a three dimensional (3D) interpolation on the 10x10x20 matrix to create a 50x50x100 matrix.

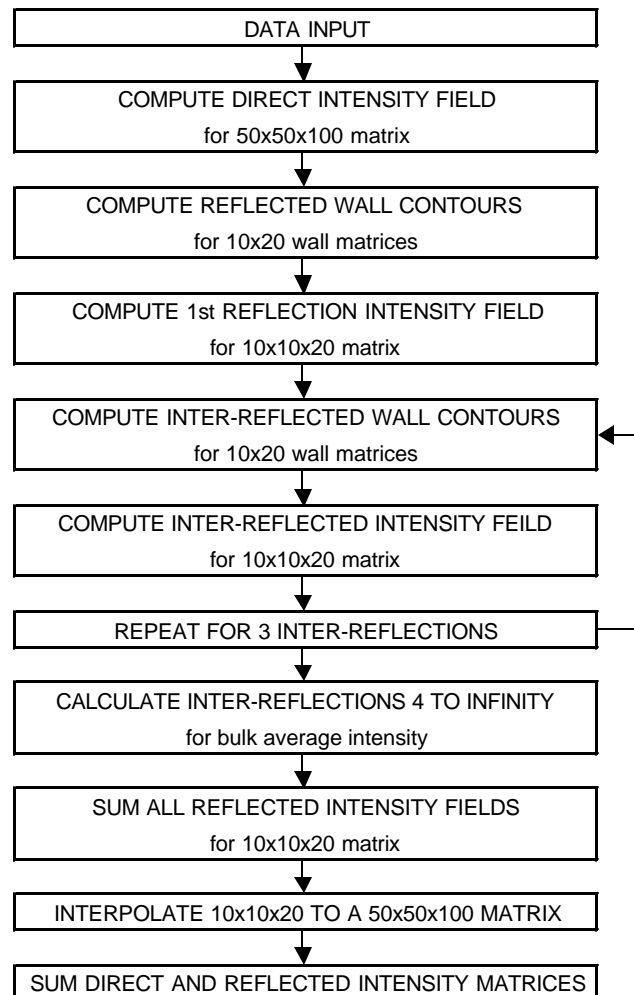


Figure 6.2: Flow Chart for Calculation of Overall Intensity Field

Once the complete 3D intensity field has been filled in, it becomes possible to compute the average intensity and the average dose. This average dose represents the theoretical bounding condition of complete mixing. Given the average intensity the overall survival of the test microbe can be simply computed by using the basic exponential decay equation, equation (5-1) in Chapter 5.

The opposite bounding condition, completely unmixed flow in which all streamlines remain approximately parallel, is computed as described in Chapter 4, where the integrated dose is the result. This is done by computing the survival of the test microbe through each streamline and then averaging the resulting survival rates. Since the matrix has a resolution of 50x50, this

means that 2500 streamlines are taken into account. However, each streamline is divided into 100 segments and the survival is computed for each of these segments, with the result that $2500 \times 100 = 250000$ calculations are performed and the results averaged to obtain the integrated survival.

Both of the bounding conditions, mixed and unmixed flow are illustrated in Figure 6.3, which shows a schematic of a typical UVGI system in an air handling unit.

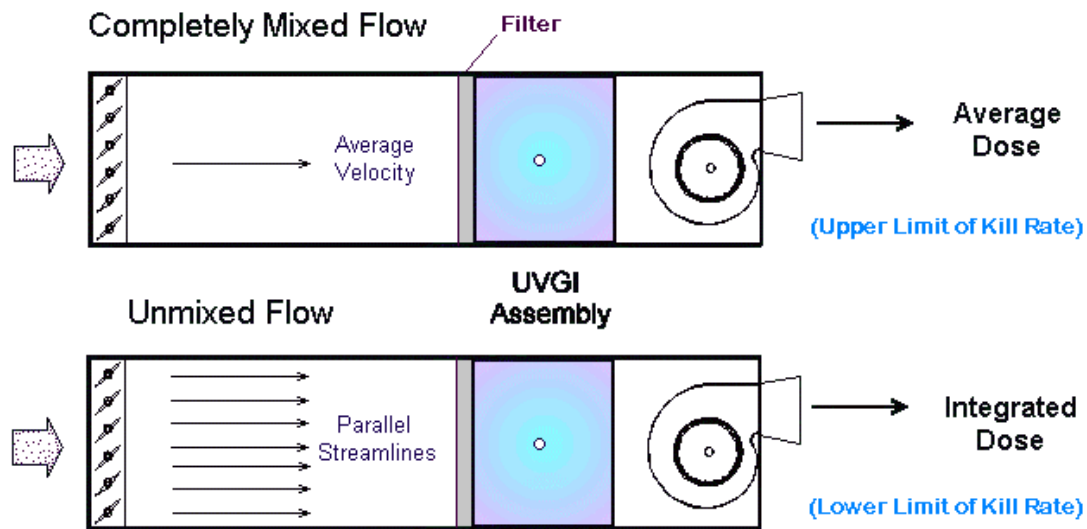


Figure 6.3: Illustration of the Two Bounding Conditions, completely mixed flow and unmixed flow.

The 3D intensity field is averaged to obtain the average intensity, which represents the mixed air condition. This average intensity is used to directly compute the average survival or kill rate. The unmixed air kill rate is obtained by using the complete detailed 3D intensity field and computing the kill rate at each increment of the $50 \times 50 \times 100$ matrix, and then summing the incremental kill rates. The kill rates are summed along the theoretical parallel streamlines, which produces the kill zones diagram such as shown in Figure 6.4, and these kill rates are summed for the entire microbial population to obtain the integrated kill rate.

Once the intensity field is computed it can be used to determine the survival rates of all microbes in the database, but for the purposes of this research only the test microbe *Serratia marcescens* is used for computations. Since the airborne rate constant has been established for this microbe through testing, it can be considered a reliable predictor of system performance and is therefore used exclusively.

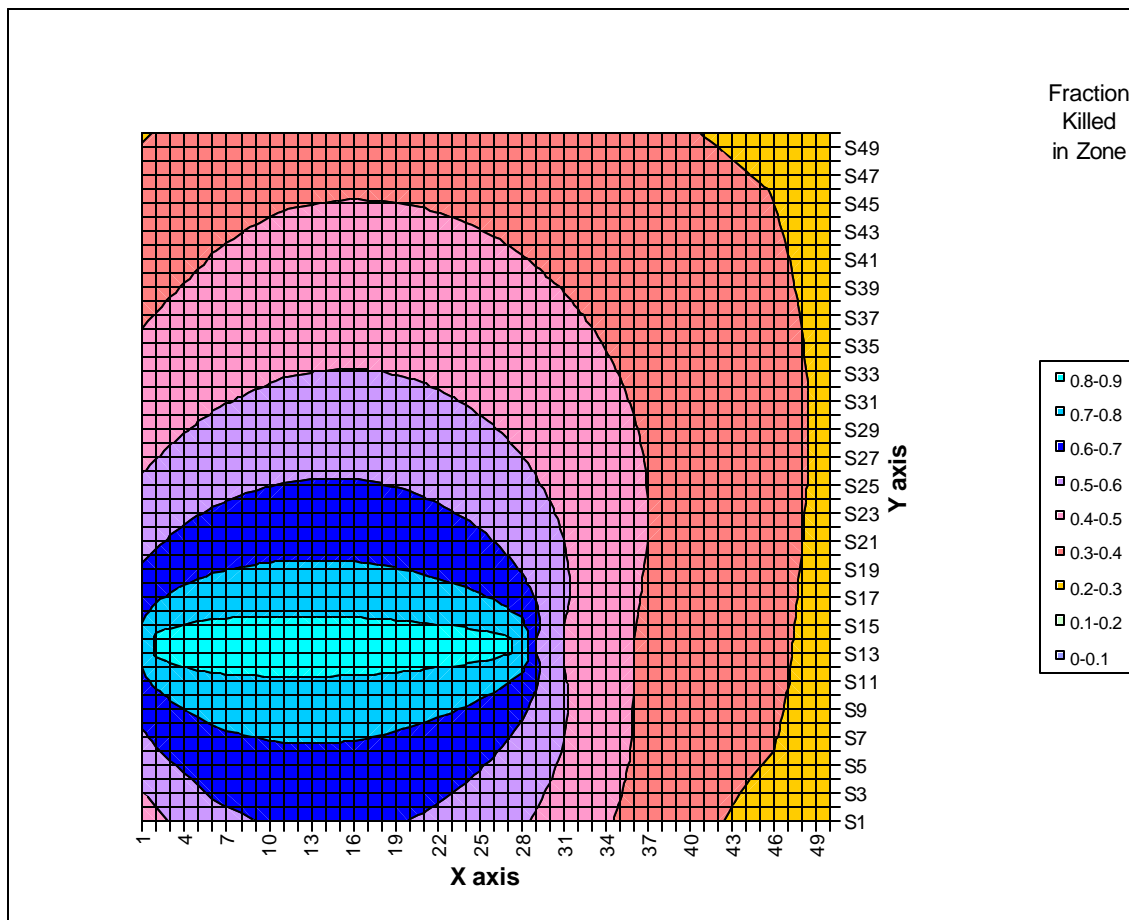


Figure 6.4: Kill Zones for the Unmixed Air Condition. The view represents the face area of the duct with X as the width and Y as the height.

The overall flow chart for the operation of the program is shown in Figure 6.5. This is, however, a greatly simplified representation of the program mechanics since each aspect of the calculations, from the intensity field calculations to the matrix operations, posed formidable challenges. For additional information on the program operation refer to the comments embedded in the source code and the variable and subroutine descriptions.

Flow charts for the direct intensity, first reflection intensity, and inter-reflected intensity are shown in Figure 6.6, Figure 6.7, and Figure 6.8, respectively. Refer to the source code in Appendix G for more detailed information on internal program computations and operation.

The version of the program used for this research incorporates a series of macroscopic loops that cycle through all variations of input parameters. A total of 273 runs are performed by this program in order to exhaustively evaluate all essential configurations necessary to meet the requirements of the factorial analysis discussed in Chapter 8. The input parameters through which the program is cycled are defined in terms of dimensionless parameters per the

dimensional analysis in Chapter 7. Only single lamp models have been used in the analyses performed here, although the program is capable of analyzing multiple lamps. Appendix D provides a list of all UVGI lamps in the current program database. Appendix E and Appendix F provide databases of material reflectivity and rate constants used in the program.

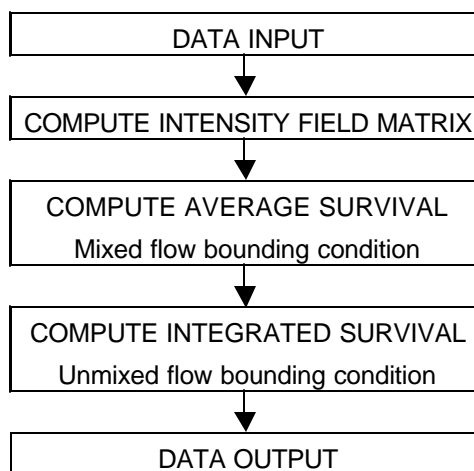


Figure 6.5: Simplified flow chart for program operation.

In the program listing in Appendix G the primary file is `uvxDlg.cpp` and the associated header files `uvxDlg.h` and `global.h`. Only the code that is involved in the computations is shown in these listings, for clarity. The main control subroutine in `uvxDlg.cpp` is called `OnBrun()` and this routine calls the subroutine `Analysis()`, which handles the computations.

Figure 6.9 shows the program screen display. This display summarizes some of the input data for each run and shows the progress of the computations. The program is run by clicking the Analysis button.

As an example of the final kill rate computation, the first line in the output file in Appendix I shows the total average intensity field to be $161.495 \mu\text{W}/\text{cm}^2$. The exposure time can be computed from the airflow and duct dimensions shown in Appendix I as follows:

$$t = \frac{WHL}{Q} = \frac{(160/100)(160/100)(200/100)}{390} (60) = 0.788 \text{ sec}$$

Per equation (5-1), the single stage decay model:

$$S = e^{-kt} = e^{-0.0028(275.77)(0.788)} = 0.544$$

The kill rate is then $K = 1 - 0.544 = 0.456$ or 45.6%, which matches the kill rate shown in the output in Appendix I.

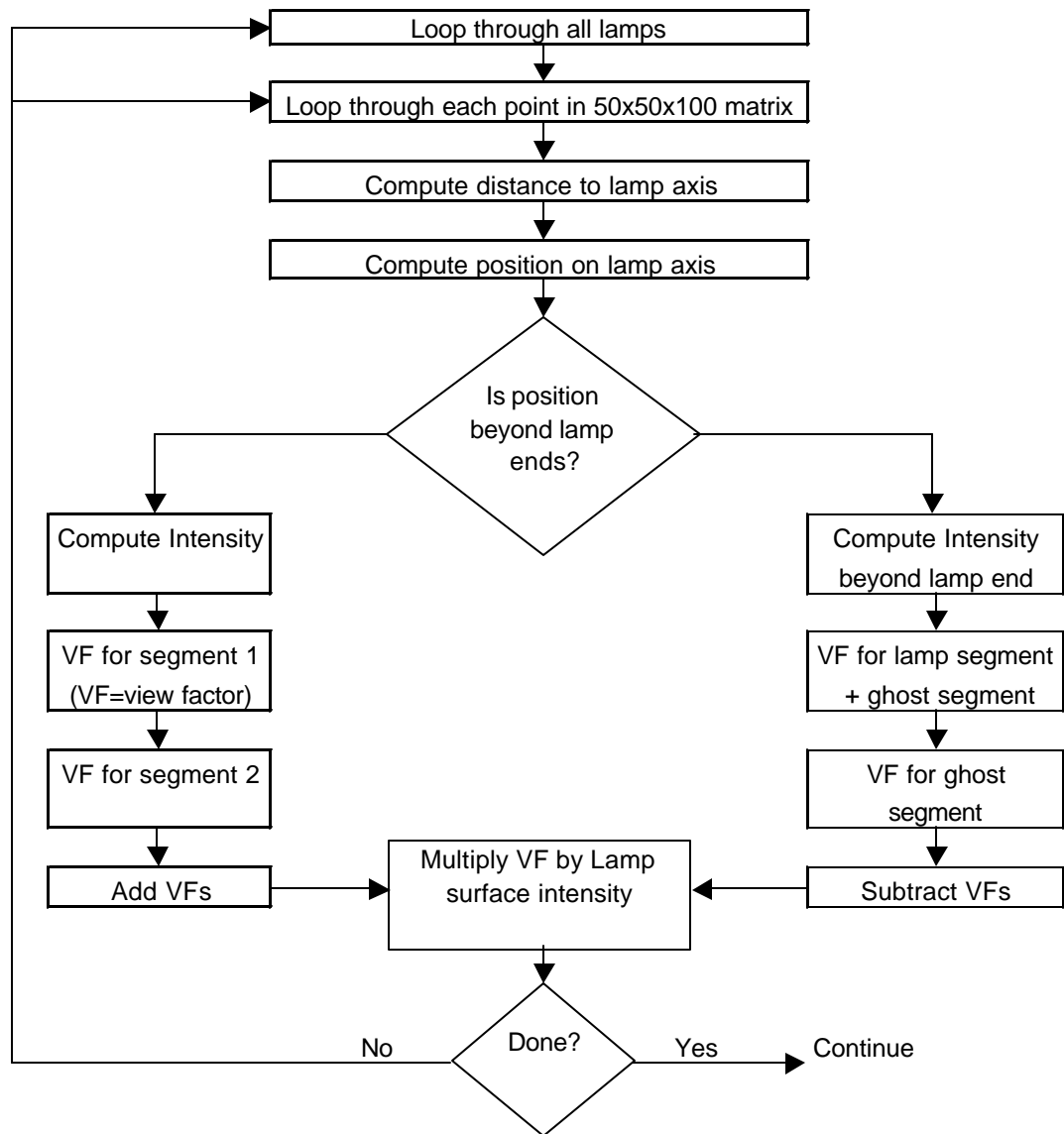


Figure 6.6: Direct Intensity Algorithm Flowchart

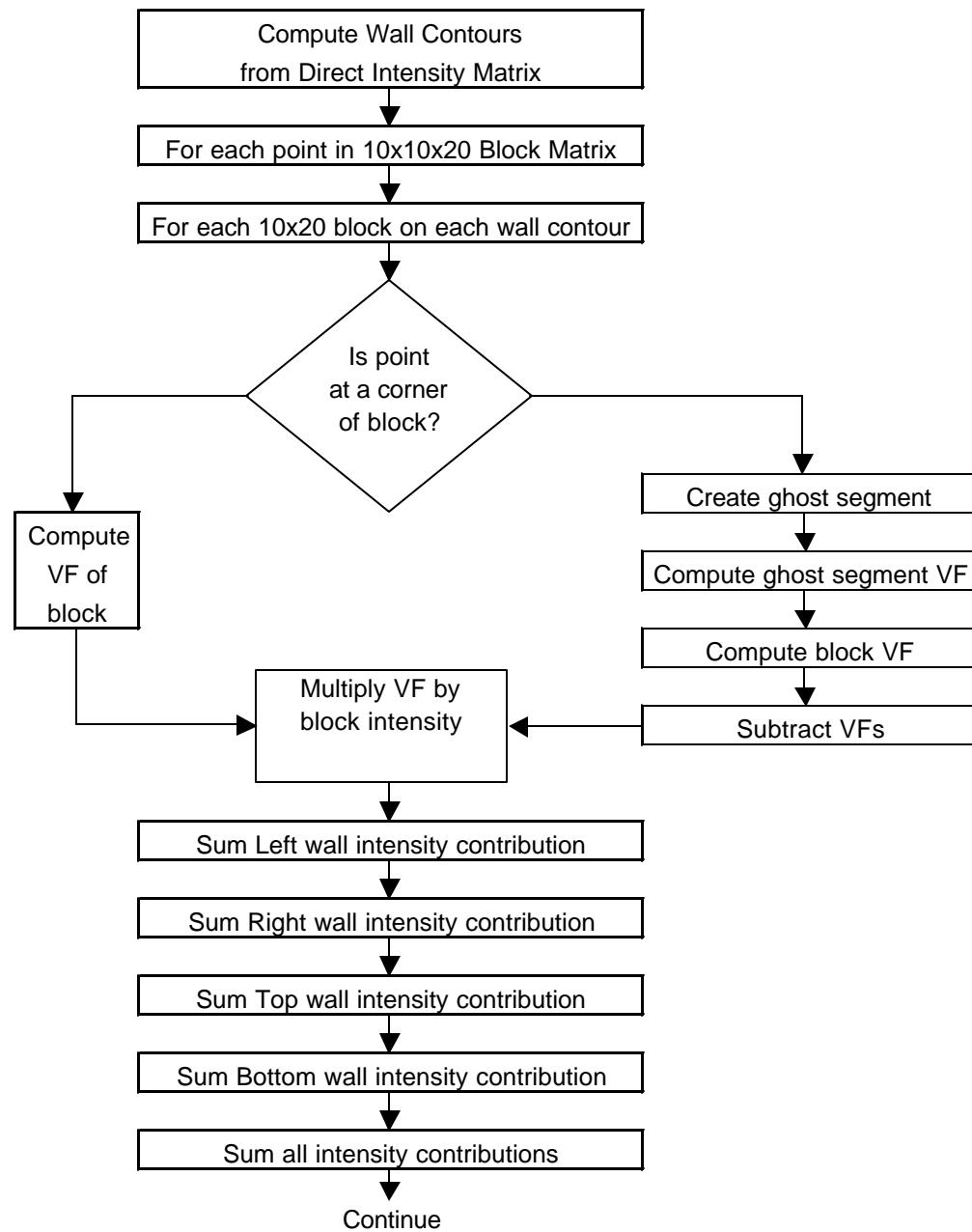


Figure 6.7: Flowchart for Reflected Intensity Algorithm

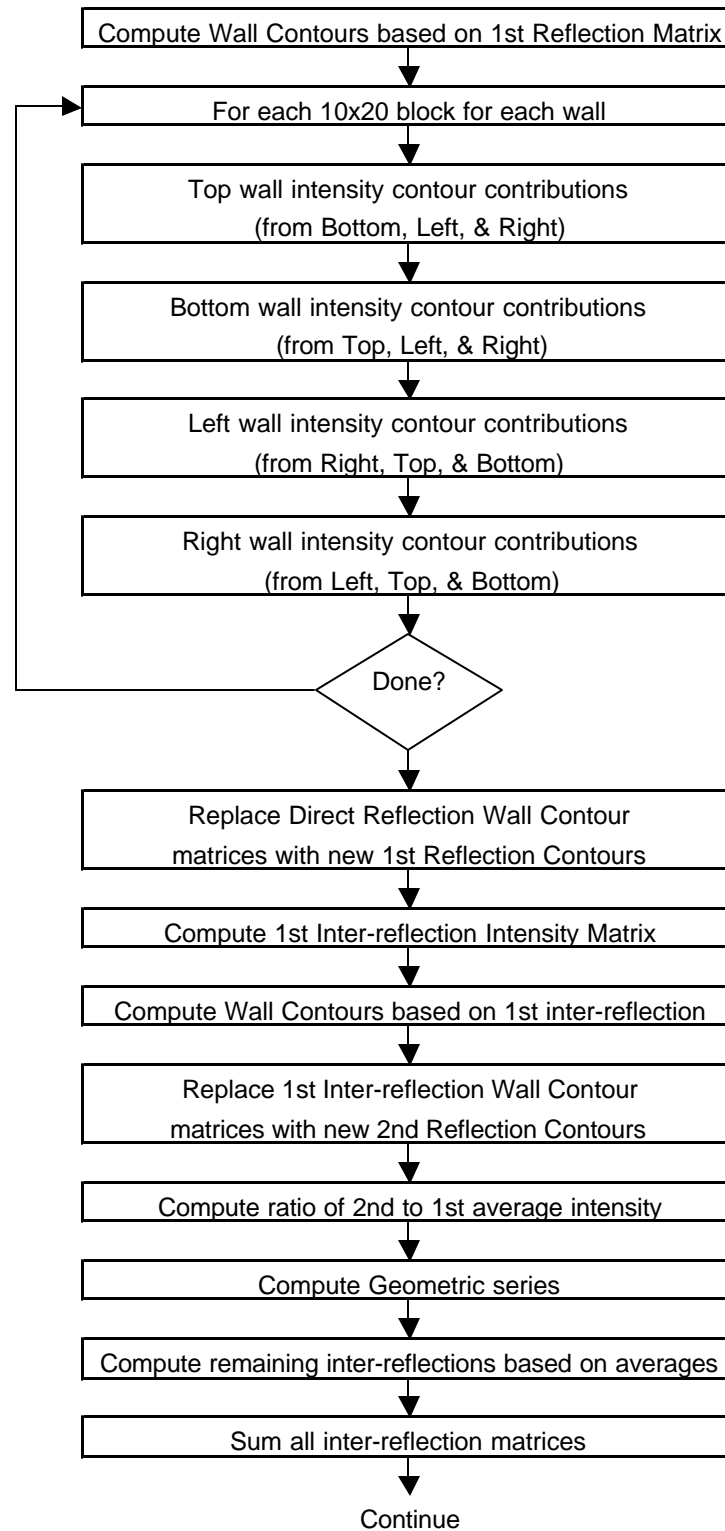


Figure 6.8: Flowchart for Inter-reflection Algorithm

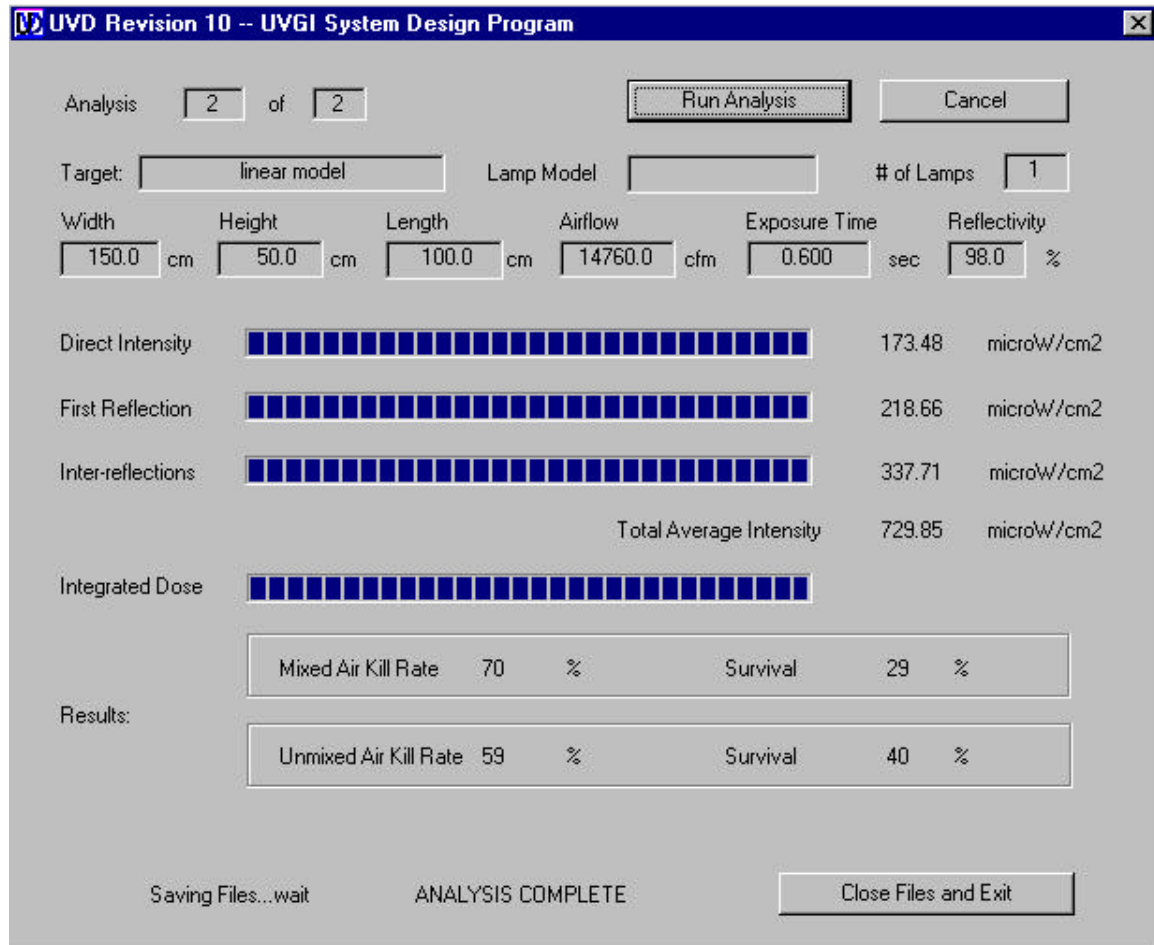


Figure 6.9: Program Window showing results of second of two analyses.

6.2 Program Input and Output

The program reads data input from a file called "params.txt" and outputs results to a file called "adata.txt." The input data is contained in a text file called "params.txt" which is shown in Appendix H, in which the input variables are identified and units given. The input consists of the twelve essential variables listed in a horizontal row. Multiple analyses can be run in one batch – the first number in the first row denotes the number of data sets that follow. The input is assumed to represent an orthogonally oriented lamp. The program is capable of evaluating non-orthogonal lamps, and multiple lamp arrays, but such were not used in the analyses performed here.

The output data is a text file called "adata.txt" which is described in Appendix I. The output variables and units are tabulated in Appendix I also. The output consists of a reiteration of the eight dimensionless parameters, the Kill Rate, the Integrated Kill Rate, the Average Intensity, the Average Direct Intensity, the Average First Reflection Intensity, and the Average Inter-reflection Intensity.

Chapter 7. Model Validation

7.1 Lamp Model Validation

The success of the view factor model in predicting lamp intensity fields is demonstrated in comparisons with photosensor data in Figure 7.1 and Figure 7.2. Figure 7.1 also illustrates two variations on the ISL – one in which it is based on the lamp surface intensity and one in which it is based on the lamp rating. Neither of these models provides an accurate description of the actual lamp intensity field over the entire range while the view factor model provides excellent agreement at all points.

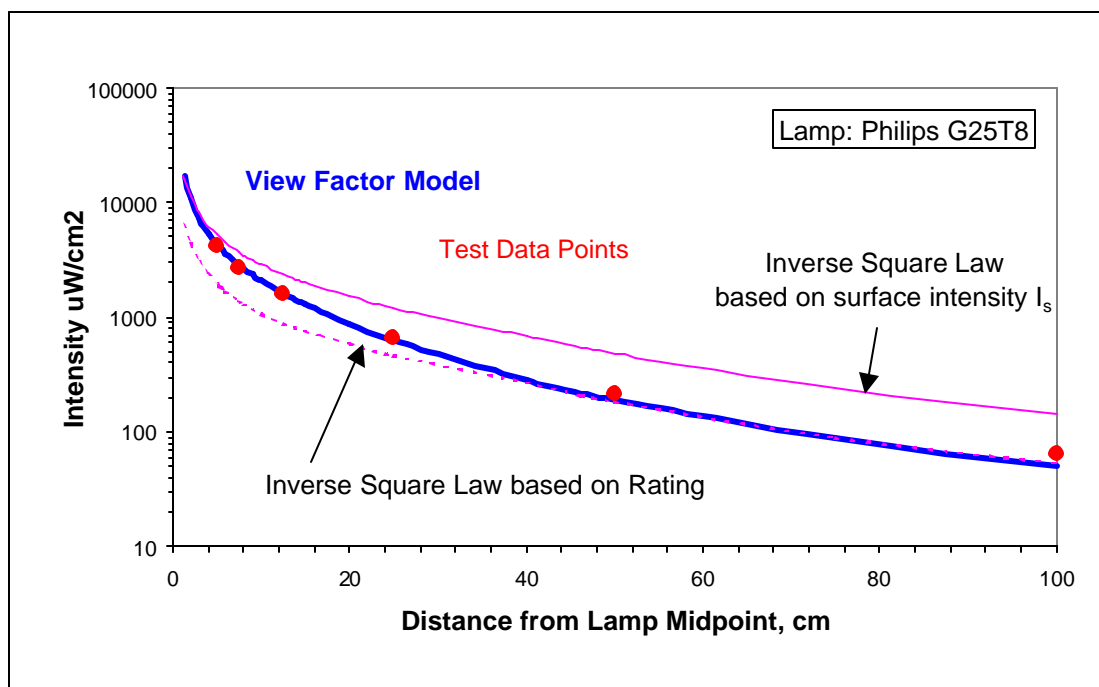


Figure 7.1: Comparison of View Factor model with ISL and photosensor readings for a Philips model G25T8 lamp. Based on lamp data from UVDI (1999).

Figure 7.2 shows a variation on the ISL in which it is used to model a lamp as a line source. In this case the ISL deviates both in the near field and the far field, while the view factor model again provides good agreement everywhere.

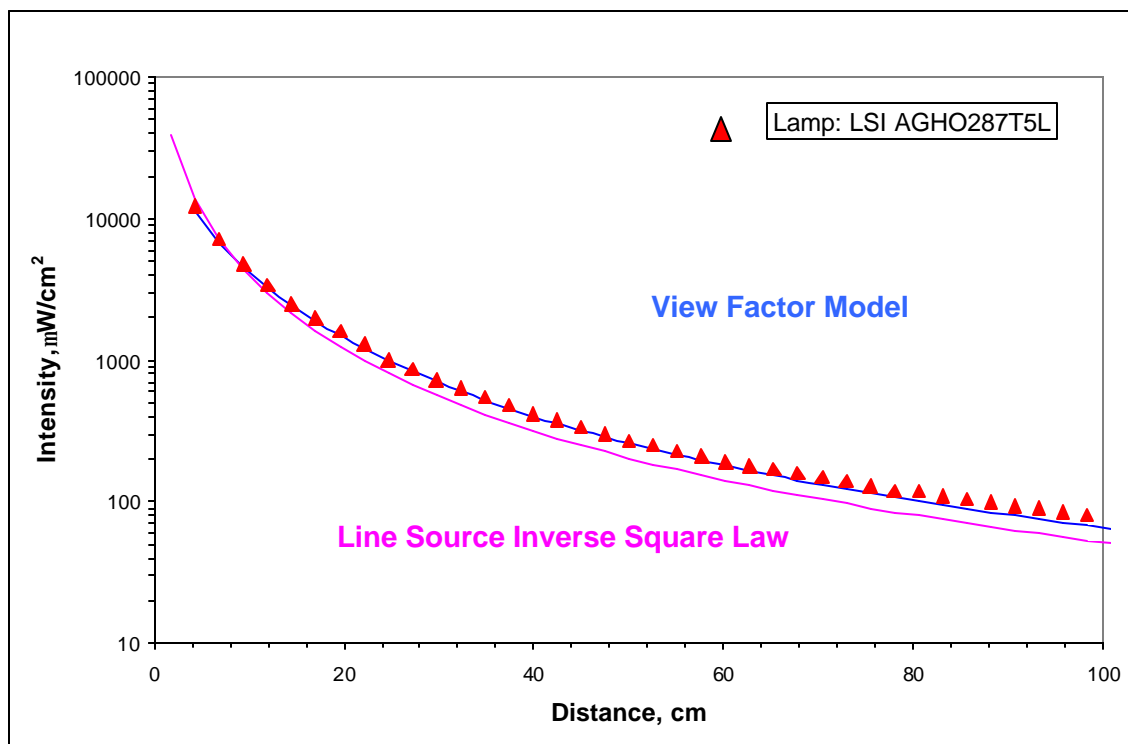


Figure 7.2: Comparison of View Factor Model with photosensor data and line source Inverse Square Law. Based on lamp data from UVDI (1999).

An example of the above model compared with lamp data and with the ISL is shown in Figure 7.3. Discrepancies that exist here between the view factor model and the data may be due to errors in the photosensor readings.

The reflected intensity field is not so easy to validate with photosensor readings because of the assumption that a spherical microbe will always face a reflecting surface. In the model a spherical microbe is exposed to reflected intensity from all four reflecting surfaces. Photosensors can only face one direction and as a result they will exclude the intensity contribution due to surfaces at right angles or behind the photosensor.

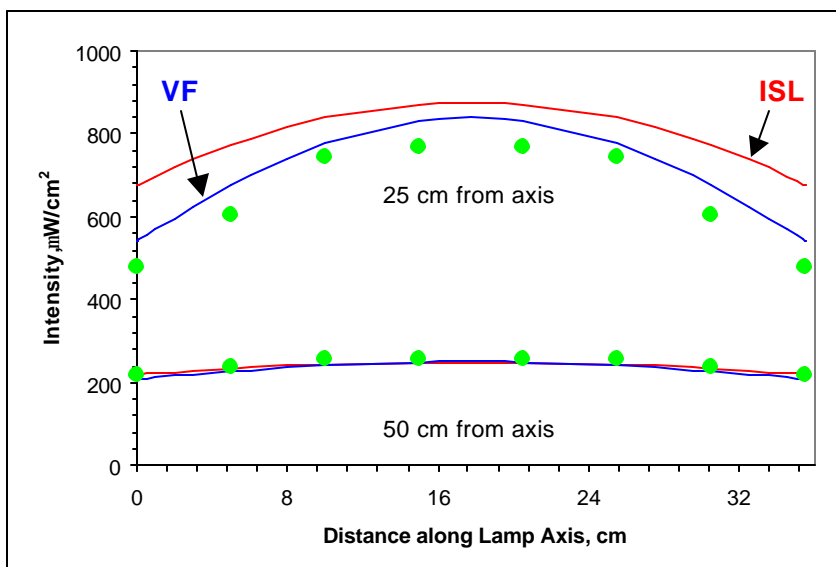


Figure 7.3: Comparison of View Factor (VF) model with data and the ISL along the length of a Philips model G25T8 lamp. Based on data from UVDI (1999).

One alternative is to use spherical actinometry (Rahn and Miller 1999) to obtain an integrated intensity contribution from all four surfaces, but this technology is in a developmental stage and has proven somewhat difficult to use. In lieu of performing any kind of validation of the reflected intensity model the entire model is simply validated by comparison with bioassay results from UVDI (2000).

7.2 Bioassays for *Serratia Marcescens*

Tests performed at two independent laboratories were used to confirm the predictive results of the UVD program (UVDI 2000). Twenty-six tests overall were performed using the target microbe *Serratia marcescens* in a variety of duct and lamp configurations. Table 7-1 summarizes the results of the tests and the predictions of the model. Results are also summarized graphically in Figure 7.4a and Figure 7.4b.

Results showed an error range of approximately +/-14% in 85% of cases. Average error was 14% for mixed air. Tests 15, 16, 24, & 25 showed huge deviations but some of these, and perhaps all, are dubious results. Without the four outlier tests the average error would have been +/-9%. The mixed air kill rate and the unmixed air predicted kill rate both tend to slightly overpredict kill rates on the average and so are conservative predictors.

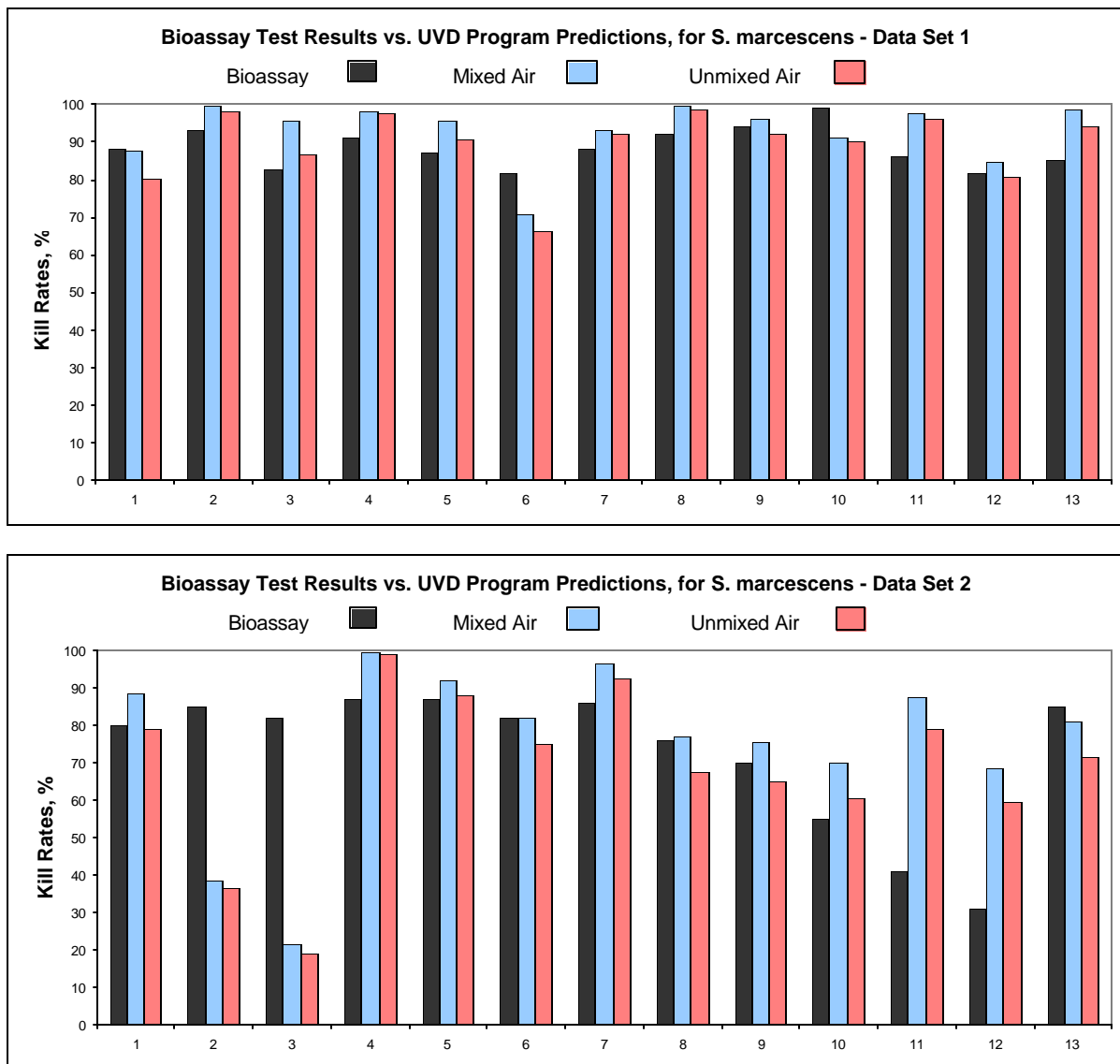


Figure 7.4a & 7.4b: Bioassay results for *Serratia marcescens* compared against model predictions for 26 different duct configurations.

Based on the above test results, computations determined the rate constant for *Serratia marcescens* to be approximately $0.002867 \text{ cm}^2/\mu\text{W-s}$. Previously, with an earlier version of the UVD program, twenty data sets, and less refined estimates of cooling effects, the rate constant was determined to be $0.002909 \text{ cm}^2/\mu\text{W-s}$ (Kowalski and Bahnfleth 2000b). The 1.4% difference between these rate constants has a negligible effect on model predictions, and the earlier published rate constant provides a better overall predictive error, therefore the original rate constant of $0.2909 \text{ cm}^2/\mu\text{W-s}$ is used in lieu of future data. Actually, the average rate constant for all microbes, $0.00275 \text{ cm}^2/\mu\text{W-s}$, is used throughout most of the analyses in this research but it is

so close to the measured value for *Serratia* that it is considered to be effectively identical. Data used for developing the *Serratia* rate constant is summarized in Appendix J.

7.3 Bioassays for *Bacillus subtilis*

Two tests were run using *Bacillus subtilis* (UVDI 2000). There is an insufficient number of tests to establish a conclusive airborne rate constant since tests were either plate-based (Rentschler and Nagy 1940, IES 1981) or consisted of mixed spores and vegetative bacteria in an airborne test (Sharp 1939). Data from the two bioassays on *Bacillus subtilis* from the bioassay tests was used to compute the rate constant of $0.000449 \text{ cm}^2/\mu\text{W-s}$. Although the data set is limited, the computed rate constant falls within the range of rate constants in the published studies, and closely matches the rate constant for the closely related *Bacillus anthracis* in air, $0.000462 \text{ cm}^2/\mu\text{W-s}$ (Sharp 1939). Figure 7.5 shows the results of the bioassays when the computed rate constant is used for predicting the kill rate.

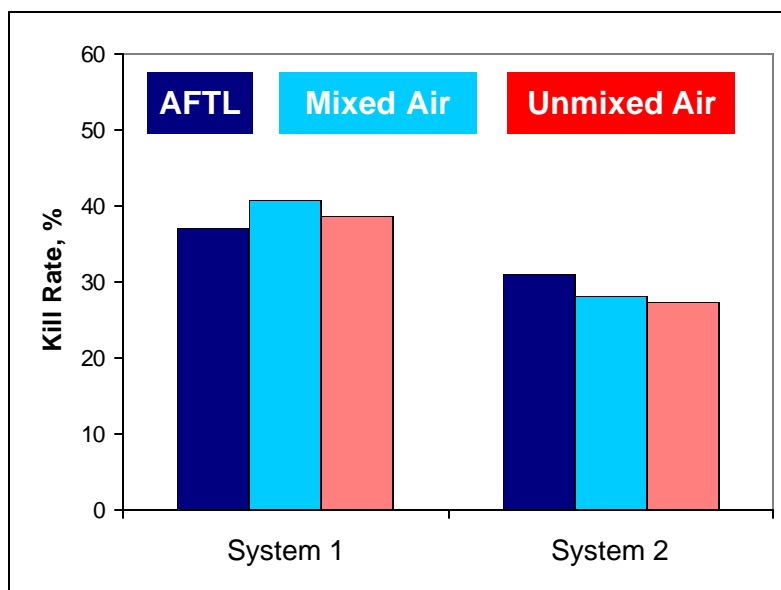


Figure 7.5: Bioassay results for *Bacillus Subtilis* compared against model predictions. Based on data from UVDI (2000).

7.4 Shoulder and Second Stage Model Verification

The UVD program evaluates the 3D intensity field and makes predictions based on single stage rate constants for a variety of microbes, but does not evaluate the effects of the shoulder or the second stage of the decay curve. Insufficient data exists to quantify the shoulder and second stage parameters for all microbes in the rate constant database (Appendix B). Although some data have been evaluated (Table 5.1 and Table 5.2), these results cannot be verified on the basis of the data in the published references.

A series of tests was conducted by an independent source on two species of mold, *Aspergillus niger* and *Rhizopus nigricans* (UVDI 2001). These tests were primarily designed to evaluate the effects of different levels of intensity and so provide data to interpret the shoulder constants necessary for making predictions at other intensities. In addition to studying the shoulder, some of the data provided indication of the second stage rate constants, which, as it turned out, play a significant role in the determination of both the shoulder constants and the overall kill rates.

The complete mathematical model for the decay curve of any microorganism exposed to UVGI (equation 5-15) is restated here in a simplified form. The simplified equation defining the complete survival curve is as follows:

$$S(t) = (1 - f)e^{-k_f It'} + fe^{-k_s It'} \quad (7-1)$$

$$t' = \begin{cases} \frac{t^2}{4t_c} & t \leq 2t_c \\ (t - t_c) & t \geq 2t_c \end{cases}$$

where I = Intensity, $\mu\text{W}/\text{cm}^2$

t = exposure time, sec

k_f = rate constant for fast decay population, $\text{cm}^2/\mu\text{W}\cdot\text{s}$

k_s = rate constant for slow decay population, $\text{cm}^2/\mu\text{W}\cdot\text{s}$

t_c = threshold, sec

f = resistant fraction of population

The shape of the complete curve is illustrated in Figure 7.6.

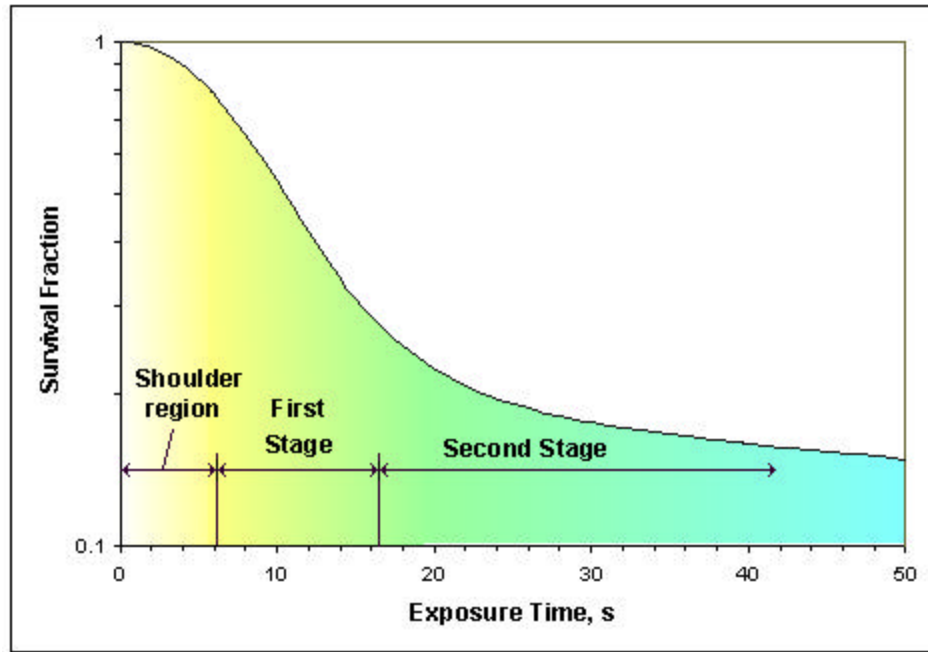


Figure 7.6: The Complete Survival Curve, including shoulder, first stage and second stage. This generic curve has an exaggerated shoulder to make the components distinct.

The threshold t_c , which defines the end of the shoulder and the beginning of the first stage of the survival curve, has been theorized to be predictable by the following relation:

$$t_c = Ae^{-BI} \quad (7-2)$$

where A = a constant defining the intercept at $I=0$

B = a constant defining the slope of the plotted line of $\ln(t_c)$ vs. I

Given any two sets of data at different intensities, equation (7-2) can be solved for the constant coefficients A and B . With A and B determined, the threshold t_c can then be determined for any intensity, and the complete survival curve will then be established.

Data presented in these sections demonstrate the ability of the new model to predict the complete survival curve. The previous model of the survival curve, based on a single stage rate constant, will be shown in the next section to be an inadequate model in comparison with the complete model for applications where the exposure time is either very short or very long.

The implications for the design of UVGI systems are twofold. First, the presence of a shoulder in the survival curve will limit the predicted kill rate in comparison with the prediction of a single stage rate constant for air disinfection systems where the exposure time tends to be short. This is likely to be the case for all spores since their natural resistance to UVGI will tend to result

in a shoulder. This will be as true for bacterial spores like *Bacillus anthracis*, as it is for fungal spores.

In regard to viruses, which tend to be vulnerable to UVGI, the shoulder is likely to be insignificant and the predictions of single stage models should approach reality. Bacteria, however, are a mixture of both resistant and vulnerable species, and therefore it is difficult to say in advance whether the presence of any shoulder would affect the predicted kill rates.

The second major implication of the complete survival curve is that the presence of a second stage will cause non-conservative errors in predictions when the exposure time is extended. This is likely to be the situation when UVGI is used to control microbial growth on surfaces or when it is used to disinfect equipment or even foodstuffs. Under extended exposure the second stage will predominate and result in higher predicted survival rates than would be obtained using the single stage survival curves alone. Inadequate exposure in such situations can potentially lead to selection of resistant microbes that could subsequently multiply in the right environmental conditions. Of course, under continuous 24-hour exposure as occurs with current microbial growth control systems it is unlikely that there would be any survivors at all.

The following sections describe in detail the test results and analysis that lead to establishing shoulder constants and second stage rate constants for these two microbes. The materials and methods are described in an as-yet unpublished manuscript (Kowalski et al 2001).

7.4.1 Bioassays for *Aspergillus niger*

Tests were run at six different intensities for *Aspergillus niger* and the results are summarized in Table 1. The number of data points is the number of petri dishes that were exposed, including controls. The first stage is shown along with the intercept of the y-axis. This intercept was then used to calculate the threshold t_c . The second stage was determined using a sum-of-squares error to find the best fit for the two-stage curve. The resistant fraction is the intercept of the second stage with the y-axis. Analysis of the sum total data yielded the shoulder coefficients A and B, which were used to compute the derived threshold for comparison.

Table 7.1: Test Results & Derived Constants for *Aspergillus niger*

Test Intensity mW/cm^2	Number of Data points	Test 1st Stage k $\text{cm}^2/\text{mW-s}$	Test Intercept Si	Test Threshold tc sec	Derived Threshold tc sec
321	30	0.0001745	1.949	11.915	8.139
372	18	0.0000857	1.291	8.000	7.612
372	18	0.0000446	1.219	11.915	7.612
372	27	0.0000849	1.296	8.193	7.612
434	30	0.0000488	1.120	5.352	7.016
666	33	0.0000562	1.178	4.378	5.173
898	30	0.0000974	1.164	1.740	3.813
930	18	0.0000396	1.136	3.453	3.656
930	18	0.0000267	1.104	4.000	3.656
930	30	0.0000419	1.128	3.089	3.656
1780	18	0.0000962	1.409	2.001	1.197
1780	18	0.0000557	1.220	2.000	1.197
1780	27	0.0000360	1.042	0.644	1.197
Average 1st Stage Rate Constant		0.0000731			$\text{cm}^2/\mu\text{W-s}$
Average 2nd Stage Rate Constant		0.00000427			$\text{cm}^2/\mu\text{W-s}$
Resistant Fraction f		0.27			
Shoulder Coefficient A		12.41			sec
Shoulder Coefficient B		0.001314			

The first stage rate constant was determined by isolating those points that clearly defined the first stage and that were not confused with the shoulder or the second stage. In Figure 7.7, for example, the portion of the curve between 2 seconds and 12 seconds approximately defines the first stage. In spite of the apparent subjectivity of the choice of defining data points, there is actually little room here for arbitrariness. The point at 2 seconds is the last point with a survival of 1 and no points below this could be chosen. The other bounding point at 15 seconds could conceivably be ignored without having much effect, but the next point, at 309 seconds, is definitely not to be included. The true test of which points belong to the first stage can be accomplished in a more analytical fashion by performing a sum-of-squares analysis, that is, by minimizing the sum-of-squares error.

The first stage plate-based rate constant for *A. niger* is $k = 0.0000753 \text{ cm}^2/\mu\text{W-s}$. This is a standardized rate constant, that is, it is considered to be at an intensity of $1 \mu\text{W/cm}^2$. This value does not exactly match either of the rate constants from Table 1, but is within an order of magnitude of the 95% dose. The rate constant, being embedded within the exponential decay equation, can vary over a range this large without necessarily producing major changes in the kill rates. That is, the decay rate is not extremely sensitive to the rate constant, especially at high kill rates. The second stage rate constant for *A. niger* is $k = 0.0000044 \text{ cm}^2/\mu\text{W-s}$.

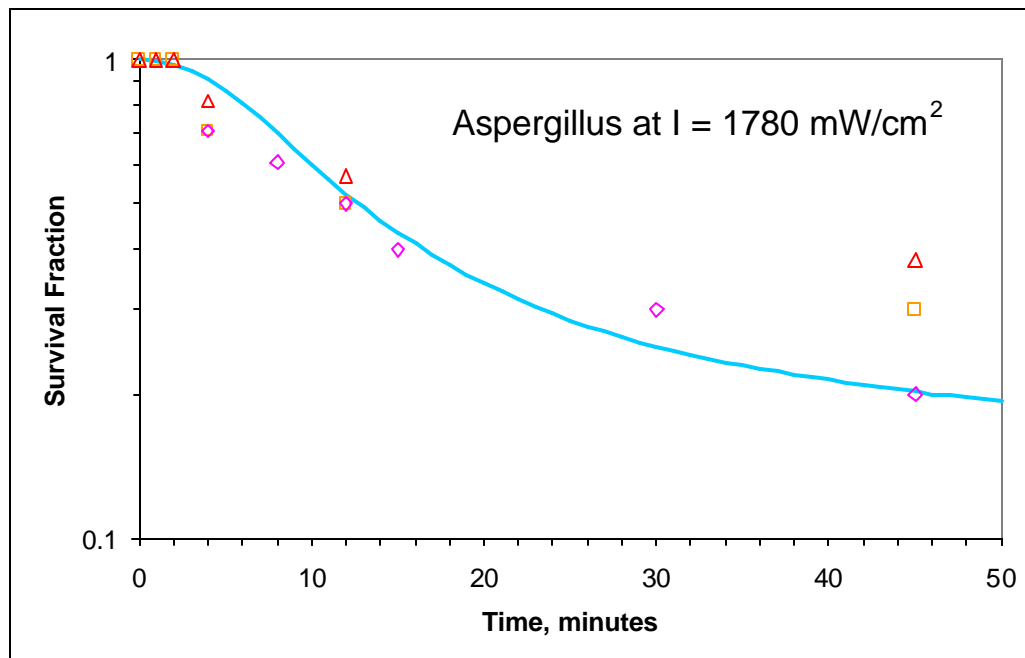


Figure 7.7: Results of Three Tests for *Aspergillus niger* at indicated intensity. Line represents the complete decay model at the specified intensity.

The difference between use of the complete survival curve for *A. niger* and the single stage survival curve is illustrated in Figure 7.8. The single stage rate constant for *A. niger* is given in various sources as $k = 0.000017 \text{ cm}^2/\mu\text{W-s}$ (Philips 1985, etc). In this diagram the survival curve based on the single stage rate constant is plotted along with the complete curve based on the present data. Obviously there will be only two points past the origin at which the curves agree, while large discrepancies may occur elsewhere. The single stage rate constant can be conservative for moderate exposure times but can become non-conservative for extended exposures.

Figure 7.9 shows a set of typical curves for the *A. niger* at different intensities. The intensity is seen to decrease the length of the shoulder and at high intensities the shoulder can become effectively insignificant. At low intensities, however, the shoulder can cause overestimation of the kill rate if only a single stage model is used.

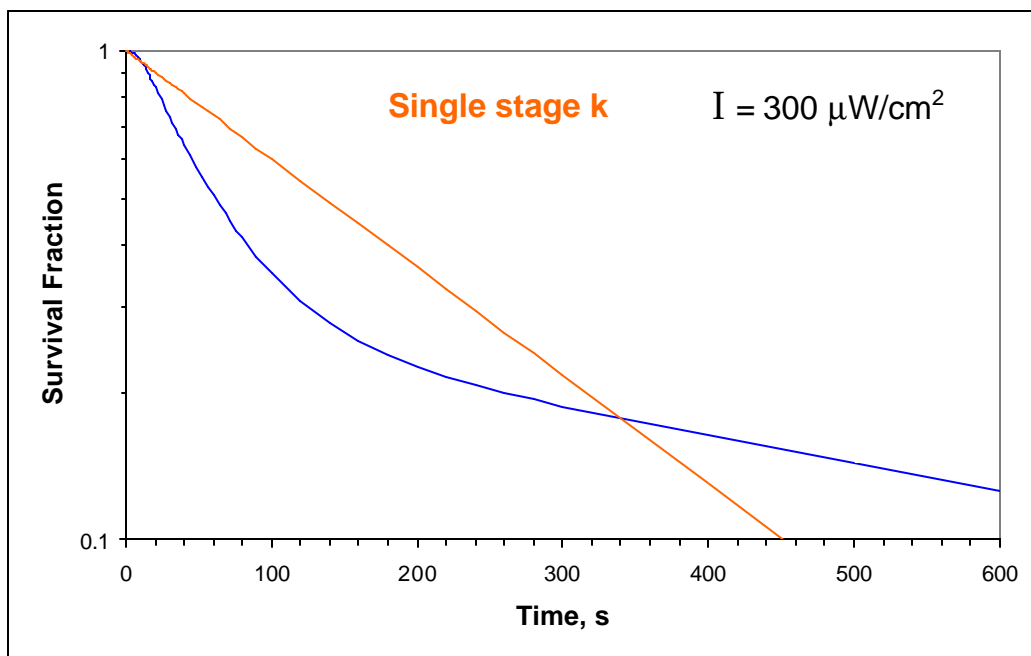


Figure 7.8: Comparison of the Complete Survival Curve of *Aspergillus niger* with a curve based on the published single stage rate constant.

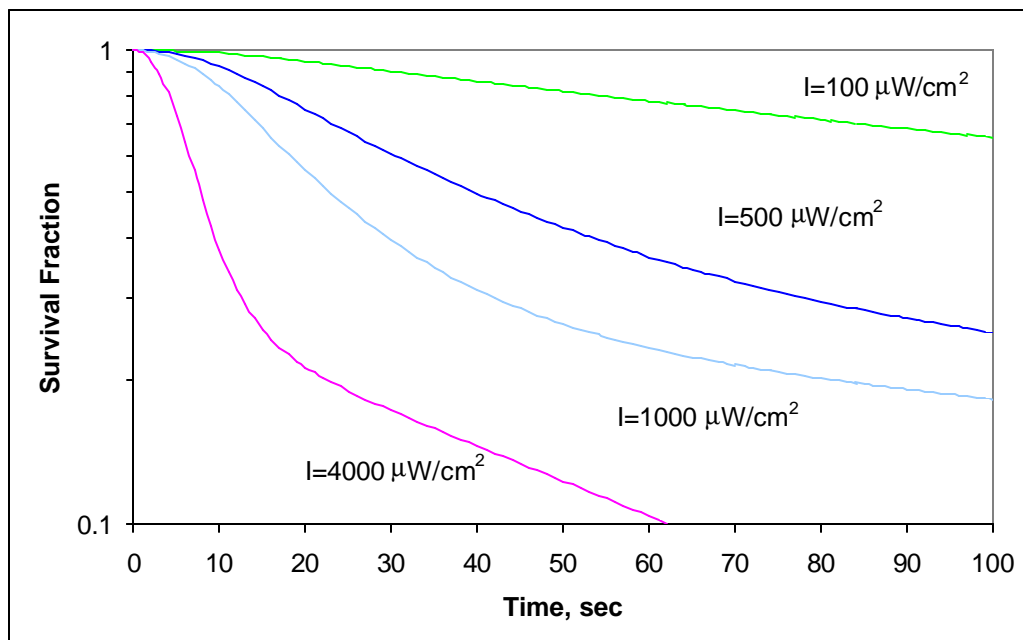


Figure 7.9: Predicted Survival Curves of *Aspergillus niger* at various intensities

7.4.2 Bioassays for *Rhizopus nigricans*

The test results for *Rhizopus nigricans* are summarized in Table 7.2. The results and constants were determined as described above. Problems occurred with plate overgrowth prevented countability in some cases. Low counts on plates also caused some unacceptable variability in results and three tests had to be discarded.

A peculiar feature observed during this test was that typically no growth would be observed for the first 48 hours after exposure, after which some colonies would experience a spurt of growth and overgrow surrounding colonies. It was found that the use of a slower growth medium, combined with microscopy, aided in the counting of the colonies.

Table 7.2: Test Results & Derived Constants for *Rhizopus nigricans*

Test Intensity $\mu\text{W}/\text{cm}^2$	Number of Data points	Test 1st Stage k $\text{cm}^2/\mu\text{W}\cdot\text{s}$	Test Intercept Si	Test Threshold tc sec	Derived Threshold tc sec
206	18	0.0000456	1.028	2.948	4.860
372	12	0.0005078	2.041	3.777	4.233
372	12	0.0004306	1.852	3.845	4.233
642	18	0.0001643	1.782	5.475	3.381
930	12	0.0003033	2.658	3.466	2.661
930	12	0.0002687	2.609	3.837	2.661
1780	18	0.0002884	1.604	0.920	1.312
1780	18	0.0002712	1.833	1.255	1.312
Average 1st Stage Rate Constant			0.0002850		$\text{cm}^2/\mu\text{W}\cdot\text{s}$
Average 2nd Stage Rate Constant			0.00001098		$\text{cm}^2/\mu\text{W}\cdot\text{s}$
Resistant Fraction f			0.08		
Shoulder Coefficient A			5.7686		sec
Shoulder Coefficient B			0.000832		

Figure 7.10 shows the results of two tests at the same intensity. The shoulder is fairly obvious here, as it was in Figure 7.1, and the second stage is more clearly manifest than it was with *Aspergillus*. In this example, the data points from 1 second to 4 seconds defined the first stage. Again, there is little room for variation in this choice of bounding points, since the next data points, at 12 seconds, are clearly manifesting primarily second stage behavior.

The first stage plate-based rate constant for *R. nigricans* is $k = 0.000285 \text{ cm}^2/\mu\text{W}\cdot\text{s}$. This again is a standardized rate constant, and is considered to be at an intensity of $1 \mu\text{W}/\text{cm}^2$. The second stage rate constant for *R. nigricans* is $k = 0.000011 \text{ cm}^2/\mu\text{W}\cdot\text{s}$.

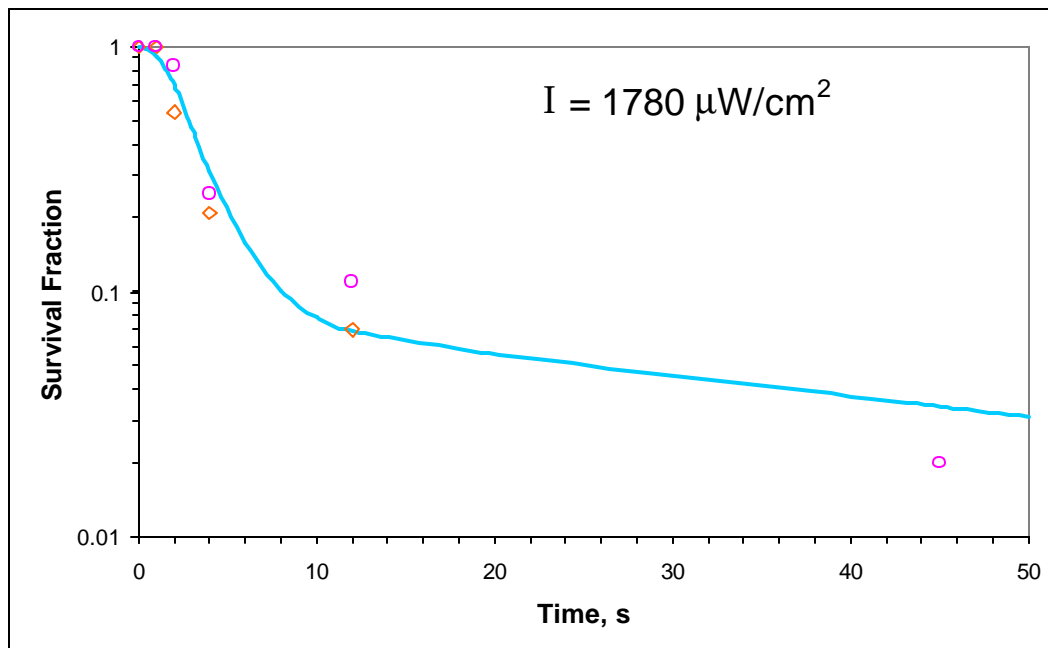


Figure 7.10: Results for Two Tests of *Rhizopus nigricans* at indicated intensity

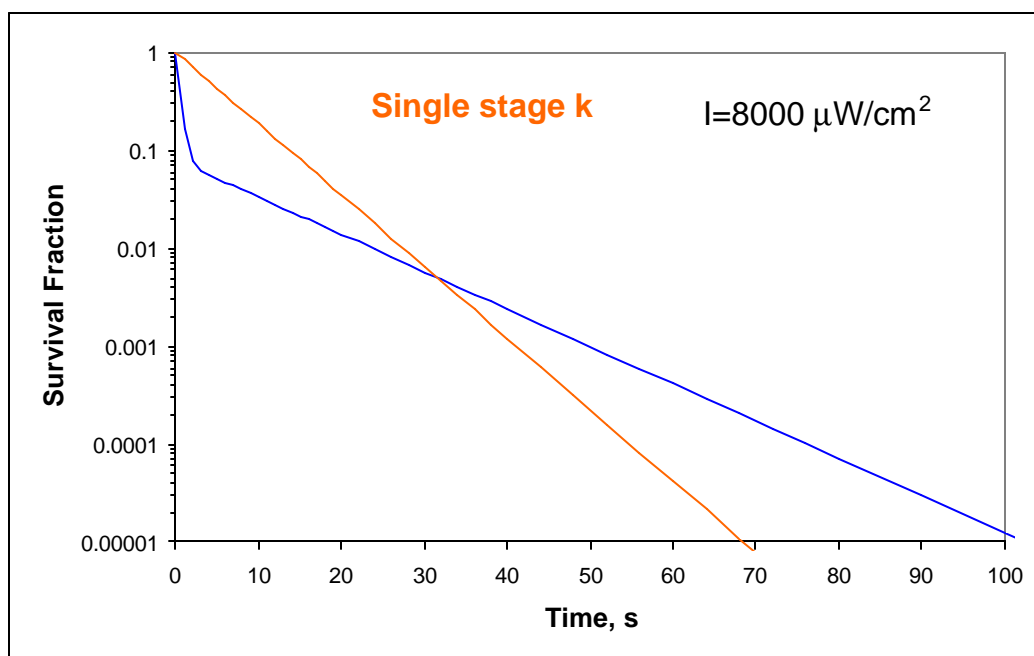


Figure 7.11: Comparison of the Complete Survival Curve of *R. nigricans* with a curve based on the published single stage rate constant

Figure 7.11 shows a similar comparison for *R. nigricans* in which the discrepancies between the curves are even greater. Clearly *R. nigricans* is more susceptible to UVGI than

Aspergillus niger, and this may be observed in the first and second stage rate constants in Table 7.1 and Table 7.2. Figure 7.12 shows the predicted response for *R. nigricans* at various intensities.

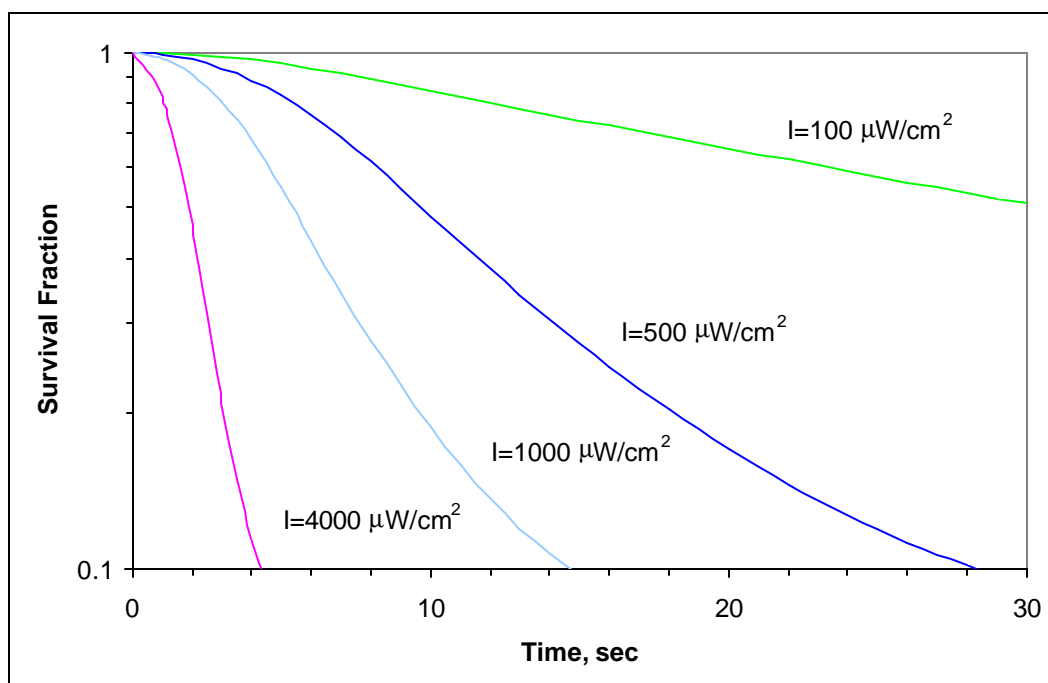


Figure 7.12: Predicted Survival Curves of *R. nigricans* at various intensities

For microbial growth control in air handling units or on cooling coils, this may not be a problem since exposure is typically continuous, that is, 24 hours a day. In the food industry, however, where surface exposure for the control of fungal or bacterial pathogens is of interest, and where too much exposure may be harmful, the complete survival curve will allow more accurate prediction of the required exposure time. For example, a typical definition of sterilization is a 6-log (base 10) reduction, or a 1 in 1,000,000 survival. As shown in Figure 7.13 for *R. nigricans*, at 4000 $\mu\text{W}/\text{cm}^2$ this would be predicted to occur at approximately $t = 55$ seconds with the published single stage model, while the complete survival curve shows that it would actually take approximately 87 seconds. This is merely an example of what the difference might be – the actual second stage rate constant determined for *Rhizopus* may not be statistically significant since there were an insufficient number of survivors to establish certainty.

Due to uncertainty and limited data, the second stage rate constants for both *Aspergillus niger* and *Rhizopus nigricans* need further study. Most of the data assembled here supports the computed shoulder constants, although they too could use further study. In spite of limitations in

the data, the complete survival curves for both these microbes are, in all likelihood, more accurate predictors of microbial response than the previous single stage models, and will, at the very least, provide conservative estimates for both low doses and high doses.

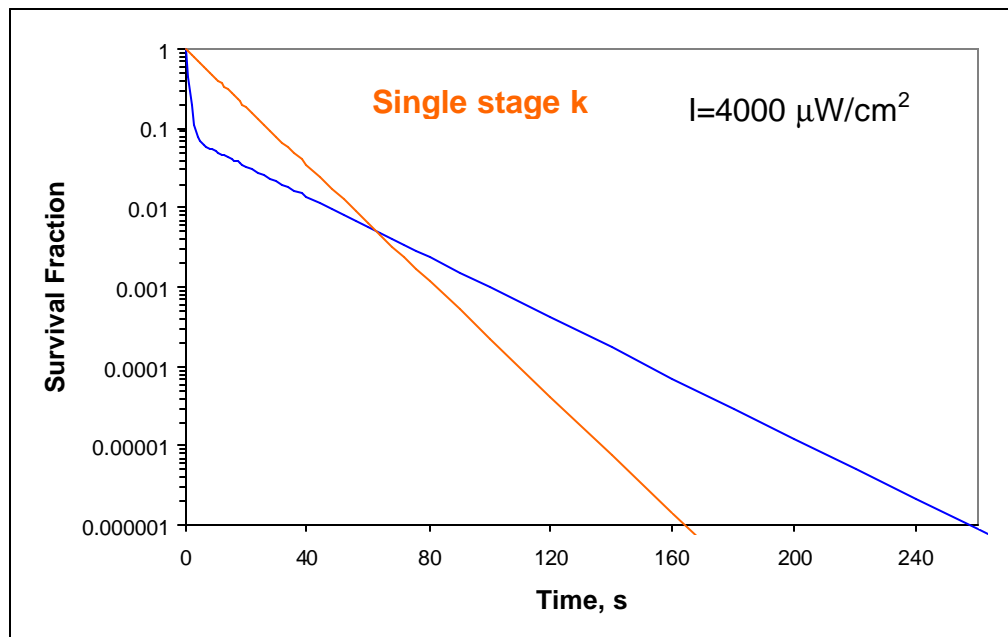


Figure 7.13: Time to Obtain Sterilization of *R. nigricans* at $I=4000 \mu\text{W}/\text{cm}^2$. Comparison of single stage model with the complete survival curve.

Data for establishing the complete survival curves for airborne and other pathogens has been scarce for viruses and bacteria, and previously non-existent for fungal spores. With the present demonstration of this mathematical model, researchers are now able to use these tools to re-evaluate the complete survival curves for microbes that have previously been studied and those airborne pathogens that have not yet been studied.

Chapter 8. Dimensional Analysis of UVGI Systems

Dimensional analysis involves a definition of all relevant dimensional variables for any system, identification of the minimum number of dimensionless parameters that result from a formal application of the Buckingham Pi theorem (Kundu 1990). The set of all variables that are relevant to UVGI design can be written in a single equation as follows:

$$S = f(W, H, L, l, r, P, t, x, y, z, Re, k, T, RH, r, Af, Q) = 0 \quad (8-1)$$

The above variables are identified with their units in Table 8-1. The exposure time t is redundant because it is implicitly defined in the variables Q , W , H , and L .

Table 8-1: Physical parameters relevant to UVGI systems

W	Duct Width	L
H	Duct Height	L
L	Duct Length	L
l	Lamp arclength (assumed same as physical length)	L
r	Lamp radius	L
P	Lamp UV Power	ML^2/T^3
t	Exposure time	T
x	Location of lamp end (base at $x = 0$)	L
y	Lamp Y position or distance above bottom surface	L
z	Lamp Z position or distance from duct entrance	L
Re	Degree of air mixing or turbulence, Reynolds number	
k	UVGI rate constant	T^2/M
T	Air Temperature	Temp.
RH	Relative Humidity	
ρ	Surface reflectivity	
Af	Surface Area Fraction	
Q	Airflow rate	M^3/T
S	Survival fraction	

Some of the factors in Table 8-1 can be ignored. The air temperature is a negligible factor, based on previous studies (see Chapter 3), and is not part of the current model. The Relative Humidity has an unknown effect, based on the results of several studies (see Chapter 3) and is not included as part of the model.

The degree of air mixing is dealt with by two separate parts of the computer analyses, completely mixed and completely unmixed conditions, which represent limits or bounds on performance, and therefore the Reynolds Number does not form an analytical part of the current model.

The surface fraction is a parameter that indicates how much light is contained inside the geometry (or not lost through the openings). Although the necessity for this parameter may not be

obvious, there is no other reasonable means of accounting for the effect of the view factors that form such an important part of the model. It was initially left out of the model but then had to be added back in when it became obvious that an uncontrolled parameter was producing distortions of the results. Although it has limited use on its own, when the area ratio is controlled, it allows for truer interpretation of the effects of the other parameters. The area fraction is defined as:

$$Af = \frac{SurfaceArea}{TotalArea} = \frac{(W + H)L}{(W + H)L + WH} \quad (8-2)$$

The minimum set of parameters are shown in Table 8.2

Table 8-2: Minimum Set of Parameters for UVGI Model

Variable	Description	Units
W	Duct Width	L
H	Duct Height	L
L	Duct Length	L
<i>I</i>	Lamp arclength	L
r	Lamp radius	L
P	Lamp UV Power	ML ² /T ³
t	Exposure time	T
x	Location of lamp end (base at x = 0)	L
y	Lamp Y position or distance above bottom surface	L
z	Lamp Z position or distance from duct entrance	L
k	UVGI rate constant	T ² /M
ρ	Surface reflectivity	
Af	Surface Area Fraction	
S	Survival fraction	

Therefore, we have 13 parameters but $n = 11$ parameters with dimensions. Selecting $r = 3$ primary dimensions MLT, the resulting table of units is

Table 8-3: Array of Units for UVGI System Minimum Parameters

Unit	W	H	L	<i>I</i>	r	P	t	x	y	z	k
M	0	0	0	0	0	1	0	0	0	0	-1
L	1	1	1	1	1	2	0	1	1	1	0
T	0	0	0	0	0	-3	1	0	0	0	2

The number of repeating parameters $m = r = 3$. We select the parameters $k =$ rate constant, $P =$ Power, and $L =$ Length as our three repeating parameters. These parameters

embody the three dimensions M, L, and T with exponents indicated as in the form $M^a L^b T^c$.

We have $n - m = 11 - 3 = 8$ dimensionless groups as summarized in Table 8-4.

Table 8-4: Dimensionless Groups

Π_1	k	P	L	W
Π_2	k	P	L	H
Π_3	k	P	L	l
Π_4	k	P	L	r
Π_5	k	P	L	t
Π_6	k	P	L	x
Π_7	k	P	L	y
Π_8	k	P	L	z

For the first group kPLW:
$$\left(\frac{T^2}{M}\right)^a \left(\frac{ML^2}{T^3}\right)^b (L)^c (L) = M^0 L^0 T^0 \quad (8-3)$$

Equating the exponents yields the following relations for each dimension:

$$M : -a + b = 0$$

$$L : 2b + c + 1 = 0$$

$$T : 2a - 3b = 0$$

therefore $a = 0 \quad b = 0 \quad c = -1$

The first group is, therefore:
$$\Pi_1 = \frac{W}{L} \quad (8-4)$$

For the second group kPLH, by similarity:
$$\Pi_2 = \frac{H}{L} \quad (8-5)$$

For the third group kPL l :
$$\Pi_3 = \frac{l}{L} \quad (8-6)$$

For the fourth group kPL r :
$$\Pi_4 = \frac{r}{L} \quad (8-7)$$

For the fifth group kPL t :
$$\left(\frac{T^2}{M}\right)^a \left(\frac{ML^2}{T^3}\right)^b (L)^c (T) = M^0 L^0 T^0 \quad (8-8)$$

$$M: -a + b = 0$$

$$L: 2b + c = 0$$

$$T: 2a - 3b + 1 = 0$$

and $a = 1 \quad b = 1 \quad c = -2$

$$\Pi_5 = \frac{kPt}{L^2} \quad (8-9)$$

For the sixth group kPLx: $\Pi_6 = \frac{x}{L} \quad (8-10)$

For the seventh group kPLy: $\Pi_7 = \frac{y}{L} \quad (8-11)$

For the eighth group kPLz: $\Pi_8 = \frac{z}{L} \quad (8-12)$

Therefore we have the following set of 10 dimensionless parameters as follows:

$$S = f\left(\frac{W}{L}, \frac{H}{L}, \frac{l}{L}, \frac{r}{L}, \frac{kPt}{L^2}, \frac{x}{L}, \frac{y}{L}, \frac{z}{L}, \mathbf{r}, Af\right) \quad (8-13)$$

Some new parameters that may be useful can be formed by combining the previous set of parameters, and this will provide more useful parameters and also reduce the total number of dimensionless parameters. The aspect ratio can be formed from equation (8-4) and (8-5), or

$$\Pi_a = \frac{\Pi_1}{\Pi_2} = \frac{W}{L} \frac{L}{H} = \frac{W}{H} \quad (8-14)$$

The lamp aspect ratio can be formed from equation (8-6) and (8-7), or

$$\Pi_b = \frac{\Pi_4}{\Pi_3} = \frac{r}{L} \frac{L}{l} = \frac{r}{l} \quad (8-15)$$

The X ratio can be formed from equation (8-4) and (8-10), or

$$\Pi_c = \frac{\Pi_6}{\Pi_1} = \frac{x}{L} \frac{L}{W} = \frac{x}{W} \quad (8-16)$$

The Y ratio can be formed from equation (8-5) and (8-11), or

$$\Pi_d = \frac{\Pi_7}{\Pi_2} = \frac{y}{L} \frac{L}{H} = \frac{y}{H} \quad (8-17)$$

The fifth group can be modified by multiplying by equation (8-4) and (8-5):

$$\Pi_5 = \frac{kPt}{L^2} \Pi_1 \Pi_2 = \frac{kPt}{L^2} \left(\frac{L}{W}\right) \left(\frac{L}{H}\right)$$

and $\Pi_5 = \frac{kPt}{WH} \quad (8-18)$

The fifth group can be made into a more useful form, one that incorporates both the airflow Q and the length L, by defining the exposure time in terms of the volume and flowrate, and

multiplying by equation (8-5) and (8-6):

$$\Pi_5 = \frac{kPt}{L^2} \Pi_1 \Pi_2 = \frac{kP}{L^2} \left(\frac{WHL}{Q} \right) \left(\frac{L}{W} \right) \left(\frac{L}{H} \right) = \frac{kPL}{Q}$$

and $\Pi_5 = \frac{kPL}{Q}$ (8-19)

In this dimensionless parameter the term P/WH has the units of intensity and can be viewed as a version of kIt . We refer to this parameter as the specific dose.

Finally, we can simplify later analysis and interpretation by using the logarithm of the kill rate K in place of the survival S . Since the survival, or the kill rate, is known in advance to be essentially an exponential function (i.e. the decay curve) of several of the variables, using the natural log of the kill rate will facilitate the analysis later. The form of the relationship between the natural log of K and the final set of eight dimensionless parameters becomes:

$$\ln K = f \left(\frac{W}{H}, \frac{r}{l}, \frac{kPL}{Q}, \frac{x}{W}, \frac{y}{H}, \frac{z}{L}, r, Af \right) \quad (8-19)$$

The range of values for the above dimensionless parameters are shown in Table 8-5, along with the values of the variable that the maximums and minimums to which the parameters correspond. The range for the lamp aspect ratio was established by reviewing actual lamp dimensions.

Figure 8.1 illustrates the three geometric ratios in relation to the side view and the face view of the duct. This depiction will be useful in interpreting the results of the performance evaluations in Chapter 10. The coordinate system used throughout this research is $z = 0$ at the front face of the duct, $x = 0$ at the left side of the duct, and $y = 0$ at the bottom side of the duct. The left end of the lamp is considered to be at $x = 0$, therefore x is equivalent to the lamp arclength. This arrangement, in which the lamp is orthogonally oriented and perpendicular to the direction of airflow, is known as a crossflow arrangement.

Table 8-5: Ranges for Dimensionless Parameters

Parameter		Description	Minimum	Maximum
A	$\frac{W}{H}$	Aspect Ratio	1	5
B	$\frac{r}{l}$	Lamp Aspect Ratio	0.0046	0.04
C	$\frac{kPL}{Q}$	Specific Dose	0.0136	2.11
D	$\frac{x}{W}$	X Ratio	0.0633	1
E	$\frac{y}{H}$	Y Ratio	0.0079	0.5
F	$\frac{z}{L}$	Z Ratio	0.1042	0.91
G	ρ	Reflectivity	0.37	0.93
J	$\frac{L(W+H)}{L(W+H)+WH}$	Area Fraction	0.1	0.9

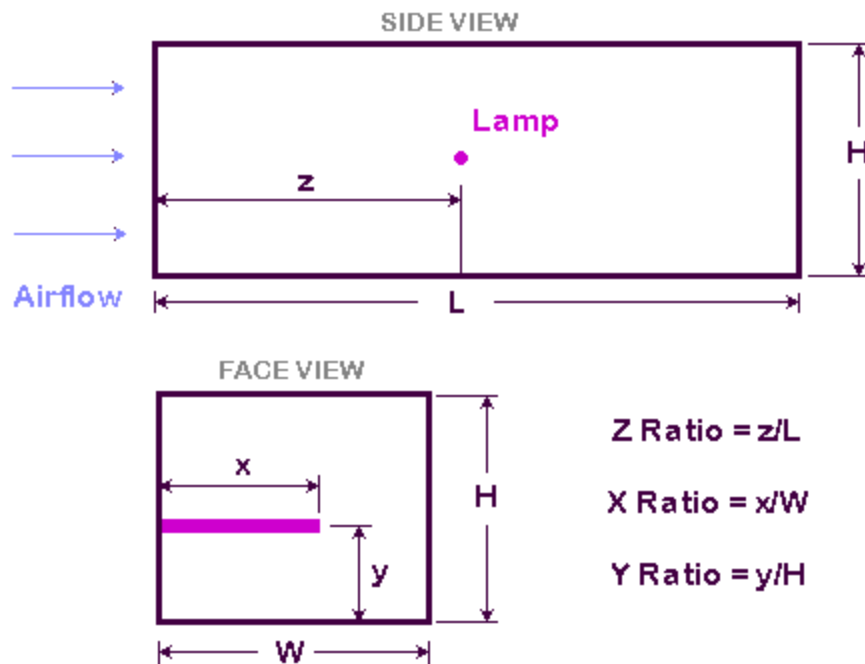


Figure 8.1: The Three Geometric Ratios, shown in relation to the position of a lamp in a duct of Length L, Width W, and Height H.

Chapter 9. Factorial Analysis

The kill rate of any microbial population subject to irradiation in a UVGI system is dependent on the dimensionless parameters that were developed in Chapter 8. The relationship between these eight parameters, from equation (8-19) is:

$$\ln K = f\left(\frac{W}{H}, \frac{r}{l}, \frac{kPt}{WH}, \frac{x}{W}, \frac{y}{H}, \frac{z}{L}, r, Af\right) \quad (9-1)$$

In equation (9-1) the Kill Rate K is used in place of the Survival S. The Kill Rate is simply the complement of the Survival, or $K = 1 - S$. This change makes for convenience of perspective – we seek to maximize K rather than minimize S. Equation (9-1) is considered to apply to both the mixed air kill rate and the integrated (unmixed) kill rate, which are both analyzed here but are analyzed separately.

The relative importance of these parameters in determining overall Kill Rate can be determined by performing a 2^k factorial analysis (Montgomery 2001). Once the critical parameters are identified, a more detailed study using Response Surface Methodology can be used to establish the exact relationships between the parameters.

Such statistical procedures are normally used to analyze experimental data. In this case the computer model serves as the experiment since it is based on simulation of physical processes. The only difference between computer modeling and experiment is that we need run only one replicate since there will be no variability in results for the same data sets.

The statistical analysis is performed in three stages. First a 2^k Factorial analysis is performed to identify the main effects based on a first order model. Next, a Response Surface Methodology (RSM) analysis is performed on a Central Composite Design using a 2^{nd} order model.

9.1 The 2^k Factorial Screening Analysis

The 2^k factorial analysis involves establishing a high and a low value of each parameter and analyzing all possible permutations. The minimums and maximums for the dimensionless parameters have been established previously in Table 8-5. Since there are $k = 8$ parameters (Kill Rate K being output by the program) with 2 possible values each we have a total number of permutations of:

$$2^k = 2^8 = 256 \quad (9-2)$$

The 256 permutations are summarized in Appendix K. The program only takes as its input the variables W, H, L, P, k, Q, r, l, p, x, y, and z and so the minimum and maximum dimensionless parameters must be converted to representative dimensional variables. The computation of the variables from the dimensionless parameters was described in the last

chapter. The minimum and maximum values for the eleven input variables shown in Table 9-1 have been selected based on reasonable size limits or were established based on data for typical lamps, materials and microbes.

Some variables were held constant to provide for practical interpretation and comparison. The rate constant used is an average that closely approximates that of *Serratia marcescens*. This is no coincidence since *Serratia* was originally selected for being representative of the average bacterial rate constant for airborne pathogens.

The power is held constant at a value that will provide kill rates in a range that is expected to be relatively log-linear, or about 1%-99%. The power and airflow are held constant to allow optimization of other parameters and to provide a fair basis, an equal energy consumption basis, for comparing all systems. Obviously, if the power was allowed to increase, a continuous increase in kill rate would result, until it reached a plateau, and no optimization would be possible. The power term is therefore varied by adjusting the component variable L, but of course this is essentially the same as varying k, P, or Q in the power term C so the results are unaffected by assuming a constant energy comparative basis. It is done merely for convenience in interpreting and comparing the results.

The eleven variables and eight dimensionless parameters are mutually dependent and cannot be arbitrarily assigned values. The values of the parameters had to be carefully selected, then the variables calculated, and the process repeated until all values were defined. The results of these computations and selections are shown in Appendix K.

Table 9-1: Variable minimum and maximum values

Variable	Minimum	Maximum	Units	Description
W	0.6	858.8	cm	Width
H	0.2	285.8	cm	Height
L	1.5	239.4	cm	Length
l	0.2	477.7	cm	lamp arclength
r	0.004449	10.86834	cm	lamp radius
P	4	4	W	Power
t	1.7E-07	46.99679	s	Exposure time
x	0.195554	477.7291	cm	lamp x2 coordinate
y	0.008164	79.76449	cm	lamp y coordinate
z	0.1606	214.4254	cm	lamp z coordinate
k	0.00275	0.00275	cm ² /μW-s	rate constant
p	25.00	93.00		reflectivity
Af	0.10	0.8958		Area Fraction
Q	75	75	m ³ /min	Airflow
V	0.050933	90756.08	m/s	Velocity

The range of the dimensionless parameters used in the 2k factorial analysis is summarized in Table 9-2. Although the range could be further extended for some of the dimensionless parameters, these values represent reasonable limits.

Table 9-2: Limits of Dimensionless Parameters

Parameter		Level	
		Min	Max
A	W/H	1.0040	5.01
B	r/l	0.0046	0.04
C	kPL/Q	0.0136	2.11
D	x/W	0.0633	1.00
E	y/H	0.0079	0.50
F	ρ	0.37	0.93
G	z/L	0.1042	0.90
J	Af	0.10	0.8958

The variable values shown in Appendix K were used as input to the UVX program. The output of the program included a recapitulation of the input variables, the re-calculated dimensionless parameters, and the two bounding kill rates – for mixed air and unmixed air. The 256 sets of dimensionless parameters and kill rates represent the complete input for a 2^k factorial analysis.

Given that the 2^k factorial data set is complete and in standard order, it was necessary only to analyze it as a General Linear Model (Montgomery 2001). This analysis considered all 2-way, 3-way, 4-way, and 5-way interactions between the dimensionless parameters. This model provides the Analysis of Variance (AOV) of K, the kill rate, which is shown in Appendix M. It is clear that parameter C, the specific dose, is the most influential factor, and that most of the interactions are of negligible importance.

The results of the 2^k factorial screening analysis are shown in Appendix M for the case of the Mixed Air Kill Rate. In this analysis the natural log of the Kill Rate is used as this more closely reflects the physical process, which is one of exponential decay.

Figure 9.1 shows the Normal Probability plot of the residuals from the 2k factorial analysis. The plot, although a reasonably good fit to the data, exhibits curvature suggestive of a second order polynomial.

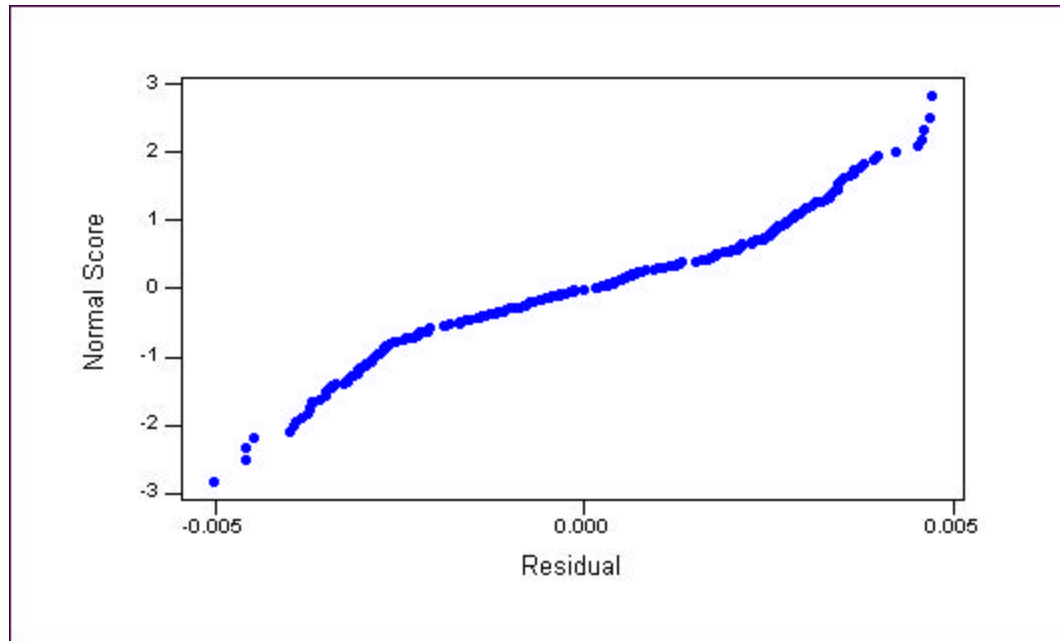


Figure 9.1: Normal Probability plot of Residuals for LnK (mixed air condition)

Based on the analysis, several two-way interactions appear to contribute significantly to the curve fit. Only one three-way interaction showed any significant contribution to the fitted first order curve.

Having screened the variables in the linear model, they can now be used for the second order model. Just to be sure, however, all the two-way effects are be used in addition to the selected two-way and three-way effects. This is because some of these effects may come back into play in the second order model.

9.2 RSM Analysis of the Central Composite Design

The previous analysis of the linear model, particularly the normal probability plot of the residuals, suggests that at least some of the relationships are nonlinear and so it is necessary to examine additional data points to provide resolution of the 2nd order polynomials. These additional data points will form the input into a statistical model known as a Central Composite Design. The data points to be added are known as center points and star points (Montgomery 2001).

The center point for this model is the set of all medians of the dimensionless parameters. Normally, multiple center points would be added so as to provide an accurate estimate of the random error. However, in this case there is no random error since the program will output identical results for any set of inputs, and therefore only one center point is needed.

The star points are determined by taking the distance of the minimum (low) or maximum (high) value of each dimensionless parameter and multiplying by a constant called alpha, typically with a value of 1.414, as in this case. This value, the square root of 2, is commonly used to represent a balanced set of data points encircling a square (in 2 dimensions) that defines the high and low points. It is convenient, if not absolutely necessary, to use high and low parameter values such that there is room to assign the star points. This explains why the original set of parameters does not represent absolute minimums and maximums. Several iterations were performed to establish a complete set of parameters and variables that fell within these limits and that simultaneously made physical sense.

The final set of star points and the center point are summarized along the minimums and maximums in Table 9-3. The complete data set is shown in Appendix K.

Table 9-3: Star Points and Center Point for Parameters

Parameter	A	B	C	D	E	F	G	J
	W/H	r/l	kPL/Q	x/W	y/H	ρ	z/L	Af
α	1.4141	1.4141	1.414	1.4141	1.4141	1.414	1.414	1.414
Lo Star	1.00405	0.00458	0.014	0.06335	0.00795	0.37	0.10	0.10
Min	1.59	0.0099	0.32	0.2	0.08	0.45	0.22	0.22
Center	3.005	0.02275	1.06	0.53	0.254	0.65	0.50	0.50
Max	4.42	0.0356	1.8	0.86	0.428	0.85	0.78	0.78
Hi Star	5.00595	0.04092	2.106	0.99665	0.50005	0.93	0.90	0.90
α	1.4141	1.4141	1.414	1.4141	1.4141	1.414	1.414	1.414

The results for the Regression of the CCD model are shown in Appendix N for the mixed air case. Table 9-4 summarizes the results for all parameters that contributed 0.17% or more to the complete model. This model accounts for over 99.9% of the total sum of squares error for the extended data set. Also shown is a reduced data set for those factors with a sum of squares error less than 0.5%. This reduced data set, in spite of the R-squared value of 97.46, proved to have significant deviations for high kill rates and was therefore not very useful.

Table 9-4: Model Sum of Square Error % Contributions

Source	Description	Seq SS	% of Total	Factors >.5%
A	W/H	0.306	0.24	
B	r/l	0.017	0.01	
C	kPL/Q	93.36	73.64	73.64
D	x/W	1.1687	0.92	0.92
E	y/H	0.4551	0.36	
F	z/L	11.7297	9.25	9.25
G	ρ	0.0611	0.05	
J	A_f	7.4	5.84	5.84
AA	$(W/H)^2$	0.017	0.01	
CC	$(kPL/Q)^2$	4.1408	3.27	3.27
DD	$(x/W)^2$	0.7529	0.59	0.59
EE	$(y/H)^2$	0.4473	0.35	
FF	$(z/L)^2$	0.2066	0.16	
GG	ρ^2	0.03	0.02	
AC	kPLW/QH	0.0413	0.03	
CD	kPLx/QW	0.179	0.14	
CE	kPLy/QH	0.0802	0.06	
CF	kPz/Q	1.3727	1.08	1.08
CJ	kPLA _f /Q	0.4017	0.32	
DF	xz/WL	0.0522	0.04	
EF	yz/HL	0.0839	0.07	
FJ	zA _f /L	0.3941	0.31	
CDF	kPxz/QW	0.0431	0.03	
CEF	kPyz/QH	0.0352	0.03	
CCC	$(kPL/Q)^3$	3.639	2.87	2.87
sqrtC	sqrt(kPL/Q)	0.2227	0.18	
atJ	atan(A _f)	0.0296	0.02	
JJJ	A_f^3	0.0134	0.01	
Total		126.78	99.92	97.46

The complete equation for the Average (mixed air) case can now be written as:

$$\ln K = \left\{ \begin{aligned} &-1.71 - 0.0495 \frac{W}{H} - 0.631 \frac{r}{l} - 8.27 \frac{kPL}{Q} - 0.35 \frac{x}{W} - 0.312 \frac{y}{H} + 1.81r + 0.692 \frac{z}{L} \\ &+ 12.8Af + 0.00207 \left(\frac{W}{H} \right)^2 + 1.64 \left(\frac{kPL}{Q} \right)^2 + 0.336 \left(\frac{x}{W} \right)^2 + 1.14 \left(\frac{y}{H} \right)^2 - 0.037 r^2 \\ &- 0.717 \left(\frac{z}{L} \right)^2 + 0.121 \frac{W}{H} \frac{kPL}{Q} - 0.0643 \frac{kPL}{Q} \frac{x}{W} - 0.159 \frac{kPL}{Q} \frac{y}{H} - 0.751 \frac{kPL}{Q} r \\ &+ 0.261 \frac{kPL}{Q} Af - 0.498 \frac{x}{W} r - 1.00 \frac{y}{H} r + 0.695 r Af + 0.266 \frac{kPL}{Q} \frac{x}{W} r \\ &+ 0.455 \frac{kPL}{Q} \frac{y}{H} r - 0.165 \left(\frac{kPL}{Q} \right)^3 + 12.3 \sqrt{\frac{kPL}{Q}} - 13.7a \tan(Af) - 3.86 Af^3 \end{aligned} \right. \quad (9-3)$$

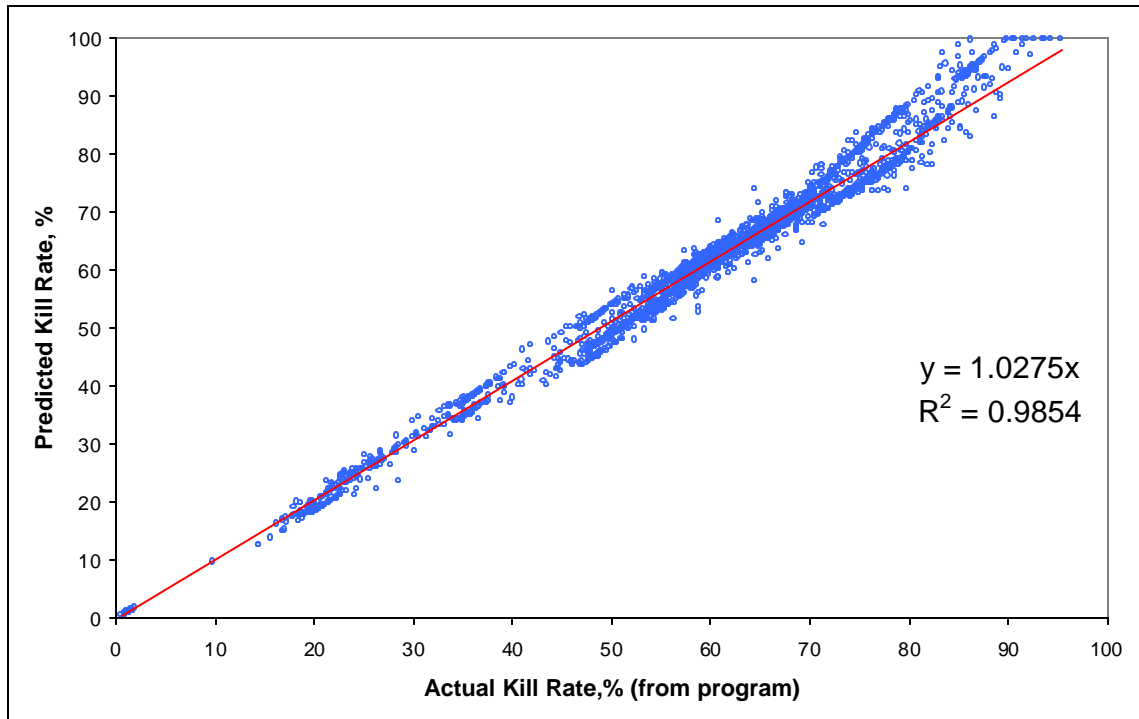


Figure 9.2: Predictive Scatter Plot for Regression Model

Figure 9.2 illustrates the predictive ability of equation (9-3). In this figure some 3300 data sets spanning the entire range of dimensionless parameters were used as input and the kill rates predicted by the program were compared against the kill rates predicted by equation (9-3). Although the agreement is remarkable over most of the range, the deviation can be as great as

+/-15%. Since the program error is already approximately +/-15%, the total error could possibly reach +/-30% and so equation (9-3) may not be an accurate substitute for the program itself. It may, however, provide a quick method of zeroing in on a set of design parameters, which can later be evaluated in detail by the program.

If the equation had proved to be simpler it might have provided insight into the relationships of the component variable functions, however, no reduction or extension of this equation resulted in any improvement, and all attempts to modify it resulted in increased scatter in the random predictions in Figure 9.2. Therefore, we are limited to interpreting only the error sum of squares values in Table 9-4 in order to understand the relationships that may be implied.

The integrated, or unmixed air case, was evaluated but because the results have no specific application they are not shown here. The value of the integrated case is primarily in what it tells us about the system, and not so much in its predictive ability. For example, the integrated case is used to produce kill zone diagrams and can assist in assessing system inefficiencies. The unmixed air case represents a lower limit on the kill rate, but, as explained in previous chapters, is an improbable condition since air mixing is unavoidable.

Chapter 10. Optimization of Performance and Economics

Information provided in the previous dimensional analysis and in Appendix K may be sufficient to establish the optimum parameters that will maximize performance of any UVGI system. In this section we seek a more exact solution to the question of what the optimal design parameters and variables might be for any given set of design criteria.

10.1 Performance Optimization

Prior to examining the economics, it is useful to consider how the various dimensionless parameters affect performance and how they may be manipulated to increase performance. Because of the negligible interactions between the eight dimensionless parameters they can be optimized independently of each other.

The dimensionless parameters have been shown in previous chapters to have little significant interaction. Therefore, a comparison of the parameters on a one-to-one basis (e.g. each parameter compared against each other parameter with all others held constant) provides insight into the relative significance and behavior of each parameter. A complete summary of the response surfaces is provided in Appendix L, but some of the contours are repeated here to illustrate and explain their behavior and impact.

Figure 10.1 shows the response surface model (RSM) for the dimensionless parameter kPL/Q , the specific dose, vs. W/H , the duct aspect ratio. The labels on the axes represent the range of the parameter values where 1 or S_1 represents the lowest value and 10 or S_{10} represents the highest value. Refer to Appendix L for the actual parameter values.

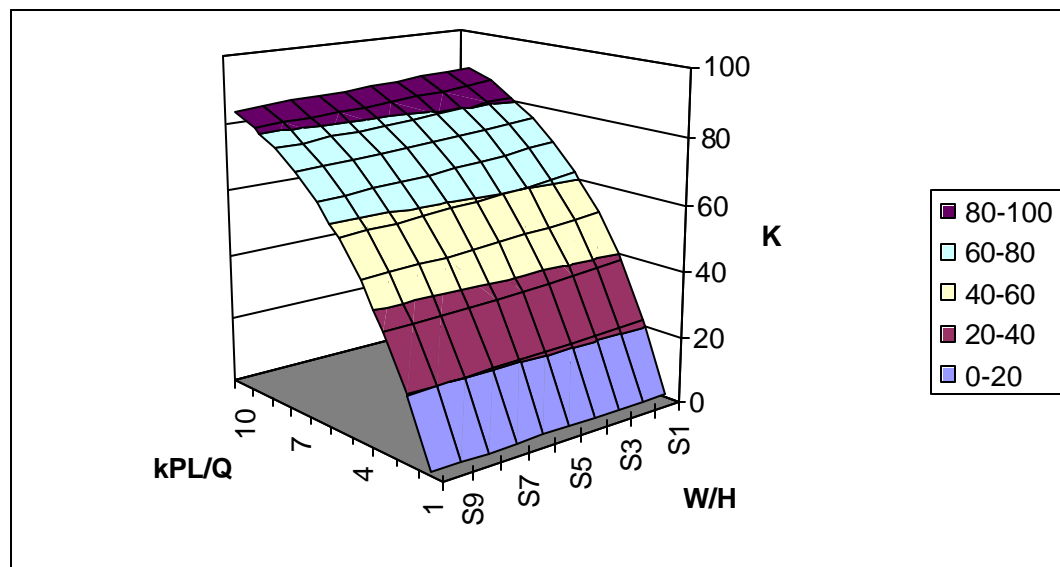


Figure 10.1: RSM for % Kill Rate of Specific Dose vs. Duct Aspect Ratio

It is observed in Figure 10.1 that the kill rate responds non-linearly to an increase in the specific dose, and the rate of increase decreases as the specific dose is increased. The kill rate increases a few percent as duct aspect ratio decreases towards the minimum of 1.0, which represents a square duct. The maximum duct aspect ratio (at S10) is 5, or a ratio of 5 to 1.

Figure 10.2 shows that the kill rate responds approximately linearly to an increase in reflectivity while the duct aspect ratio is again seen to increase to its optimum for square duct. It can be concluded that, after some specific dose is achieved, that there is more benefit to increasing reflectivity than increasing power. This will be demonstrated to be an economic approach in subsequent sections.

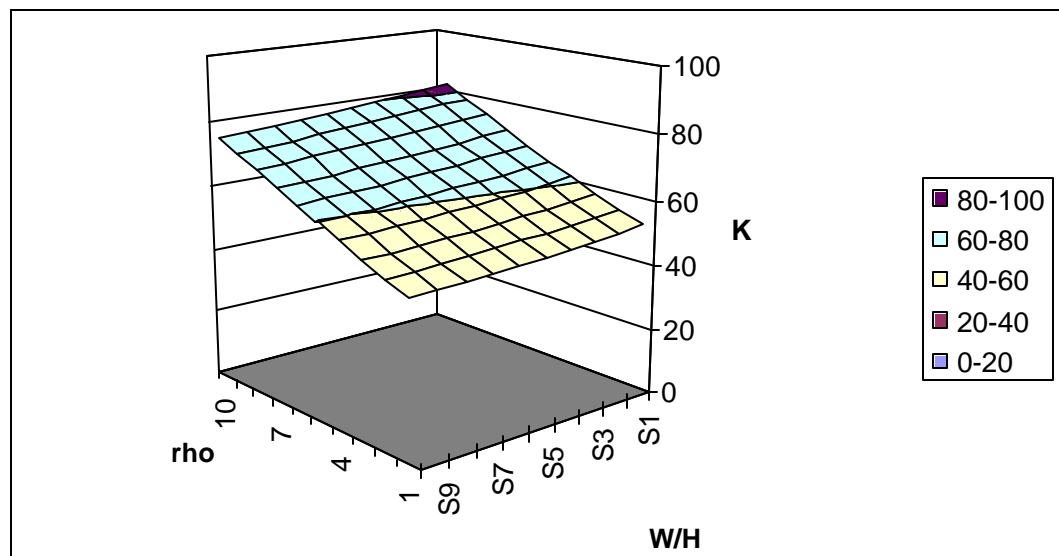


Figure 10.2: RSM for % Kill Rate of Reflectivity vs. Duct Aspect Ratio

Figure 10.3 shows the response surface of lamp aspect ratio, r/l , vs. the Y ratio, y/L . The Y ratio represents the height of the lamp above the lower duct surface (see Figure 8.1). It is observed that the lamp aspect ratio has an almost insignificant effect (i.e. less than 1%) and this is true for all cases examined, since the interactions are negligible for all parameters. The Y ratio, however, shows a most interesting result – the kill rate increases up to 15% as the lamp is moved toward the surface. This occurs because the reflective surface is amplifying a higher intensity field when the lamp is close as opposed to amplifying a lower intensity field when the lamp is further away.

This phenomena is here termed the proximity effect. It is interesting in two regards, first the common practice is to place lamps in the central location in a duct, and second is the fact that this boost in system efficiency comes for no additional cost, since it merely involves placement of

the lamp. It is not known exactly how close a lamp can actually be placed near the surface since airflow around the lamp and between the duct will experience interference at some point. This matter remains to be studied further but it is assumed for convenience that the limit is approximately one lamp diameter and none of the studies shown here place the lamp any closer than this.

One caveat here is that the proximity effect must be dependent in some degree on the kill rate. That is, if a high kill rate is already being achieved, then the gains from relocating the lamp closer to the surface may not be significant. An alternate view of this phenomena is that if the intensity field near the lamp is producing, say, a 40% kill rate, then moving the lamp close to a surface of, say, 99% reflectivity will approximately double the kill rate in the local area to about 80% (assuming a linear kill rate response merely for the sake of argument). If however, the local kill rate around the lamp is already high, say 80%, then relocating the lamp close to the surface won't produce 160%, of course, it will only produce a maximum of 100%, meaning the extra intensity goes to waste -- it represents an inefficiency. The conclusion can be drawn that, depending on the kill rates being achieved, there must exist some optimum Y ratio, but this is difficult to establish in advance or for general situations and so is left as a matter for future research.

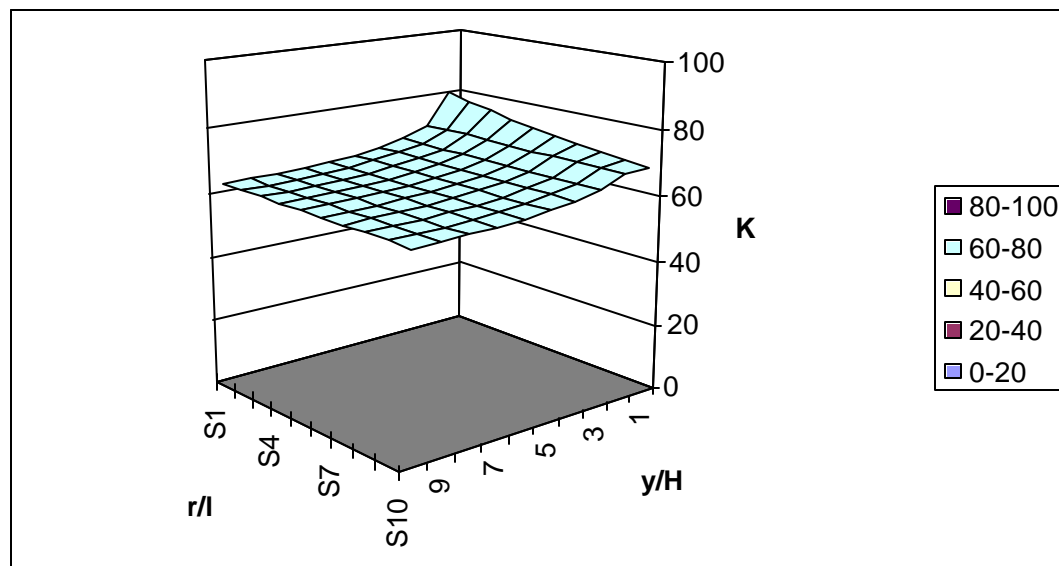


Figure 10.3: RSM for % Kill Rate of Lamp Aspect Ratio vs. Y Ratio

Figure 10.4 shows the response surface for the X ratio vs. the Y ratio. The X ratio is the arclength of the lamp, with one end located at the right side surface, divided by the duct width (see Figure 8.1). Here also we see the proximity effect in a slightly different form – the kill rate is boosted by about 15% as the lamp length is shortened relative to the duct width. In effect, as the

lamp intensity field is compressed towards the surface it is perpendicular to the intensity field is increased due to the reflection of a higher intensity field.

Because the effects of the parameters are essentially additive, the combination of minimizing both the Y ratio and the X ratio results in a maximum $15\% + 15\% = 30\%$ boost in the kill rate, in this example. The same caveat applies as with the Y ratio – the effect may be somewhat dependent on the actual kill rates achieved and so it cannot be concluded that the effect would be manifest in all situations. It is likely, however, that the situation can be set up to produce a proximity effect in most cases. Clearly, the manipulation of the proximity effect can result in considerable energy savings at no additional cost of materials.

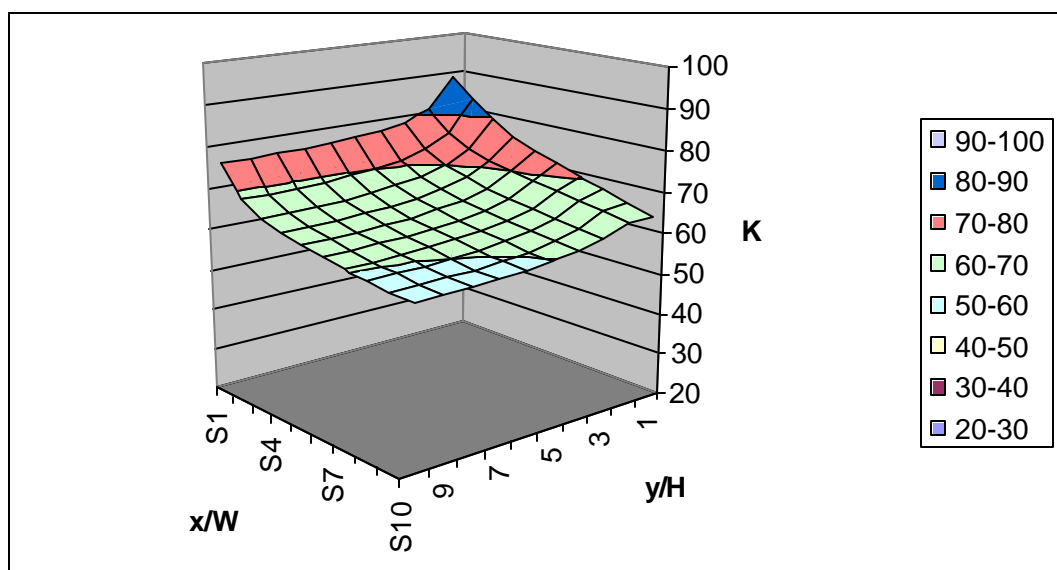


Figure 10.4: RSM for % Kill Rate of X Ratio vs. Y Ratio

Figure 10.5 shows the response surface of the Z ratio vs. the specific dose. The Z ratio represents the depth within the duct at which the lamp is placed (see Figure 8.1). In this case the Z ratio varies from a minimum (1) at approximately the face of the duct inlet, to a maximum (10) at approximately the duct outlet. Normally, lamps are located at the middle portion of any duct, where it is intuitively expected that the intensity and kill rates will be maximized. This turns out to be exactly the case as the Z ratio proves to always be a maximum at a value of 0.5, or exactly centered along the length of the duct. In this figure it is again observed that the effects of both parameters are superposed, or directly additive.

No further examples are analyzed here because the remaining response surfaces are basically additive repetitions of the effects described here. They are provided for review, along with the data on which they are based, in Appendix L.

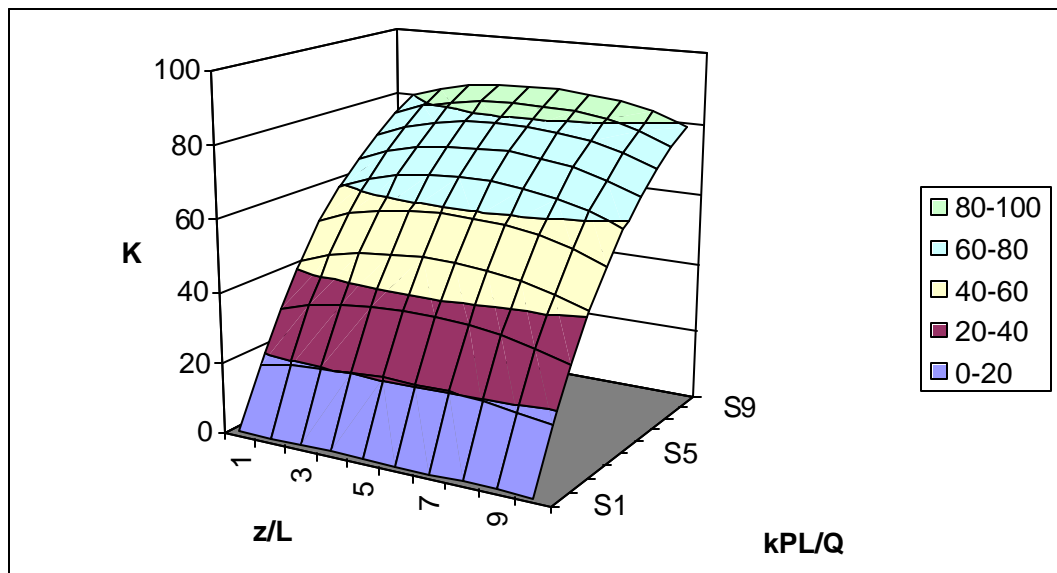


Figure 10.5: RSM for % Kill Rate of Z ratio vs. Specific Dose

Table 10-1 lists the values of the dimensionless parameters that result in optimum performance. Some of these optimum parameters are obvious, either intuitively or based on the results presented so far. It is clear, for example, that the specific dose, reflectivity, and the surface fraction should all be maximized, while the aspect ratio and the Y ratio should be minimized. The Z ratio is optimum at 0.5 (lamp should be at mid-depth of duct).

Table 10-1: Optimum Values for Parameters

Dimensionless Parameter		Description	Optimum Value
A	W/H	Aspect Ratio	1
B	r/l	Lamp Aspect Ratio	none
C	kPL/Q	Specific Dose	MAX
D	x/W	X Ratio	MIN/MAX
E	y/H	Y Ratio	MIN
F	z/L	Z Ratio	0.5
G	ρ	Reflectivity	MAX
J	A_f	Area Fraction	MAX

The X ratio will produce optimum kill rates if it is minimized, however, if it is greater than 0.5 then it should be maximized. That is, if the reflectivity is high enough, there will be an increase in kill rate when the lamp spans the entire duct. More simply put, the length of the lamp is preferably short, but that if it is over one-half the duct width, then it is best to span the entire duct. This is a direct result of the proximity effect discussed previously. In addition, real world values for

lamp dimensions constrain the parameter – it may not be possible to obtain the optimum value for the X ratio for any given system.

The lamp aspect ratio has no significant effect under most conditions and so has no significantly optimum value. There may be situations where it has a minor impact, such as in ducts with very small cross-sections, but such cases may have to be evaluated on an individual basis.

One problem with defining the minimum value for the parameter y/H is the fact that some value other than zero is likely optimum since zero implies the lamp sits directly on the surface. Not only is this not possible because the lamp has a finite diameter, but also placing a lamp so close to a surface would disturb the air currents and reduce local airflow between the lamp and the surface. The airflow problem is not studied here and so it is arbitrarily assumed that a lamp can be no closer than one diameter from a surface. This matter remains to be studied later in more detail to determine the specific optimum distance any given lamp can be placed from the surface, ideally with the aid of computational fluid dynamics.

Since equation (9-4), which represents a statistical curve fit of the entire response surface model, failed to produce predictability within an acceptable error range, the program must be used to exhaustively search for the performance optimums. These optimums exist either as points, ridges or hilltops in the response surfaces of the eight-dimensional space defined by the dimensionless parameters.

In fact, the pronounced lack of interaction between the terms means that these optimums can be identified by individual comparisons of the parameters on a one-to-one basis. Each of these parameters can be independently maximized since the interactions are relatively minor. The Y ratio, or lamp height, for example, can be minimized regardless of the X ratio, the Z ratio or the duct aspect ratio.

Some cases exist where there is no optimum for a given parameter, but these do not constrain or impact the optimization of other parameters. For example, if the reflectivity is too low, the gains from reducing the X ratio become negligible, but reducing the X ratio does no harm to the kill rate in this condition.

The optimum values for parameters are illustrated in Figure 10.6a thru 10.6h. In these diagrams the kill rate due to each subject parameter is shown against each of the other seven parameters as these other parameters vary across their entire range. That is, each of the lines represents the subject parameter vs. each one of the other seven parameters with the other six held constant. It can be observed in each and every case that the relationships follow a consistent pattern and the maximum for each subject parameter occurs at the same point regardless of which other parameter it is compared against.

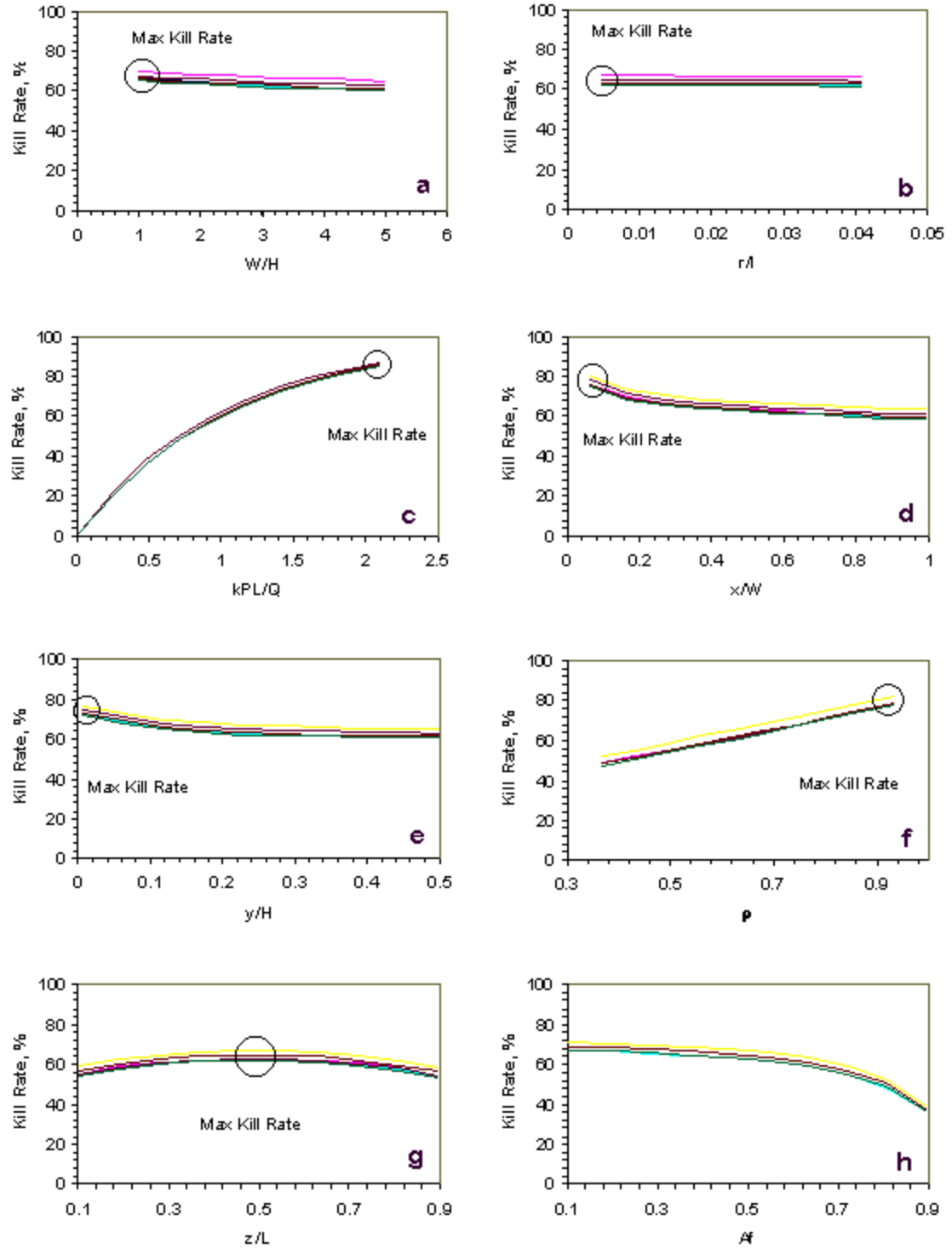


Figure 10.6a-h: Optimum Values of Dimensionless Parameters. The seven lines on each chart represent each of the other parameters varied across their entire range.

In all the comparisons in table 10.6a through 10.6h the optimum point is seen to be obvious and singular at the point of highest kill rate. The one qualified exception is the area fraction, which, although it has an apparent maximum, the maximum is without significance. As explained previously, the area fraction cannot be independently controlled without the use of light baffles, and light baffles are beyond the current analysis capability of the program. To reiterate, the area fraction effectively serves as a control constant when the duct length is varied, thereby allowing accurate interpretation of the response of the specific dose.

Because of the fact that the power and airflow are held constant in this study to provide comparisons based on equal energy consumption and equal volumes of disinfected air, the area fraction becomes dependent on the exposure time. The exposure time has more impact than the area fraction and so the kill rates decrease overall when the area fraction increases.

One way in which the area fraction can be divorced from the exposure time is through the use of light baffles. In a system in which light baffles were used at the inlet and outlet the area fraction could be increased without altering airflow, although pressure losses would increase fan energy consumption. The analysis of light baffles is beyond the current capabilities of the UVX program, but the subject will be discussed further in the next chapter.

10.2 Economic Optimization

Having established the performance of UVGI systems as a function of the eight dimensionless parameters, a study of economic optimization can be pursued. First, typical economic analysis is performed here for each of the two types of UVGI systems – an air disinfection system, and a surface disinfection system. Next, an optimization study is performed to evaluate the economic relation between those parameters with which costs are associated.

10.2.1 Life Cycle Cost of UVGI Systems

UVGI systems exist for both air and surface disinfection. The UVX program can analyze both types. Air disinfection systems are used to process building air in air handling units or in stand-alone recirculation units. The second type of system is used to control microbial growth on surfaces. For convenience of comparison, only the in-duct air disinfection system (not the stand-alone recirculation type) is used in the following life cycle cost comparison. Recirculation systems will be studied further in the next section.

Table 10.3 summarizes the costs associated with purchasing, installing, and operating two different types of UVGI systems, an airstream disinfection system and a microbial growth control system. The ventilation system is identical in both cases. These systems were sized using the techniques described in the article with predicted disinfection rates as shown.

The location used in the energy analysis is Philadelphia, and so the heat added by the lamps results in a cooling energy penalty for about 70% of the year. No credit is taken for energy input during the heating season, when heating the air may be desirable in most buildings. Clearly, the first cost of each of these systems is minor, while the maintenance cost eclipses the energy cost.

Although the microbial growth control system uses less wattage, it is considered to operate continuously, while the airstream system operates only while the building is occupied. The power requirements of the former system are appropriate for disinfection of duct surfaces or filter faces. Depending on the type of cooling coil, some systems may require higher intensities due to the problem of obtaining penetration through the fins and coils. Each system is assumed to have 75% reflective surfaces on four sides.

The energy consumption of both these systems is largely influenced by the filters, not the fans. The air disinfection system is assumed to include a 60% high efficiency filter with an average lifetime pressure loss of 0.56 in.w.g. A 25% filter is assumed for the microbial growth control system since the purpose is to destroy spores and so they need not be filtered to a higher efficiency. Prefilters (dust filters) are assumed to be present within the existing system and so are not accounted for in the UVGI system cost. Prefilters extend the life of high efficiency filters.

It may be plausibly argued that the added benefit to the indoor air quality from using a 60% filter on the microbial growth control system could be justified, but assessment of the actual risks and benefits is difficult in the absence of data. It may also be argued that the use of a 60% filter warrants the use of a 25% pre-filter to extend the life, but it is not entirely clear that this approach necessarily saves life cycle costs, especially in locations where energy costs are skyrocketing. Many buildings, such as hospitals, already use 25% pre-filters anyway. Therefore the air disinfection system does not account for any 25% pre-filters and it is simply noted here that their use must be evaluated economically on a case-by-case basis.

Table 10-2: Life Cycle Cost of Typical UVGI Systems

TYPE OF APPLICATION	Airstream Disinfection		Microbial Growth Control	
Design Airflow	10,000	cfm	10,000	cfm
	283	m ³ /min	283	m ³ /min
Velocity	413	fpm	413	fpm
	2.1	m/s	2.1	m/s
UVGI Lamp Model	GPH436T5		TUV18W	
UV Power	14	W	3.2	W
Number of Lamps	2		1	
Height	150	cm	150	cm
Width	150	cm	150	cm
Length	150	cm	150	cm
Lamp Total Power (ea.)	36	W	18	W
Hours of Operation	3744	hrs	8760	hrs
Power drop off at end-of-life	30	%	30	%
System Pressure Losses				
Diameter of lamp	1.5	cm	1.6	cm
Length of lamp	29.2	cm	28.83	cm
Face Area	22500	cm ²	22500	cm ²
Side area	43.8	cm ²	46.128	cm ²
Total area	87.6	cm ²	46.128	cm ²
Framing/Fittings	17.52	cm ²	9.2256	cm ²
Total Area	105.12	cm ²	55.3536	cm ²
Free Area Ratio	0.9953		0.9975	
Loss Coefficient (ASHRAE CR6-1)	0.0014		0.00018	
Press Loss (lamps & fixtures)	1.468E-05	in.w.g.	1.887E-06	in.w.g.
Energy Costs				
Heat Generated	0.072	kW	0.018	kW
Total dP (lamps, fixtures, filters)	0.560	in.w.g.	0.290	in.w.g.
Total Fan Energy (80% eff.)	8016	kW-hrs	4151	kW-hrs
Electrical Energy	270	kW-hrs	158	kW-hrs
Cooling Load Energy	189	kW-hr	110	kW-hr
Total Energy	8475	kW-hrs	4419	kW-hrs
Rate	0.08	\$/kW-hr	0.08	\$/kW-hr
(a) Annual Energy Cost	678	\$	354	\$
Maintenance costs				
Average tube life	9000	hrs	9000	hrs
tube hours/year (# of tubes x hours of operation)	7488	hrs	8760	hrs
Replacements/year	0.83		0.97	
(b) Cost / tube	85	\$	85	\$
(c) Annual cost	71	\$	181	\$
# 24" filters by height	2.5		2.5	
# 24" filters by length	2.5		2.5	
Number of filters	6		6	
Filter Type	60%	High Efficiency	25%	
Filter replacements/year	6	(1x per year)	24	(4x per year)
(d) Cost / filter	32.7	\$	4.1	\$
(e) Annual filter replacement cost	196	\$	98	\$
(f) Maintenance (assumed)	50	\$	50	\$
(g) Annual Maintenance Cost (a+c+f)	799	\$	585	\$
First Costs				
(h) UVGI system (AU prices)	765	\$	550	\$
(i) Labor (estimated)	1000	\$	1000	\$
(j) Total Installation Cost (h+i)	1,765	\$	1,550	\$
Life Cycle	20	years	20	years
Interest rate	8	%	8	%
(k) Life Cycle Cost	180	\$	158	\$
Total Annual Cost	1656	\$	1096	\$

10.2.2 Basic Cost Relationships of UVGI System Components

Before proceeding with an economic optimization of UVGI systems, it is necessary to qualify the various cost relationships. These include the relationship between lamp assembly first cost and lamp UV power, the cost of reflective materials as a function of reflectivity, the cost of sheet metal ductwork, the cost of a filter assembly, the cost of a fan and motor, and the cost of assembly or construction of a UVGI system. These cost estimates are based on quotes from various sources, including estimates from catalogs and Internet sources. These are not meant to be conclusive costs, as they may vary considerably from one source to another and depend on quantity, but are merely representative and so not all are given with specific references.

The lamp UV power depends on the model of lamp used and the number of lamps. The pressure losses associated with different lamps and numbers of lamps are assumed identical here due to their relative insignificance (i.e. see Table 10-3). Appendix O summarizes these costs along with those of the other cost parameters.

Figure 10.7 shows the variation of UV Power with cost for some 33 lamp assemblies. A second order polynomial has been fitted to the data yielding a general relation between the cost of UV Power UVP\$, and UV power P as follows:

$$UVP\$ = -0.0493P^2 + 24.83P + 209.8 \quad (10-3)$$

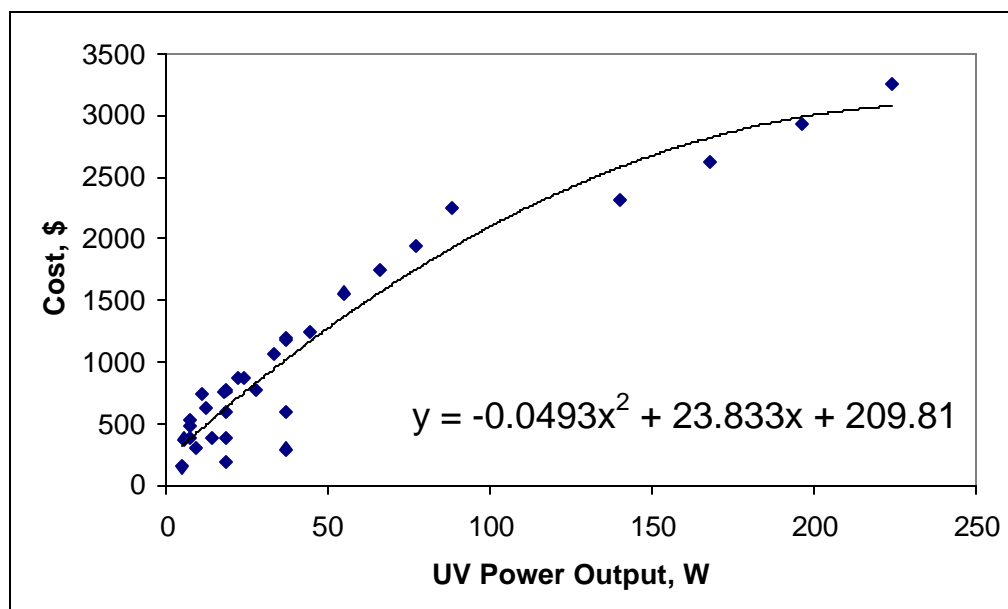


Figure 10.7: Variation of cost with increasing UV power. Based on combinations of various model lamps.

The ductwork cost depends on the total duct surface area, in terms of W , H , and L . See Appendix O for these tabulated costs. Galvanized 16 gauge ductwork typically costs \$4.83 per sq. ft. and so the cost relationship can be written as:

$$Duct\$ = 4.83(2L(W + H)) = 9.66L(W + H) \quad (10-4)$$

The reflective material cost is also dependent on total surface area, but the reflectivity depends on the type of material, as shown in Figure 10.8. Several materials have been identified and tabulated in terms of their cost in Appendix O. The relation for the reflective material is based on costs for three materials, ordinary galvanized duct, sheet aluminum (rough), polished sheet aluminum, and estimated costs for Alzak sheet aluminum. The UV reflectivities for these materials are typically 54%, 65%, 75%, and 85%, respectively. The galvanized duct has a cost of zero since it is the duct surface already present in the system. The following relationship summarizes a curve-fit of these data:

$$Cost / ft^2 = 0.0882r - 4.8286 \quad (10-5)$$

The total cost per sq. ft. of reflective material $RF\$$ becomes:

$$RF\$ = (0.0882r - 4.8286)(2L(W + H)) \quad (10-6)$$

Simplifying equation (10-6) we have:

$$RF\$ = (0.1764r - 9.66)L(W + H) \quad (10-7)$$

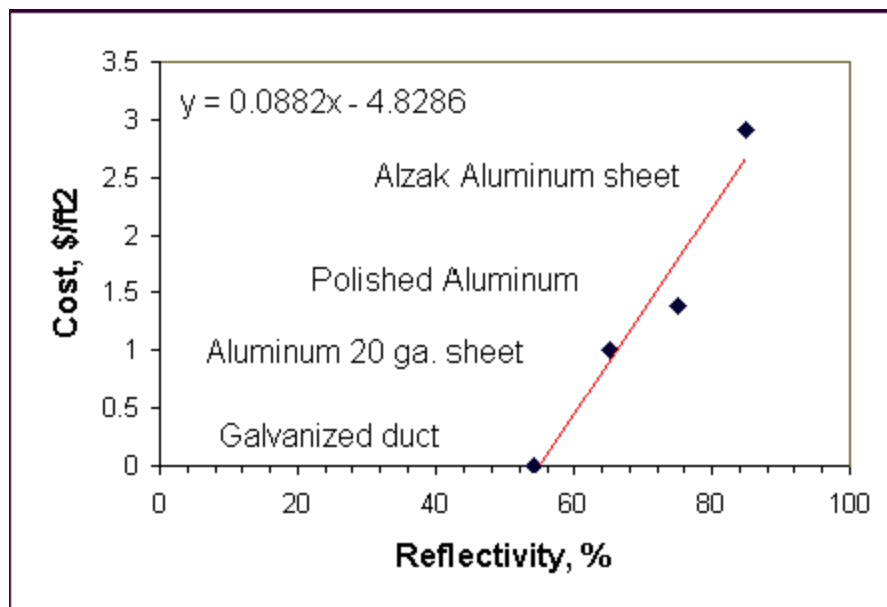


Figure 10.8: Cost of Reflective Materials per sq. ft. vs. Reflectivity

Based on some industry construction estimates for UVGI systems, the labor for construction of the duct plus reflective materials are estimated to consist of a baseline cost of about \$460 (for systems of the size we are interested in) with a nominal increase for square footage that yields the following estimated relationship:

$$Labor\$ = 460 + 0.5(2L(W + H)) = 460 + L(W + H) \quad (10-4)$$

In-duct systems include no fans, but recirculation systems must have one. The fan, including motor, has a cost roughly dependent on the air moving capacity. This cost is estimated to be approximately 0.01452 \$/cfm, and is therefore:

$$FanFC\$ = 0.01452(35.315)Q = 0.5128Q \quad (10-5)$$

The filter assembly for any UVGI system has some nominal first cost that depends on filter face area and this relationship is estimated to be about \$10 per sq. ft. or:

$$FilterFC\$ = 10WH \quad (10-6)$$

We can now write the total first cost FC\$ of a UVGI system, including the first cost of the fan (applies only to recirculation units) as follows:

$$FC\$ = UVP\$ + Duct\$ + RF\$ + Labor\$ + FanFC\$ + FilterFC\$ \quad (10-7)$$

Substituting the previous cost relationships we get:

$$FC\$ = \begin{cases} -0.0493P^2 + 24.83P + 209.8 + 9.66L(W + H) \\ + (0.1764r - 9.657)L(W + H) \\ + 460 + L(W + H) + 0.5128Q + 10WH \end{cases} \quad (10-8)$$

Simplifying this summation and making the appropriate conversions to metric units (W, H, & L must be in cm for program input) we get:

$$FC\$ = \begin{cases} -0.0493P^2 + 24.83P + 669.8 \\ + (0.001076 + 0.0001898r)L(W + H) \\ + 0.5128Q + 0.0108WH \end{cases} \quad (10-9)$$

10.2.3 Annual Costs of UVGI Systems

Now, the energy and maintenance costs must be evaluated. There is an energy cost due to the total power consumption of the UVGI lamp, or LP\$. There is also an energy cost due to the excess heat the lamp puts into the ventilation system, LH\$. Finally there is a pressure loss associated with both the lamp assembly and the duct. It is assumed, furthermore, that the UVGI system comes complete with an 80% filter to maintain cleanliness. This data is summarized from manufacturer's catalogs in Appendix O.

The energy cost of the lamp is computed based on the total power consumption (at an efficiency of 76%), and at a cost of 0.08 kWh for full-time operation:

$$LP\$ = \frac{0.08 * 8760 * P}{0.34(1000)} = 2.06118P \quad (10-10)$$

The cooling cost of the lamp is based on a location of Philadelphia, Pennsylvania, where the cooling load will be present for approximately 70% of the year, and in which all the lamp energy is assumed to be converted ultimately to heat.

$$CP\$ = \frac{0.08 * 0.70 * 8760 * P}{0.34(1000)} = 1.443P \quad (10-11)$$

Pressure losses are based on a combined entry and exit loss (for recirculation systems) that has a combined loss coefficient of 1.5. The lamp losses depend on the cross-sectional area of the lamp. Assuming the lamp spans the entire duct (a conservative assumption) the loss coefficient for the entry, exit and the lamp can be written as a function of the radius. The loss coefficient (ASHRAE 1981) for lamps in the size range, and in the air velocity range, we are interested in is approximately 0.11, conservatively, for all cases. The pressure loss relationship can be written as:

$$dPL = (1.5 + 0.11) * 0.075 \left(\frac{Q}{WH1097} \right)^2 = 0.12075 \left(\frac{Q}{WH1097} \right)^2 \quad (10-12)$$

The pressure loss due to filters associated with the UVGI systems account for these energy costs. The design pressure loss of a 60% filter over its life is estimated as approximately 0.56 in.w.g. at the design velocity of 500 fpm. This yields a pressure loss coefficient of $C_0 = 35.94$, which is used to account for variations in air velocity in some of the performance evaluations. The relationship is

$$dPF = 35.94 * 0.075 \left(\frac{Q}{WH1097} \right)^2 \quad (10-13)$$

The total energy loss due to the pressure drop of the duct, lamp, and filters is then calculated based on the air horsepower with a fan efficiency of 0.75 and a fan motor efficiency of 0.75. Based on the same energy costs as previously, the resulting relationship is:

$$PL\$ = 0.08 * 8760 \frac{745.7 * 0.0001575 * Q}{0.75 * 0.75 * 1000} 2.696 \left(\frac{Q}{WH1097} \right)^2 = \frac{0.3957Q^3}{(WH1097)^2} \quad (10-14)$$

Maintenance is assumed at a flat rate of \$50 per year, regardless of system size. Lamp replacements are estimated to occur at a rate of 1.027 per year, based on the normal life of 9000 hours for such lamps, with all lamps operating for 3744 hours per year (12 hours per day/6 days

per week). Assuming for ease of computation that lamps are 5.33 UV watts and cost \$28.23 each (or \$85 for a 16 Watt lamp) and can be divided continuously between the minimum and maximum power levels in this study, we can write the lamp maintenance annual cost as:

$$LM \$ = 1.027 * 28.23 \frac{P}{5.33} = 5.439P \quad (10-15)$$

Filter replacements are based on a cost of \$8.18 per square foot of filter surface area (for a 60% filter). Assuming again that they are continuously distributable over the size range, and that they are replaced yearly, we have the relation:

$$FM \$ = 8.18WH \quad (10-16)$$

The total annual maintenance and energy costs can now be written as:

$$ME\$ = LP\$ + CP\$ + PL\$ + LM\$ + FM\$ + 50 \quad (10-17)$$

Substituting the previous equations, and converting to the appropriate metric units (W, H, & L are in cm) we have:

$$ME\$ = 2.0612P + 1.443P + \frac{11168Q^3}{(WH)^2} + 5.439P + 0.0088WH + 50 \quad (10-18)$$

Simplifying we get:

$$ME\$ = 8.943P + \frac{11168Q^3}{(WH)^2} + 0.0088WH + 200 \quad (10-19)$$

The first cost can be annualized with the capital recovery factor as follows:

$$AFC\$ = \frac{0.08 * (1.08)^{20}}{(1.08)^{20} - 1} FC\$ = 0.10185FC\$ \quad (10-20)$$

Substituting the first cost relation we get:

$$AFC\$ = \begin{cases} -0.00502P^2 + 2.529P + 68.19 \\ + (0.0001095 + 0.00000193r)L(W + H) \\ + 0.0522Q + 0.000116WH \end{cases} \quad (10-21)$$

The Annual Cost of a UVGI system can now be written as:

$$AC\$ = \begin{cases} 8.943P + \frac{11168Q^3}{(WH)^2} + 0.0088WH + 50 \\ - 0.00502P^2 + 2.529P + 68.19 \\ + (0.0001095 + 0.0000193r)L(W + H) \\ + 0.0522Q + 0.000116WH \end{cases} \quad (10-22)$$

Simplifying, we have:

$$AC\$ = \begin{cases} 11.47P - 0.00502P^2 + \frac{11168Q^3}{(WH)^2} + 0.0522Q + 118.19 \\ + (0.0001095 + 0.0000193r)L(W + H) + 0.0089WH \end{cases} \quad (10-23)$$

The relationships developed above are used in the ensuing calculations for optimization of in-duct and recirculation units. The input data and costs used in the optimization calculations are summarized in Appendix O (Input Data), Appendix P (First Costs), and Appendix Q (Annual Costs).

10.2.4 Economic Optimization of In-Duct UVGI Systems

The two basic types of UVGI systems are stand-alone recirculation units and in-duct systems. The in-duct systems can be sub-classified into complete units that can be added to a ductwork system and add-on components without duct that are added to existing ductwork. Because of the self-contained nature of recirculation UVGI units (i.e. independence from any ventilation system parameters), they are treated here exclusively. The same methods, however, can be applied to in-duct systems.

The eight dimensionless parameters depend on thirteen variables (see Table 8-2), not all of which have costs associated with them. The factors that affect the cost of a UVGI system include the lamp power, the ductwork, the reflective material, the reflectivity (type of reflective material), and the pressure loss through the duct.

The lamp aspect ratio r/l has too insignificant an effect to warrant its inclusion. Also, the costs that may be associated with placement of lamps in proximity to surfaces, as opposed to typical central locations, are taken as zero.

Not all of the cost factors can be defined as continuous functions since they involve some degree of discontinuity. However, continuous functions have been fitted and superposed on the data for the purposes of analysis. Obviously any selected operating point will require evaluation at specific real-world operating points but the results of this analysis can be used to identify bracketing conditions. In practice, these bracketing conditions (i.e. lamp model #1 vs. lamp model #2) can be evaluated in detail by the program to make a final selection.

As a sideline of some interest, Figure 10.9 shows the cost of typical UVGI air disinfection systems vs. their predicted kill rates, in which power is uncontrolled. An approximately linear relationship exists between the kill rate and the cost up until about 90%, at which point any increase in total system power provides diminishing results. This chart suggests that systems in this size range (i.e. 12,000 cfm) with more than about \$3000 each in annualized cost provide no additional benefit. Of course, this relates to kill rates for *Serratia marcescens* only, and although it is a representative microorganism, there are some more resistant microbes for which higher power systems might conceivably be justified.

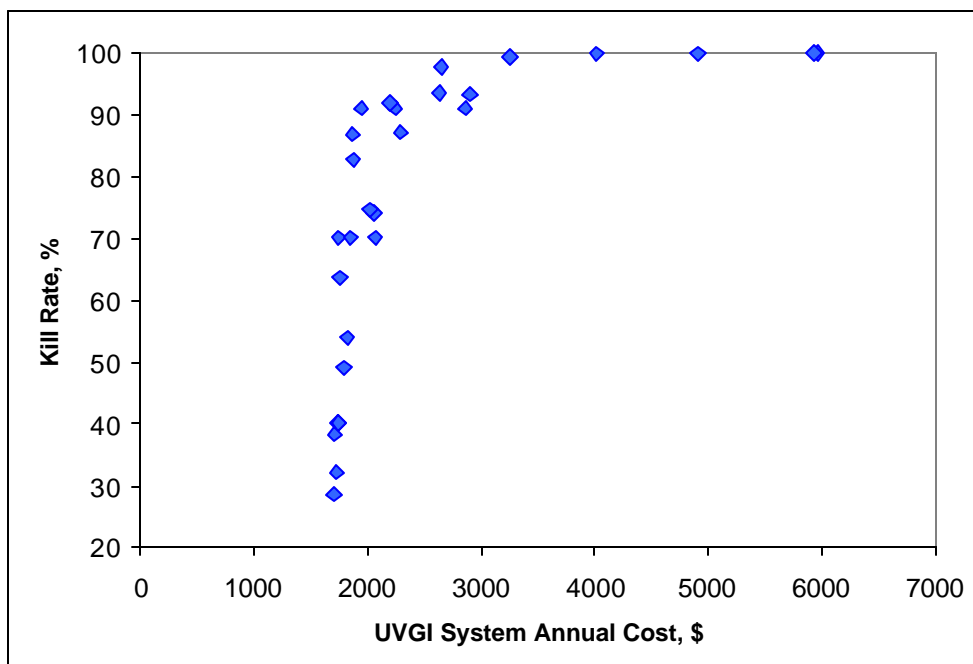


Figure 10.9: Kill Rate of *S. marcescens* vs. Annual Cost for Typical UVGI Systems

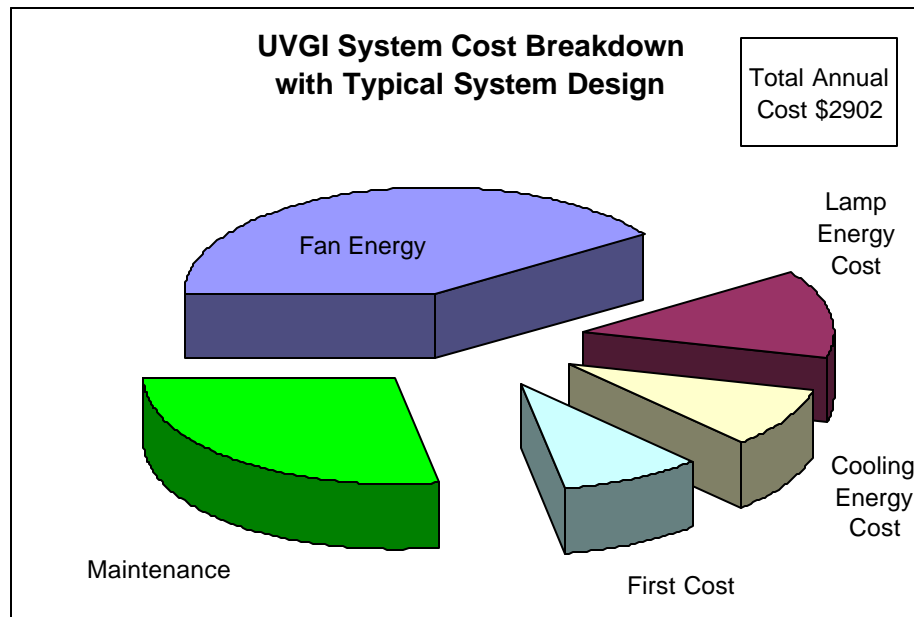


Figure 10.10: Cost Breakdown for Typical System design

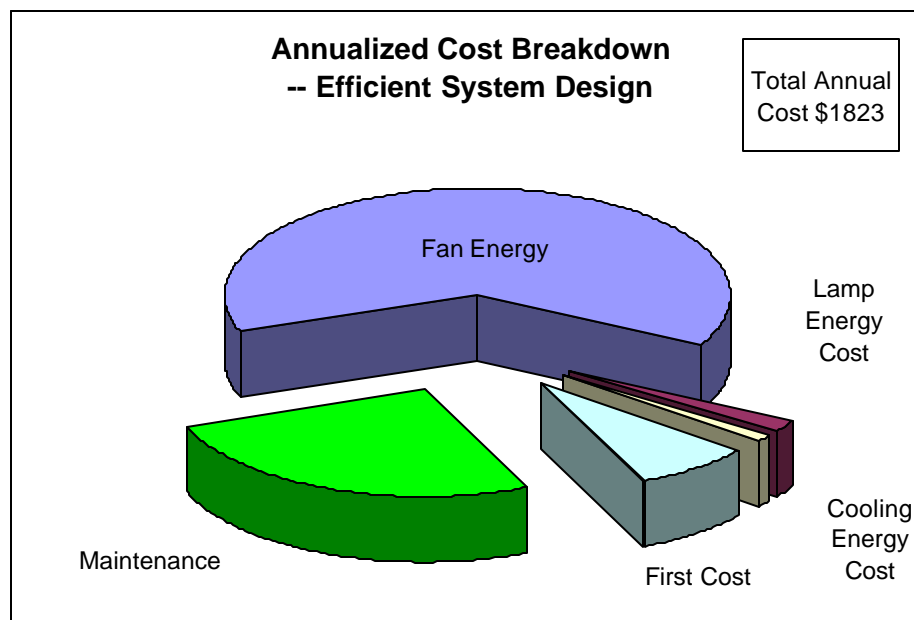


Figure 10.11: Cost Breakdown for Energy-Efficient System Design

Figure 10.12 compares the UVGI Cost Efficiency (CE), which is the kill rate divided by the annual cost, for 33 typical systems, arranged from left to right in order of kill rate. Power is uncontrolled in these systems – they are simply selected as representative “off-the-shelf” systems. Systems with high CE values, around 0.03 or higher, are characterized by power levels that are appropriate for the intended kill rate. Overpowered systems typically have a low rating.

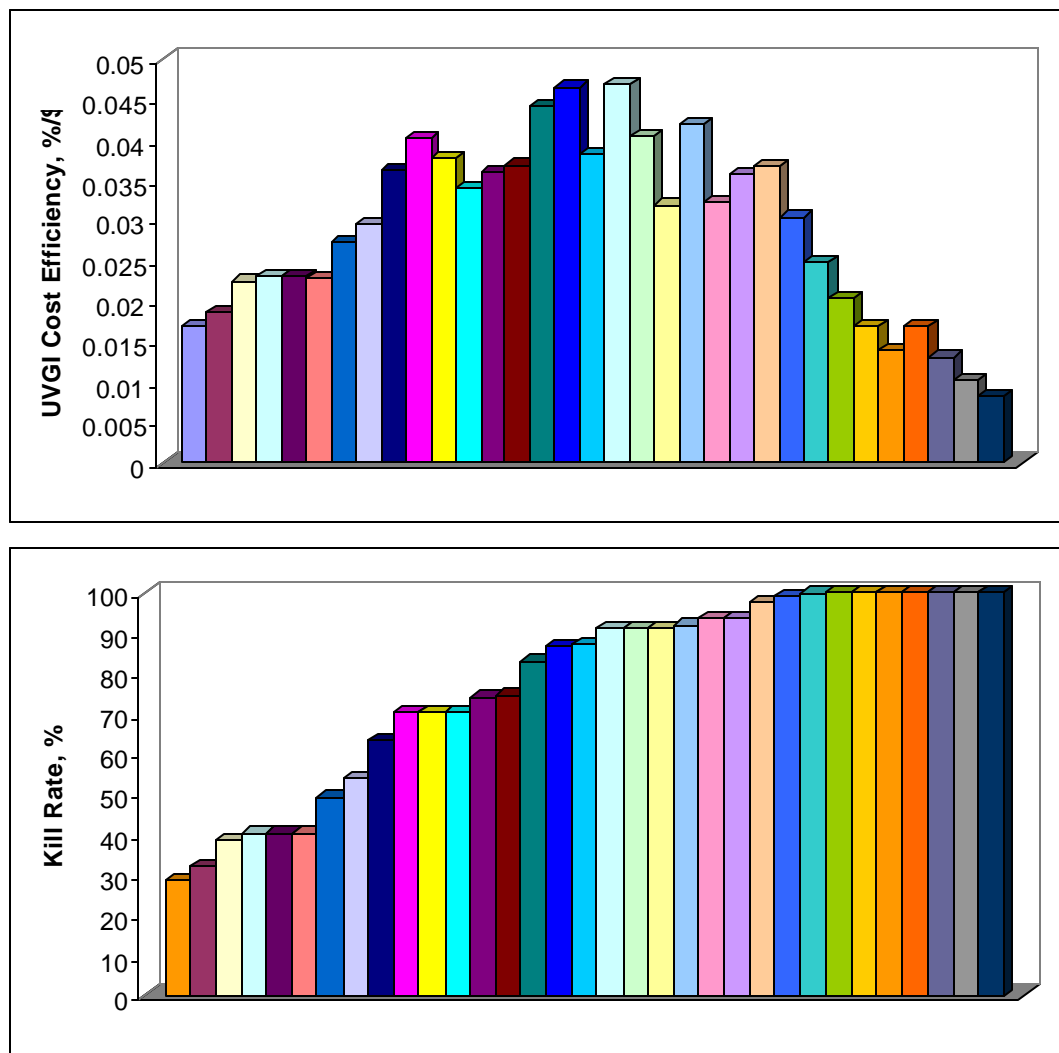


Figure 10.12a and 10.12b: UVGI Cost Efficiency for Typical Systems (upper). Lower figure shows the resulting kill rates for comparison.

The CE values are based on kill rates for *Serratia marcescens* and the annual cost summaries, along with program results, are shown in Appendix Q. One of the conclusions of this survey, apart from the fact that there is wide divergence in the cost and effectiveness of systems, is that the cost of increasing lamp power brings diminishing returns in terms of kill rates. Clearly, as the kill rate approaches the upper 90% range, the cost efficiency (and the cost) decrease. In comparison, the costs and results of increasing reflectivity show approximately linear responses.

The cost efficiency CE can be evaluated in terms of the dimensionless parameters, but only two of the dimensionless parameters figure significantly in the cost of a UVGI system, the power term C and the reflectivity G . The lamp aspect ratio has an insignificant effect on the

pressure loss, which is itself almost insignificant in the total life cycle cost. The aspect ratio does not reflect the duct area and so does not play a part in the cost.

Only the parameters C, the specific dose, and G, the reflectivity, can be individually evaluated against CE. The specific dose C, however, contains the power P the duct length L, and the airflow Q, each of which has different costs associated with it. No specific values of either the dimensionless parameters or the variables themselves can be used to define the critical point of the optimum, since they are highly dependent on factors like the cost of ductwork, the reflectivity, and even the fan power. It can only be concluded that there exists some unique combination of variables for any given system at which an optimum will occur, and beyond which the cost efficiency will decrease.

10.2.5 Economic Optimization of Recirculation UVGI Systems

Based on equation (10-24) only five variables contribute to the life cycle cost of a UVGI system and they are P, Q, W, H, and ρ . The other variables have no cost associated with them and only affect the performance. At least two approaches could be used here for optimization – the calculus method and the exhaustive search.

A comparison of the life cycle costs is valid only if the performance of different UVGI systems is essentially identical and if they disinfect equal quantities of air. Therefore the airflow Q must be held constant. The performance will be assumed equivalent if the systems produce a high rate of air disinfection, say approximately 85-99%. Furthermore, it is already known from the performance evaluations that the aspect ratio should ideally be 1.0, or square, and since this makes for great convenience mathematically, we will assume $W = H$. Equation (10-24) becomes:

$$AC\$ = \begin{cases} 11.47P - 0.00502P^2 + \frac{11168Q^3}{W^4} + 0.0522Q + 118.19 \\ + (0.0001095 + 0.0000193r)L(2W) + 0.0089W^2 \end{cases} \quad (10-25)$$

It is obvious that the calculus approach, which requires partial derivatives to be taken and the result set equal to zero, will not produce a solvable equation because of the number and type of variables. Furthermore, and realistically, the air velocity should be held constant since both the filters and the UVGI lamps have a design velocity specified. This requires both Q and W^2 to be held constant and allows us to optimize P and L. Selecting $Q = 390 \text{ m}^3/\text{min}$ and $W = H = 160 \text{ cm}$, we have:

$$AC\$ = \begin{cases} 11.47P - 0.00502P^2 + 1011 + 20.36 + 118.19 \\ + (0.0001095 + 0.0000193r)L(320) + 228.25 \end{cases} \quad (10-26)$$

Simplifying we get:

$$AC\$ = 11.47P - 0.00502P^2 + (0.03504 + 0.006176r)L + 1467.8 \quad (10-27)$$

This relation is used to assess the optimums for Length and Width later in this chapter. First, we examine the optimums for all the variables that factor into the costs, as an exercise in understanding the relationships. Here we examine a square duct and the Cost Efficiency (CE) for L vs. P, ρ vs. P, L vs. ρ , P vs. Q, L vs. Q, Q vs. ρ , W vs. P, W vs. L, and W vs. Q. The range of variable values is summarized for convenience in Table 10-3.

Table 10-3: Range of Variables for Cost Efficiency Evaluation

Increment #	Length cm	Power UV Watts	Reflectivity %	Airflow m ³ /min	Width cm	Height cm
1	100.0	16.0	54.0	100.0	160	160
2	166.7	21.3	58.4	164.4	160	160
3	233.3	26.7	62.7	228.9	160	160
4	300.0	32.0	67.1	293.3	160	160
5	366.7	37.3	71.5	357.8	160	160
6	433.3	42.7	75.8	422.2	160	160
7	500.0	48.0	80.2	486.7	160	160
8	566.7	53.3	84.6	551.1	160	160
9	633.3	58.7	88.9	615.6	160	160
10	700.0	64.0	93.3	680.0	160	160

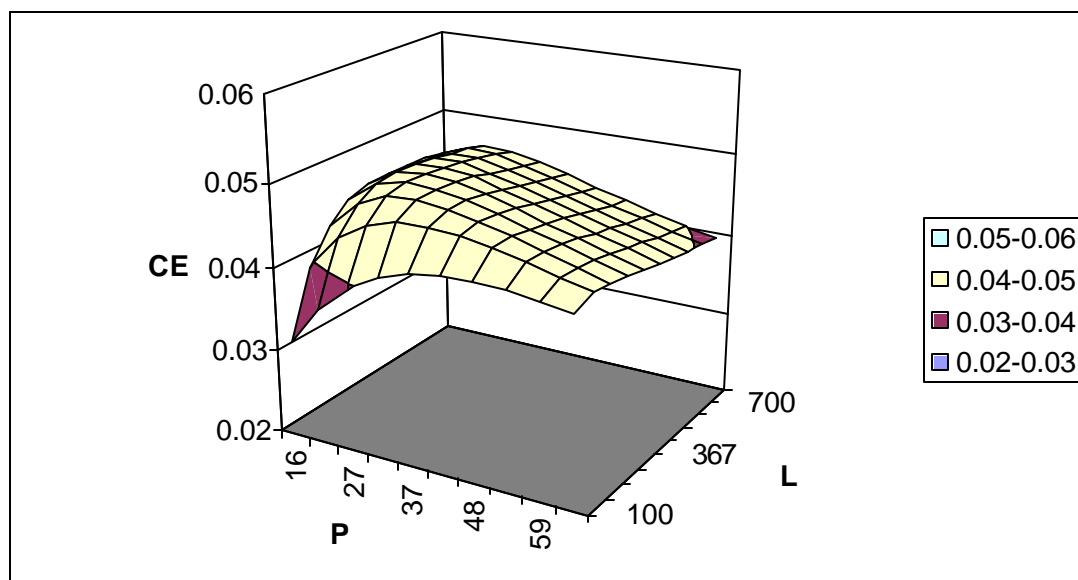


Figure 10.13: Response Surface for the Cost Efficiency (CE) of Length vs. Power

Figure 10.13 shows the CE for Length vs. Power with all other variables held constant. It has a reasonably well-defined optimum (high CE) at a Power value of about 26.7 (the 3rd

increment in Table 10-4) and a Length of between 300 cm (the 4th increment in Table 10-4) and 366.7 cm (the 5th increment in Table 10-4).

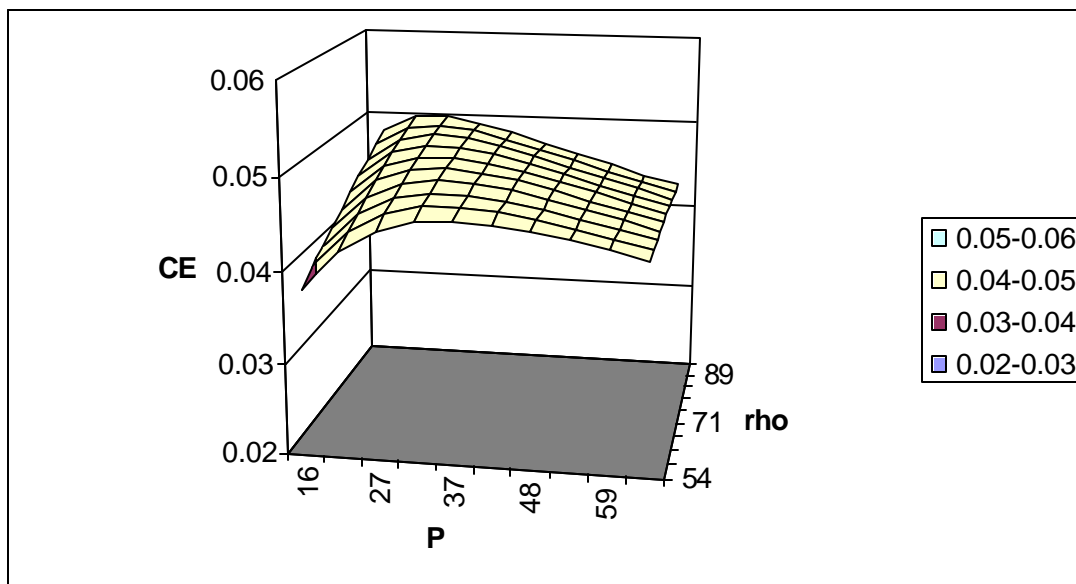


Figure 10.14: Response Surface for the CE of Reflectivity vs. Power

Figure 10.14 shows the CE values for Reflectivity vs. Power. The optimum clearly exists at the highest reflectivity, 93%, and with an optimum power between 21.3 and 26.7 watts, or about 24 watts if we interpolate. Notice how the optimum power shifts higher for lower reflectivity.

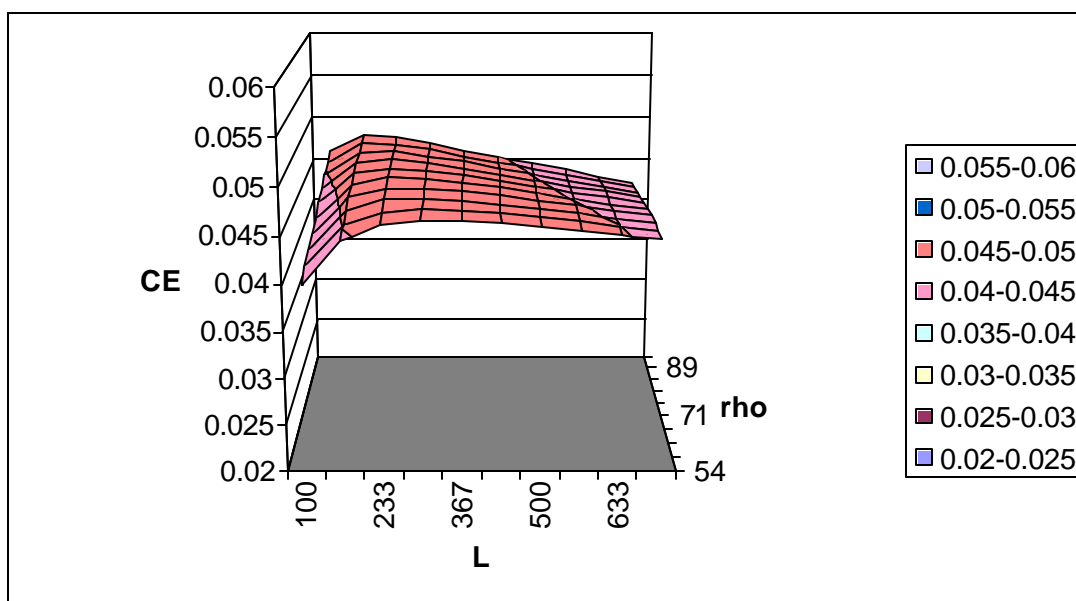


Figure 10.15: Response Surface for CE of Reflectivity vs. Length

Figure 10.15 shows that the optimum CE exists at maximum reflectivity (93%) and a length of 166.7 cm. This length is, of course, relative to the duct size of 160 cm by 160 cm.

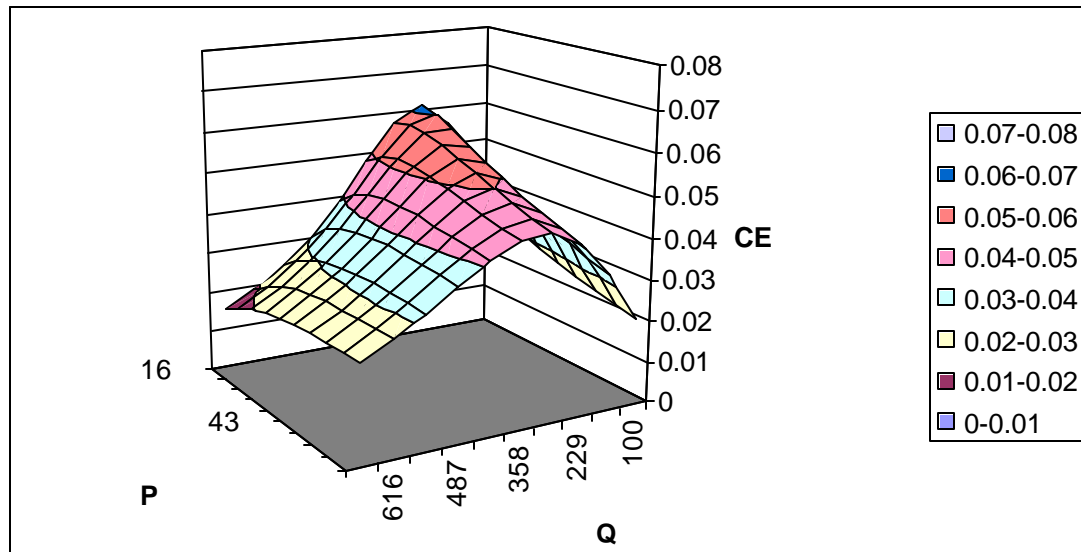


Figure 10.16: Response Surface for CE of Airflow vs. Power

Figure 10.16 indicates that an optimum exists at an airflow of $293.3 \text{ m}^3/\text{min}$ and minimum power at 16 UV watts. The airflow, and therefore the air velocity at the constant square duct width, is varied in this example as a test of the methods and the system. The airflow in this example is rated on a per volume basis, so that it represents the cost of disinfection per unit volume. Normally, airflow is defined by the face area and the filter or lamp design velocity and so this example is for illustrative purposes only and can not be directly applied to system design due to violation of the velocity restrictions.

This example does, however, suggest that an optimum airflow must exist for any system on a per volume basis. The volumetric flowrate in this case proves to be lower than the design flowrate of $390 \text{ m}^3/\text{min}$ and so this system does not perform the same amount of air disinfection. The optimum here mainly reflects the fact that pressure losses through the filter are lower at low velocity.

This airflow optimum also ignores the cost of space, which has an unknown value but is dependent on local conditions or limitations. Reducing the airflow, as in this example, might indeed lower overall annual costs but the system would have to be sized larger to provide the full airflow of $390 \text{ m}^3/\text{min}$. The system would effectively be saving energy by reducing pressure loss through the filter but this may only be feasible where space is not at a premium and where the UV lamp output is unaffected by lowered air velocity.

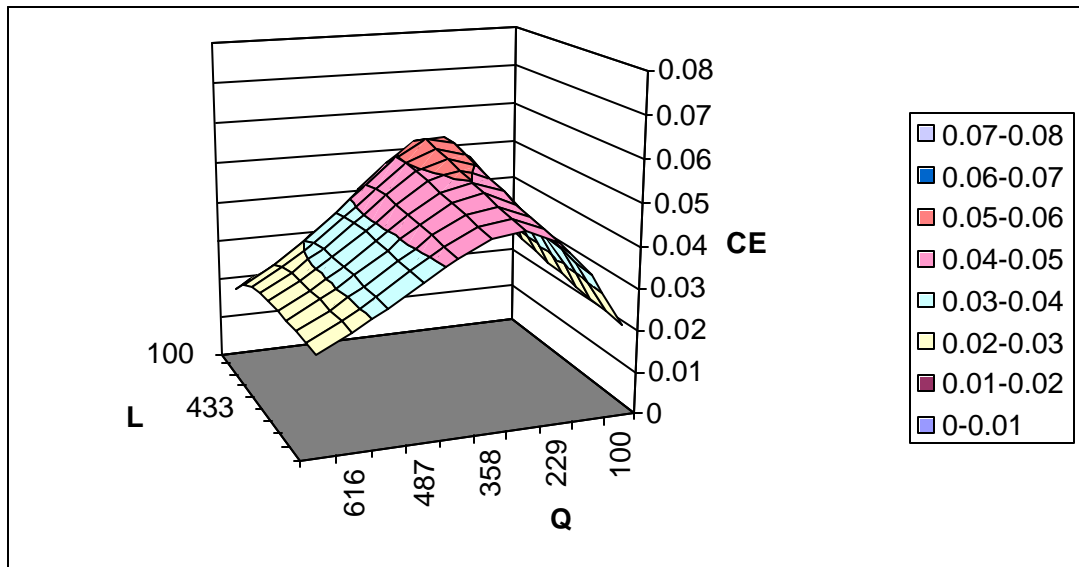


Figure 10.17: Response Surface for CE of Airflow vs. Length

Figure 10.17 also shows that an optimum airflow exists, on a per volume basis, and that it is essentially independent of the length of the ductwork. In gain, this example is illustrative only and the design velocity of the lamp and filters, typically 500 fpm, should preferably be used unless it can be otherwise justified.

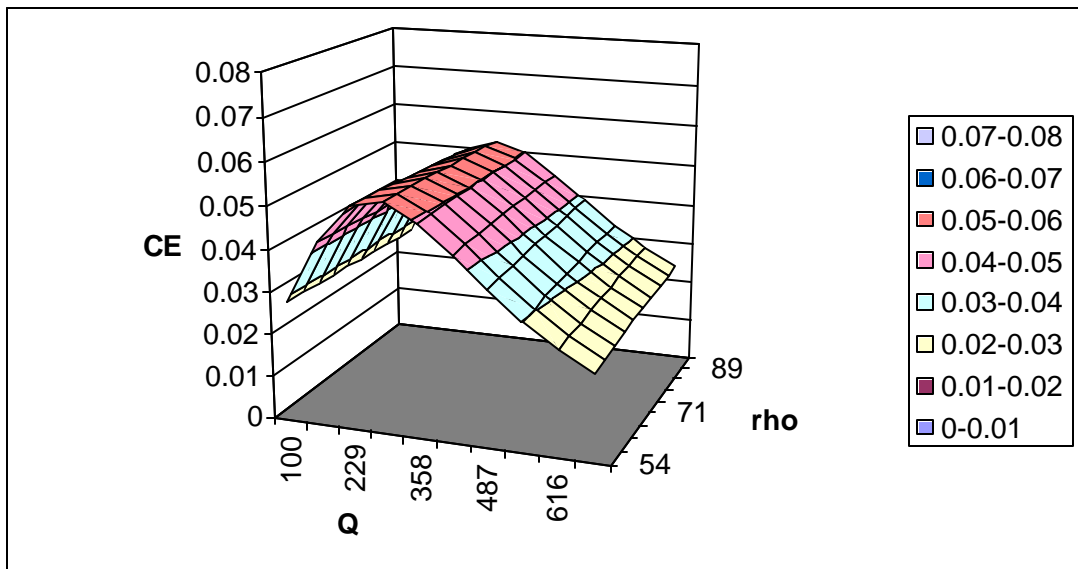


Figure 10.18 : Response Surface for CE of Airflow vs. Reflectivity

Figure 10.18 confirms that the airflow has an optimum value for any given system on a per volume basis, and it is likely that this is true for most, if not all, systems. We also observe that maximum reflectivity is optimum, as we have seen previously in all comparisons.

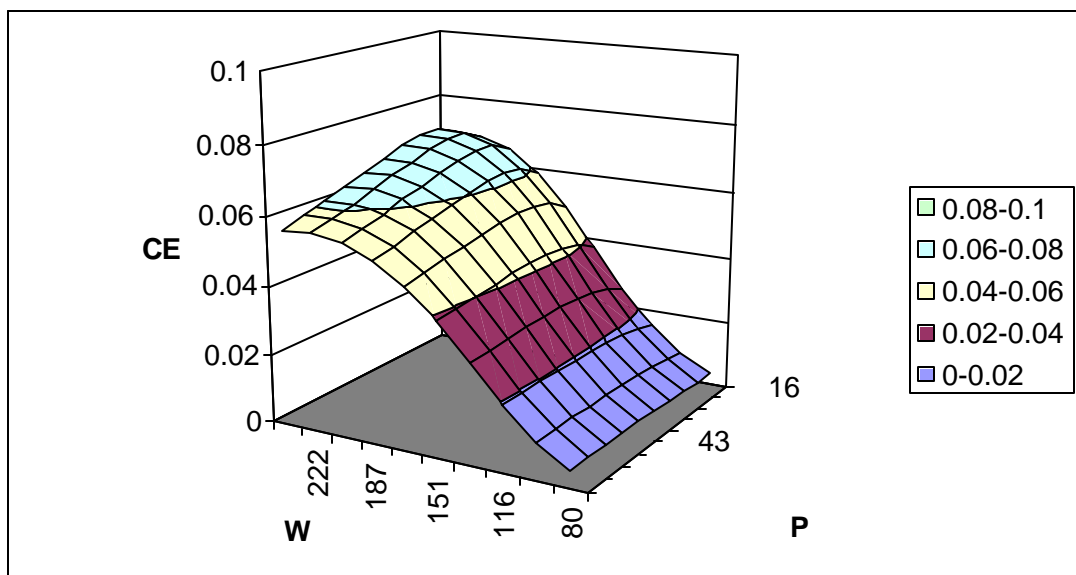


Figure 10.19: Response Surface for CE of Power vs. Width of Square Duct

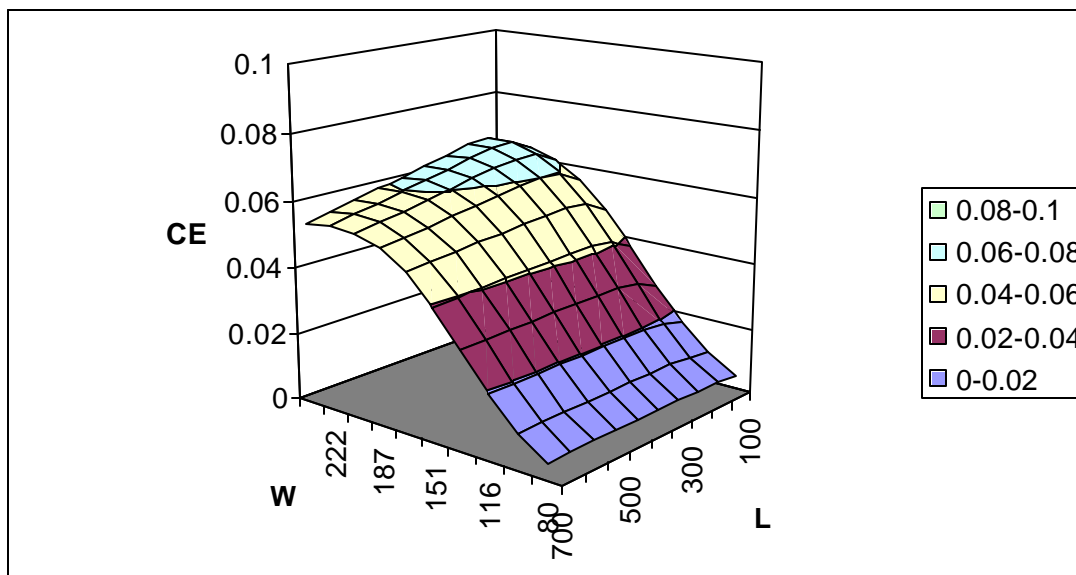


Figure 10.20: Response Surface for CE of Length vs. Width of Square Duct

From Figure 10.19, 10.20, 10.216, and 10.22 we can observe the existence of an optimum for any parameter (power, length, airflow, and reflectivity, respectively) associated with the maximum width. Of course, the maximum widths that show up as optimum are due to lowered

air velocity through the filter and the associated decrease in fan energy consumption. Since such large ducts would require excessive space and the cost of space isn't easy to generalize, these optimums are likely not practical. In addition, the filters and the lamps normally have a specified design velocity of 500 fpm (2.54 m/s) and it would be appropriate to maintain such criteria. In the event that space and design velocities were not constraints, it is clear that not only can costs be lowered with large face areas, but according to Figure 10.22, a definitive relationship exists between the optimum width and optimum airflow.

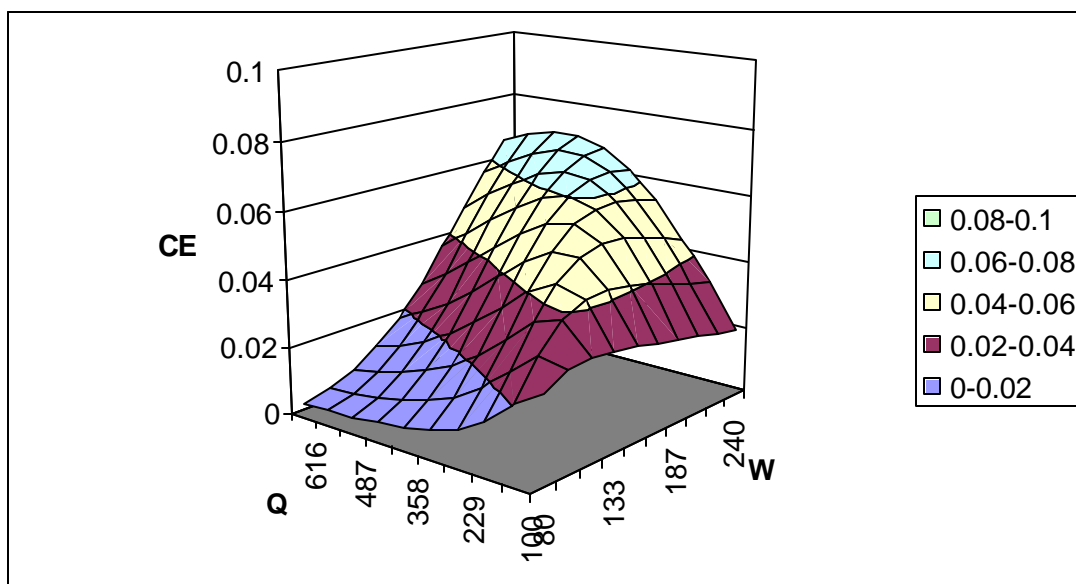


Figure 10.21: Response Surface for CE of Width vs. Airflow for Square Duct

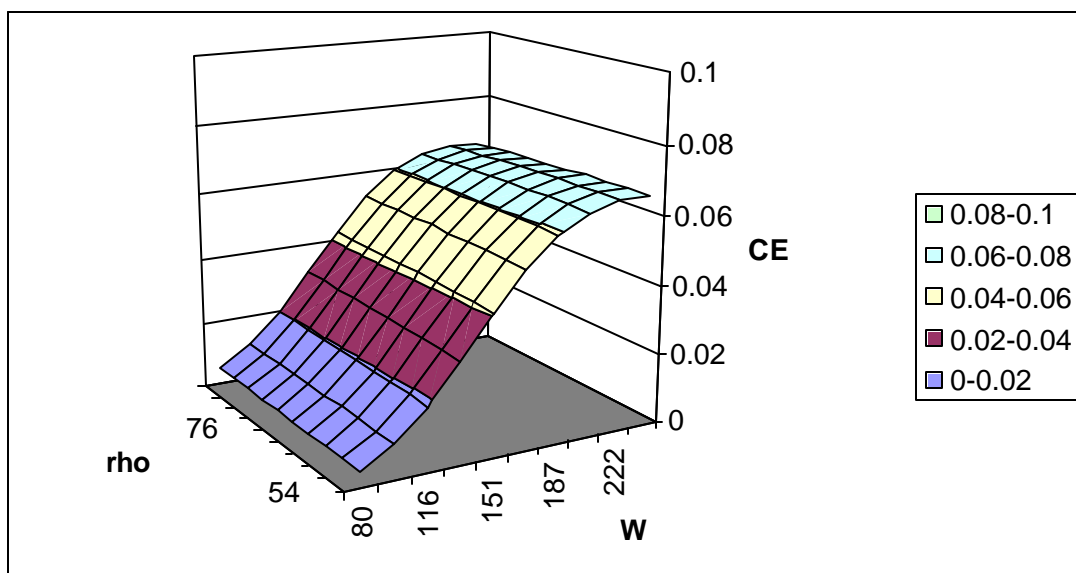


Figure 10.22: Response Surface for CE of Width vs. Reflectivity for Square Duct

Real world applications require certain constraints, such as the design velocity and minimization of space usage. Furthermore, some minimum disinfection criteria may be required for certain applications. Therefore, as a practical example of the optimization methods developed here a system is optimized for a given square duct of 160 cm width, a given airflow of 390 m³/min, a design face velocity of 500 fpm (2.54 m/s), and a disinfection rate of around 95%.

Using equation (10-27) and the program output, Figure 10.23 and Figure 10.24 have been compiled to represent the Cost Efficiency at two different values of reflectivity, 75% and 93%. Kill rates were approximately 95% at the optimum and beyond. The input data are summarized in Appendix U.

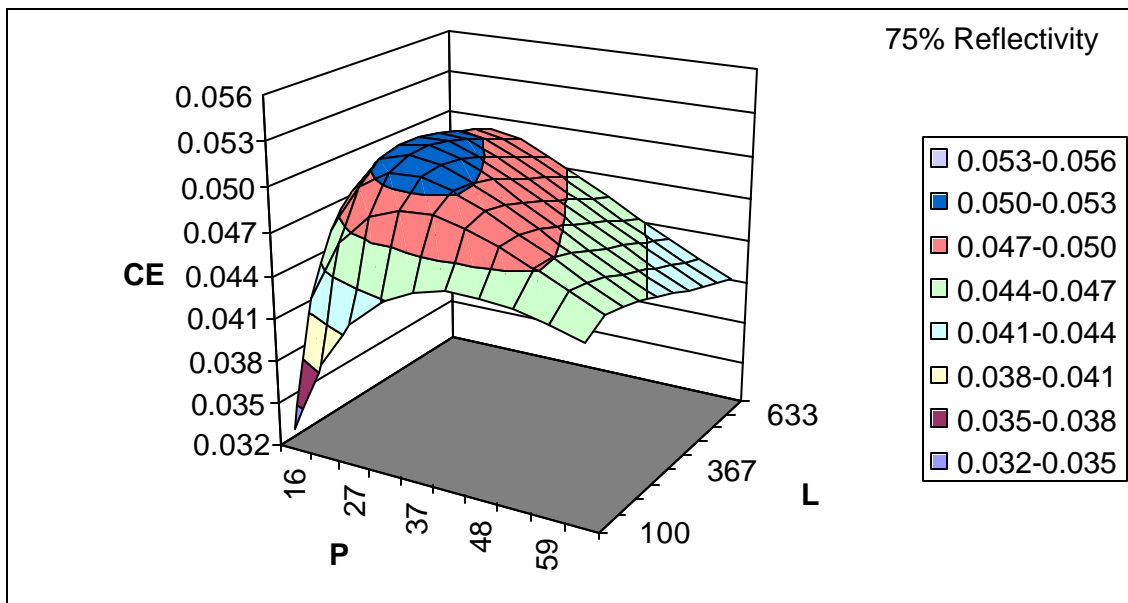


Figure 10.23: CE for Square Duct of Constant Area and Velocity, 75% Reflectivity

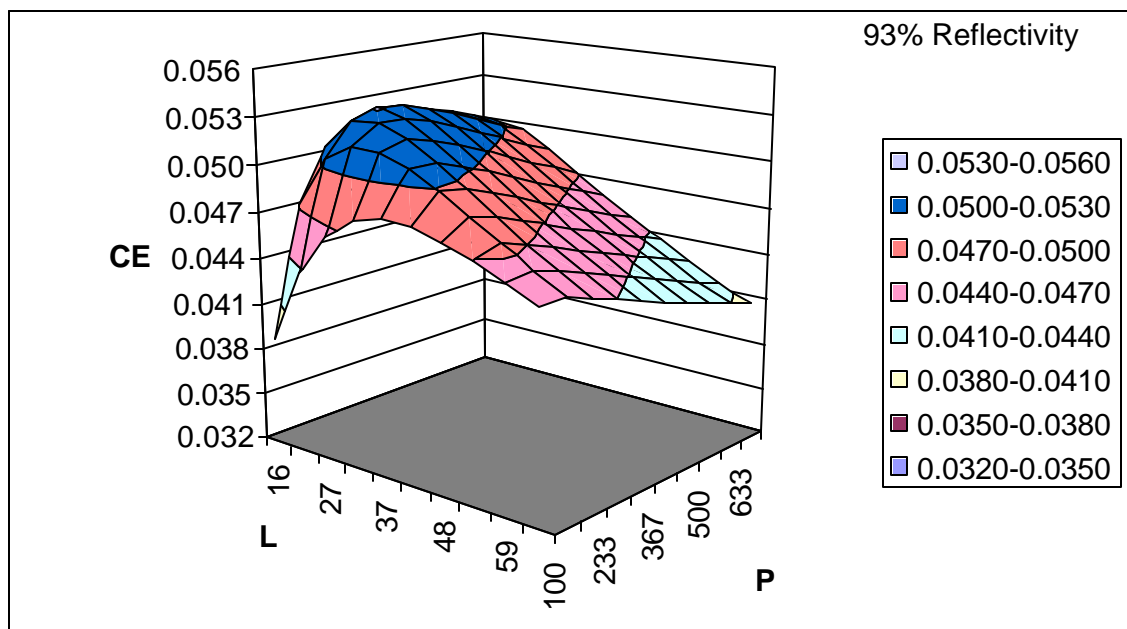


Figure 10.24: CE for Square Duct of Constant Area and Velocity, 93% Reflectivity

It can be observed in Figure 10.23 and Figure 10.24 that a definite optimum exists for the configuration as defined and the reflectivity as indicated on the charts. These optimums only apply to this particular case, and are sensitive to the material and energy costs, but it does suggest that a definite optimum exist for any given set of input parameters. For 75% reflectivity, power is optimized at 29.5 watts of UV power, and a length of 333 cm, after interpolation. For 93% reflectivity, the optimum exists at a power of 29.5 UV watts and a length of 200 cm. Obviously the increased reflectivity has resulted in the economics favoring a decreased length.

One final example is presented as a test of the sensitivity of the optimization model to the cost of electrical energy. Although material costs may also affect the optimization, they vary widely and are often subject to choice, while energy costs may be an inescapable fact of geographic location. The previous examples are based on energy and cooling costs for a Philadelphia location, and a comparison with a Los Angeles location, when energy costs are currently extreme, provides an interesting example of the optimization model sensitivity.

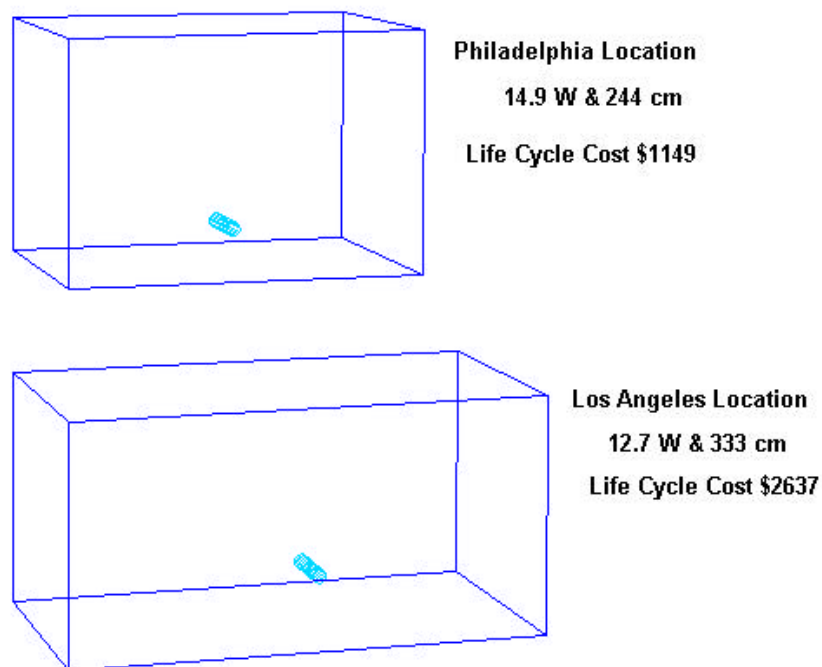


Figure 10.25: UVGI Systems Optimized for Different Geographic Locations

Figure 10.25 illustrates the sensitivity of the optimization model to energy costs. The Philadelphia location, which has a typical energy cost of 0.035 \$/kWh and cooling requirements about 70% of the year, produces a shorter duct with higher UV power. The Los Angeles location, with current energy costs of about 0.135 \$/kWh and cooling requirements about 95% of the year produces an optimal design that is longer and has lower lamp power. Both systems produce a 92% disinfection rate, but the LA system is obviously more than twice as expensive to own and operate.

10.2.6 Performance of Multiple Lamp and Axial Configurations

The previous performance and economic evaluations are based on single lamp configurations in which the lamps are in the crossflow configuration, in which lamps are aligned perpendicular to the direction of airflow. Two major variations are addressed here – multiple lamp configurations and axial lamp configurations.

When multiple lamps are placed centrally in a duct in crossflow configurations, as is commonly the case, it has been found that results do not differ significantly from the use of a single lamp with the same total wattage. This is implied in Figure 10.6e, which is a graph of the kill rates as a function of the parameter y/H compared with all other parameters. It can be

observed that in the y/H range of approximately 0.25 to 0.5 (or the span of the entire width from 0.25 to 0.75), that performance is essentially unchanged. This means that placement of a lamp anywhere in this range will produce approximately the same result. If the lamp is divided into several smaller lamps of equal total wattage, we would expect the performance to be approximately additive. This would not be true, however, if the lamps were located in proximity to the reflective surfaces, where the proximity effect would increase the average intensity field and the system performance.

It has been shown that the placement of a lamp near the sides, and the use of shorter lamps with one end at the side of a surface can boost the average intensity field and the kill rates. This result is, however, based on the assumption of complete mixing. Although real world systems approach complete mixing, there is no guarantee that this limiting condition will be reached. Therefore, the use of a single lamp in only one corner may not necessarily produce the full benefits in the kill rate since microbes passing through the opposite corner, for example, may not receive the average dose. A practical means of dealing with unevenly mixed flow is simply to use multiple lamps in more than one corner.

The axial lamp configuration, in which the lamp is aligned parallel to the airstream, is another possibility. Such designs are occasionally used but they invariably locate the lamps in the center of the duct, whether rectangular or round. Analysis shows that the proximity effect can be used to advantage for axial lamp configurations as well. In principle, the axial lamp should be placed nearer the sides or in the corner for maximum effect. The same problem with incomplete air mixing could be highlighted by such a configuration if only one lamp is used. Therefore, as a hedge against poor mixing, for axial lamp configurations that are optimized with corner or side locations, multiple lamps should be used.

Both of the above configurations have been analyzed using the proprietary version of the program (the UVD program). The UVX program is quite capable of analyzing multiple lamps and is set up to do so (in the Analysis() subroutine in Appendix G) except for the data input routine (the DataInput() subroutine in Appendix G) must be modified to read the lamp data and the defining coordinates for each lamp.

Figure 10.26 shows the results of analysis of multiple lamps in crossflow and multiple axial lamps compared against each other and with single lamp configurations. The total lamp wattage is 8 UV watts in all cases. The lamp lengths are divided up by the number of lamps. That is, the single lamp is 20 cm long while the double lamps are 10 cm long, etc. The duct is square with 40 cm sides and is 80 cm in length. For this particular case, the single lamp in one corner produces the highest average intensity field, whether in crossflow (1c) or axial configuration (1ac). The four-lamp crossflow configuration (4c), in which the lamps are located in the four corners, produces slightly less average intensity than the single lamp (1c) arrangement, however, as

explained previously, this configuration may be superior in real world situations where air mixing is not quite complete.

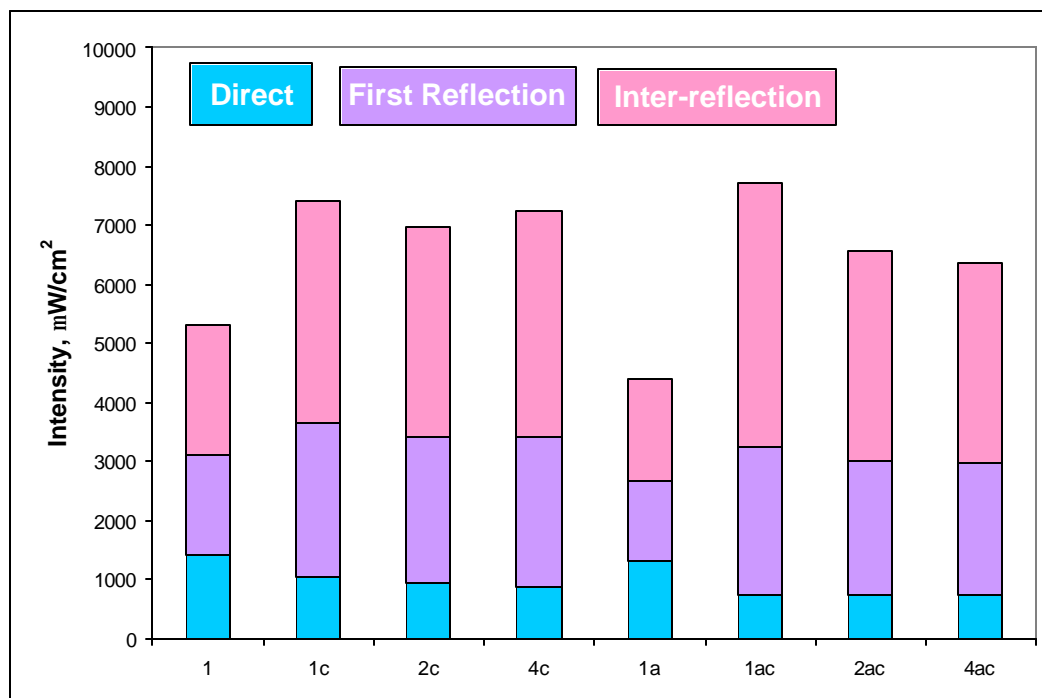


Figure 10.26: Comparison of Multiple Lamp Configurations in crossflow and axial arrangements. Number indicates number of lamps. The letter 'c' signifies corner location, while the letter 'a' signifies an axial lamp configuration.

Although the single corner axial lamp configuration (1ac) produces the highest overall average intensity, it may be subject to the same problem of incomplete mixing in real world situations. The multiple lamp version of the axial configuration (4ac) produces less overall average intensity than the crossflow arrangement (4c) and so the optimum configuration may be the four lamp crossflow arrangement (4c). This is, of course, a somewhat speculative choice and remains to be verified by actual laboratory tests.

Chapter 11. Summary and Conclusions

This research has demonstrated a methodology for predicting the effectiveness of UVGI systems for disinfecting air and surfaces. The method allows more accurate prediction of kill rates than has previously been possible. The success of the model permits cost-effective systems to be designed on computers. This method also facilitates the determination of UVGI rate constants from airborne laboratory tests.

The program written to do the analysis has an estimated error of less than +/-15% in most cases. The program results have elucidated the effects of all design parameters to the point that new principles can now be used to improve the design of UVGI systems. One of the principles identified is here termed the proximity effect, which describes the fact that positioning lamps closer to reflective surfaces tends to boost overall average intensity, and therefore boosts kill rates, for any system which approaches the limits of complete air mixing. The proximity effect can be manipulated to boost system efficiency by as much as 15-30% for single lamp systems, based on the results of this research. It also entails no significant cost as it involves lamp position only. For multiple lamp systems the efficiency gains may be even higher.

Given the program's ability to interpret UVGI rate constants, these can now be more accurately established for microbes than has previously been possible. It is hoped that the availability of the software and mathematical models presented here will stimulate new research and finally resolve the airborne rate constants for the entire array of known airborne pathogens. These methods can also be used to finally establish the effect of Relative Humidity on the rate constants of airborne pathogens, a subject that has been enveloped in debate and confusion for decades. Thanks to these design tools, such information could be acquired for much less cost and difficulty than has previously been possible. The data acquired on rate constants and Relative Humidity effects would be a boon for designers and may even lead to further improvements in UVGI system design.

This thesis includes the first attempt to perform dimensional analysis for UVGI systems and has identified eight dimensionless parameters that together can determine the effectiveness of any UVGI system. The optimum dimensionless parameters have been shown to be mostly unimodal with distinct values corresponding to maximum kill rates. Application of the program results have produced a linear regression model that can be used to estimate system disinfection rates, although the accuracy is limited, particularly in the high kill rate range above 90%.

Figure 11-1 summarizes the values of the dimensionless parameters that will optimize performance for single lamp systems. It is likely that these same optimums apply to multiple lamp systems but this subject remains to be studied in more detail.

The economics of a UVGI system are dependent only those variables that contribute to defining the Life Cycle cost of a UVGI system – W, H, L, P, Q, and ρ . The costs associated with

these variables can be highly variable depending on quantities and system size, and therefore only examples of cost optimization could be given here. These examples, presented in Chapter 10, indicate that optimum values exist for the power and length of any system, given any reflectivity, design air velocity, and disinfection criteria. These optimums can be determined by evaluating the system with the methods shown, using whatever specific cost data is applicable to the system under consideration.

It has been furthermore demonstrated that the sensitivity of the optimization model to energy costs can result in systems of different size and lamp power. An example provided shows that higher electrical energy costs may result in systems with longer ductwork and lower lamp power.

Table 11-1: Optimum Values for Dimensionless Parameters

Parameter		Optimum
$\frac{W}{H}$	Aspect Ratio	1.0
$\frac{r}{l}$	Lamp Aspect Ratio	None
$\frac{kPL}{Q}$	Power term	Maximum
$\frac{x}{W}$	X Ratio	Minimum
$\frac{y}{H}$	Y Ratio	Minimum
$\frac{z}{L}$	Z Ratio	0.5
ρ	Reflectivity	Maximum
$\frac{L(W+H)}{L(W+H)+WH}$	Area Fraction	Maximum

The criteria for optimizing Cost Efficiency can be summarized as follows:

- ❖ Maximum reflectivity improves Cost Efficiency
- ❖ Length has some optimum value for any given set of parameters
- ❖ Power has some optimum value for any given set of parameters
- ❖ Exceeding the optimum values will cause a decrease in Cost Efficiency

In general, a high Cost Efficiency correlates with a high kill rate, but this may not always be the case. If a criteria for kill rates is specified, then the concept of cost efficiency could be applied to the comparison of all systems that satisfy this criteria.

As noted previously, the air velocity should be maintained at the design value for the filters and the lamps, and this is typically 500 fpm. If the air velocity were not constrained, then expanding the duct face area can decrease costs but would also impact the cost of space, for which values can be application specific, or for which definite limits on size may be imposed externally.

The energy analysis and life cycle costs analyzed here make it clear that the bulk of the energy consumption of a UVGI system will often be due to the filter pressure losses. Since filters are used to maintain the lamp cleanliness and allow peak performance, and also since they remove spores from the airstream, it is recommended that they always be used in conjunction with UVGI. However, it is clear from previous studies that the level of filtration commonly used, that is, HEPA filters, is often unnecessary since lower efficiency filters will perform just as well for the intended purposes. The key to improving the energy efficiency of UVGI systems beyond that demonstrated in the current research is to control filter pressure losses, either by selecting more appropriate filters or by developing new types of filters that more precisely complement UVGI system performance.

The development of the dimensionless parameter called the area fraction proved to be useful as a means of controlling aspects of the performance evaluation that could have distorted some results. The area fraction cannot normally be varied without affecting system dimensions. Holding the area fraction constant allowed for valid comparisons to be made between the systems studied in this research. The area fraction can be independently varied only through the use of light baffles, which do not affect duct dimensions but enclose more surface area.

The possibility of improving system performance by use of the area fraction exists implicitly for the application of light baffles. Light baffles have previously been used to trap light and prevent its escape from the irradiation chamber, but they could clearly be applied to enhance the internal intensity field. The use of light baffles enables the manipulation of the dimensionless area fraction to seek improved system performance. This matter is left as an area of future research and requires the development of analytical tools beyond those used in this research.

Multiple lamp configurations have been reviewed as a means of dealing with situations in which the airflow may not be completely mixed. Analysis of multiple lamp configurations suggest that location of lamps in all four corners, in which the lamps were of shorter lengths and same total UV wattage, would provide a hedge against poor air mixing, and may therefore represent an optimum configuration.

Axial lamp configurations, both single and multiple, were also shown to have improved performance when located near the corners. An axial lamp configuration, with a single lamp located in the corner, has been shown to be slightly superior to a crossflow arrangement with a single lamp in the corner. This type of arrangement, however, may be subject to losses in predicted performance under conditions of poor air mixing. Multiple axial lamp configurations, with the lamps located in the corners produced performance that approached that of multiple lamps in a crossflow configuration where the lamps were located in the corners.

The principles of design that have been developed by this analysis have been applied to the proposed design of a UVGI system as shown in Figure 10.1. This system represents one possible configuration of an optimized design. This unit has a square cross-section and a length to width ratio of 5:1. Unlike current UVGI systems, this proposed prototype places short lamps in all four corners, taking full advantage of the proximity effect. It also employs light baffles at the inlet and outlet, increasing the effective area fraction without significantly increasing system size. The baffles require optimizing so as to minimize the constriction of airflow. Ideally, the most reflective material available, and that would be ePTFE, would be used on all the inside surfaces, including the inside of the light baffles, to maximize the benefits of reflectivity.

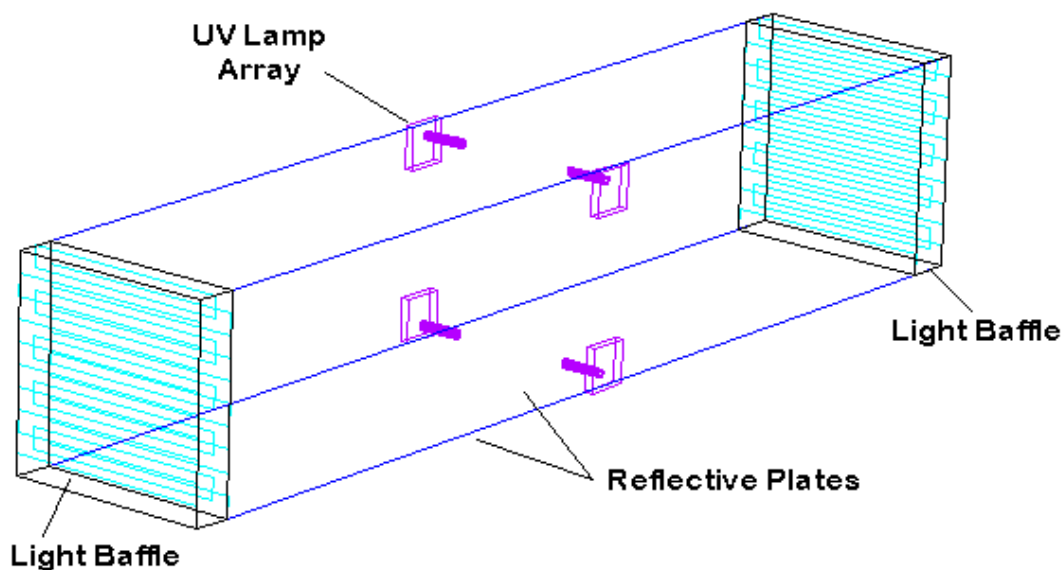


Figure 11.1: Proposed Configuration of an Optimized UVGI System employing light baffles at the inlet and outlet, and internal reflective plates

Areas of further research remain from both limitations of present knowledge and from the fact that new areas of research and improvement of current research are now possible with these

research and design tools. The following modeling tools would enhance program capability and create more flexibility and extend applicability to essentially all types of UVGI air and surface disinfection applications:

- A specular reflective model
- A combined specular & diffuse reflective model
- A model to handle more complex geometries
- A model to handle the design of light baffles

All of the above items could be completed by the development of a ray tracing routine, or a program that uses probabilistic ray tracing to determine the intensity field inside enclosures of any shape or size. This routine would augment the existing view factor routines that currently drive the program, and provide solid ground for corroborating results.

Studies of the airflow dynamics inside UVGI systems need to be performed to establish the exact distance and orientation of UV lamps that will produce the least pressure losses and greatest kill rates. It may be necessary to use computational fluid dynamics software for this purpose.

The areas of research that remain to be pursued are summarized here:

- ❖ Development of a Ray Tracing Program
- ❖ Computational Fluid Dynamics Studies on airflow inside UVGI chambers
- ❖ Further study of multiple lamp and axial lamp configurations
- ❖ Study of the proximity effect as a possible function of local intensity fields and kill rates
- ❖ Aerosolization studies of bacterial rate constants
- ❖ Studies of the effect of Relative Humidity on rate constants
- ❖ Development and application of new highly reflective materials such as ePTFE
- ❖ Establishment of guidelines for acceptable levels of airstream disinfection criteria
- ❖ Research and development of filtration systems that complement UVGI performance and reduce energy costs

Finally, it is our hope at Penn State that an actual prototype system designed according to the principles established herein will be built and tested to verify the expected performance improvements and energy savings, and that this will lead to reduced costs for general applications in the industry, thereby contributing to the reduction of disease and the preservation of public health worldwide.

References

- Abshire, R. L., and Dunton, H. (1981). "Resistance of selected strains of *Pseudomonas aeruginosa* to low-intensity ultraviolet radiation." *Appl. Envir. Microb.*, 41(6), 1419-1423.
- Ager, B. P., and Tickner, J. A. (1983). "The control of microbiological hazards associated with air-conditioning and ventilation systems." *Ann. Occup. Hyg.*, 27(4), 341-358.
- AIA. (1993). "Guidelines for construction and equipment of hospital and medical facilities." Mechanical Standards, Amer. Inst. of Architects, ed., Washington.
- Allegra, L., Blasi, F., Tarsia, P., Arosio, C., Fagetti, L., and Gazzano, M. (1997). "A novel device for the prevention of airborne infections." *J. Clinical Microb.*, 35(7), 1918-1919.
- Allen, E. G., Bovarnick, M. R., and Snyder, J. C. (1954). "The effect of irradiation with ultraviolet light on various properties of typhus rickettsiae." *J. Bact.*, 67, 718-723.
- Alpen, E. L. (1990). *Radiation Biophysics*, Prentice-Hall, Englewood.
- Alper, T. (1979). *Cellular Radiobiology*, Cambridge University Press, Cambridge.
- Anellis, A., Grecz, N., and Berkowitz, D. (1965). "Survival of *Clostridium botulinum* spores." *Appl. Microbiol.*, 13(3), 397-401.
- Antopol, S. C., and Ellner, P. D. (1979). "Susceptibility of *Legionella pneumophila* to ultraviolet radiation." *Appl. & Environ. Microb.*, 38(2), 347-348.
- ASHRAE. (1985). *Handbook of Fundamentals*, ASHRAE, Atlanta.
- ASHRAE. (1991). "Health Facilities." ASHRAE Handbook of Applications, ASHRAE, ed., Atlanta.
- Asthana, A., and Tuveson, R. W. (1992). "Effects of UV and phototoxins on selected fungal pathogens of citrus." *Int. J. Plant Sci.*, 153(3), 442-452.
- Austin, B. (1991). *Pathogens in the Environment*, Blackwell Scientific Publications, Oxford.
- AWWA. (1971). *Water Quality and Treatment*, McGraw-Hill, New York.
- Banrud, H., and Moan, J. (1999). "The use of short wave ultraviolet radiation for disinfection in operating rooms." *Tidsskrift for den Norske Laegeforening*, 119(18), 2670-2673.
- Beebe, J. M. (1958). "Stability of disseminated aerosols of *Pastuerella tularensis* subjected to simulated solar radiations at various humidities." *Journal of Bacteriology*, 78, 18-24.
- Bishop, J. M., Quintrell, N., and Koch, G. (1967). "Poliovirus double-stranded RNA: Inactivation by ultraviolet light." *J. Mol. Biol.*, 24, 125-128.
- Blatchley, E. F. (1997). "Numerical modelling of UV intensity: Application to collimated-beam reactors and continuous-flow systems." *Wat. Res.*, 31(9), 2205-2218.
- Braude, A. I., Davis, C. E., and Fierer, J. (1981). "Infectious Diseases and Medical Microbiology, 2nd Edition." W. B. Saunders Company, Philadelphia.
- Casarett, A. P. (1968). *Radiation Biology*, Prentice-Hall, Englewood.
- Castle, M., and Ajemian, E. (1987). *Hospital infection control*, John Wiley & Sons, New York.
- Cerf, O. (1977). "A review : Tailing of survival curves of bacterial spores." *J. Appl. Bact.*, 42, 1-19.
- Chick, H. (1908). "An investigation into the laws of disinfection." *J. Hygiene*, 8, 92.
- Coggle, J. E. (1971). *Biological effects of radiation*, Wykeham Publ., London.
- Collier, L. H., McClean, D., and Vallet, L. (1955). "The antigenicity of ultra-violet irradiated vaccinia virus." *J. Hyg.*, 53(4), 513-534.
- Collins, F. M. (1971). "Relative susceptibility of acid-fast and non-acid fast bacteria to ultraviolet light." *Appl. Microbiol.*, 21, 411-413.
- Collins, C. H. (1993). *Laboratory-acquired Infections*, Buterworth-Heinemann Ltd., Oxford.
- Corporation, C. (1999). *Selection Guide: Ultraviolet Germicidal Lamp*, .
- Darken, M. A., and Swift, M. E. (1962). "Effects of ultraviolet-absorbing compounds on spore germination and cultural variation in microorganisms." *Applied Microbiology*, 11, 154-156.
- David, H. L., Jones, W. D., and Newman, C. M. (1971). "Ultraviolet light inactivation and photoreactivation in the mycobacteria." *Infect. and Immun.*, 4, 318-319.
- David, H. L. (1973). "Response of mycobacteria to ultraviolet radiation." *Am. Rev. Resp. Dis.*, 108, 1175-1184.
- Davidovich, I. A., and Kishchenko, G. P. (1991). "The shape of the survival curves in the inactivation of viruses." *Mol. Gen., Microb. & Virol.*, 6, 13-16.

- DeGiorgi, C. F., Fernandez, R. O., and Pizarro, R. A. (1996). "Ultraviolet-B lethal damage on *Pseudomonas aeruginosa*." *Current Microb.*, 33, 141-146.
- Dring, G. J., Ellar, D. J., and Gould, G. W. (1985). *Fundamental and Applied Aspects of Bacterial Spores*, Academic Press, London.
- Dumyahn, T., and First, M. (1999). "Characterization of ultraviolet upper room air disinfection devices." *Am. Ind. Hyg. Assoc. J.*, 60(2), 219-227.
- Eisenstark, A. (1989). "Bacterial genes involved in response to near-ultraviolet radiation." *Advances in Genetics*, 26, 99-147.
- El-Adhami, W., Daly, S., and Stewart, P. R. (1994). "Biochemical studies on the lethal effects of solar and artificial ultraviolet radiation on *Staphylococcus aureus*." *Arch. Microbiol.*, 161, 82-87.
- Elasri, M. O., and Miller, R. V. (1999). "Response of a biofilm bacterial community to UV Radiation." *Appl. & Environ. Microbiol.*, 65(5), 2025-2031.
- Elmer, W. B. (1989). *The optical design of reflectors*, TLA Lighting Consultants, Inc., Salem, MA.
- Erhardt, L., and C.P.Steinmetz. (1977). *Radiation, Light, and Illumination*, Camarillo Reproduction Center, Camarillo.
- Fahlberg, W. J., and Groschel, D. (1978). *Occurrence, diagnosis, and sources of Hospital-acquired infections*, Marcel Dekker, New York.
- Fernandez, R. O. (1996). "Lethal effect induced in *Pseudomonas aeruginosa* exposed to ultraviolet-A radiation." *Photochem. & Photobiol.*, 64(2), 334-339.
- Field, A. A. (1973). "Operating theater air conditioning." *HPAC*, October, 91-93.
- Fields, B. N., and Knipe, D. M. (1991). *Fundamental Virology*, Raven Press, New York.
- First, M. W., Nardell, E. A., Chaisson, W., and Riley, R. (1999). "Guidelines for the application of upper-room ultraviolet germicidal irradiation for preventing transmission of airborne contagion." *ASHRAE J.*, 105.
- Folmsbee, T. W., and Ganatra, C. P. (1996). "Benefits of membrane surface filtration." *World Cement*, 27(10), 59-61.
- Fraenkel-Conrat, H. (1985). *The Viruses: Catalogue, Characterization, and Classification*, Plenum Press, New York.
- Freeman, B. A. ed. (1985). *Burrows Textbook of Microbiology*, W. B. Saunders Co., Philadelphia.
- Fuerst, C. R. (1960). "Inactivation of bacterial viruses by physical means." *Annals of the New York Academy of Sciences*, 82, 684-691.
- Fujikawa, H., and Itoh, T. (1996). "Tailing of thermal inactivation curve of *Aspergillus niger* spores." *Appl. Microb.*, 62(10), 3745-3749.
- Futter, B. V. (1967). "Inactivation of bacterial spores by visible radiation." *J. Appl. Bact.*, 30(2), 347-353.
- Galasso, G. J., and Sharp, D. G. (1965). "Effect of particle aggregation on the survival of irradiated Vaccinia virus." *J. Bact.*, 90(4), 1138-1142.
- Gates, F. L. (1929). "A study of the bactericidal action of ultraviolet light." *J. Gen. Physiol.*, 13, 231-260.
- Gilpin, R. W. (1984). "Laboratory and Field Applications of UV Light Disinfection on Six Species of Legionella and Other Bacteria in Water." *Legionella: Proceedings of the 2nd International Symposium*, C. Thornsberry, ed., American Society for Microbiology, Washington.
- Glassner, A. S. (1989). "An Introduction to Ray Tracing." , Academic Press, London.
- Glaze, W. H., Payton, G. R., Huang, F. Y., Bureson, J. L., and Jones, P. C. (1980). "Oxidation of water supply refractory species by ozone with ultraviolet radiation." 600, U.S. EPA.
- Godish, T. (1995). *Sick Buildings : Definition, Diagnosis and Mitigation*, Lewis Publishers, Boca Raton.
- Goldstein, M. A., and Tauraso, N. M. (1970). "Effect of formalin, B-propiolactone, merthiolate, and ultraviolet light upon Influenza virus infectivity, chicken cell agglutination, hemagglutination, and antigenicity." *Appl. Microb.*, 19(2), 290-294.
- Grun, L., and Pitz, N. (1974). "U.V. radiators in humidifying units and air channels of air conditioning systems in hospitals." *Zbl. Bakt. Hyg.*, B159, 50-60.

- Hannon, G. E., McGregor, G. L., and Raymond, B. (1997). "Light reflectant surface and method for making and using same." , USA Patent No. 5,596,450.
- Harm, W. (1980). *Biological effects of ultraviolet radiation*, Cambridge University Press, New York.
- Harstad, J. B., H.M.Decker, and A.G.Wedum. (1954). "Use of ultraviolet irradiation in a room air conditioner for removal of bacteria." *American Industrial Hygiene Association Journal*, 2, 148-151.
- Hill, W. F., Hamblet, F. E., Benton, W. H., and Akin, E. W. (1970). "Ultraviolet devitalization of eight selected enteric viruses in estuarine water." *Appl. Microb.*, 19(5), 805-812.
- Holah, J. T., Rogers, S. J., Holder, J., Hall, K. E., Taylor, J., and Brown, K. L. (1995). "The evaluation of air disinfection systems." *R&D Report No. 13*, Campden & Chorleywood Food Research Association, Gloucestershire.
- Hollaender, A. (1943). "Effect of long ultraviolet and short visible radiation (3500 to 4900) on *Escherichia coli*." *J. Bact.*, 46, 531-541.
- Howard, D. H., and Howard, L. F. (1983). *Fungi pathogenic for Humans and Animals*, Marcel Dekker, Inc., New York.
- Howell, J. R. (1982). *A Catalog of Radiation View Factors*, McGraw-Hill, New York.
- Huber, T. W., Reddick, R. A., and Kubica, G. P. (1970). "Germicidal effect of ultraviolet irradiation on paper contaminated with mycobacteria." *Appl. Microbiol.*, 19, 383-384.
- Huntley, H. E. (1967). *Dimensional Analysis*, Dover Publications, Inc., New York.
- IES. (1981). *Lighting Handbook Application Volume*, Illumination Engineering Society.
- Jagger, J. (1967). *Ultraviolet Photobiology*, Prentice-Hall, Inc., Englewood Cliffs.
- Jensen, M. M. (1964). "Inactivation of airborne viruses by ultraviolet irradiation." *Applied Microbiology*, 12(5), 418-420.
- Jensen, M. (1967). "Bacteriophage aerosol challenge of installed air contamination control systems." *Appl. Microbiol.*, 15(6), 1447-1449.
- Johnson, E., Jaax, N., White, J., and Jahrling, P. (1995). "Lethal experimental infections of Rhesus monkeys by aerosolized Ebola virus." *Intl. J. Experim. Path.*, 76, 227-236.
- Kafka, C. E. "Benefits of membrane surface filtration in the non-ferrous industries." *TMS Annual Meeting*, Orlando, FL, 191-203.
- Kapur, V., Whittam, T. S., and Musser, J. M. (1994). "Is *Mycobacterium tuberculosis* 15,000 years old?" *J. Infect. Dis.*, 170, 1348-1349.
- Keller, L. C., Thompson, T. L., and Macy, R. B. (1982). "UV light-induced survival response in a highly radiation-resistant isolate of the *Moraxella-Acinetobacter* group." *Appl. & Environ. Microb.*, 43(2), 424-429.
- Kelner, A. (1949). "Effect of visible light on the recovery of *Streptomyces griseus* conidia from ultraviolet irradiation injury." *Proc. Nat. Acad. Sci.*, 35(2), 73-79.
- Klein, B., Filon, A. R., Zeeland, A. A. v., and Eb, A. J. v. d. (1994). "Survival of UV-irradiated vaccinia virus in normal and xeroderma pigmentosum fibroblasts; evidence for repair of UV-damaged viral DNA." *Mut. Res.*, 307(1), 25-32.
- Knudson, G. B. (1985). "Photoreactivation of UV-irradiated *Legionella pneumophila* and other *Legionella* species." *Appl/ Environ. Microbiol.*, 49(4), 975-980.
- Koch, A. L. (1966). "The logarithm in biology: Mechanisms generating the lognormal distribution exactly." *J. Theoret. Biol.*, 12, 276-290.
- Koch, A. L. (1995). *Bacterial Growth and Form*, Chapman & Hall, New York.
- Koller, L. R. (1952). *Ultraviolet Radiation*, John Wiley & Sons, New York.
- Kortepeter, M. G., and Parker, G. W. (1999). "Potential biological weapons threats." *Emerg. Infect. Dis.*, 5(4), 523-527.
- Kowalski, W. J. (1997). "Technologies for controlling respiratory disease transmission in indoor environments: Theoretical performance and economics." M.S., The Pennsylvania State University.
- Kowalski, W. J., Bahnfleth, W. P., and Whittam, T. S. (1998). "Bactericidal effects of high airborne ozone concentrations on *Escherichia coli* and *Staphylococcus aureus*." *Ozone Science & Engineering*, 20(3), 205-221.

- Kowalski, W., and Bahnfleth, W. P. (1998). "Airborne respiratory diseases and technologies for control of microbes." *HPAC*, 70(6).
- Kowalski, W. J., W. P. Bahnfleth, T. S. Whittam. (1999). "Filtration of Airborne Microorganisms: Modeling and prediction." *ASHRAE Transactions*, 105(2), 4-17.
- Kowalski, W. J., and Bahnfleth, W. P. (2000a). "UVGI Design Basics for Air and Surface Disinfection." *HPAC*, 72(1), 100-110.
- Kowalski, W. J., and Bahnfleth, W. P. (2000b). "Effective UVGI system design through improved modeling." *ASHRAE Transactions*, 106(2), 4-15.
- Kowalski, W. J. (2000). "Shedding Light on Moldy Ductwork." *Home Energy*, 17(3), 6.
- Kowalski, W. J. (2000). "Indoor mold growth: Health hazards and remediation." *HPAC Engineering*, August.
- Kowalski, W. J., Bahnfleth, W. P., Severin, B. F., and Whittam, T. S. (2001). "Mathematical modeling of UVGI for air disinfection." *Quantitative Microbiology*, (submitted).
- Kuluncsics, Z., Perdiz, D., Brulay, E., Muel, B., and Sage, E. (1999). "Wavelength dependence of ultraviolet-induced DNA damage distribution: Involvement of direct or indirect mechanisms and possible artefacts." *J. Photochem. & Photobiol.*, 49(1), 71-80.
- Kundsins, R. B. (1966). "Characterization of Mycoplasma aerosols as to viability, particle size, and lethality of ultraviolet radiation." *J. Bacteriol.*, 91(3), 942-944.
- Kundsins, R. B. (1968). "Aerosols of Mycoplasmas, L forms, and bacteria: Comparison of particle size, viability, and lethality of ultraviolet radiation." *Applied Microbiology*, 16(1), 143-146.
- Kundsins, R. B. (1988). *Architectural design and indoor microbial pollution*, Oxford Press.
- Kundu, P. K. (1990). *Fluid Mechanics*, Academic Press, San Diego.
- Kunkle, R. S., and Phillips, G. B. (1969). *Microbial Contamination Control Facilities*, Van Nostrand Reinhold, New York.
- Lacey, J., and Crook, B. (1988). "Fungal and actinomycete spores as pollutants of the workplace and occupational illness." , 32, 515-533.
- Langmuir, A. D. (1961). "Epidemiology of airborne infection." *Bacteriology Reviews*, 25, 173-181.
- Lash, D. J. (2000). "Performance Benefits of Highly Reflective Diffuse Materials in Lighting Fixtures." *Journal of the Illuminating Engineering Society*, Winter, 11-16.
- Lidwell, O. M., and Lowbury, E. J. (1950). "The survival of bacteria in dust." *Annual Review of Microbiology*, 14, 38-43.
- Lindsey, J. L. (1997). *Applied Illumination Engineering*, The Fairmont Press, Inc., Lilburn.
- Linscomb, M. (1994). "AIDS clinic HVAC system limits spread of TB." *HPAC*, February.
- Linton, A. H. (1982). *Microbes, man, and animals: The natural history of microbial interactions*, Wiley & Sons, New York.
- Litonski, B. (1974). "Air conditioning as decontamination unit for the air of operating theatres." *Zbl. Bakt. Hyg.*, B159, 244-271.
- Little, J. S., Kishimoto, R. A., and Canonico, P. G. (1980). "In vitro studies of interaction of rickettsia and macrophages: Effect of ultraviolet light on *Coxiella burnetii* inactivation and macrophage enzymes." *Infect. Immun.*, 27(3), 837-841.
- Luciano, J. R. (1977). *Air Contamination Control in Hospitals*, Plenum Press, New York.
- Luckiesh, M., and Holladay, L. L. (1942a). "Designing installations of germicidal lamps for occupied rooms." *General Electric Review*, 45(6), 343-349.
- Luckiesh, M., and Holladay, L. L. (1942b). "Tests and data on disinfection of air with germicidal lamps." *General Electric Review*, 45(4), 223-231.
- Luckiesh, M. (1945). "Disinfection with germicidal lamps: Control -- I." *Electrical World*, Sep.29, 72-73.
- Luckiesh, M. (1945). "Disinfection with germicidal lamps: Air -- II." *Electrical World*, Oct.13, 109-111.
- Luckiesh, M. (1945). "Disinfection with germicidal lamps: Water -- III." *Electrical World*, Oct.27, 90-91.
- Luckiesh, M. (1946). *Applications of Germicidal, Erythral and Infrared Energy*, D. Van Nostrand Co., New York.

- Luckiesh, M., Taylor, A. H., and Knowles, T. (1947). "Killing air-borne microorganisms with germicidal energy." *Journal of the Franklin Institute*, Oct., 267-290.
- Macher, J. M., Alevantis, L. E., Chang, Y. L., and Liu, K. S. (1992). "Effect of ultraviolet germicidal lamps on airborne microorganisms in an outpatient waiting room." *Appl. Occup. Environ. Hyg.*, 7(8), 505-513.
- Maniloff, J., McElhaney, R. N., Finch, L. R., and Baseman, J. B. (1992). *Mycoplasmas: Molecular Biology and Pathogenesis*, ASM Press, Washington, D.C.
- Miller, W. R., Jarrett, E. T., Willmon, T. L., Hollaender, A., Brown, E. W., Lewandowski, T., and Stone, R. S. (1948). "Evaluation of ultraviolet radiation and dust control measures in control of respiratory disease at a naval training center." , 82, 86-100.
- Mitscherlich, E., and Marth, E. H. (1984). *Microbial Survival in the Environment*, Springer-Verlag, Berlin.
- Moats, W. A., Dabbah, R., and Edwards, V. M. (1971). "Interpretation of nonlogarithmic survivor curves of heated bacteria." *J. Food of Science*, 36, 523-526.
- Modest, M. F. (1993). *Radiative Heat Transfer*, McGraw-Hill, New York.
- Mongold, J. (1992). "DNA repair and the evolution of transformation in *Haemophilus influenzae*." *Genetics*, 132, 893-898.
- Montgomery. (2001). *Design of Experiments*, .
- Montgomery, D. C. (2001). *Design and Analysis of Experiments*, John Wiley, New York.
- Montz, W. E. (2000). "Contamination control in hospitals." *Engineered Systems*, 17(6), 68-72.
- Morey, P., Feeley, J., and Otten. (1990). *Biological Contaminants in Indoor Environments*, ASTM.
- Morrissey, R. F., and Phillips, G. B. (1993). *Sterilization Technology*, Van Nostrand Reinhold, New York.
- Mumma, S. A. (2001). "Dedicated Outside Air Systems." *ASHRAE IAQ Applications*, 2(1).
- Munakata, N., Saito, M., and Hieda, K. (1991). "Inactivation action spectra of *Bacillus subtilis* spores in extended ultraviolet wavelengths (50-300 nm) obtained with synchrotron radiation." *Photochem. & Photobiol.*, 54(5), 761-768.
- Murray, P. R. (1999). *Manual of Clinical Microbiology*, ASM Press, Washington, D.C.
- Myers, R. H., and Montgomery, D. C. (1995). *Response Surface Methodology*, Wiley Interscience, New York.
- Nakamura, H. (1987). "Sterilization efficacy of ultraviolet irradiation on microbial aerosols under dynamic airflow by experimental air conditioning systems." *Bull. Tokyo Med. Dent. Univ.*, 34(2), 25-40.
- Nicas, M., and Miller, S. L. (1999). "A multi-zone model evaluation of the efficacy of upper-room air ultraviolet germicidal irradiation." *Appl. & Environ. Occup. Hyg. J.*, 14, 317-328.
- Ortiz-Ortiz, L., Bojalil, L. F., and Yakoleff, V. (1984). *Biological, biochemical, and biomedical aspects of actinomycetes*, Academic Press, Orlando.
- Pannkoek, T. (1973). "Modern clean room concepts." *HPAC*, October, 63-70.
- Pattison, J. R. (1988). *Parvoviruses and Human Disease*, CRC Press, Boca Raton.
- Philips. (1985). *UVGI Catalog and Design Guide*, Catalog No. U.D.C. 628.9, Netherlands.
- Phillips, G. B., and Novak, F. E. (1955). "Applications of germicidal ultraviolet in infectious disease laboratories." *Appl. Microb.*, 4, 95-96.
- Pizzarello, D. J., and Witcofski, R. L. (1982). *Medical Radiation Biology*, Lea & Febiger, Philadelphia.
- Pollard, E. C. (1960). "Theory of the physical means of the inactivation of viruses." *Annals of the New York Academy of Sciences*, 82, 654-660.
- Pope, A. M., Patterson, R., and Burge, H. (1993). "Indoor Allergens." , I. o. Medicine, ed., National Academy Press, Washington, DC.
- Prescott, L. M., Harley, J. P., and Klein, D. A. (1996). "Microbiology." , Wm. C. Brown Publishers, Dubuque, IA.
- Pruitt, K. M., and Kamau, D. N. (1993). "Mathematical models of bacterial growth, inhibition and death under combined stress conditions." *J. Ind. Microb.*, 12, 221-231.
- Qualls, R. G., and Johnson, J. D. (1983). "Bioassay and dose measurement in UV disinfection." *Appl. Microb.*, 45(3), 872-877.

- Qualls, R. G., and Johnson, J. D. (1985). "Modeling and efficiency of ultraviolet disinfection systems." *Water Res.*, 19(8), 1039-1046.
- Rahn, R. O., Xu, P., and Miller, S. L. (1999). "Dosimetry of room-air germicidal (254 nm) radiation using spherical actinometry." *Photochem. and Photobiol.*, 70(3), 314-318.
- Rainbow, A. J., and Mak, S. (1973). "DNA damage and biological function of human adenovirus after U.V. irradiation." *Int. J. Radiat. Biol.*, 24(1), 59-72.
- Rauth, A. M. (1965). "The physical state of viral nucleic acid and the sensitivity of viruses to ultraviolet light." *Biophysical Journal*, 5, 257-273.
- Rentschler, H. C., and Nagy, R. (1940). "Advantages of bactericidal ultraviolet radiation in air conditioning systems." *HPAC*, 12, 127-130.
- Rentschler, H. C., Nagy, R., and Mouromseff, G. (1941). "Bactericidal effect of ultraviolet radiation." *J. Bacteriol.*, 42, 745-774.
- Rentschler, H. C., and Nagy, R. (1942). "Bactericidal action of ultraviolet radiation on air-borne microorganisms." *J. Bacteriol.*, 44, 85-94.
- Rice, E. W., and Hoff, J. C. (1999). "Inactivation of *Giardia lamblia* cysts by ultraviolet irradiation." *Appl. & Environ. Microbiol.*, 42(3), 546-547.
- Riley, R. L., and O'Grady, F. (1961). *Airborne Infection*, The Macmillan Company, New York.
- Riley, R. L., and Kaufman, J. E. (1972). "Effect of relative humidity on the inactivation of airborne *Serratia marcescens* by ultraviolet radiation." *Applied Microbiology*, 23(6), 1113-1120.
- Riley, R. L. (1972). "The ecology of indoor atmospheres: Airborne infection in hospitals." *J. Chron. Dis.*, 25, 421-423.
- Riley, R. L., Knight, M., and Middlebrook, G. (1976). "Ultraviolet susceptibility of BCG and virulent tubercle bacilli." *Am. Rev. Resp. Dis.*, 113, 413-418.
- Riley, R. L., and Nardell, E. A. (1989). "Clearing the air: The theory and application of ultraviolet disinfection." *Am. Rev. Resp. Dis.*, 139, 1286-1294.
- Rohsenow, W. M., and Hartnett, J. P. (1973). *Handbook of Heat Transfer*, McGraw-Hill, New York.
- Russell, A. D. (1982). *The destruction of bacterial spores*, Academic Press, New York.
- Ryan, K. J. e. (1994). *Sherris Medical Microbiology*, Appleton & Lange, Norwalk.
- Sakuma, S., and Abe, K. "Prevention of fungal growth on a panel cooling system by intermittent operation." *The 7th International Conference on IAQ and Climate*, Nagoya, Japan, 179-184.
- Schall, K. P., and Pulverer, G. "Actinomycetes." *Proceedings of the Fourth International Symposium on Actinomycete Biology*, Cologne.
- Scheir, R., and Fencl, F. B. (1996). "Using UVC Technology to Enhance IAQ." *HPAC*, Feb.
- Schoenen, D., Kolch, A., and Gebel, J. (1993). "Influence of geometrical parameters in different irradiation vessels on UV disinfection rate." *Zbl. Hyg. Umweltmed*, 194(3), 313-320.
- Seagal-Maurer, S., and Kalkut, G. E. (1994). "Environmental control of tuberculosis: Continuing controversy." *Clinical Infectious Diseases*, 19, 299-308.
- Severin, B. F., Suidan, M. T., and Englebrecht, R. S. (1983). "Kinetic modeling of U.V. disinfection of water." *Water Res.*, 17(11), 1669-1678.
- Severin, B. F., Suidan, M. T., Rittmann, B. E., and Englebrecht, R. S. (1984). "Inactivation kinetics in a flow-through UV reactor." *J. Water Pollution Control*, 56(2), 164-169.
- Severin, B. F. (1986). "Ultraviolet disinfection for municipal wastewater." *Chemical Engineering Progress*, 81, 37-44.
- Severin, B. F., and Roessler, P. F. (1998). "Resolving UV photometer outputs with modeled intensity profiles." *Wat. Res.*, 32(5), 1718-1724.
- Shama, G. (1992). "Inactivation of *Escherichia coli* by ultraviolet light and hydrogen peroxide in a thin film contactor." *Letters in Appl. Microb.*, 15, 259-260.
- Shama, G. (1992). "Ultraviolet irradiation apparatus for disinfecting liquids of high ultraviolet absorptivities." *Letters in Appl. Microb.*, 15, 69-72.
- Sharp, D. G. (1938). "A quantitative method of determining the lethal effect of ultraviolet light on bacteria suspended in air." *J. Bact.*, 35, 589-599.
- Sharp, G. (1939). "The lethal action of short ultraviolet rays on several common pathogenic bacteria." *J. Bact.*, 37, 447-459.

- Sharp, G. (1940). "The effects of ultraviolet light on bacteria suspended in air." *J. Bact.*, 38, 535-547.
- Shaughnessy, R., Levetin, E., and Rogers, C. (1999). "The effects of UV-C on biological contamination of AHUs in a commercial office building: Preliminary results." *Indoor Environment* '99, 195-202.
- Siegel, R., and Howell, J. R. (1981). *Thermal Radiation Heat Transfer*, Hemisphere, New York.
- Smerage, G. H., and Teixeira, A. A. (1993). "Dynamics of heat destruction of spores: a new view." *J. Ind. Microb.*, 12, 211-220.
- Smith, J. M. B. (1989). *Opportunistic mycoses of man and other animals*, BPCC Wheatons, Exeter.
- Sommer, R., Cabaj, A., Schoenen, D., Gebel, J., Kolsch, E., and Havalaar, A. H. (1995). "Comparison of three laboratory devices for UV-inactivation of microorganisms." *Wat. Sci. Technol.*, 31, 147-156.
- Sparrow, E. M., and Cess, R. D. (1997). *Radiation Heat Transfer*, Brooks/Cole Publ., Belmont.
- Spendlove, J. C., and Fannin, K. F. (1983). "Source, significance, and control of indoor microbial aerosols: Human health aspects." *Public Health Reports*, 98(3), 229-244.
- Steril-Aire, Inc. (2000). "UVC lights save on energy while cleaning coils." *HPAC Engineering*, 72(1), 131-132.
- Streifel, A. J. (1996). "Controlling aspergillosis and Legionella in hospitals." *Indoor Air and Human Health*, CRC Press, Boca Raton.
- Suidan, M. T., and Severin, B. F. (1986). "Light intensity models for annular UV disinfection reactors." *AIChE Journal*, 32(11), 1902-1909.
- Sylvania. (1981). "Sylvania Engineering Bulletin 0-342, Germicidal and Short-Wave Ultraviolet Radiation." , GTE Products Corp.
- Tamm, I., and Fluke, D. J. (1950). "The effect of monochromatic ultraviolet radiation on the infectivity and hemagglutinating ability of the influenza virus type A strain PR-8." *J. Bact.*, 59, 449-461.
- Taylor, A. R. (1960). "Effects of nonionizing radiations of animal viruses." *Annals of the New York Academy of Sciences*, 82, 670-683.
- Thompson, L. R. (1962). *Microbiology and epidemiology*, W. B. Saunders Co., Philadelphia.
- Thornsberry, C., Balows, A., Feeley, J., and Jakubowski, W. "Legionella: Proceedings of the 2nd International Symposium." , Atlanta.
- UVDI. (1999). "Report on Lamp Photosensor Data for UV Lamps." , Ultraviolet Devices, Inc., Valencia, CA.
- UVDI. (2000). "Report on Bioassays of *S. marcescens* and *B. subtilis* exposed to UV." , Ultraviolet Devices, Inc., Valencia, CA.
- UVDI. (2001). "Report on Survival Data for *A. niger* and *R. nigricans* Under UVGI exposure." , Valencia.
- von Brodrotti, H. S., and Mahnel, H. (1982). "Comparative studies on susceptibility of viruses to ultraviolet rays." *Zbl. Vet. Med. B.*, 29, 129-136.
- von Sonntag, C. (1986). "Disinfection by free radicals and UV-radiation." *Water Supply*, 4, 11-18.
- Walter, C. W. (1969). "Ventilation and air conditioning as bacteriologic engineering." *Anesthesiology*, 31, 186-192.
- Wang, Y., and Casadevall, A. (1994). "Decreased susceptibility of melanized *Cryptococcus neoformans* to UV light." *Appl. Microb.*, 60(10), 3864-3866.
- Watson, H. E. (1908). "A note on the variation of the rate of disinfection with change in the concentration of disinfectant." *J. Hyg.*, 8, 536.
- Weinstein, R. A. (1991). "Epidemiology and control of nosocomial infections in adult intensive care units." *Am. J. Med.*, 91(suppl 3B), 179S-184S.
- Wekhof, A. (2000). "Disinfection with flashlamps." *PDA J. of Pharmaceutical Science and Technology*, May-June, 263-267.
- Wells, W. F. (1955). *Airborne Contagion*, New York Academy of Sciences, New York.
- Westinghouse. (1982). "Booklet A-8968." , Westinghouse Electric Corp., Lamp Div.

- Whiting, R. C. (1991). "Predictive Modeling." Food Microbiology, M. P. Doyle, ed., ASM Press, Washington, 728-739.
- Woods, J. E., Grimsrud, D. T., and Boschi, N. (1997). *Healthy Buildings / IAQ '97*, ASHRAE, Washington, DC.
- Zemke, V., and Schoenen, D. (1989). "UV disinfecting experiments with E. coli and actinometric determination of the irradiation intensity." *Zbl. Hyg. Umweltmed*, 188(3-4), 380-384.
- Zemke, V., Podgorsek, L., and Schoenen, D. (1990). "Ultraviolet disinfection of drinking water." *Zbl. Hyg. Umweltmed*, 190(1-2), 51-61.

APPENDIX A: Airborne Pathogen and Allergen Database

AIRBORNE PATHOGEN	GROUP	TYPE	SOURCE	DISEASE	Mean diameter	Annual Cases	Fatalities	BSL
Adenovirus	DNA Virus	C	Humans, sewage	colds, fever, pharyngitis, Acute Respiratory	0.080	common	-	2
Coronavirus	RNA Virus	C	Humans	colds, croup	0.110	1,700,000	-	2
Coxsackievirus	RNA Virus	C	Humans, feces, sewage.	colds, Acute Respiratory Disorder.	0.027	common	-	2
Echovirus	RNA Virus	C	Humans	colds, meningitis possible	0.027	common	-	2
Hantaan virus	RNA Virus	NC	Rodents	hemorrhagic fever, Korean Hem. Fever	0.095	44	22	3
Influenza A virus	RNA Virus	C	Humans, birds, pigs, nosocomial	flu, secondary pneumonia	0.098	2,000,000	20000	2
Junin virus	RNA Virus	C	Rodents	hemorrhagic fever	0.120	2,000	rare	6
Marburg virus	RNA Virus	C	Humans, monkeys	hemorrhagic fever	0.039	rare	rare	4
Measles virus	RNA Virus	C	Humans, nosocomial	measles (rubeola)	0.158	500,000	rare	2
Mumps virus	RNA Virus	C	Humans	mumps, viral encephalitis	0.164	10,000	rare	2
Parainfluenza virus	RNA Virus	C	Humans, nosocomial	flu, colds, croup, pneumonia	0.194	common	-	2
Parvovirus B19	DNA Virus	C	Humans	fifth Disease, anemia, fever	0.022	uncomm.	rare	2
Reovirus	RNA Virus	C	Humans	colds, fever, pneumonia, rhinorrhea	0.075	-	-	2
Respiratory Syncytial Virus	RNA Virus	C	Humans, nosocomial	pneumonia, bronchiolitis	0.190	common	rare	2
Rhinovirus	RNA Virus	C	Humans	colds	0.023	common	-	2
Rubella virus	RNA Virus	C	Humans, nosocomial	rubella (German measles)	0.061	3,000	none	2
Vaccinia virus	DNA Virus	NC	Agricultural.	smallpox	0.224	rare	none	2
Varicella-zoster virus	DNA Virus	C	Humans, nosocomial	chickenpox	0.173	common	250	2
Acinetobacter	Gram- Bacteria	E	Environ., soil, sewage, nosocomial	OI, septic infections, meningitis	1.220	147	-	2
Actinomyces israelii	Gram+ Bacteria	E	Humans, cattle	actinomycosis	0.901	uncomm.	-	2
Aeromonas	Gram- Bacteria	NC	Environ., nosocomial	Non-respiratory OI, bacteremia.	2.100	-	-	2
Alcaligenes	Gram- Bacteria	E	Humans, soil, water, nosocomial	OI	0.775	rare	rare	2
Bacteroides fragilis	Gram- Bacteria	E	Humans	OI.	3.160	uncomm.	-	2
Bordetella pertussis	Gram- Bacteria	C	Humans, nosocomial	whooping cough, toxins	0.245	6,564	15	2

APPENDIX A: Airborne Pathogen and Allergen Database

AIRBORNE PATHOGEN	GROUP	TYPE	SOURCE	DISEASE	Mean diameter	Annual Cases	Fatalities	BSL
Burkholderia cepacia	Gram- Bacteria	NC	Environ.	OI.	0.707	-	-	1
Burkholderia mallei	Gram- Bacteria	NC	Environ., Horses, mules, nosocomial.	Glanders, fever, OI	0.674	-	none	-
Burkholderia pseudomallei	Gram- Bacteria	NC	Environ., rodents, soil, nosocomial.	meliodosis, OI	0.494	rare	rare	2-3
Brucella	Gram- Bacteria	NC	Goats, cattle, swine, dogs.	Brucellosis, undulant fever	0.566	98	rare	3
Cardiobacterium	Gram- Bacteria	E	Humans, nosocomial.	OI, endocarditis	0.612	rare	-	2
Chlamydia pneumoniae	Gram- Bacteria	C	Humans, nosocomial	pneumonia, bronchitis, pharyngitis.	0.548	uncomm.	-	2
Chlamydia psittaci	Gram- Bacteria	NC	Birds, fowl	psittacosis/ornithosis , pneumonitis	0.283	33	rare	2
Clostridium perfringens	Gram+ Bacteria	NC	Environ., Humans, Animals, soil.	sepsis, toxins, food poisoning.	5.000	10,000	10	2
Corynebacterium diphtheriae	Gram+ Bacteria	C	Humans, sewage, nosocomial	diphtheria, toxin produced.	0.698	10	-	2
Coxiella burnetii	Gram- Bacteria	NC	Cattle, sheep	Q fever	0.283	rare	-	3
Enterobacter cloacae	Gram- Bacteria	E	Humans, Environ., soil, water.	OI	1.410	uncomm.	-	1
Enterococcus	Gram+ Bacteria	NC	Humans.	OI,	1.410	rare	-	1-2
Enterococcus faecalis	Gram+ Bacteria	NC	Feces.	Endocarditis, neonatal septicemia, meningitis	0.707	-	-	1
Francisella tularensis	Gram- Bacteria	NC	Animals, natural waters	tularemia, pneumonia, fever	0.200	rare	-	3
Haemophilus influenzae	Gram- Bacteria	C	Humans, nosocomial.	OI, conjunctivitis, pneumonia, meningitis	0.285	1,162	-	2
Haemophilus parainfluenzae	Gram- Bacteria	E	Humans, nosocomial.	OI, conjunctivitis, pneumonia, meningitis	1.730	common	-	2
Klebsiella pneumoniae	Gram- Bacteria	E	Environ., soil, Humans, nosocomial.	OI, pneumonia	0.671	1,488	-	2
Legionella pneumophila	Gram- Bacteria	NC	Environ., cooling towers, nosocomial.	Legionnaire's Disease, Pontiac fever, OI	0.520	1,163	10	2
Moraxella	Gram- Bacteria	E	Humans, nosocomial.	otitis media, OI	1.225	rare	0	2
Mycobacterium avium	Bacteria	NC	Environ., water, dust, plants.	cavitary pulmonary disease.	1.120	uncomm.	rare	3

APPENDIX A: Airborne Pathogen and Allergen Database

AIRBORNE PATHOGEN	GROUP	TYPE	SOURCE	DISEASE	Mean diameter	Annual Cases	Fatalities	BSL
<i>Mycobacterium kansasii</i>	Bacteria	NC	unknown	cavitary pulmonary disease.	0.637	rare	rare	2
<i>Mycobacterium tuberculosis</i>	Bacteria	C	Humans, sewage, nosocomial.	tuberculosis, TB	0.637	20,000	-	3
<i>Mycoplasma pneumoniae</i>	Bacteria	E	Humans	pneumonia	0.177	uncomm.	rare	2
<i>Neisseria meningitidis</i>	Gram- Bacteria	E	Humans	meningitis, pharyngitis	0.775	3,308	rare	2
<i>Proteus mirabilis</i>	Gram- Bacteria	E	Humans	OI.	0.494	-	-	2
<i>Pseudomonas aeruginosa</i>	Gram- Bacteria	NC	Environ., sewage, nosocomial	pneumonia, toxins	0.494	2,626	-	1
<i>Serratia marcescens</i>	Gram- Bacteria	E	Environ., indoor growth, nosocomial.	OI, bacteremia, endocarditis, pneumonia.	1.225	479	-	1
<i>Staphylococcus aureus</i>	Gram+ Bacteria	E	Humans, sewage, nosocomial.	staphylococcal pneumonia, OI	0.866	2,750	-	2
<i>Staphylococcus epidermis</i>	Gram+ Bacteria	E	Humans, sewage, nosocomial.	OI, bacteremia	0.866	common	-	1
<i>Streptococcus pneumoniae</i>	Gram+ Bacteria	C	Humans, nosocomial.	pneumonia, meningitis, otitis media, toxins	0.707	500,000	50000	2
<i>Streptococcus pyogenes</i>	Gram+ Bacteria	C	Humans, nosocomial.	scarlet fever, pharyngitis, toxins	0.894	213,962	-	2
<i>Yersinia pestis</i>	Gram- Bacteria	C	Rodents, fleas, Humans	bubonic plague, pneumonic plague, sylvatic plague.	0.707	4	-	2-3
<i>Bacillus anthracis</i>	Bacterial Spore	NC	Cattle, sheep, Animals, soil.	anthrax, woolsorter's disease.	1.118	rare	rare	2
<i>Micromonospora faeni</i>	Bacterial Spore	NC	Agricultural, moldy Hay, indoor growth	Farmer's Lung, pulmonary fibrosis, AR	0.866	uncomm.	-	-
<i>Micropolyspora faeni</i>	Bacterial Spore	NC	Agricultural, indoor growth	Farmer's Lung, alveolitis, asthma	1.342	-	-	2
<i>Nocardia asteroides</i>	Bacterial Spore	NC	Environ., sewage, nosocomial.	nocardiosis, pneumonia	1.118	uncomm.	rare	2
<i>Nocardia brasiliensis</i>	Bacterial Spore	NC	Environ., sewage, nosocomial.	nocardiosis, pneumonia	1.414	uncomm.	-	2
<i>Thermoactinomyces sacchari</i>	Bacterial Spore	NC	Agricultural, bagasse	bagassosis, alveolitis, HP	0.855	-	-	2
<i>Thermoactinomyces vulgaris</i>	Bacterial Spore	NC	Agricultural, indoor growth	Farmer's Lung, AR, asthma, HP	0.866	uncomm.	rare	1
<i>Thermomonospora viridis</i>	Bacterial Spore	NC	Agricultural	Farmer's Lung, HP	0.520	-	-	1
<i>Absidia</i>	Fungal Spore	NC	Environ.	zygomycosis, OI	3.536	rare	-	2
<i>Acremonium</i>	Fungal Spore	NC	Environ., indoor growth	AA, mycetoma, toxins, keratitis	2.449	-	-	1-2
<i>Alternaria alternata</i>	Fungal Spore	NC	Environ., indoor growth	AA, rhinitis, asthma, toxins	11.225	-	-	1

APPENDIX A: Airborne Pathogen and Allergen Database

AIRBORNE PATHOGEN	GROUP	TYPE	SOURCE	DISEASE	Mean diameter	Annual Cases	Fatalities	BSL
Aspergillus	Fungal Spore	NC	Environ., nosocomial, indoor growth	aspergillosis, alveolitis, asthma, toxins, VOC	3.354	uncomm.	-	2
Aureobasidium pullulans	Fungal Spore	NC	Environ., indoor growth	AA, sequoiosis	4.899	-	-	1
Blastomyces dermatitidis	Fungal Spore	NC	Environ., nosocomial.	blastomycosis, Gilchrist's Disease	12.649	rare	-	2
Candida	Fungal Spore	E	Humans	candidamycosis, candidiasis, bronchitis.	4.900	uncomm.	-	1
Chaetomium globosum	Fungal Spore	NC	Environ., indoor growth	AA, VOC	5.455	-	-	1
Cladosporium	Fungal Spore	NC	Environ., indoor growth	chromoblastomycosis, AR, rhinitis, asthma	8.062	-	-	1
Coccidioides immitis	Fungal Spore	NC	Environ., soil, nosocomial.	coccidioidomycosis, valley fever, desert rheumatism	3.464	uncomm.	-	3
Cryptococcus neoformans	Fungal Spore	NC	Environ., nosocomial, indoor growth	cryptococcosis, cryptococcal meningitis, SBS/BRI	5.477	high	rare	2
Cryptostroma corticale	Fungal Spore	NC	Environ.	alveolitis, asthma, maple bark pneumonitis	3.742		-	2
Emericella nidulans	Fungal Spore	NC	Environ.	AA	3.240	-	-	1
Epicoecum nigrum	Fungal Spore	NC	Environ., indoor growth	AA, rhinitis	17.321	-	-	1
Eurotium	Fungal Spore	NC	Environ., indoor growth	AA	5.612	-	-	1
Exophiala	Fungal Spore	NC	Environ., indoor growth	AR	1.410	-	-	2
Fusarium	Fungal Spore	NC	Environ., indoor growth	AA, toxins, VOC	11.225	-	-	1
Helminthosporium	Fungal Spore	NC	Environ., indoor growth	AA, AR, UR irritation, SBS/BRI	11.580	-	-	1
Histoplasma capsulatum	Fungal Spore	NC	Environ., nosocomial, pigeon roosts.	histoplasmosis, fever, malaise	2.236	common	-	3
Mucor plumbeus	Fungal Spore	NC	Environ., sewage, nosocomial	mucormycosis, rhinitis	7.071	rare	rare	1
Paecilomyces variotii	Fungal Spore	NC	Environ., indoor growth	paecilomycosis, AA, toxins, VOC	2.828	-	-	1
Paracoccidioides	Fungal Spore	NC	Environ.	paracoccidioidomycosis	4.472	rare	-	2
Penicillium	Fungal Spore	NC	Environ., indoor growth	alveolitis, rhinitis, asthma, AR, toxins, VOC	3.262	rare	-	1
Phialophora	Fungal Spore	NC	Environ., indoor growth	AA, chromomycosis	1.470	-	-	2
Phoma	Fungal Spore	NC	Environ., indoor growth	AA	3.162	-	-	1

APPENDIX A: Airborne Pathogen and Allergen Database

AIRBORNE PATHOGEN	GROUP	TYPE	SOURCE	DISEASE	Mean diameter	Annual Cases	Fatalities	BSL
<i>Pneumocystis carinii</i>	Fungal Spore	NC	Environ., nosocomial.	pneumocystosis	2.000	rare	rare	1
<i>Rhizomucor pusillus</i>	Fungal Spore	NC	Environ.	AA, mucormycosis	4.183	rare	-	1
<i>Rhizopus stolonifer</i>	Fungal Spore	NC	Environ., nosocomial	zygomycosis, AR	6.928	rare	-	2
<i>Rhodoturula</i>	Fungal Spore	NC	Environ., indoor growth	AA	13.856	-	-	-
<i>Scopulariopsis</i>	Fungal Spore	NC	Environ., indoor growth	onychomycosis, AR	5.916	-	-	2
<i>Sporothrix schenckii</i>	Fungal Spore	NC	Environ., plant material.	sporotrichosis, rose gardener's disease.	6.325	rare	-	2
<i>Stachybotrys atra</i>	Fungal Spore	NC	Environ., indoor growth	lung disease, AA, toxins	5.623	-	-	1
<i>Trichoderma</i>	Fungal Spore	NC	Environ., indoor growth	AA, toxins, VOC	4.025	-	-	1
<i>Ulocladium</i>	Fungal Spore	NC	Environ., indoor growth	AA	14.142	-	-	1
<i>Ustilago</i>	Fungal Spore	NC	Environ.	rhinitis, asthma	5.916	-	-	1
<i>Wallemia sebi</i>	Fungal Spore	NC	Environ., indoor growth	AA	2.958	-	-	1

Abbreviations:

NC: Non-communicable AR: allergic reactions

BSL: Biosafety Level

C: Communicable OI: opportunistic infections

E: Endogenous AA: allergic alveolitis
VOC: Volatile Organic Compounds

Appendix B: Summary of UVGI Rate Constants Results for Airborne Pathogens

Microorganism	Type	Reference	Test Medium Air/Plt/Wtr	k = Standard Rate Constant cm ² /μW-s
Adenovirus	Virus	Jensen 1964	Air	0.000546
		Rainbow 1973 (Type 2)	Plates	0.000047
Vaccinia	Virus	Jensen 1964	Air	0.001528
		Galasso 1965	Plates	0.001542
Coxsackievirus	Virus	Jensen 1964	Air	0.001108
		Hill 1970 (B-1)	Water	0.000159
		Hill 1970 (A-9)	Water	0.000202
Influenza A	Virus	Jensen 1964	Air	0.001187
Echovirus	Virus	Hill 1970	Water	0.000217
Reovirus Type 1	Virus	Hill 1970	Water	0.000132
Staphylococcus aureus	Gram + Bacteria	Sharp 1939	Plates	0.000886
		Sharp 1940	Air	0.003476
		Gates 1929	Plates	0.001184
		Abshire 1981	Plates	0.000419
		Luckiesh 1946	Air	0.009602
Streptococcus pyogenes	Gram + Bacteria	Lidwell 1950	Plates	0.006161
		Mitscherlich 1984	Air	0.001066
Mycobacterium tuberculosis	Mycobacteria	David 1973	Air	0.000987
		Riley 1961	Air	0.004721
		Collins 1971	Air	0.002132
Mycobacterium kansasii	Mycobacteria	David 1973	Air	0.000364
Mycobacterium avium-intra.	Mycobacteria	David 1973	Air	0.000406
E. coli (reference only)	Gram - Bacteria	Sharp 1939	Plates	0.000927
		Sharp 1940	Air	0.003759
Corynebacterium diptheriae	Gram + Bacteria	Sharp 1939	Plates	0.000701
Moraxella-Acinetobacter	Gram - Bacteria	Keller 1982	Water	0.0000021
Haemophilus influenzae	Gram - Bacteria	Mongold 1992	Plates	0.000599
Pseudomonas aeruginosa	Gram - Bacteria	Collins 1971	Air	0.002375
		Abshire 1981	Water	0.000640
		Sharp 1940	Air	0.005721
		Zelle (Antopol 1979)	Water	0.000419
Legionella pneumophila	Gram - Bacteria	Gilpin 1984	Water	0.002047
		Antopol 1979	Water	0.002503
Serratia marcescens	Gram - Bacteria	Collins 1971	Air	0.002208
		Zelle (Antopol 1979)	Water	0.001047
		Riley 1972	Air	0.049900
		Sharp 1940	Air	0.004449
		Sharp 1939	Air	0.001047
		Rentschler 1941	Air	0.001225
Coxiella burnetti	Rickettsiae	Little 1980	Water	0.001535
Bacillus anthracis	Bacterial spore	Sharp 1939	Plates	0.000509
Cryptococcus neoformans	Fungal spore	Wang 1994	Plates	0.000102
Fusarium oxysporum	Fungal spore	Asthana 1992	Plates	0.000112
Fusarium solani	Fungal spore	Asthana 1992	Plates	0.0000706
Penicillium italicum	Fungal spore	Asthana 1992	Plates	0.0001259
Penicillium digitatum	Fungal spore	Asthana 1992	Plates	0.0000718
Rhizopus nigricans spores	Fungal spore	Luckiesh 1946	Air	0.0000861
Cladosporium herbarum	Fungal spore	Luckiesh 1946	Air	0.0000370
Scopulariopsis brevicaulis	Fungal spore	Luckiesh 1946	Air	0.0000344
Mucor mucedo	Fungal spore	Luckiesh 1946	Air	0.0000399
Penicillium chrysogenum	Fungal spore	Luckiesh 1946	Air	0.0000434
Aspergillus amstelodami	Fungal spore	Luckiesh 1946	Air	0.0000344

APPENDIX C: Units of Intensity and Dose

Conversion Factors for Intensity				
(Read down from units to gray block and then horizontally for unit equivalence.)				
microW/mm²	erg/mm²-s	microW/cm²	erg/cm²-s	W/ft²
W/m²				
J/m²-s				
1	10	100	1000	0.107639
0.1	1	10	100	0.010764
0.01	0.1	1	10	0.001076
0.001	0.01	0.1	1	0.000108
9.29	92.90	929.0	9290	1
J/m²				
W-s/m²				
microW-s/mm²	erg/mm²	microW-s/cm²	erg/cm²	W-s/ft²
Conversion factors for Dose, Exposure Time = 1 second				
(Read up from units to gray block and then horizontally for unit equivalence.)				

NOTE: This conversion chart is presented in spreadsheet form in the attached CDR.

APPENDIX D: UVGI Lamp Database

Model	UVPower	Arclength	Radius	#Coils	Rating	Diameter	Reference
782H10	2.8	22.2	0.79	1	28	1.58	American Ultraviolet
782H20	5.5	47.6	0.79	1	52	1.58	American Ultraviolet
782H30	8.3	73	0.79	1	73	1.58	American Ultraviolet
782L10	2	22.2	0.79	1	20	1.58	American Ultraviolet
782L20	3.9	47.6	0.79	1	35	1.58	American Ultraviolet
782L25_1/2	7.3	64.8	0.79	1	75	1.58	American Ultraviolet
782L30	5.2	73	0.79	1	46	1.58	American Ultraviolet
782VH29_1	5.7	70.8	0.79	1	50	1.58	American Ultraviolet
782VH29_2	9.1	70.8	0.79	1	80	1.58	American Ultraviolet
83A-1	3.1	27.3	0.875	1	35	1.75	IES Handbook
84A-1	4.1	62.8	0.65	1	46	1.3	IES Handbook
86A-45	1.4	11.4	0.875	1	16	1.75	IES Handbook
87A-45	4.3	26.7	0.875	1	47	1.75	IES Handbook
88A-45	10.4	62.2	0.875	1	113	1.75	IES Handbook
93A-1	1.9	29.2	0.65	1	21	1.3	IES Handbook
94A-1	7.2	62.8	0.875	1	80	1.75	IES Handbook
AGH0287T5L	6.5	20.6	0.8	1	70	1.6	LSI
G10T5_1/2H	5.3	27.6	0.79	1	55	1.58	American Ultraviolet
G10T5_1/2L	5.3	27.6	0.79	1	55	1.58	American Ultraviolet
G10T5_1/2VH	5.3	27.6	0.79	1	55	1.58	American Ultraviolet
G10T8	2.6	24.5	1.275	1	27	2.55	T-W
G11T5	3	15.5	0.75	1	30	1.5	Philips
G12T5_1/2L	6	21.6	0.79	1	66	1.58	American Ultraviolet
G12T5_1/2VH	6	21.6	0.79	1	66	1.58	American Ultraviolet
G15T8	3.6	36.5	1.27	1	38	2.54	American Ultraviolet
G20T10	4.2	0	1.625	1	0	3.25	T-W
G25T8	6.6	35.56	1.27	1	65.5	2.54	Philips
G25T8(W)	5	36.5	1.27	1	54	2.54	American Ultraviolet
G30T8	11.6	81.3	1.27	1	117	2.54	T-W
G30T8(W)	8.3	81.3	1.27	1	85	2.54	American Ultraviolet
G36T5L	13.9	75.9	0.75	1	181	1.5	Philips
G36T6	12.7	76.2	0.95	1	110	1.9	American Ultraviolet
G36T6H	13.8	76.2	0.79	1	120	1.58	American Ultraviolet
G36T6L	13.8	76.2	0.75	1	176	1.5	LSI
G36T6L(W)	13.8	76.2	0.79	1	120	1.58	American Ultraviolet
G36T6VH	15.2	78.7	0.79	1	124	1.58	American Ultraviolet
G37T6VH	14.3	78.5	0.79	1	130	1.58	IES Handbook
G40T10	11.5	0	1.625	1	0	3.25	T-W
G4S11	0.1	0.95	1.745	1	1.1	3.49	American Ultraviolet
G4T4	0.7	7.8	0.675	1	10	1.35	American Ultraviolet
G4T4/1	1.1	15	0.65	1	12	1.3	American Ultraviolet
G4T5	0.8	8.1	0.775	1	8.3	1.55	T-W
G4T5(W)	0.5	6.3	0.79	1	5.4	1.58	American Ultraviolet
G64T5L	26.7	147.3	0.79	1	190	1.58	American Ultraviolet
G64T5VH	26.7	147.3	0.79	1	190	1.58	American Ultraviolet
G64T6	25	147	0.95	1	200	1.9	IES Handbook
G64T6L	25.5	147.3	0.95	1	208	1.9	American Ultraviolet
G67T5L	25.6	152.5	0.79	1	205	1.58	American Ultraviolet
G67T5VH	25.6	152.5	0.79	1	205	1.58	American Ultraviolet
G6T5	1.6	15.7	0.775	1	16.7	1.55	T-W

APPENDIX D: UVGI Lamp Database

G6T5(W)	1	14	0.79	1	11	1.58	American Ultraviolet
G8T5	2.5	23.3	0.775	1	26	1.55	T-W
G8T5(W)	1.6	21.6	0.79	1	17	1.58	American Ultraviolet
GCC369H	2.4	22.9	0.79	1	23.7	1.58	American Ultraviolet
GCC369N	1.6	22.9	0.79	1	16	1.58	American Ultraviolet
GHO287T5L	3.2	20.6	0.8	1	35	1.6	LSI
GPH212T5L	2.9	13.21	0.75	1	0	1.5	LSI
GPH287T5-H	3	20	0.8	1	33	1.6	IES Handbook
GPH287T5L	3.2	20.57	0.75	1	35	1.5	LSI
GPH287T5-VH	3	20	0.8	1	33	1.6	IES Handbook
GPH435T5	9.6	35	0.75	1	88	1.5	LSI
GPH436T5/HO/40	14	29.2	0.75	1	140	1.5	LSI
GPH436T5LHO/40	8	36	0.75	1	75	1.5	LSI
GPH846T5LHO/40	17	76.71	0.75	1	165	1.5	LSI
GPH893T5LHO/40	17	81.53	0.75	1	0	1.5	LSI
GTL2	0.12	0	1	1	1	2	T-W
GTL3	0.18	0	1	1	2	2	T-W
GUL4	0.7	15	0.675	1	10	1.35	T-W
HUV5W	0.1	0	0.75	1	0	1.5	LSI
LSI436T5	8	36	1	1	0	2	LSI
OZ4S11	0.1	0.95	1.745	1	1.1	3.49	American Ultraviolet
OZ4T5	0.6	15.2	0.79	1	6.5	1.58	American Ultraviolet
OZ6T5	1.2	22.9	0.79	1	13	1.58	American Ultraviolet
OZ8T5	1.8	21.6	0.79	1	19.5	1.58	American Ultraviolet
PL-S9W/TUV	2.5	0	0.5	1	0	1	Philips
Special1	34	46.7	0.9	1	0	1.8	Philips
TUV10W	2.2	33.15	1.4	1	0	2.8	Philips
TUV115W	33.5	119.94	2.025	1	300	4.05	Philips
TUV115WVHO	38.8	119.94	2.025	1	300	4.05	Philips
TUV11W	2.2	42.42	0.45	2	0	0.9	Philips
TUV11WPL-S	3.6	39.6	0.45	2	0	0.9	Philips
TUV15W	4.7	43.74	1.4	1	0	2.8	Philips
TUV16T5	5	22.86	0.76	1	46	1.5	Philips
TUV16W	3.2	28.83	0.8	1	0	1.6	Philips
TUV18W	5.5	39	0.45	2	90	0.9	Philips
TUV18WPL-L	4.6	31.75	0.9	2	46	1.8	Philips
TUV30W	11.2	89.46	1.4	1	0	2.8	Philips
TUV36W	14	112.5	1.3	1	110	2.6	Philips
TUV36WPL-L	12	73	0.45	2	90	0.9	Philips
TUV4W	0.9	8.6	0.8	1	6.5	1.6	Philips
TUV55W	18	178.92	0.45	2	0	0.9	Philips
TUV55WPL-L	17	94.65	0.9	2	290	1.8	Philips
TUV55WHO	17	78.2	1.3	1	0	2.6	Philips
TUV59W	9	21.6	0.45	2	0	0.9	Philips
TUV6W	1.5	16.2	0.8	1	14.3	1.6	Philips
TUV75W	26	119.94	1.4	1	0	2.8	Philips
TUV75WHO	25	112.5	1.3	1	0	2.6	Philips
TUV8W	2.1	23.8	0.8	1	17	1.6	Philips
TUV9WPL-S	2.4	25.8	0.45	2	0	0.9	Philips
SA5000(min)	12.5	27.94	0.9	1	158	1.8	Steril-Aire
SA5000(max)	30	27.94	0.9	1	0	1.8	Steril-Aire

APPENDIX E: Material Reflectivity Database

MATERIAL	REFLECTIVITY %	MATERIAL	REFLECTIVITY %
ePTFE	98.5	Molybdenum	25
Spectralon	95	White botting paper	25
Smoked magnesium oxide	93	AZO photographic paper, unexposed	24
Evaporated aluminum	87	Silver	23
Alzak sheet aluminum, brightened	87	White water paint	23
Alzak sheet aluminum	84	White wallpaper	22
Magnesium oxide	81	Stainless steel	20
Aluminum - sputtered on glass	80	Brownish figured wallpaper	18
Pressed calcium carbonate	78	Tungsten	18
Pressed magnesium oxide	77	Linen	17
Calcium carbonate	75	Fluorescent lamp phosphors	17
Magnesium carbonate	75	Duralumin	16
Aluminum - treated surface	74	Kalsomine white water paint	12
Aluminum foil	73	Medusa cement	11
Aluminum paint	65	Alabastine white water paint	10
Barytes	65	White baked enamel	9
New plaster	58	White oil paint	8
Galvanized duct - smooth	57	Black paint	7
Galvanized duct - rough	53	Brass	7
Aluminum - untreated surface	50	Brown wrapping paper	7
White wall plaster	46	Titanium oxide	6
Stellite	46	AZO photographic paper, exposed black	6
Chromium	44	Celluloid	6
AZO photographic paper, white back	39	Pongee silk	6
Chrome steel	39	Brown baked enamel	6
Rhodium	38	Casein vehicle	6
Nickel	37	Flat black Egyptian lacquer	5
S.W. white Decotint paint	33	Lithopone	5
Ivory wallpaper	31	Zinc oxide in clear lacquer	5
Pink figured wallpaper	31	Black lacquer paint	5
Speculum	30	White porcelain enamel	5
Bleached cotton	30	Zinc oxide paint	5
Tin plated steel	28	Lantern slide glass	4
Stainless steel	28	China clay	4
Tin plate	28	Zinc oxide casein paint	4
Ivory figured wallpaper	26	Pressed zinc oxide	3

APPENDIX F: Program Database for UVGI Rate Constants

Microbe	Rate Constant cm ² /μW-s	D37 μW-s/cm ²	D90 μW-s/cm ²	D99.9 μW-s/cm ²	Test Medium
<i>Serratia marcescens</i>	0.002909	159	792	2375	Air
<i>Escherichia coli</i>	0.003759	123	613	1838	Air
<i>Staphylococcus aureus</i>	0.003476	133	662	1987	Air
<i>Streptococcus pyogenes</i>	0.006161	75	374	1121	Air
<i>Pseudomonas aeruginosa</i>	0.005721	81	402	1207	Air
<i>Legionella pneumophila</i>	0.002047	226	1125	3375	Air
Adenovirus	0.000546	846	4217	12652	Air
Vaccinia (Poxvirus)	0.001528	302	1507	4521	Air
Coxsackievirus	0.001108	417	2078	6234	Air
Influenza A virus	0.001187	389	1940	5820	Air
Echovirus	0.000217	2129	10611	31833	Plates
Reovirus Type 1	0.001849	250	1245	3736	Plates
<i>Staphylococcus aureus</i>	0.000886	521	2599	7797	Water
<i>Mycobacterium tuberculosis</i>	0.002132	217	1080	3240	Plates
<i>Mycobacterium tuberculosis</i>	0.000691	669	3332	9997	Water
<i>Escherichia coli</i>	0.000284	1627	8108	24323	Water
<i>Corynebacterium diptheriae</i>	0.000683	676	3371	10114	Water
<i>Moraxella-Acinetobacter</i>	2.00E-06	231018	1151293	3453878	Water
<i>Haemophilus influenzae</i>	0.000656	704	3510	10530	Water
<i>Pseudomonas aeruginosa</i>	0.000419	1103	5495	16486	Water
<i>Legionella pneumophila</i>	0.002503	185	920	2760	Plates
<i>Serratia marcescens</i>	0.000718	644	3207	9621	Plates
<i>Serratia marcescens</i>	0.001047	441	2199	6598	Water
<i>Bacillus anthracis</i> (mixed)	0.000509	908	4524	13571	Water
<i>Bacillus anthracis</i> spores	0.000794	582	2900	8700	Plates
<i>Bacillus subtilis</i> spores	0.000324	1426	7107	21320	Plates
<i>Cryptococcus neoformans</i> spores	0.000102	4530	22574	67723	Plates
<i>Mucor racemosus</i> spores	0.000135	3422	17056	51169	Plates
<i>Aspergillus niger</i> spores	1.70E-05	27179	135446	406339	Plates
<i>Aspergillus glaucus</i> spores	5.20E-05	8885	44280	132841	Plates
<i>Rhizopus nigricans</i> spores	2.10E-05	22002	109647	328941	Plates
<i>Fusarium oxysporum</i> spores	0.000112	4125	20559	61676	Plates
<i>Fusarium solani</i> spores	7.10E-05	6508	32431	97292	Plates
<i>Penicillium italicum</i> spores	0.000126	3667	18274	54823	Plates
<i>Penicillium digitatum</i> spores	7.20E-05	6417	31980	95941	Plates
<i>Penicillium expansum</i> spores	0.000177	2610	13009	39027	Plates
<i>Cladosporium</i> spores	3.80E-05	12159	60594	181783	Plates
<i>Scopulariopsis</i> spores	2.90E-05	15932	79399	238198	Plates
Blue-green algae	4.60E-06	100442	500562	1501686	Plates
<i>Bacillus subtilis</i> (average)	0.00056	825	4112	12335	--
<i>Listeria monocytogenes</i>	0.002303	201	1000	2999	Plates
<i>Salmonella enteritidis</i>	0.00223	207	1033	3098	Plates
<i>Giardia lamblia</i>	0.0000233	19830	98823	296470	Water
<i>Shigella paradysenteriae</i>	0.000688	672	3347	10040	Water

APPENDIX G: UVX Program Listing

The program used in this research consists of ten files, of which only three are related to the computations. The remaining files are devoted to windows applications, non-computational class definitions, and overhead.

These three files include routines that are used in the computations:

global.h	--	global header file (variable definitions)
uvxDlg.h	--	header file for uvxDlg.cpp (variable definitions)
uvxDlg.cpp	--	source file for main computations

NOTE: Computations begin in the uvxDlg.cpp subroutine called OnBrun().

These files provides windows overhead and resources only:

uvx.cpp	--	source file for windows modules
uvx.h	--	header file for uvx.cpp windows modules
uvx.rc	--	resource file for windows modules
Resource.h	--	header file for resources
Uvx.idl	--	IDL files
StdAfx.cpp	--	standard afx include file
StdAfx.h	--	header file for StdAfx.cpp

global.h

```

// Global variables and arrays

double DirectField[IRES+10][JRES+10][KRES+10]; // Direct Intensity Field
double DistanceMtx[IRES+10][JRES+10][KRES+10];
double PositionMtx[IRES+10][JRES+10][KRES+10];
double FirstField[IBLOCK+10][JBLOCK+10][KBLOCK+10]; // First Reflection Intensity Field
double LeftWall[JBLOCK+10][KBLOCK+10]; // Left Wall Block Intensity Contour
double RightWall[JBLOCK+10][KBLOCK+10]; // Right Wall Block Intensity Contour
double BotWall[IBLOCK+10][KBLOCK+10]; // Bottom Wall Block Intensity Contour
double TopWall[IBLOCK+10][KBLOCK+10]; // Top Wall Block Intensity Contour
double AvgFirst; // Average First Reflection Intensity
double InterField[IBLOCK+10][JBLOCK+10][KBLOCK+10]; // Inter-reflection Intensity Field
double InterFieldTotal[IBLOCK+10][JBLOCK+10][KBLOCK+10]; // Inter-reflection Total field
double RField[IBLOCK+10][JBLOCK+10][KBLOCK+10];
double AvgInter[12]; // Average Inter-reflection Intensity
double AvgTotal; // Average of Total intensity Field
double kSM; // UVDI rate constant for Serratia marcescens
char Microbe[100], Title[100], Model[50];
double SurvivalSM; // Survival of Serratia marcescens
double IntegratedSurvival, Smin, Ce;
double AvgSurvival;
double LogmeanDia;
double FilterEff[5];
double OverallRemoval[5];
double AirVelocity, AirVel, FVel[5];
double Corners[10], MinI, Spores[30];
double MDBrc[100], MDBs[100], MDBk[100]; // Microbe Database rate const surv. & kill
double KZ[IRES+10][JRES+10]; // Kill zones matrix
double NextField[IBLOCK+10][JBLOCK+10][KBLOCK+10];
double EFF[IRES+10][JRES+10][KRES+10]; // Expanded First Field
double EIF[IRES+10][JRES+10][KRES+10]; // Expanded Inter Field
double EBA[IBLOCK+10][JBLOCK+10][KBLOCK+10]; // Block Field
double EFA[IRES+10][JRES+10][KRES+10]; // Expanded Field Total
double TopIR[12][12][22], BotIR[12][12][22], LeftIR[12][12][22], RightIR[12][12][22]; // IR Contours
double RfL1[12][22], RfT1[12][22], RfB1[12][22];
double LfR1[12][22], LfT1[12][22], LfB1[12][22];
double TfB1[12][22], TfL1[12][22], TfR1[12][22];
double BfT1[12][22], BfL1[12][22], BfR1[12][22];
double LeftWallInt[JBLOCK+10][KBLOCK+10]; // Left Wall Block Inter Contour
double RightWallInt[JBLOCK+10][KBLOCK+10]; // Right Wall Block Inter Contour
double BotWallInt[IBLOCK+10][KBLOCK+10]; // Bottom Wall Block Inter Contour
double TopWallInt[IBLOCK+10][KBLOCK+10];
double InterAverage[12], TotalAvgInter, BlockIntAvg;
double AvgTop1, AvgBot1, AvgLeft1, AvgRight1, IR4etc;
int MDB; // # microbes in database
int lcount, IM, checkassign;
int NN, IP, PI;
double P1, P2, P3, P4, P5, P6, P7, P8; // DIMENSIONLES PARAMETERS a-f
double P[2000][15]; // array for input variables

```

uvxDlg.h

```

// uvxDlg.h : header file
//
#ifdef !defined(AFX_UVXDLG_H__1F507046_6081_11D4_8047_FDFE4C9EA26A__INCLUDED_)
#define AFX_UVXDLG_H__1F507046_6081_11D4_8047_FDFE4C9EA26A__INCLUDED_
#if _MSC_VER > 1000
#pragma once
#endif // _MSC_VER > 1000
#include <iostream.h>
#include <fstream.h>
#include <math.h>
#include <stdlib.h>
    const double Pi = 3.14159;
    const int MAXSIZE = 50;
    const int IRES=50, JRES=50, KRES=100; // Resolution x, y, z
    const int IR = 51, JR = 51, KR = 101; // Matrix Size
    const int IBLOCK=10, JBLOCK=10, KBLOCK=20; // Surface Block Resolution
    const int IB = 11, JB = 11, KB = 21; // Matrix Size
    const int NameLen = 20;

////////////////////////////////////
// CUvxDlg dialog
class CUvxDlg : public CDialog
{
// Construction
public:
    void Dimensionless();
    void ABCfill();
    void InterReflections();
    int SaveContours(int i);
    void AvgIR1Contours();
    double PerpRect(double a, double b, double c);
    double ParaRect(double a, double b, double c);
    void AvgIR2();
    void RightIR1();
    void LeftIR1();
    void BotIR1();
    void TopIR1();
    void ScaleDimensions();
    void CheckAssignment();
    double rightPavg;
    double leftPavg;
    double bottomPavg;
    double topPavg;
    double exitPavg;
    double entrancePavg;
    CString m_gfilename;
    void EntPlaneRes();
    void EntPlaneBlock();
    void InitializeMatrices();
    void IDIntensity();
    void AddFields();
    void ExpandFirstField();
    void ExpandInterField();
    //void AddFieldsBlock();

```

```

void IntegratedIntensity();
double Survival(double k, double I, double t);
double VFPerpendicularGhost(double c, double a, double b, double d, double e);
double VFPerpendicularPlane(double c, double a, double b);
double VFRightPPWall(double x, double y, double z);
double VFLeftPPWall(double x, double y, double z);
double VFTopPPWall(double x, double y, double z);
double VFBotPPWall(double x, double y, double z);
double VFTopWall(double x, double y, double z);
double VFBotWall(double x, double y, double z);
double VFRightWall(double x, double y, double z);
double VFLeftWall(double x, double y, double z);
double AverageInter();
void ExchangeWallFields();
void InterReflectField();
double AverageFirst();
double VFParallelGhost(double c, double a, double b, double d, double e);
double VFParallelPlane(double c, double a, double b);
double VFHorizWall(double y, double x, double z);
double VFVerticalWall(double x, double y, double z);
void FirstRefField();
void BlockAvg();
double AverageDirect();
double VFCylinder(double I, double r, double h);
double IBeyondEnds(double IS, double arcl, double r, double x, double db);
double Intensity(double IS, double arcl, double r, double x, double I);
double Position(int i, int j, int k, int l);
double PointLine(double x, double y, double z, int l);
double Distance(int i, int j, int k, int l);
void DirectIntField();
void DataInput();
void Analysis();
void Graphs();
int m_nProgress1;
int m_nProgress2;
int m_nProgress3;
int m_nProgress6;
CUvxDlg(CWnd* pParent = NULL);    // standard constructor
int NUMLAMPS, REALNUMLAMPS;
// Lamp Data Arrays
int lamptype[MAXSIZE];           // Type 1 = cylindrical, Type 2 = U-tube
double UVPower[MAXSIZE];         // Array for Lamp UV powers
double UVPoweractual[MAXSIZE];   // storage array for U-tube power
double arclength[MAXSIZE];       // Array for Lamp arclengths
double radius[MAXSIZE];          // Array for Lamp radii
double SurfInt[MAXSIZE];         // Array for Lamp Surface Intensities
double lampx1[MAXSIZE], lampy1[MAXSIZE], lampz1[MAXSIZE]; // Lamp Endpoints
double lampx2[MAXSIZE], lampy2[MAXSIZE], lampz2[MAXSIZE]; // Lamp Endpoints
char Project[22];
double Width, Height, Length;    // Enclosure dimensions
double xincr, yincr, zincr;       // Increments x, y, z
double Reflectivity, Rho;         // Surface Reflectivity
double Et;                        // Exposure time
double Airflow;                   // Airflow in cu. meters/sec
double AvgDirect;                 // Average Direct Intensity
double KillRate, IntKillRate;

```

```

        double U[5];                                // filter air velocity, m/s

// Dialog Data
//{{AFX_DATA(CUvxDlg)
enum { IDD = IDD_UVX_DIALOG };
CString m_averagedirect;
CString m_averagefirst;
CString m_averageinter;
CString m_killrate;
CString m_averagetotal;
CString m_integratedkill;
CString m_savingfiles;
CString m_complete;
CString m_intsurvival;
CString m_survival;
CString m_target;
CString m_rho;
CString m_exptime;
CString m_showairflow;
CString m_showheight;
CString m_showlength;
CString m_showmodel;
CString m_showwidth;
CString m_shownlamps;
CString m_PI;
CString m_ip;
//}}AFX_DATA

// ClassWizard generated virtual function overrides
//{{AFX_VIRTUAL(CUvxDlg)
protected:
virtual void DoDataExchange(CDataExchange* pDX);    // DDX/DDV support
//}}AFX_VIRTUAL

// Implementation
protected:
    HICON m_hIcon;

    // Generated message map functions
//{{AFX_MSG(CUvxDlg)
virtual BOOL OnInitDialog();
afx_msg void OnSysCommand(UINT nID, LPARAM lParam);
afx_msg void OnPaint();
afx_msg HCURSOR OnQueryDragIcon();
afx_msg void OnBrun();
afx_msg void OnKeyDown(UINT nChar, UINT nRepCnt, UINT nFlags);
//}}AFX_MSG
    DECLARE_MESSAGE_MAP()
};

//{{AFX_INSERT_LOCATION}}
// Microsoft Visual C++ will insert additional declarations immediately before the previous line.
#endif //
#ifdef AFX_UVXDLG_H__1F507046_6081_11D4_8047_FDFE4C9EA26A__INCLUDED_

```


uvxDlg.cpp

```

// uvxDlg.cpp : implementation file
//

#include "stdafx.h"
#include "iostream.h"
#include "fstream.h"
#include "iomanip.h"
#include "uvx.h"
#include "uvxDlg.h"
#include "global.h"
#include "math.h"

#ifdef _DEBUG
#define new DEBUG_NEW
#undef THIS_FILE
static char THIS_FILE[] = __FILE__;
#endif

////////////////////////////////////
// CAboutDlg dialog used for App About

class CAboutDlg : public CDialog
{
public:
    CAboutDlg();

// Dialog Data
//{{AFX_DATA(CAboutDlg)
enum { IDD = IDD_ABOUTBOX };
//}}AFX_DATA

// ClassWizard generated virtual function overrides
//{{AFX_VIRTUAL(CAboutDlg)
protected:
virtual void DoDataExchange(CDataExchange* pDX);    // DDX/DDV support
//}}AFX_VIRTUAL

// Implementation
protected:

//{{AFX_MSG(CAboutDlg)
//}}AFX_MSG
    DECLARE_MESSAGE_MAP()
};

CAboutDlg::CAboutDlg() : CDialog(CAboutDlg::IDD)
{
    // comment
    {{{AFX_DATA_INIT(CAboutDlg)
    }}}AFX_DATA_INIT
}

```

```

void CAboutDlg::DoDataExchange(CDataExchange* pDX)
{
    CDialog::DoDataExchange(pDX);
   //{{AFX_DATA_MAP(CAboutDlg)
   //}}AFX_DATA_MAP
}

BEGIN_MESSAGE_MAP(CAboutDlg, CDialog)
   //{{AFX_MSG_MAP(CAboutDlg)
    // No message handlers
   //}}AFX_MSG_MAP
END_MESSAGE_MAP()

////////////////////////////////////
// CUvxDlg dialog

CUvxDlg::CUvxDlg(CWnd* pParent /*=NULL*/)
: CDialog(CUvxDlg::IDD, pParent)
{
   //{{AFX_DATA_INIT(CUvxDlg)
    m_averagedirect = _T("0.0");
    m_averagefirst = _T("0.0");
    m_averageinter = _T("0.0");
    m_killrate = _T("0.0");
    m_averagetotal = _T("0.0");
    m_integratedkill = _T("0.0");
    m_savingfiles = _T("");
    m_complete = _T("");
    m_intsurvival = _T("0.0");
    m_survival = _T("0.0");
    m_target = _T("");
    m_rho = _T("");
    m_exptime = _T("");
    m_showairflow = _T("");
    m_showheight = _T("");
    m_showlength = _T("");
    m_showmodel = _T("");
    m_showwidth = _T("");
    m_shownlamps = _T("");
    m_PI = _T("");
    m_ip = _T("");
    m_nProgress1 = 0;
    m_nProgress2 = 0;
    m_nProgress3 = 0;
   //}}AFX_DATA_INIT
    // Note that LoadIcon does not require a subsequent DestroyIcon in Win32
    m_hIcon = AfxGetApp()->LoadIcon(IDR_MAINFRAME);
}

```



```

BOOL CUvxDlg::OnInitDialog()
{

    // IDM_ABOUTBOX must be in the system command range.
    ASSERT((IDM_ABOUTBOX & 0xFFF0) == IDM_ABOUTBOX);
    ASSERT(IDM_ABOUTBOX < 0xF000);

    CMenu* pSysMenu = GetSystemMenu(FALSE);
    if (pSysMenu != NULL)
    {
        CString strAboutMenu;
        strAboutMenu.LoadString(IDS_ABOUTBOX);
        if (!strAboutMenu.IsEmpty())
        {
            pSysMenu->AppendMenu(MF_SEPARATOR);
            pSysMenu->AppendMenu(MF_STRING, IDM_ABOUTBOX,
strAboutMenu);
        }
    }

    // Set the icon for this dialog. The framework does this automatically
    // when the application's main window is not a dialog
    SetIcon(m_hIcon, TRUE);           // Set big icon
    SetIcon(m_hIcon, FALSE);          // Set small icon

    // TODO: Add extra initialization here
    CProgressCtrl* pProg1 = (CProgressCtrl*) GetDlgItem(IDC_PROGRESS1);
    pProg1->SetRange(0,100);
    pProg1->SetPos(m_nProgress1);

    CProgressCtrl* pProg2 = (CProgressCtrl*) GetDlgItem(IDC_PROGRESS2);
    pProg2->SetRange(0,100);
    pProg2->SetPos(m_nProgress2);

    CProgressCtrl* pProg3 = (CProgressCtrl*) GetDlgItem(IDC_PROGRESS3);
    pProg3->SetRange(0,30);
    pProg3->SetPos(m_nProgress3);

    CProgressCtrl* pProg6 = (CProgressCtrl*) GetDlgItem(IDC_PROGRESS6);
    pProg6->SetRange(0,100);
    pProg6->SetPos(m_nProgress6);

    return TRUE; // return TRUE unless you set the focus to a control
}

```

```

void CUvxDlg::OnSysCommand(UINT nID, LPARAM lParam)
{
    if ((nID & 0xFFFF) == IDM_ABOUTBOX)
    {
        CAboutDlg dlgAbout;
        dlgAbout.DoModal();
    }
    else
    {
        CDialog::OnSysCommand(nID, lParam);
    }
}

```

// If you add a minimize button to your dialog, you will need the code below
 // to draw the icon. For MFC applications using the document/view model,
 // this is automatically done for you by the framework.

```

void CUvxDlg::OnPaint()
{
    if (IsIconic())
    {
        CPaintDC dc(this); // device context for painting

        SendMessage(WM_ICONERASEBKGND, (LPARAM) dc.GetSafeHdc(), 0);

        // Center icon in client rectangle
        int cxIcon = GetSystemMetrics(SM_CXICON);
        int cyIcon = GetSystemMetrics(SM_CYICON);
        CRect rect;
        GetClientRect(&rect);
        int x = (rect.Width() - cxIcon + 1) / 2;
        int y = (rect.Height() - cyIcon + 1) / 2;

        // Draw the icon
        dc.DrawIcon(x, y, m_hIcon);
    }
    else
    {
        CDialog::OnPaint();
    }
}

```

// The system calls this to obtain the cursor to display while the user drags
 // the minimized window.

```

HCURSOR CUvxDlg::OnQueryDragIcon()
{
    return (HCURSOR) m_hIcon;
}

```

```

//-----
//-----
//-----

```

```

void CUvxDlg::OnBrun()
{
    UpdateData(TRUE);
    ABCfill();
    ofstream outfile("adata.txt",ios::out);
    outfile<<"A B C D E F G J KillRate IntKill Iavg AvgDir AvgFirst AvgInter";
    outfile<<endl;
    for(PI=1; PI<=IP; PI++){
        UpdateData(TRUE);
        m_PI.Format("%d ",PI);
        UpdateData(FALSE);
        NUMLAMPS=1;
        REALNUMLAMPS=1;
        InitializeMatrices();      // Initialize
        DataInput();               // Get file data
        Analysis();               // Perform UVGI Analysis
        Dimensionless();
        outfile<<P1<<" "<<P2<<" "<<P3<<" "<<P4<<" "<<P5<<" "
        <<P6<<" "<<P7<<" "<<P8<<" "<<KillRate<<" "<<IntKillRate<<" "
        <<AvgTotal<<" "<<AvgDirect<<" "<<AvgFirst<<" "<<TotalAvgInter<<" "<<endl;
    }

    m_complete.Format("ANALYSIS COMPLETE ");
    UpdateData(FALSE);
}

```

```

void CUvxDlg::Analysis()
{
    // Scale
    ScaleDimensions();
    // Compute Intensity Matrix
    DirectIntField();

    AvgDirect = AverageDirect();
    m_averagedirect.Format("%7.2f ",AvgDirect);
    UpdateData(FALSE);

    // Compute Reflected Intensity Field
    if (Reflectivity!=0){
        // Compute Block Average Wall Intensities
        BlockAvg();
        // Compute First Reflection Intensity Field
        FirstRefField();
        ExpandFirstField();
        AvgFirst = AverageFirst();
        m_averagefirst.Format("%7.2f ",AvgFirst);

        UpdateData(FALSE);
        // Compute Inter-reflection Intensity Field
        InterReflections();
        m_averageinter.Format("%7.2f ",TotalAvgInter);
        UpdateData(FALSE);
    }

    AvgTotal = TotalAvgInter + AvgFirst + AvgDirect;
    m_averagetotal.Format("%7.2f ",AvgTotal);
    UpdateData(FALSE);

    // Compute Survival
    AvgSurvival = 100.0*Survival(kSM, AvgTotal, Et);
    KillRate = 100.0-AvgSurvival;
    m_killrate.Format("%d ", (int)KillRate);
    m_survival.Format("%d ", (int)AvgSurvival);
    UpdateData(FALSE);
    // Compute Integrated Intensity
    IntegratedIntensity();
    m_integratedkill.Format("%d ",(int)IntKillRate);
    m_intsurvival.Format("%d ",(int)IntegratedSurvival);

    UpdateData(FALSE);

}

//-----
//-----
//-----

```

```

void CUvxDlg::DataInput()
{
    // Read data input file
    // Convert data input file P[i][j]
    Width = P[PI][1];
    Height = P[PI][2];
    kSM = P[PI][5];
    Airflow = P[PI][7];
    Length = P[PI][11];
    Reflectivity = P[PI][12];
    Rho = Reflectivity/100;
    lamptype[0] = 1;
    UVPower[0]= 1000000.0*P[PI][6];
    arclength[0] = P[PI][4];
    radius[0] = P[PI][3];
    lampx1[0] = 0.0;
    lampx2[0] = P[PI][4];
    lampy1[0] = P[PI][9];
    lampy2[0] = P[PI][9];
    lampz1[0] = P[PI][10];
    lampz2[0] = P[PI][10];

    // Compute Surface Intensity
    SurfInt[0]= UVPower[0]/(2*Pi*radius[0]*arclength[0]);

    double Qcfm;
    // Air Velocity in UVGI System
    AirVel = (Airflow/60)/((Height/100)*(Width/100));;
    AirVelocity = AirVel*196.8;
    Qcfm = Airflow*196.8;
    Et = (Length/100)/(Airflow/(60*Width*Height/10000));
    m_ip.Format("%d ",IP);
    m_rho.Format("%.3f ", Reflectivity);
    m_exptime.Format("%.5f ", Et);
    m_showmodel=Model;
    m_showheight.Format("%.7f ", Height);
    m_showlength.Format("%.7f ", Length);
    m_showwidth.Format("%.7f ", Width);
    m_showairflow.Format("%.7f ", Qcfm);
    m_shownlamps.Format("%d ", NUMLAMPS);
    UpdateData(FALSE);
}

```



```

void CUvxDlg::DirectIntField()
// Computes Intensity Matrix of Direct Intensity Field
{
    //ofstream outfile("dex.txt",ios::out);
    //outfile<<"i j k x paxis db DirectField"<<endl;
    int i, j, k, l;
    double tempsum = 0.0, x, paxis, db=0.0;
    for (i=0; i<=IRES; i++){
        CProgressCtrl* pProg1 =
            (CProgressCtrl*) GetDlgItem(IDC_PROGRESS1);
        pProg1->SetRange(0, 100);
        pProg1->SetPos(i*2);

        for (j=0; j<=JRES; j++){
            for (k=0; k<=KRES; k++){
                db=0.0;
                for (l=0; l<NUMLAMPS; l=l+1) {
                    // Compute distance x to lamp axis
                    x = Distance(i,j,k,l);
                    DistanceMtx[i][j][k]=x;
                    // Compute position on lamp axis
                    paxis = fabs(Position(i,j,k,l));
                    PositionMtx[i][j][k]=paxis;
                    // Are we within lamp arclength?
                    if (paxis < arclength[l]){
                        // Compute Intensity within Lamp arclength
                        tempsum = Intensity(SurfInt[l],arclength[l],radius[l],x,paxis);
                    }
                    else { // Compute Intensity beyond Lamp end
                        db = paxis-arclength[l];
                        tempsum = lBeyondEnds(SurfInt[l],arclength[l],radius[l],x,db);
                    }
                    // Add intensities for all lamps
                    DirectField[i][j][k] = DirectField[i][j][k] + tempsum;
                    tempsum = 0;
                }
            }
        }
    }
}

```

```

double CUvxDlg::Distance(int i, int j, int k, int l)
{ // Compute shortest Distance to Lamp Axis
  double xi, yj, zk;
  xi = i;
  yj = j;
  zk = k;
  double x = xi*xincr;
  double y = yj*yincr;
  double z = zk*zincr;
  double dist = PointLine(x, y, z, l);
  return dist;
}

double CUvxDlg::PointLine(double x, double y, double z, int l)
{ // Compute Distance from a Point to a Line
  double x1=x-lampx1[l];
  double y1=y-lampy1[l];
  double z1=z-lampz1[l];
  double x2=lampx2[l]-lampx1[l];
  double y2=lampy2[l]-lampy1[l];
  double z2=lampz2[l]-lampz1[l];
  double dist, DotProd, a;
  double p1=x1*x1+y1*y1+z1*z1;
  double p2=x2*x2+y2*y2+z2*z2;
  if (p1*p2>0){
    DotProd = (x1*x2+y1*y2+z1*z2)/sqrt(p1*p2);
    a = acos(DotProd);
    dist=fabs(sin(a))*sqrt(p1);
  }
  else {
    dist = 0;
  }
  return dist;
}

```

```

double CUvxDlg::Position(int i, int j, int k, int l)
{
    // Compute Position along lamp axis
    double xi, yj, zk, p1, p2;
    double DotProd, a, x, y, z, posit, x1, y1, z1, x2, y2, z2;
    double pc, pa, pd, p3, p4, p5, posit1, posit2;
    xi = i;
    yj = j;
    zk = k;
    x = xi*xincr;
    y = yj*yincr;
    z = zk*zincr;
    posit = 1;
    x1=x-lampx1[l];
    y1=y-lampy1[l];
    z1=z-lampz1[l];
    x2 = lampx2[l]-lampx1[l];
    y2 = lampy2[l]-lampy1[l];
    z2 = lampz2[l]-lampz1[l];
    p1 = x1*x1+y1*y1+z1*z1;
    p2 = x2*x2+y2*y2+z2*z2;
    pc = x1*x2+y1*y2+z1*z2;
    pa =p1*p2;
    if (pa>0){
        DotProd = pc/sqrt(pa);
        a = acos(DotProd);
        posit1 = cos(a)*sqrt(p1);
    }
    else {
        posit1 = 0.000001;
    }
    x1=x-lampx2[l];
    y1=y-lampy2[l];
    z1=z-lampz2[l];
    x2 = lampx1[l]-lampx2[l];
    y2 = lampy1[l]-lampy2[l];
    z2 = lampz1[l]-lampz2[l];
    p3 = x1*x1+y1*y1+z1*z1;
    p4 = x2*x2+y2*y2+z2*z2;
    pd = x1*x2+y1*y2+z1*z2;
    p5 =p3*p4;
    if (p5>0){
        DotProd = pd/sqrt(p5);
        a = acos(DotProd);
        posit2 = cos(a)*sqrt(p3);
    }
    else {
        posit2 = 0.000001;
    }
    //posit = max(posit1,posit2);
    if (posit1>=posit2) posit = posit1;
    else posit = posit2;
    return posit;
}

```

```

double CUvxDlg::Intensity(double IS, double arcl, double r, double x, double l)
{
    // Compute Intensity Field
    // IS=Surface Intensity, arcl=arclength, r=radius,
    // x=distance from axis, l = distance along axis
    double intense;
    double VF, VF1, VF2;
    // Compute VF Lamp segment 1
    VF1 = VFCylinder(l,r,x);
    // Compute Lamp segment 2
    VF2 = VFCylinder((arcl-l),r,x);
    // Total VF for Lamp
    VF = VF1 + VF2;
    // Compute intensity at the point
    intense = IS*VF;
    return intense;
}

double CUvxDlg::IBeyondEnds(double IS, double arcl, double r, double x, double db )
{
    // Compute Intensity field beyond the ends of the LAMP
    // IS=Surface Intensity, arcl=arclength, r=radius
    // x=distance from axis, db=distance beyond lamp end
    double intense;
    double VF, VF1, VF2;
    // Compute Lamp + Ghost Lamp segment
    VF1 = VFCylinder((arcl+db),r,x);
    // Compute Ghost Lamp segment
    VF2 = VFCylinder(db,r,x);
    // Compute Lamp VF
    VF = VF1 - VF2;
    // Compute intensity at the point
    // use absolute value since near zero values may be negative
    intense = fabs(IS*VF);
    return intense;
}

double CUvxDlg::VFCylinder(double l, double r, double h) // Modest VF #15
{
    // l=length, r=radius, h=height above axis
    double H, L, X, Y, p1, p2, p3, VF;
    if (h<r) h=r+0.000001; // Not inside lamp
    H = h/r;
    L = l/r;
    if (L==0) L=0.000001;
    if (H==1) H=H+0.000001;
    X = (1+H)*(1+H)+L*L;
    Y = (1-H)*(1-H)+L*L;
    // Compute Parts of View Factor
    p1 = atan( L/sqrt(H*H-1) )/L;
    p2 = (X-2*H)*atan( sqrt( (X/Y)*(H-1)/(H+1) ) )/sqrt(X*Y);
    p3 = atan( sqrt((H-1)/(H+1)) );
    VF = L*(p1+p2-p3)/(Pi*H);
    return VF;
}

```

```

double CUvxDlg::AverageDirect()
{
    int IR, JR, KR;
    double total = 0;
    double Avg = 0;
    IR = IRES+1;
    JR = JRES+1;
    KR = KRES+1;
    for (int i=0; i<=IRES; i++){
        for (int j=0; j<=JRES; j++){
            for (int k=0; k<=KRES; k++){
                total = total + DirectField[i][j][k];
                // Remove Lamp Volume contribution
            }
        }
    }
    Avg = total/(IR*JR*KR);
    return Avg;
}

void CUvxDlg::BlockAvg() // Computes Block Averages of Reflected Wall Intensity
{
    int i, k, ib, kb;
    double s1, s2, s3, s4;
    for (ib=0; ib<=IB; ib++){
        for (kb=0; kb<=KB; kb++){
            s1 = 0;
            s2 = 0;
            s3 = 0;
            s4 = 0;
            for (i=ib*5; i<(ib+1)*5; i++){
                for (k=kb*5; k<(kb+1)*5; k++){
                    s1 = s1 + DirectField[i][0][k];
                    s2 = s2 + DirectField[i][JRES][k];
                    s3 = s3 + DirectField[0][i][k];
                    s4 = s4 + DirectField[IRES][i][k];
                }
            }

            BotWall[ib][kb] = Rho*s1/25.0;
            TopWall[ib][kb] = Rho*s2/25.0;
            LeftWall[ib][kb] = Rho*s3/25.0;
            RightWall[ib][kb]= Rho*s4/25.0;
        }
    }
}

```

```

void CUvxDlg::FirstRefField() // Computes Intensity Matrix of First Reflection
{
    int i,j,k;
    double dx, dy, dz;
    double frv, frh, id, jd, kd;
        id =xincr*IRES/IBLOCK;
        jd =yincr*JRES/JBLOCK;
        kd =zincr*KRES/KBLOCK;
    for (i=0; i<IB; i++){
        dx = i*id; // Distance to Left Wall
        for (j=0; j<JB; j++){
            dy = j*jd; // Distance to Bottom Wall
            CProgressCtrl* pProg2 =
                (CProgressCtrl*) GetDlgItem(IDC_PROGRESS2);
            pProg2->SetRange(0, 100);
            pProg2->SetPos(i*10+j);
            for (k=0; k<KB; k++){
                dz = k*kd; // Distance along z axis
                // Compute Intensity from Left & Right Walls
                frv = VFVerticalWall(dx, dy, dz);
                // Compute Intensity from Bottom & Top Walls
                frh = VFHorizWall(dy, dx, dz);
                FirstField[i][j][k] = frv+frh;
                frv = 0;
                frh = 0;
            }
        }
    }
}

```

```

double CUvxDig::VFVerticalWall(double x, double y, double z)
{
    int jb, kb;
    double y1, y2, z1, z2, dy, dz, c, a, b;
    double vf, vfl, vfr, fr, frl, frr, wr, id, jd, kd;
    fr = 0;    // zero out sum
    vf = 0;
    id = xincr*IRES/IBLOCK;
    jd = yincr*JRES/JBLOCK;
    kd = zincr*KRES/KBLOCK;
    // Compute block dims & dist

    c = x;
    a = jd;
    b = kd;
    wr = Width - c;
    for (jb=0; jb<JB; jb++){
        y1 = jb*jd;
        y2 = (jb+1)*jd;
        dy = min(fabs(y-y1), fabs(y-y2));
        for (kb=0; kb<KB; kb++){
            // Define four coordinates of block
            z1 = kb*kd;
            z2 = (kb+1)*kd;
            // Find distance to closest coordinates
            dz = min(fabs(z-z1), fabs(z-z2));

            // Compute View Factors & Field from left & right
            if (dy==0 && dz==0){    // We're right at a corner
                vfl = VFParallelPlane(c,a,b);    // VF left wall
                frl = vfl*LeftWall[jb][kb];    // Field intensity
                vfr = VFParallelPlane(wr,a,b);    // VF right wall
                frr = vfr*RightWall[jb][kb];    // Field intensity
            }
            else {    // We're not at a corner
                vfl = VFParallelGhost(c,a,b,dy,dz);    // VF left
                frl = vfl*LeftWall[jb][kb];    // Field
                vfr = VFParallelGhost(wr,a,b,dy,dz);    // VF right
                frr = vfr*RightWall[jb][kb];    // Field
            }
            fr = fr + frl + frr;    // Total Field intensity left & right
            vf = vf + vfl + vfr;
        }
    }
    return fr;
}

```

```

double CUvxDlg::VFHorizWall(double y, double x, double z)
{
    int ib, kb;
    double x1, x2, z1, z2, dx, dz, c, a, b;
    double vf, vfb, vft, fr, frb, frt, wr, id, jd, kd;
    fr = 0;    // zero out sum
    vf = 0;
    id = xincr*IRES/IBLOCK;
    jd = yincr*JRES/JBLOCK;
    kd = zincr*KRES/KBLOCK;
    // Compute block dims & dist

    c = y;
    a = id;    // Define coordinates of block
    b = kd;
    wr = Height - c;
    for (ib=0; ib<IB; ib++){
        x1 = ib*id;
        x2 = (ib+1)*id;
        dx = min(fabs(x-x1),fabs(x-x2));
        for (kb=0; kb<KB; kb++){
            // Define coordinates of block
            z1 = kb*kd;
            z2 = (kb+1)*kd;
            // Find distance to closest coordinates
            dz = min(fabs(z-z1),fabs(z-z2));
            // Compute View Factors & Field from left & right
            if (dx==0 && dz==0){    // We're right at a corner
                vfb = VFParallelPlane(c,a,b);    // VF bottom wall
                frb = vfb*BotWall[ib][kb];    // Field intensity
                vft = VFParallelPlane(wr,a,b);    // VF top wall
                frt = vft*TopWall[ib][kb];    // Field intensity
            }
            else {    // We're not at a corner
                vfb = VFParallelGhost(c,a,b,dx,dz);    // VF bot
                frb = vfb*BotWall[ib][kb];    // Field
                vft = VFParallelGhost(wr,a,b,dx,dz);    // VF top
                frt = vft*TopWall[ib][kb];    // Field
            }
            fr = fr + frb + frt;    // Total Field intensity left & right
            vf = vf + vft + vfb;
        }
    }
    return fr;
}

```



```

double CUvxDlg::VFParallelPlane(double c, double a, double b)
{ // View Factor to a Parallel Plane at the corner
  // a=width or height, b=length, c=distance to corner
  double A, B, p1, p2, vf;
  if (c==0) c=0.000001; // Can't be closer than 1 micron
  A = a/c;
  B = b/c;
  p1 = (A/sqrt(1+A*A))*atan(B/sqrt(1+A*A));
  p2 = (B/sqrt(1+B*B))*atan(A/sqrt(1+B*B));
  vf = (p1+p2)/(2*Pi);
  if(vf>1.0) vf=1.0;
  return vf;
}

double CUvxDlg::VFParallelGhost(double c, double a, double b, double d, double e)
{ // View factor to Parallel Plane beyond the corner
  // a=width or height, b=length, c=perpendicular distance
  // d = y distance beyond corner, e = z distance beyond corner
  double vft, vf1, vf2, vf34, vf2a, vf2b; // Total vft, & sections 1,2,3,4

  // Compute VF to Total Area
  vft = VFParallelPlane(c,a+d,b+e);
  // Compute VF to Ghost sections 2,3,4
  vf2a = VFParallelPlane(c,a+d,e);
  vf2b = VFParallelPlane(c,d,e);
  vf2 = vf2a-vf2b;
  vf34 = VFParallelPlane(c,d,b+e);
  // Subtract to obtain VF to Real Section vf1
  vf1 = vft - vf2 - vf34;
  return vf1;
}

double CUvxDlg::AverageFirst()
{
  double total=0, Avg;
  for (int i=0; i<=IBLOCK; i++){
    for (int j=0; j<=JBLOCK; j++){
      for (int k=0; k<=KBLOCK; k++){
        total = total + FirstField[i][j][k];
        // Remove Lamp Volume contribution
      }
    }
  }
  Avg = total/(IB*JB*KB);
  return Avg;
}

```

```

//***** INTER-REFLECTIONS *****

void CUvxDlg::InterReflections() // Computes Intensity Matrix of Inter-reflections
{
    //int i;
    double Fraction21, GeomSeries;
    lcount = 0;
    AvgInter[1] = 0;
    AvgInter[2] = 0;
    IR4etc = 0;
    //SaveContours(0);
        // Compute wall contours from 1st inter-reflection

    TopIR1();        // Compute TopWallInt = 1st Inter Contour
    BotIR1();        // Compute BotWallInt
    LeftIR1();       // Compute LeftWallInt
    RightIR1();      // Compute RightWallInt


    ExchangeWallFields(); // Exchange Direct for 1st IR Contours
    //SaveContours(1);      // Save Wall Contours
    InterReflectField();    // Compute IR1 Intensity Field
    AvgInter[1] = AverageInter(); // Computes Avg IR1 Field
    AvgIR1Contours();      // Flattens IR1 Contours
    AvgIR2();              // Compute Avg IR2 Contours
    ExchangeWallFields(); // Exchange Wall Fields
    InterReflectField();    // Compute IR2 Intensity Field
    AvgInter[2] = AverageInter(); // Compute Average IR2 Field
    // Compute ratio of 3rd to second Inter-reflection
    Fraction21 = AvgInter[2]/AvgInter[1];
    AvgInter[3] = Fraction21*AvgInter[2];
    AvgInter[4] = Fraction21*AvgInter[3];
    AvgInter[5] = Fraction21*AvgInter[4];
    AvgInter[6] = Fraction21*AvgInter[5];
    // Compute the Geometric Series Factor
    GeomSeries = Fraction21/(1-Fraction21);
    // Compute remaining reflections 4 to infinity as a series
    IR4etc = GeomSeries*AvgInter[2];
    TotalAvgInter = AvgInter[1]+AvgInter[2]+IR4etc;
}

```

```

void CUvxDlg::TopIR1()
{
    // Top IR contour from other walls
    int i, k;
    double dx, dy, dz, dt, id, jd, kd;
    id = xincr*IRES/IBLOCK;
    jd = yincr*JRES/IBLOCK;
    kd = zincr*KRES/KBLOCK;
    dy = Height; // Distance to Left
    // Top from Bottom
    for (i=0; i<IBLOCK; i++){
        dx = i*id; // Distance to Bottom
        for (k=0; k<KBLOCK; k++){
            dz = k*kd; // Distance along z axis
            TfB1[i][k] = Rho*VFBotWall(dy,dx,dz);
        }
    }
    // Top from Left
    for (i=0; i<IBLOCK; i++){
        dx = i*id; // Distance to Left
        for (k=0; k<KBLOCK; k++){
            dz = k*kd; // Distance along z axis
            TfL1[i][k] = Rho*VFLeftPPWall(dx,dy,dz);
        }
    }
    // Top from Right
    for (i=0; i<IBLOCK; i++){
        dx = i*id; // Distance to Left
        dt = Width - dx;
        for (k=0; k<KBLOCK; k++){
            dz = k*kd; // Distance along z axis
            TfR1[i][k] = Rho*VFRightPPWall(dt,dy,dz);
        }
    }
    for (i=0; i<IBLOCK; i++){
        for (k=0; k<KBLOCK; k++){
            TopWallInt[i][k]=TfB1[i][k]+TfL1[i][k]+TfR1[i][k];
        }
    }
}

```

```

void CUvxDlg::BotlR1()
{
    int i, k;
    double dx, dy, dz, dt, id, jd, kd;
    id = xincr*IRES/IBLOCK;
    jd = yincr*JRES/IBLOCK;
    kd = zincr*KRES/KBLOCK;
    dy = Height;          // Distance to Left
    // Bottom from Top
    for (i=0; i<IBLOCK; i++){
        dx = i*id;          // Distance to Bottom
        for (k=0; k<KBLOCK; k++){
            dz = k*kd;      // Distance along z axis
            BfT1[i][k] = Rho*VFTopWall(dy,dx,dz);
        }
    }
    // Bottom from Left
    dy = 0; // Distance to Bottom
    for (i=0; i<IBLOCK; i++){
        dx = i*id; // Distance to Left
        for (k=0; k<KBLOCK; k++){
            dz = k*kd; // Distance along z axis
            BfL1[i][k] = Rho*VFLeftPPWall(dx,dy,dz);
        }
    }
    // Bottom from Right
    for (i=0; i<IBLOCK; i++){
        dx = i*id; // Distance to Left
        dt = Width - dx;
        for (k=0; k<KBLOCK; k++){
            dz = k*kd; // Distance along z axis
            BfR1[i][k] = Rho*VFRightPPWall(dt,dy,dz);
        }
    }
    for (i=0; i<IBLOCK; i++){
        for (k=0; k<KBLOCK; k++){
            BotWallInt[i][k]= BfT1[i][k] +BfL1[i][k] +BfR1[i][k] ;
        }
    }
}

```

```

void CUvxDlg::LeftIR1()
{
    int j, k;
    double dx, dy, dz, dt, id, jd, kd;
    id = xincr*IRES/IBLOCK;
    jd = yincr*JRES/JBLOCK;
    kd = zincr*KRES/KBLOCK;
    dx = Width;          // Distance to Left
    // Left from Right
    for (j=0; j<JBLOCK; j++){
        dy = j*jd;      // Distance to Bottom
        for (k=0; k<KBLOCK; k++){
            dz = k*kd;   // Distance along z axis
            LfR1[j][k] = Rho*VFRightWall(dx,dy,dz);
        }
    }
    // Left from Top
    dx = 0.0;
    for (j=0; j<JBLOCK; j++){
        dy = j*jd;      // Distance to Bottom
        dt = Height - dy;
        for (k=0; k<KBLOCK; k++){
            dz = k*kd;   // Distance along z axis
            LfT1[j][k] = Rho*VFTopPPWall(dx,dt,dz);
        }
    }
    // Left from Bottom
    dx = 0;
    for (j=0; j<JBLOCK; j++){
        dy = j*jd;      // Distance to Bottom
        for (k=0; k<KBLOCK; k++){
            dz = k*kd;   // Distance along z axis
            LfB1[j][k] = Rho*VFBotPPWall(dx,dy,dz);
        }
    }
    for (j=0; j<JBLOCK; j++){
        for (k=0; k<KBLOCK; k++)
            LeftWallInt[j][k] = LfR1[j][k]+LfT1[j][k]+LfB1[j][k];
    }
}

```

```

void CUvxDlg::RightIR1()
{
    int j, k;
    double dx, dy, dz, dt, id, jd, kd;
    id = xincr*IRES/IBLOCK;
    jd = yincr*JRES/JBLOCK;
    kd = zincr*KRES/KBLOCK;
    dx = Width;           // Distance to Left
    // Right from Left
    for (j=0; j<JBLOCK; j++){
        dy = j*jd;        // Distance to Bottom
        for (k=0; k<KBLOCK; k++){
            dz = k*kd;     // Distance along z axis
            RfL1[j][k] = Rho*VFLeftWall(dx,dy,dz);
        }
    }
    // Right from Top
    dx = 0.0;
    for (j=0; j<JBLOCK; j++){
        dy = j*jd;        // Distance to Bottom
        dt = Height - dy;
        for (k=0; k<KBLOCK; k++){
            dz = k*kd;     // Distance along z axis
            RfT1[j][k] = Rho*VFTopPPWall(dx,dt,dz);
        }
    }
    // Right from Bottom
    for (j=0; j<JBLOCK; j++){
        dy = j*jd;        // Distance to Bottom
        for (k=0; k<KBLOCK; k++){
            dz = k*kd;     // Distance along z axis
            RfB1[j][k] = Rho*VFBotPPWall(dx,dy,dz);
        }
    }
    for (j=0; j<JBLOCK; j++){
        for (k=0; k<KBLOCK; k++){
            RightWallInt[j][k] = RfL1[j][k]+RfT1[j][k]+RfB1[j][k];
        }
    }
}

```

```

void CUvxDlg::AvgIR1Contours()
{
    // Average the intermediate contours from IR 1
    int i,k;
    double s1=0, s2=0, s3=0, s4=0;
    for (i=0; i<=IBLOCK; i++){
        for (k=0; k<=KBLOCK; k++){
            s1 = s1 + TopWallInt[i][k];
            s2 = s2 + BotWallInt[i][k];
            s3 = s3 + LeftWallInt[i][k];
            s4 = s4 + RightWallInt[i][k];
        }
    }
    AvgTop1 = s1/(IB*KB);
    AvgBot1 = s2/(IB*KB);
    AvgLeft1 = s3/(IB*KB);
    AvgRight1 = s4/(IB*KB);
    for (i=0; i<=IBLOCK; i++){
        for (k=0; k<=KBLOCK; k++){
            TopWallInt[i][k]=AvgTop1;
            BotWallInt[i][k]=AvgBot1;
            LeftWallInt[i][k]=AvgLeft1;
            RightWallInt[i][k]=AvgRight1;
        }
    }
}

```

```

void CUvxDlg::AvgIR2()
{
    // Compute Inter-reflection 2 from parallel rectangles

    double TfB2, TfL2, TfR2, BfT2, BfL2, BfR2, vfpara, vfperp;
    double LfR2, LfT2, LfB2, RfL2, RfT2, RfB2;
    double TopTot2, BotTot2, LeftTot2, RightTot2;
    double a, b, c;
    a = Width;
    b = Height;
    c = Length;
    vfpara = ParaRect(a, b, c);
    vfperp = PerpRect(a, b, c);
    // Top Planes
    TfB2 = Rho*AvgBot1*vfpara;
    TfL2 = Rho*AvgLeft1*vfperp;
    TfR2 = Rho*AvgRight1*vfperp;
    TopTot2 = TfB2+TfL2+TfR2;
    // Bottom Planes
    BfT2 = Rho*AvgTop1*vfpara;
    BfL2 = Rho*AvgLeft1*vfperp;
    BfR2 = Rho*AvgRight1*vfperp;
    BotTot2 = BfT2+BfL2+BfR2;
    vfpara = ParaRect(b, a, c);
    vfperp = PerpRect(b, a, c);
    // Left Planes
    LfR2 = Rho*AvgRight1*vfpara;
    LfT2 = Rho*AvgTop1*vfperp;
    LfB2 = Rho*AvgBot1*vfperp;
    LeftTot2 = LfR2+LfT2+LfB2;
    // Right Planes
    RfL2 = Rho*AvgLeft1*vfpara;
    RfT2 = Rho*AvgTop1*vfperp;
    RfB2 = Rho*AvgBot1*vfperp;
    RightTot2 = RfL2+RfT2+RfB2;
    // Fill In Wall Contours with averages
    int j, k;
    for (j=0; j<IB; j++){
        for (k=0; k<KB; k++){
            BotWallInt[j][k] = BotTot2;
            TopWallInt[j][k] = TopTot2;
            LeftWallInt[j][k] = LeftTot2;
            RightWallInt[j][k] = RightTot2;
        }
    }
}

```



```

int CUvxDlg::SaveContours(int i)
{
    int j, k;
    for (j=0; j<IBLOCK; j++){
        for (k=0; k<KBLOCK; k++){
            BotlR[i][j][k] = BotWall[j][k];
            ToplR[i][j][k] = TopWall[j][k];
            LeftlR[i][j][k] = LeftWall[j][k];
            RightlR[i][j][k] = RightWall[j][k];
        }
    }
    return 0;
}

double CUvxDlg::ParaRect(double a, double b, double c)
{
    // a=width of both, b=distance between, c=length
    double X, Y, d, e, f, g, h, F12;
    X = a/c;
    Y = b/c;
    d = log( pow((1+X*X)*(1+Y*Y)/(1+X*X+Y*Y), 0.5));
    e = X*sqrt(1+Y*Y)*atan(X/sqrt(1+Y*Y));
    f = Y*sqrt(1+X*X)*atan(Y/sqrt(1+X*X));
    g = X*atan(X);
    h = Y*atan(Y);
    F12 = (2/(Pi*X*Y))*(d+e+f-g-h);
    return F12;
}

double CUvxDlg::PerpRect(double a, double b, double c)
{
    // a=width of receiver 1, b=height of sender 2, c=length
    double H, W, d, e, f, g, h, h2, t, t2, F12;
    H = b/c;
    W = a/c;
    d = W*atan(1/W);
    e = H*atan(1/H);
    f = sqrt(H*H+W*W)*atan(1/sqrt(H*H+W*W));
    g = (1+W*W)*(1+H*H)/(1+W*W+H*H);
    h = W*W*(1+W*W+H*H)/((1+W*W)*(W*W+H*H));
    h2 = pow(h,(W*W));
    t = H*H*(1+H*H+W*W)/((1+H*H)*(H*H+W*W));
    t2 = pow(t,H*H);
    F12 = (1/(Pi*W))*(d+e-f+0.25*log(g*h2*t2));
    return F12;
}

```

```

void CUvxDlg::InterReflectField()
{
    int i,j,k;
    double dx,dy,dz,frv,frh, id, jd, kd;
    id = xincr*IRES/IBLOCK;
    jd = yincr*JRES/JBLOCK;
    kd = zincr*KRES/KBLOCK;
    for(i=0; i<=IBLOCK; i++){
        dx = i*id; // Distance to Left Wall
        CProgressCtrl* pProg3 =
            (CProgressCtrl*) GetDlgItem(IDC_PROGRESS3);
        pProg3->SetRange(0, 20);
        pProg3->SetPos(i+IBLOCK*Icount);
        for(j=0; j<=JBLOCK; j++){
            dy = j*jd; // Distance to Bottom Wall
            for(k=0; k<=KBLOCK; k++){
                dz = k*kd; // Distance along z axis
                // Compute Intensity from Left & Right Walls
                frv = VFVerticalWall(dx, dy, dz);
                // Compute Intensity from Bottom & Top Walls
                frh = VFHorizWall(dy, dx, dz);
                InterField[i][j][k] = frv+frh;
                InterFieldTotal[i][j][k] = InterFieldTotal[i][j][k] + frv+frh;
            }
        }
    }
    Icount++;
}

```

```

void CUvxDlg::ExchangeWallFields()
{
    int i,k;
    for (i=0; i<IB; i++){
        for (k=0; k<KB; k++){
            TopWall[i][k] = TopWallInt[i][k];
            BotWall[i][k] = BotWallInt[i][k];
            LeftWall[i][k] = LeftWallInt[i][k];
            RightWall[i][k] = RightWallInt[i][k];
        }
    }
}

double CUvxDlg::AverageInter()
{
    int i, j, k;
    double total=0, Avg;
    for (i=0; i<IB; i++){
        for (j=0; j<JB; j++){
            for (k=0; k<KB; k++){
                total = total + InterField[i][j][k];
                // Remove Lamp Volume contribution
            }
        }
    }
    Avg = total/(IB*JB*KB);
    return Avg;
}

```

```

double CUvxDig::VFLeftWall(double x, double y, double z)
{
    int jb, kb;
    double y1, y2, z1, z2, dy, dz, c, a, b, jd, kd;
    double vfl, frl, frsum;
    frsum = 0;    // zero out sum
    jd = yincr*JRES/JBLOCK;
    kd = zincr*KRES/KBLOCK;
    // Compute block dims & dist
    c = x;
    a = jd;
    b = kd;
    for (jb=0; jb<JB; jb++){
        y1 = jb*jd;
        y2 = (jb+1)*jd;
        dy = min(fabs(y-y1),fabs(y-y2));
        for (kb=0; kb<KB; kb++){
            // Define four coordinates of block
            z1 = kb*kd;
            z2 = (kb+1)*kd;
            // Find distance to closest coordinates
            dz = min(fabs(z-z1),fabs(z-z2));
            // Compute View Factors & Field from left & right
            if (dy==0 && dz==0){    // We're right at a corner
                vfl = VFParallelPlane(c,a,b);    // VF left wall
                frl = vfl*LeftWall[jb][kb];    // Field intensity
            }
            else {    // We're not at a corner
                vfl = VFParallelGhost(c,a,b,dy,dz); // VF left
                frl = vfl*LeftWall[jb][kb];    // Field
            }
            frsum = frsum + frl;
        }
    }
    return frsum;
}

```

```

double CUvxDlg::VFRightWall(double x, double y, double z)
{
    int jb, kb;
    double y1, y2, z1, z2, dy, dz, c, a, b, id, jd, kd;
    double vfl, frl, frsum;
    id = xincr*IRES/IBLOCK;
    jd = yincr*JRES/JBLOCK;
    kd = zincr*KRES/KBLOCK;
    frsum = 0;    // zero out sum
    // Compute block dims & dist
    c = x;
    a = jd;
    b = kd;
    for (jb=0; jb<JB; jb++){
        y1 = jb*jd;
        y2 = (jb+1)*jd;
        dy = min(fabs(y-y1),fabs(y-y2));
        for (kb=0; kb<KB; kb++){
            // Define four coordinates of block
            z1 = kb*kd;
            z2 = (kb+1)*kd;
            // Find distance to closest coordinates
            dz = min(fabs(z-z1),fabs(z-z2));
            // Compute View Factors & Field from left & right
            if (dy==0 && dz==0){    // We're right at a corner
                vfl = VFParallelPlane(c,a,b);    // VF left wall
                frl = vfl*RightWall[jb][kb];    // Field intensity
            }
            else {    // We're not at a corner
                vfl = VFParallelGhost(c,a,b,dy,dz); // VF left
                frl = vfl*RightWall[jb][kb];    // Field
            }
            frsum = frsum + frl;
        }
    }
    return frsum;
}

```

```

double CUvxDlg::VFBotWall(double x, double y, double z)
{
    int ib, kb;
    double x1, x2, z1, z2, dx, dz, c, a, b, id,jd,kd;
    double vfl, frl, frsum;
    frsum = 0;    // zero out sum
    id = xincr*IRES/IBLOCK;
    jd = yincr*JRES/JBLOCK;
    kd = zincr*KRES/KBLOCK;
    c = x;// Distance to Bottom Wall
    // Compute block dims & dist
    a = id;
    b = kd;
    for (ib=0; ib<IB; ib++){
        x1 = ib*id;
        x2 = (ib+1)*id;
        dx = min(fabs(y-x1),fabs(y-x2));
        for (kb=0; kb<KB; kb++){
            // Define four coordinates of block
            z1 = kb*kd;
            z2 = (kb+1)*kd;
            // Find distance to closest coordinates
            dz = min(fabs(z-z1),fabs(z-z2));
            // Compute View Factors & Field
            if (dx==0 && dz==0){    // We're right at a corner
                vfl = VFParallelPlane(c,a,b);    // VF wall
                frl = vfl*BotWall[ib][kb];    // Field intensity
            }
            else {    // We're not at a corner
                vfl = VFParallelGhost(c,a,b,dx,dz); // VF
                frl = vfl*BotWall[ib][kb];    // Field
            }
            frsum = frsum + frl;
        }
    }
    return frsum;
}

```

```

double CUvxDlg::VFTopWall(double x, double y, double z)
{
    int ib, kb;
    double x1, x2, z1, z2, dx, dz, c, a, b, id, jd, kd;
    double vfl, frl, frsum;
    frsum = 0; // zero out sum
    id = xincr*IRES/IBLOCK;
    jd = yincr*JRES/JBLOCK;
    kd = zincr*KRES/KBLOCK;
    c = x; // Distance to Top Wall
    // Compute block dims & dist
    a = id;
    b = kd;
    for (ib=0; ib<IB; ib++){
        x1 = ib*id;
        x2 = (ib+1)*id;
        dx = min(fabs(y-x1), fabs(y-x2));
        for (kb=0; kb<KB; kb++){
            // Define four coordinates of block
            z1 = kb*kd;
            z2 = (kb+1)*kd;
            // Find distance to closest coordinates
            dz = min(fabs(z-z1), fabs(z-z2));
            // Compute View Factors & Field
            if (dx==0 && dz==0){ // We're right at a corner
                vfl = VFParallelPlane(c,a,b); // VF wall
                frl = vfl*TopWall[ib][kb]; // Field intensity
            }
            else { // We're not at a corner
                vfl = VFParallelGhost(c,a,b,dx,dz); // VF
                frl = vfl*TopWall[ib][kb]; // Field
            }
            frsum = frsum + frl;
        }
    }
    return frsum;
}

```

```

double CUvxDlg::VFBotPPWall(double x, double y, double z)
{
    int ib, kb;
    double x1, x2, z1, z2, dx, dz, c, a, b, id,jd,kd;
    double vfl, frl, frsum;
    frsum = 0;    // zero out sum
    id = xincr*IRES/IBLOCK;
    jd = yincr*JRES/JBLOCK;
    kd = zincr*KRES/KBLOCK;
    // Compute block dims & dist
    c = y;
    a = id;
    b = kd;
    for (ib=0; ib<IB; ib++){
        x1 = ib*id;
        x2 = (ib+1)*id;
        dx = min(fabs(x-x1),fabs(x-x2));
        for (kb=0; kb<KB; kb++){
            // Define four coordinates of block
            z1 = kb*kd;
            z2 = (kb+1)*kd;
            // Find distance to closest coordinates
            dz = min(fabs(z-z1),fabs(z-z2));
            // Compute View Factors & Field
            if (dx==0 && dz==0){    // We're right at a corner
                vfl = VFPerpendicularPlane(c,a,b);    // VF wall
                frl = vfl*BotWall[ib][kb];    // Field intensity
            }
            else {    // We're not at a corner
                vfl = VFPerpendicularGhost(c,a,b,dx,dz); // VF
                frl = vfl*BotWall[ib][kb];    // Field
            }
            frsum = frsum + frl;
        }
    }
    return frsum;
}

```



```

double CUvxDlg::VFTopPPWall(double x, double y, double z)
{
    int ib, kb;
    double x1, x2, z1, z2, dx, dz, c, a, b, id,jd,kd;
    double vfl, frl, frsum;
    frsum = 0;    // zero out sum
    id = xincr*IRES/IBLOCK;
    jd = yincr*JRES/JBLOCK;
    kd = zincr*KRES/KBLOCK;
    // Compute block dims & dist
    c = y;
    a = id;
    b = kd;
    for (ib=0; ib<IB; ib++){
        x1 = ib*id;
        x2 = (ib+1)*id;
        dx = min(fabs(x-x1),fabs(x-x2));
        for (kb=0; kb<KB; kb++){
            // Define four coordinates of block
            z1 = kb*kd;
            z2 = (kb+1)*kd;
            // Find distance to closest coordinates
            dz = min(fabs(z-z1),fabs(z-z2));
            // Compute View Factors & Field
            if (dx==0 && dz==0){    // We're right at a corner
                vfl = VFPerpendicularPlane(c,a,b);    // VF wall
                frl = vfl*TopWall[ib][kb];    // Field intensity
            }
            else {    // We're not at a corner
                vfl = VFPerpendicularGhost(c,a,b,dx,dz); // VF
                frl = vfl*TopWall[ib][kb];    // Field
            }
            frsum = frsum + frl;
        }
    }
    return frsum;
}

```

```

double CUvxDlg::VFLeftPPWall(double x, double y, double z)
{
    int jb, kb;
    double y1, y2, z1, z2, dy, dz, c, a, b, id, jd, kd;
    double vfl, frl, frsum;
    frsum = 0;    // zero out sum
    id = xincr*IRES/IBLOCK;
    jd = yincr*JRES/JBLOCK;
    kd = zincr*KRES/KBLOCK;
    // Compute block dims & dist
    c = x;
    a = jd;
    b = kd;
    for (jb=0; jb<JB; jb++){
        y1 = jb*jd;
        y2 = (jb+1)*jd;
        dy = min(fabs(y-y1),fabs(y-y2));
        for (kb=0; kb<KB; kb++){
            // Define four coordinates of block
            z1 = kb*kd;
            z2 = (kb+1)*kd;
            // Find distance to closest coordinates
            dz = min(fabs(z-z1),fabs(z-z2));
            // Compute View Factors & Field
            if (dy==0 && dz==0){    // We're right at a corner
                vfl = VFPerpendicularPlane(c,a,b);    // VF wall
                frl = vfl*LeftWall[jb][kb];    // Field intensity
            }
            else {    // We're not at a corner
                vfl = VFPerpendicularGhost(c,a,b,dy,dz); // VF
                frl = vfl*LeftWall[jb][kb];    // Field
            }
            frsum = frsum + frl;
        }
    }
    return frsum;
}

```

```

double CUvxDlg::VFRightPPWall(double x, double y, double z)
{
    int jb, kb;
    double y1, y2, z1, z2, dy, dz, c, a, b, id,jd,kd;
    double vfl, frl, frsum;
    frsum = 0;    // zero out sum
    id = xincr*IRES/IBLOCK;
    jd = yincr*JRES/JBLOCK;
    kd = zincr*KRES/KBLOCK;
    // Compute block dims & dist
    c = x;
    a = jd;
    b = kd;
    for (jb=0; jb<JB; jb++){
        y1 = jb*jd;
        y2 = (jb+1)*jd;
        dy = min(fabs(y-y1),fabs(y-y2));
        for (kb=0; kb<KB; kb++){
            // Define four coordinates of block
            z1 = kb*kd;
            z2 = (kb+1)*kd;
            // Find distance to closest coordinates
            dz = min(fabs(z-z1),fabs(z-z2));
            // Compute View Factors & Field
            if (dy==0 && dz==0){    // We're right at a corner
                vfl = VFPerpendicularPlane(c,a,b);    // VF wall
                frl = vfl*RightWall[jb][kb];    // Field intensity
            }
            else {    // We're not at a corner
                vfl = VFPerpendicularGhost(c,a,b,dy,dz); // VF
                frl = vfl*RightWall[jb][kb];    // Field
            }
            frsum = frsum + frl;
        }
    }
    return frsum;
}

```

```

double CUvxDlg::VFPerpendicularPlane(double c, double a, double b)
{
    // View factor to a Perpendicular Plane at the corner
    // a=width or height, b=length, c=distance to corner
    double X, Y, p1, p2, vf;
    if (b==0) b=0.000001; // Can't be closer than 1 micron
    if (c==0) c=0.000001;
    X = a/b;
    Y = c/b;
    p1 = atan(1/Y);
    p2 = (Y/sqrt(X*X+Y*Y))*atan(1/sqrt(X*X+Y*Y));
    vf = (p1-p2)/(2*Pi);
    if(vf>1.0) vf=1.0;    // or 0.5??
    return vf;
}

```

```

double CUvxDlg::VFPerpendicularGhost(double c, double a, double b, double d, double e)
{ // View factor to Perpendicular Plane beyond the corner
  // a=width or height, b=length, c=perpendicular distance
  // d = y distance beyond corner, e = z distance beyond corner
  double vft, vf1, vf2, vf34; // Total t and sections 1,2,34
  // Compute VF to Total Area
  vft = VFPerpendicularPlane(c,a+d,b+e);
  // Compute VF to Ghost sections 2,3,4
  vf2 = VFPerpendicularPlane(c,d,b+e)-VFPerpendicularPlane(c,d,e);
  vf34 = VFPerpendicularPlane(c,a+d,e);
  // Subtract to obtain VF to Real Section vf1
  vf1 = vft - vf2 - vf34;
  return vf1;
}

void CUvxDlg::IntegratedIntensity()
{
  int i,j,k, IR, JR, KR;
  IR=IRES+1;
  JR=JRES+1;
  KR=KRES+1;
  //Add First field & Inter field, then Interpolate

  ExpandInterField();
  // Add all field matrices
  AddFields();
  // Compute Eit = exposure Time for integrated fields
  double Eit = Et/KR;
  // Compute Survival over each streamline segment i
  double Sint[IRES+10][JRES+10];
  double Si, Sintsum=0;
  for (i=0; i<IR; i++){
    CProgressCtrl* pProg6 = (CProgressCtrl*) GetDlgItem(IDC_PROGRESS6);
    pProg6->SetRange(0,100);
    pProg6->SetPos(i*2);
    for (j=0; j<JR; j++){
      Sint[i][j] = 1;
      for (k=0; k<KR; k++){
        Si = Survival(kSM,EFA[i][j][k],Eit);
        Sint[i][j] = Sint[i][j]*Si;
      }
      Sintsum = Sintsum + Sint[i][j];
      KZ[i][j] = 1 - Sint[i][j];
    }
  }
  IntegratedSurvival = 100.0*Sintsum/(IR*JR);
  IntKillRate = 100.0-IntegratedSurvival;
}

```

```

void CUvxDlg::ExpandFirstField()
{
    // Expand First Reflection matrix from BLOCK resolution to full RES
    int i, j, k, jd, kd, id;
    double deli, delj, delk;
    // Fill Expanded Matrix EFF with corner points from Block matrix
    for (i=0; i<=IRES; i=i+5){
        for (j=0; j<=JRES; j=j+5){
            for (k=0; k<=KRES; k=k+5)
                EFF[i][j][k] = FirstField[i/5][j/5][k/5];
        }
    }
    // Interpolate to fill blanks along k axis in EFF
    for (i=0; i<=IRES; i=i+5){
        for (j=0; j<=JRES; j=j+5){
            for (k=0; k<=KRES; k=k+5){
                delk = EFF[i][j][k+5]-EFF[i][j][k];
                for (kd=1; kd<5; kd++)
                    EFF[i][j][k+kd] = EFF[i][j][k]+kd*delk/5.0;
            }
        }
    }
    // Interpolate to fill blanks along i axis in EFF
    for (k=0; k<=KRES; k++){
        for (j=0; j<=JRES; j=j+5){
            for (i=0; i<=IRES; i=i+5){
                deli = EFF[i+5][j][k]-EFF[i][j][k];
                for (id=1; id<5; id++)
                    EFF[i+id][j][k] = EFF[i][j][k]+id*deli/5.0;
            }
        }
    }
    // Interpolate to fill blanks along j axis
    for (k=0; k<=KRES; k++){
        for (i=0; i<=IRES; i++){
            for (j=0; j<=JRES; j=j+5){
                delj = EFF[i][j+5][k]-EFF[i][j][k];
                for (jd=1; jd<5; jd++)
                    EFF[i][j+jd][k] = EFF[i][j][k]+jd*delj/5.0;
            }
        }
    }
}

```

```

void CUvxDlg::ExpandInterField()
{
    // Expand First Reflection matrix from BLOCK resolution to full RES
    int i,j,k,jd,kd, id;
    double deli, delj, delk;
    // Fill Expanded Matrix EFF with corner points from Block matrix
    for (i=0; i<=IRES; i=i+5){
        for (j=0; j<=JRES; j=j+5){
            for (k=0; k<=KRES; k=k+5){
                EIF[i][j][k] = InterFieldTotal[i/5][j/5][k/5];
            }
        }
    }
    // Interpolate to fill blanks along k axis in EFF

    for (i=0; i<=IRES; i=i+5){
        for (j=0; j<=JRES; j=j+5){
            for (k=0; k<=KRES; k=k+5){
                delk = EIF[i][j][k+5]-EIF[i][j][k];
                for (kd=1; kd<5; kd++){
                    EIF[i][j][k+kd] = EIF[i][j][k]+kd*delk/5.0;
                }
            }
        }
    }

    // Interpolate to fill blanks along i axis in EFF
    for (k=0; k<=KRES; k++){
        for (j=0; j<=JRES; j=j+5){
            for (i=0; i<=IRES; i=i+5){
                deli = EIF[i+5][j][k]-EIF[i][j][k];
                for (id=1; id<5; id++){
                    EIF[i+id][j][k] = EIF[i][j][k]+id*deli/5.0;
                }
            }
        }
    }

    // Interpolate to fill blanks along j axis
    for (k=0; k<=KRES; k++){
        for (i=0; i<=IRES; i++){
            for (j=0; j<=JRES; j=j+5){
                delj = EIF[i][j+5][k]-EIF[i][j][k];
                for (jd=1; jd<5; jd++){
                    EIF[i][j+jd][k] = EIF[i][j][k]+jd*delj/5.0;
                }
            }
        }
    }
}

```

```

void CUvxDlg::AddFields()
{
    int i,j,k;
    for (i=0; i<=IRES; i++){
        for (j=0; j<=JRES; j++){
            for (k=0; k<=KRES; k++){
                // add expanded first field, interfield and direct
                EFA[i][j][k] = DirectField[i][j][k]
                    + EFF[i][j][k]+ EIF[i][j][k];
            }
        }
    }
}

```

```

void CUvxDlg::InitializeMatrices() // Init Matrices and Data
{
    // initialize InterFieldTotal
    int i,j,k;
    for (i=0; i<=IR; i++)
        for (j=0; j<=JR; j++)
            for (k=0; k<=KR; k++){
                DirectField[i][j][k] = 0;
                DistanceMtx[i][j][k] = 0;
                PositionMtx[i][j][k] = 0;
                EFF[i][j][k] = 0;
                EIF[i][j][k] = 0;
                EFA[i][j][k] = 0;
            }
    for (i=0; i<=IB; i++)
        for (j=0; j<=JB; j++)
            for (k=0; k<=KB; k++){
                FirstField[i][j][k] = 0;
                InterField[i][j][k] = 0;
                InterFieldTotal[i][j][k] = 0;
                NextField[i][j][k] = 0;
                EBA[i][j][k] = 0;
                RField[i][j][k]=0;
            }
    for (i=0; i<=IB; i++)
        for (k=0; k<=KB; k++){
            TopWall[i][k]=0;
            BotWall[i][k]=0;
            LeftWall[i][k]=0;
            RightWall[i][k]=0;
            TopWallInt[i][k]=0;
            BotWallInt[i][k]=0;
            LeftWallInt[i][k]=0;
            RightWallInt[i][k]=0;
            RfL1[i][k]=0;
            RfT1[i][k]=0;
            RfB1[i][k]=0;
            LfR1[i][k]=0;
            LfT1[i][k]=0;
            LfB1[i][k]=0;
            TfB1[i][k]=0;
            Tfl1[i][k]=0;
            TfR1[i][k]=0;
            BfT1[i][k]=0;
            BfL1[i][k]=0;
            BfR1[i][k]=0;
        }
    for (i=0; i<=7; i++)
        for (j=0; j<=JR; j++)
            for (k=0; k<=KR; k++){
                TopIR[i][j][k]=0;
                BotIR[i][j][k]=0;
                LeftIR[i][j][k]=0;
                RightIR[i][j][k]=0;
            }
    for(i=0; i<=10; i++){
        AvgInter[i] = 0;
    }
}

```



```

        InterAverage[i] = 0;
    }
    AvgFirst=0;
    AvgTotal=0;
    IntegratedSurvival=0;
    Smin=0;
    AvgSurvival=0;
    AvgTop1=0;
    AvgBot1=0;
    AvgLeft1=0;
    AvgRight1=0;
    IR4etc=0;
    for(i=0;i<=IR;i++){
        for(j=0;j<=JR;j++){
            KZ[i][j]=0;
        }
    }
    TotalAvgInter=0;
    BlockIntAvg=0;
    ifstream infile("kselect.txt",ios::in );
    infile.getline(Microbe,80);
    infile >> kSM;
    infile >> LogmeanDia;
    m_target = Microbe;
    UpdateData(FALSE);
}

```

```

double CUvxDlg::Survival(double k, double I, double t)
{
    // Survival Fraction of species with standard rate constant k
    // Intensity = I (microW/cm2), exposure time = t (sec)
    double S;
    S = exp(-k*I*t);
    return S;
}

void CUvxDlg::ScaleDimensions()
{
    // Scale dimension increments to resolution
    xincr = Width/IRES;
    yincr = Height/JRES;
    zincr = Length/KRES;
}

void CUvxDlg::ABCfill()
{
    int i, j;

    ifstream infile("params.txt",ios::in );

    infile>>IP;        // number of input data points

    for (i=1; i<=IP; i++){
        for (j=1; j<13; j++){
            infile>>P[i][j];
        }
    }
}

void CUvxDlg::Dimensionless()
{
    P1 = Width/Height;
    P2 = radius[0]/arclength[0];
    P3 = (kSM*UVPower[0]*Et/(Width*Height*100));
    P4 = lampx2[0]/Width;
    P5 = lampy1[0]/Height;
    P6 = Rho;
    P7 = lampz1[0]/Length;
    P8 = (Width*Length+Height*Length)/(Width*Length+Height*Length+Width*Height);
}

```

uvx.cpp

```

// uvx.cpp : Defines the class behaviors for the application.
//

#include "stdafx.h"
#include "uvx.h"
#include "uvxDlg.h"
#include <initguid.h>
#include "Uvx_i.c"

#ifdef _DEBUG
#define new DEBUG_NEW
#undef THIS_FILE
static char THIS_FILE[] = __FILE__;
#endif

////////////////////////////////////
// CUvxApp

BEGIN_MESSAGE_MAP(CUvxApp, CWinApp)
//{{AFX_MSG_MAP(CUvxApp)
// NOTE - the ClassWizard will add and remove mapping macros here.
// DO NOT EDIT what you see in these blocks of generated code!
//}}AFX_MSG
ON_COMMAND(ID_HELP, CWinApp::OnHelp)
END_MESSAGE_MAP()

////////////////////////////////////
// CUvxApp construction

CUvxApp::CUvxApp()
{
    // TODO: add construction code here,
    // Place all significant initialization in InitInstance
}

////////////////////////////////////
// The one and only CUvxApp object

CUvxApp theApp;

```

```

////////////////////////////////////
// CUvxApp initialization

BOOL CUvxApp::InitInstance()
{
    if (!InitATL())
        return FALSE;

    AfxEnableControlContainer();

    CCommandLineInfo cmdInfo;
    ParseCommandLine(cmdInfo);

    if (cmdInfo.m_bRunEmbedded || cmdInfo.m_bRunAutomated)
    {
        return TRUE;
    }

    // Standard initialization
    // If you are not using these features and wish to reduce the size
    // of your final executable, you should remove from the following
    // the specific initialization routines you do not need.

#ifdef _AFXDLL
    Enable3dControls();                // Call this when using MFC in a shared DLL
#else
    Enable3dControlsStatic();          // Call this when linking to MFC statically
#endif

    CUvxDlg dlg;
    m_pMainWnd = &dlg;
    int nResponse = dlg.DoModal();
    if (nResponse == IDOK)
    {
        // TODO: Place code here to handle when the dialog is
        // dismissed with OK
    }
    else if (nResponse == IDCANCEL)
    {
        // TODO: Place code here to handle when the dialog is
        // dismissed with Cancel
    }

    // Since the dialog has been closed, return FALSE so that we exit the
    // application, rather than start the application's message pump.
    return FALSE;
}

CUvxModule _Module;

BEGIN_OBJECT_MAP(ObjectMap)
END_OBJECT_MAP()

```

```

LONG CUvxModule::Unlock()
{
    AfxOleUnlockApp();
    return 0;
}

LONG CUvxModule::Lock()
{
    AfxOleLockApp();
    return 1;
}

LPCTSTR CUvxModule::FindOneOf(LPCTSTR p1, LPCTSTR p2)
{
    while (*p1 != NULL)
    {
        LPCTSTR p = p2;
        while (*p != NULL)
        {
            if (*p1 == *p)
                return CharNext(p1);
            p = CharNext(p);
        }
        p1++;
    }
    return NULL;
}

int CUvxApp::ExitInstance()
{
    if (m_bATLInited)
    {
        _Module.RevokeClassObjects();
        _Module.Term();
        CoUninitialize();
    }

    return CWinApp::ExitInstance();
}

```

```

BOOL CUvxApp::InitATL()
{
    m_bATLInited = TRUE;

#ifdef _WIN32_WINNT >= 0x0400
    HRESULT hRes = CoInitializeEx(NULL, COINIT_MULTITHREADED);
#else
    HRESULT hRes = CoInitialize(NULL);
#endif

    if (FAILED(hRes))
    {
        m_bATLInited = FALSE;
        return FALSE;
    }

    _Module.Init(ObjectMap, AfxGetInstanceHandle());
    _Module.dwThreadID = GetCurrentThreadId();

    LPTSTR lpCmdLine = GetCommandLine(); //this line necessary for _ATL_MIN_CRT
    TCHAR szTokens[] = _T("-/");

    BOOL bRun = TRUE;
    LPCTSTR lpszToken = _Module.FindOneOf(lpCmdLine, szTokens);
    while (lpszToken != NULL)
    {
        if (lstrcmpi(lpszToken, _T("UnregServer"))==0)
        {
            _Module.UpdateRegistryFromResource(IDR_UVX, FALSE);
            _Module.UnregisterServer(TRUE); //TRUE means typelib is unreg'd
            bRun = FALSE;
            break;
        }
        if (lstrcmpi(lpszToken, _T("RegServer"))==0)
        {
            _Module.UpdateRegistryFromResource(IDR_UVX, TRUE);
            _Module.RegisterServer(TRUE);
            bRun = FALSE;
            break;
        }
        lpszToken = _Module.FindOneOf(lpszToken, szTokens);
    }

    if (!bRun)
    {
        m_bATLInited = FALSE;
        _Module.Term();
        CoUninitialize();
        return FALSE;
    }

    hRes = _Module.RegisterClassObjects(CLSCTX_LOCAL_SERVER,
        REGCLS_MULTIPLEUSE);
    if (FAILED(hRes))
    {
        m_bATLInited = FALSE;
    }
}

```

```
        CoUninitialize();  
        return FALSE;  
    }  
    return TRUE;  
}
```

uvx.h

```

// uvx.h : main header file for the UVX application
//

#ifndef AFX_UVX_H__1F507044_6081_11D4_8047_FDFE4C9EA26A__INCLUDED_
#define AFX_UVX_H__1F507044_6081_11D4_8047_FDFE4C9EA26A__INCLUDED_
#if _MSC_VER > 1000
#pragma once
#endif // _MSC_VER > 1000
#ifndef __AFXWIN_H__
    #error include 'stdafx.h' before including this file for PCH
#endif
#include "resource.h"          // main symbols
#include "Uvx_i.h"

////////////////////////////////////
// CUvxApp:
// See uvx.cpp for the implementation of this class
//
class CUvxApp : public CWinApp
{
public:
    CUvxApp();
// Overrides
    // ClassWizard generated virtual function overrides
   //{{AFX_VIRTUAL(CUvxApp)
public:
    virtual BOOL InitInstance();
        virtual int ExitInstance();
   //}}AFX_VIRTUAL

// Implementation

    {{{AFX_MSG(CUvxApp)
        // NOTE - the ClassWizard will add and remove member functions here.
        // DO NOT EDIT what you see in these blocks of generated code !
    }}}AFX_MSG
    DECLARE_MESSAGE_MAP()
private:
    BOOL m_bATLInitd;
private:
    BOOL InitATL();
};

////////////////////////////////////

{{{AFX_INSERT_LOCATION}}
// Microsoft Visual C++ will insert additional declarations immediately before the previous line.

#endif // !defined(AFX_UVX_H__1F507044_6081_11D4_8047_FDFE4C9EA26A__INCLUDED_)

```


uvx.rc

(NOTE: no code is associated with this file since it consists of Windows graphic modules. See Chapter 6 for Window image)

Resource.h

```

//{{NO_DEPENDENCIES}}
// Microsoft Developer Studio generated include file.
// Used by uvx.rc
//
#define IDM_ABOUTBOX            0x0010
#define IDD_ABOUTBOX            100
#define IDS_ABOUTBOX            101
#define IDD_UVX_DIALOG           102
#define IDR_UVX                  103
#define IDR_MAINFRAME           128
#define IDD_DIALOG1              131
#define IDD_DCHECK               132
#define IDC_EFILENAME            1000
#define IDC_BRUN                 1001
#define IDC_PROGRESS1            1002
#define IDC_PROGRESS2            1005
#define IDC_SAVGDIRECT           1006
#define IDC_SAVGFIRST            1007
#define IDC_PROGRESS3            1008
#define IDC_SAVGINTER1           1009
#define IDC_STOTALAVG            1010
#define IDC_SKILLRATE            1011
#define IDC_SINTEGRATEDKILL      1012
#define IDC_SCONFIGEFF           1014
#define IDC_SCOMPLETE            1015
#define IDC_SAVING               1016
#define IDC_SURVIVAL             1017
#define IDC_SINTSURVIVAL         1018
#define IDC_PROGRESS6            1020
#define IDC_EPASS                1023
#define IDC_SPASS                1024
#define IDC_SMICROBE             1026
#define IDC_SCASSIGN             1027
#define IDC_SRHO                 1028
#define IDC_SEXPOSURETIME        1029
#define IDC_BCURRENT             1030
#define IDC_SMODEL               1032
#define IDC_SWIDTH               1033
#define IDC_SLENGTH              1034
#define IDC_SHEIGHT              1035
#define IDC_SAIRFLOW             1036
#define IDC_SLAMPS               1037
#define IDC_SPI                  1038
#define IDC_SPIMAX               1039
#define IDC_SURFI                1040

// Next default values for new objects
//

```

```

#ifdef APSTUDIO_INVOKED
#ifndef APSTUDIO_READONLY_SYMBOLS
#define _APS_NEXT_RESOURCE_VALUE        143
#define _APS_NEXT_COMMAND_VALUE        32771
#define _APS_NEXT_CONTROL_VALUE        1041
#define _APS_NEXT_SYMED_VALUE        104
#endif
#endif

```

Uvx.idl

```

// Uvx.idl : IDL source for Uvx.exe
//
// This file will be processed by the MIDL tool to
// produce the type library (Uvx.tlb) and marshalling code.
import "oaidl.idl";
import "ocidl.idl";
[
    uuid(149329C0-647F-11D4-8047-986788F9A92D),
    version(1.0),
    helpstring("Uvx 1.0 Type Library")
]
library UvxLib
{
    importlib("stdole32.tlb");
    importlib("stdole2.tlb");
};

```

stdafx.cpp

```

// stdafx.cpp : source file that includes just the standard includes
//      uvx.pch will be the pre-compiled header
//      stdafx.obj will contain the pre-compiled type information

#include "stdafx.h"

#ifdef _ATL_STATIC_REGISTRY
#include <statreg.h>
#endif
#include <atlimpl.cpp>

```

stdafx.h

```

// stdafx.h : include file for standard system include files,
// or project specific include files that are used frequently, but
// are changed infrequently
//

#if !defined(AFX_STDAFX_H__1F507048_6081_11D4_8047_FDFE4C9EA26A__INCLUDED_)
#define AFX_STDAFX_H__1F507048_6081_11D4_8047_FDFE4C9EA26A__INCLUDED_

#if _MSC_VER > 1000
#pragma once
#endif // _MSC_VER > 1000

#define VC_EXTRALEAN // Exclude rarely-used stuff from Windows headers

#include <afxwin.h> // MFC core and standard components
#include <afxext.h> // MFC extensions
#include <afxdisp.h> // MFC Automation classes
#include <afxdtctl.h> // MFC support for Internet Explorer 4 Common Controls
#ifndef _AFX_NO_AFXCMN_SUPPORT
#include <afxcmn.h> // MFC support for Windows Common Controls
#endif // _AFX_NO_AFXCMN_SUPPORT


#define _ATL_APARTMENT_THREADED
#include <atlbase.h>
//You may derive a class from CComModule and use it if you want to override
//something, but do not change the name of _Module
class CUvxModule : public CComModule
{
public:
    LONG Unlock();
    LONG Lock();
    LPCTSTR FindOneOf(LPCTSTR p1, LPCTSTR p2);
    DWORD dwThreadId;
};
extern CUvxModule _Module;
#include <atlcom.h>

//{{AFX_INSERT_LOCATION}}
// Microsoft Visual C++ will insert additional declarations immediately before the previous line.

#endif //
#endif(AFX_STDAFX_H__1F507048_6081_11D4_8047_FDFE4C9EA26A__INCLUDED_)

```

Appendix H – UVD Program Input File “params.txt”

```

2
160.0 160.00 1.373 40.00 0.0028 4.00 390 40.00 16.00 100.0 200.0 93.0
160.0 160.00 1.373 40.00 0.0028 5.56 390 40.00 16.00 100.0 200.0 93.0

```

Explanation: The first number, 2, indicates the number of analyses to be performed. The next two rows show the input variables for the analysis. These variables correspond to the data as follows:

W	H	r	l	k	P	Q	x	y	z	L	rho
160.0	160.00	1.373	40.00	0.0028	4.00	390	40.00	16.00	100.0	200.0	93.0
160.0	160.00	1.373	40.00	0.0028	5.56	390	40.00	16.00	100.0	200.0	93.0

The definitions of the variables and units are tabulated below :

Duct Width	W	cm
Duct Height	H	cm
lamp radius	r	cm
lamp diameter	l	cm
rate constant	k	cm ² /μW-s
UV Power	P	W
Airflow	Q	m ³ /min
lamp end coordinate	x	cm
lamp y coordinate	y	cm
lamp z coordinate	z	cm
Duct Length	L	cm
Reflectivity	rho	%

The above data input file is typically generated by spreadsheet, and then saved as a text file for input to the program.

Appendix I – UVD Program Output File “adata.txt”

```
A B C D E F G J KillRate IntKill Iavg AvgDir AvgFirst AvgInter
1 0.034325 0.344615 0.25 0.1 0.93 0.5 0.714286 45.5678 39.0291 275.767
46.5691 86.378 142.82
1 0.034325 0.479015 0.25 0.1 0.93 0.5 0.714286 57.0622 48.8755 383.316
64.7311 120.065 198.519
```

The above data stream is typically read as a text file into a spreadsheet, and is reorganized here for clarity:

A	B	C	D	E	F	G	J
1	0.034325	0.344615	0.25	0.1	0.93	0.5	0.714286
1	0.034325	0.479015	0.25	0.1	0.93	0.5	0.714286

KillRate	IntKill	Iavg	AvgDir	AvgFirst	AvgInter
45.5678	39.0291	275.767	46.5691	86.378	142.82
57.0622	48.8755	383.316	64.7311	120.065	198.519

Explanation: The output consists of a re-computation of the dimensionless variables A through J, and then a summary of the program results. These are defined in tabular form below:

A	Dimensionless Parameter A = duct aspect ratio
B	Dimensionless Parameter B = lamp aspect ratio
C	Dimensionless Parameter C = specific dose
D	Dimensionless Parameter D = X ratio
E	Dimensionless Parameter E = Y ratio
F	Dimensionless Parameter F = reflectivity (fraction)
G	Dimensionless Parameter G = Z ratio
J	Dimensionless Parameter J = area fraction
KillRate	Kill Rate, % (mixed air)
IntKill	Integrated Kill Rate, % (unmixed air)
Iavg	Average Intensity, $\mu\text{W}/\text{cm}^2$
AvgDir	Average Direct Intensity, $\mu\text{W}/\text{cm}^2$
AvgFirst	Average First Reflection Intensity, $\mu\text{W}/\text{cm}^2$
AvgInter	Average Inter-reflection intensity, $\mu\text{W}/\text{cm}^2$

APPENDIX J: BIOASSAY TEST RESULTS AND ANALYSIS

#	Test Results KR %	Mixed Air KR %	Unimixed Air KR %	Average Intensity mW/cm ²	Error %	Comp. k cm ² /mW-s	Height cm	Width cm	Length cm	rho %	Total UV Watts	Airflow cfm
1	88	86.80	80.60	1002	1.2	0.00305	45.72	45.72	187.96	7	11.8	1200
2	93	99.70	98.38	2964	6.7	0.001293	45.72	45.72	187.96	7	34.8	1200
3	83	95.44	86.90	2152	12.4	0.001715	60.96	60.96	182.88	7	35.8	3000
4	91	98.07	97.42	1984	7.1	0.001798	45.72	45.72	182.88	7	28.4	1200
5	87	95.73	90.90	1562	8.7	0.001935	45.72	45.72	182.88	7	17.3	1200
6	82	70.79	67.10	616	11.2	0.004124	45.72	45.72	182.88	7	8.9	1200
7	88	93.32	92.30	2041	5.3	0.002309	45.72	45.72	182.88	7	29.2	1800
8	92	99.82	98.50	3133	7.8	0.001194	45.72	45.72	182.88	7	36.5	1200
9	94	91.40	90.30	2056	2.6	0.003379	45.72	45.72	182.88	7	29.4	2000
10	99	96.40	92.50	2749	2.6	0.004136	45.72	45.72	182.88	7	64.1	2000
11	86	97.47	96.04	6647	11.5	0.001578	30.48	63.5	91.44	57.4	17.6	2000
12	82	84.94	80.77	3427	2.9	0.002669	30.48	63.5	91.44	57.4	9.1	2000
13	85	98.64	93.99	7596	13.6	0.001332	30.48	63.5	91.44	57.4	21.8	2000
14	80	88.44	79.20	3812	8.4	0.002252	30.48	63.5	91.44	57.4	11.1	2000
15	85	39.60	38.80	926	45.4	0.010927	30.48	63.5	91.44	7	15.3	2000
16	82	22.70	22.20	471	0.0	0.019417	30.48	63.5	91.44	7	7.6	2000
17	87	99.50	99.11	7899	12.5	0.001157	25.4	63.5	91.44	57.4	19.5	1400
18	87	98.00	96.80	7041	11.0	0.001545	30.48	63.5	91.44	57.4	18.6	2000
19	82	81.80	75.70	3608	0.2	0.002535	30.48	63.5	91.44	57.4	8.8	2000
20	86	96.80	92.70	7284	10.8	0.00144	30.48	63.5	91.44	57.4	17.6	2000
21	76	58.00	49.20	1540	18.0	0.004942	30.48	63.5	91.44	57.4	4.2	2000
22	70	59.10	50.60	1602	10.9	0.004008	30.48	63.5	91.44	57.4	3.5	2000
23	55	69.90	61.70	2127	14.9	0.002002	30.48	63.5	91.44	57.4	5.7	2000
24	41	87.84	79.80	3707	0.0	0.000759	30.48	63.5	91.44	57.4	10.6	2000
25	31	68.40	60.70	2028	37.4	0.000976	30.48	63.5	91.44	57.4	5.8	2000
26	85	89.39	81.12	3977	4.4	0.002544	30.48	63.5	91.44	58.4	21.5	2000
27	37	43.93	39.41	6220	6.9	0.000396	30.48	63.5	91.44	57.4	24.0	2000
28	31	35.24	29.84	3939	4.2	0.000502	30.48	63.5	91.44	57.4	24.0	2000

NOTES: KR = Kill Rate

Comp. = Computed

Tests 1-26 are for *Serratia marcescens*

Tests 27-28 are for *Bacillus subtilis*

APPENDIX K: Dimensionless Parameters and Variables for CCD Analysis

Case	A	B	C	D	E	F	G	J	Computed Values for Variables						
	W/H	r/l	kPL/Q	x/W	y/H	p	z/L	Af	W	H	r	l	y	z	L
1	4.420	0.0356	1.800	0.860	0.4280	0.85	0.780	0.780	243.9	55.2	7.467	209.75	23.62	159.5	204.5
2	1.590	0.0356	1.800	0.860	0.4280	0.85	0.780	0.780	116.6	73.3	3.568	100.23	31.37	159.5	204.5
3	4.420	0.0099	1.800	0.860	0.4280	0.85	0.780	0.780	243.9	55.2	2.077	209.75	23.62	159.5	204.5
4	1.590	0.0099	1.800	0.860	0.4280	0.85	0.780	0.780	116.6	73.3	0.992	100.23	31.37	159.5	204.5
5	4.420	0.0356	0.320	0.860	0.4280	0.85	0.780	0.780	43.4	9.8	1.328	37.29	4.20	28.4	36.4
6	1.590	0.0356	0.320	0.860	0.4280	0.85	0.780	0.780	20.7	13.0	0.634	17.82	5.58	28.4	36.4
7	4.420	0.0099	0.320	0.860	0.4280	0.85	0.780	0.780	43.4	9.8	0.369	37.29	4.20	28.4	36.4
8	1.590	0.0099	0.320	0.860	0.4280	0.85	0.780	0.780	20.7	13.0	0.176	17.82	5.58	28.4	36.4
9	4.420	0.0356	1.800	0.200	0.4280	0.85	0.780	0.780	243.9	55.2	1.737	48.78	23.62	159.5	204.5
10	1.590	0.0356	1.800	0.200	0.4280	0.85	0.780	0.780	116.6	73.3	0.830	23.31	31.37	159.5	204.5
11	4.420	0.0099	1.800	0.200	0.4280	0.85	0.780	0.780	243.9	55.2	0.483	48.78	23.62	159.5	204.5
12	1.590	0.0099	1.800	0.200	0.4280	0.85	0.780	0.780	116.6	73.3	0.231	23.31	31.37	159.5	204.5
13	4.420	0.0356	0.320	0.200	0.4280	0.85	0.780	0.780	43.4	9.8	0.309	8.67	4.20	28.4	36.4
14	1.590	0.0356	0.320	0.200	0.4280	0.85	0.780	0.780	20.7	13.0	0.148	4.14	5.58	28.4	36.4
15	4.420	0.0099	0.320	0.200	0.4280	0.85	0.780	0.780	43.4	9.8	0.086	8.67	4.20	28.4	36.4
16	1.590	0.0099	0.320	0.200	0.4280	0.85	0.780	0.780	20.7	13.0	0.041	4.14	5.58	28.4	36.4
17	4.420	0.0356	1.800	0.860	0.0800	0.85	0.780	0.780	243.9	55.2	7.467	209.75	4.41	159.5	204.5
18	1.590	0.0356	1.800	0.860	0.0800	0.85	0.780	0.780	116.6	73.3	3.568	100.23	5.86	159.5	204.5
19	4.420	0.0099	1.800	0.860	0.0800	0.85	0.780	0.780	243.9	55.2	2.077	209.75	4.41	159.5	204.5
20	1.590	0.0099	1.800	0.860	0.0800	0.85	0.780	0.780	116.6	73.3	0.992	100.23	5.86	159.5	204.5
21	4.420	0.0356	0.320	0.860	0.0800	0.85	0.780	0.780	43.4	9.8	1.328	37.29	0.78	28.4	36.4
22	1.590	0.0356	0.320	0.860	0.0800	0.85	0.780	0.780	20.7	13.0	0.634	17.82	1.04	28.4	36.4
23	4.420	0.0099	0.320	0.860	0.0800	0.85	0.780	0.780	43.4	9.8	0.369	37.29	0.78	28.4	36.4
24	1.590	0.0099	0.320	0.860	0.0800	0.85	0.780	0.780	20.7	13.0	0.176	17.82	1.04	28.4	36.4
25	4.420	0.0356	1.800	0.200	0.0800	0.85	0.780	0.780	243.9	55.2	1.737	48.78	4.41	159.5	204.5
26	1.590	0.0356	1.800	0.200	0.0800	0.85	0.780	0.780	116.6	73.3	0.830	23.31	5.86	159.5	204.5
27	4.420	0.0099	1.800	0.200	0.0800	0.85	0.780	0.780	243.9	55.2	0.483	48.78	4.41	159.5	204.5
28	1.590	0.0099	1.800	0.200	0.0800	0.85	0.780	0.780	116.6	73.3	0.231	23.31	5.86	159.5	204.5
29	4.420	0.0356	0.320	0.200	0.0800	0.85	0.780	0.780	43.4	9.8	0.309	8.67	0.78	28.4	36.4
30	1.590	0.0356	0.320	0.200	0.0800	0.85	0.780	0.780	20.7	13.0	0.148	4.14	1.04	28.4	36.4
31	4.420	0.0099	0.320	0.200	0.0800	0.85	0.780	0.780	43.4	9.8	0.086	8.67	0.78	28.4	36.4
32	1.590	0.0099	0.320	0.200	0.0800	0.85	0.780	0.780	20.7	13.0	0.041	4.14	1.04	28.4	36.4
33	4.420	0.0356	1.800	0.860	0.4280	0.45	0.780	0.780	243.9	55.2	7.467	209.75	23.62	159.5	204.5
34	1.590	0.0356	1.800	0.860	0.4280	0.45	0.780	0.780	116.6	73.3	3.568	100.23	31.37	159.5	204.5
35	4.420	0.0099	1.800	0.860	0.4280	0.45	0.780	0.780	243.9	55.2	2.077	209.75	23.62	159.5	204.5
36	1.590	0.0099	1.800	0.860	0.4280	0.45	0.780	0.780	116.6	73.3	0.992	100.23	31.37	159.5	204.5
37	4.420	0.0356	0.320	0.860	0.4280	0.45	0.780	0.780	43.4	9.8	1.328	37.29	4.20	28.4	36.4
38	1.590	0.0356	0.320	0.860	0.4280	0.45	0.780	0.780	20.7	13.0	0.634	17.82	5.58	28.4	36.4
39	4.420	0.0099	0.320	0.860	0.4280	0.45	0.780	0.780	43.4	9.8	0.369	37.29	4.20	28.4	36.4
40	1.590	0.0099	0.320	0.860	0.4280	0.45	0.780	0.780	20.7	13.0	0.176	17.82	5.58	28.4	36.4
41	4.420	0.0356	1.800	0.200	0.4280	0.45	0.780	0.780	243.9	55.2	1.737	48.78	23.62	159.5	204.5
42	1.590	0.0356	1.800	0.200	0.4280	0.45	0.780	0.780	116.6	73.3	0.830	23.31	31.37	159.5	204.5
43	4.420	0.0099	1.800	0.200	0.4280	0.45	0.780	0.780	243.9	55.2	0.483	48.78	23.62	159.5	204.5
44	1.590	0.0099	1.800	0.200	0.4280	0.45	0.780	0.780	116.6	73.3	0.231	23.31	31.37	159.5	204.5
45	4.420	0.0356	0.320	0.200	0.4280	0.45	0.780	0.780	43.4	9.8	0.309	8.67	4.20	28.4	36.4
46	1.590	0.0356	0.320	0.200	0.4280	0.45	0.780	0.780	20.7	13.0	0.148	4.14	5.58	28.4	36.4
47	4.420	0.0099	0.320	0.200	0.4280	0.45	0.780	0.780	43.4	9.8	0.086	8.67	4.20	28.4	36.4
48	1.590	0.0099	0.320	0.200	0.4280	0.45	0.780	0.780	20.7	13.0	0.041	4.14	5.58	28.4	36.4
49	4.420	0.0356	1.800	0.860	0.0800	0.45	0.780	0.780	243.9	55.2	7.467	209.75	4.41	159.5	204.5
50	1.590	0.0356	1.800	0.860	0.0800	0.45	0.780	0.780	116.6	73.3	3.568	100.23	5.86	159.5	204.5
51	4.420	0.0099	1.800	0.860	0.0800	0.45	0.780	0.780	243.9	55.2	2.077	209.75	4.41	159.5	204.5
52	1.590	0.0099	1.800	0.860	0.0800	0.45	0.780	0.780	116.6	73.3	0.992	100.23	5.86	159.5	204.5
53	4.420	0.0356	0.320	0.860	0.0800	0.45	0.780	0.780	43.4	9.8	1.328	37.29	0.78	28.4	36.4
54	1.590	0.0356	0.320	0.860	0.0800	0.45	0.780	0.780	20.7	13.0	0.634	17.82	1.04	28.4	36.4
55	4.420	0.0099	0.320	0.860	0.0800	0.45	0.780	0.780	43.4	9.8	0.369	37.29	0.78	28.4	36.4
56	1.590	0.0099	0.320	0.860	0.0800	0.45	0.780	0.780	20.7	13.0	0.176	17.82	1.04	28.4	36.4
57	4.420	0.0356	1.800	0.200	0.0800	0.45	0.780	0.780	243.9	55.2	1.737	48.78	4.41	159.5	204.5
58	1.590	0.0356	1.800	0.200	0.0800	0.45	0.780	0.780	116.6	73.3	0.830	23.31	5.86	159.5	204.5

APPENDIX K: Dimensionless Parameters and Variables for CCD Analysis

Case	A	B	C	D	E	F	G	J	Computed Values for Variables						
	W/H	r/l	kPL/Q	x/W	y/H	p	z/L	Af	W	H	r	l	y	z	L
59	4.420	0.0099	1.800	0.200	0.0800	0.45	0.780	0.780	243.9	55.2	0.483	48.78	4.41	159.5	204.5
60	1.590	0.0099	1.800	0.200	0.0800	0.45	0.780	0.780	116.6	73.3	0.231	23.31	5.86	159.5	204.5
61	4.420	0.0356	0.320	0.200	0.0800	0.45	0.780	0.780	43.4	9.8	0.309	8.67	0.78	28.4	36.4
62	1.590	0.0356	0.320	0.200	0.0800	0.45	0.780	0.780	20.7	13.0	0.148	4.14	1.04	28.4	36.4
63	4.420	0.0099	0.320	0.200	0.0800	0.45	0.780	0.780	43.4	9.8	0.086	8.67	0.78	28.4	36.4
64	1.590	0.0099	0.320	0.200	0.0800	0.45	0.780	0.780	20.7	13.0	0.041	4.14	1.04	28.4	36.4
65	4.420	0.0356	1.800	0.860	0.4280	0.85	0.220	0.780	243.9	55.2	7.467	209.75	23.62	45.0	204.5
66	1.590	0.0356	1.800	0.860	0.4280	0.85	0.220	0.780	116.6	73.3	3.568	100.23	31.37	45.0	204.5
67	4.420	0.0099	1.800	0.860	0.4280	0.85	0.220	0.780	243.9	55.2	2.077	209.75	23.62	45.0	204.5
68	1.590	0.0099	1.800	0.860	0.4280	0.85	0.220	0.780	116.6	73.3	0.992	100.23	31.37	45.0	204.5
69	4.420	0.0356	0.320	0.860	0.4280	0.85	0.220	0.780	43.4	9.8	1.328	37.29	4.20	8.0	36.4
70	1.590	0.0356	0.320	0.860	0.4280	0.85	0.220	0.780	20.7	13.0	0.634	17.82	5.58	8.0	36.4
71	4.420	0.0099	0.320	0.860	0.4280	0.85	0.220	0.780	43.4	9.8	0.369	37.29	4.20	8.0	36.4
72	1.590	0.0099	0.320	0.860	0.4280	0.85	0.220	0.780	20.7	13.0	0.176	17.82	5.58	8.0	36.4
73	4.420	0.0356	1.800	0.200	0.4280	0.85	0.220	0.780	243.9	55.2	1.737	48.78	23.62	45.0	204.5
74	1.590	0.0356	1.800	0.200	0.4280	0.85	0.220	0.780	116.6	73.3	0.830	23.31	31.37	45.0	204.5
75	4.420	0.0099	1.800	0.200	0.4280	0.85	0.220	0.780	243.9	55.2	0.483	48.78	23.62	45.0	204.5
76	1.590	0.0099	1.800	0.200	0.4280	0.85	0.220	0.780	116.6	73.3	0.231	23.31	31.37	45.0	204.5
77	4.420	0.0356	0.320	0.200	0.4280	0.85	0.220	0.780	43.4	9.8	0.309	8.67	4.20	8.0	36.4
78	1.590	0.0356	0.320	0.200	0.4280	0.85	0.220	0.780	20.7	13.0	0.148	4.14	5.58	8.0	36.4
79	4.420	0.0099	0.320	0.200	0.4280	0.85	0.220	0.780	43.4	9.8	0.086	8.67	4.20	8.0	36.4
80	1.590	0.0099	0.320	0.200	0.4280	0.85	0.220	0.780	20.7	13.0	0.041	4.14	5.58	8.0	36.4
81	4.420	0.0356	1.800	0.860	0.0800	0.85	0.220	0.780	243.9	55.2	7.467	209.75	4.41	45.0	204.5
82	1.590	0.0356	1.800	0.860	0.0800	0.85	0.220	0.780	116.6	73.3	3.568	100.23	5.86	45.0	204.5
83	4.420	0.0099	1.800	0.860	0.0800	0.85	0.220	0.780	243.9	55.2	2.077	209.75	4.41	45.0	204.5
84	1.590	0.0099	1.800	0.860	0.0800	0.85	0.220	0.780	116.6	73.3	0.992	100.23	5.86	45.0	204.5
85	4.420	0.0356	0.320	0.860	0.0800	0.85	0.220	0.780	43.4	9.8	1.328	37.29	0.78	8.0	36.4
86	1.590	0.0356	0.320	0.860	0.0800	0.85	0.220	0.780	20.7	13.0	0.634	17.82	1.04	8.0	36.4
87	4.420	0.0099	0.320	0.860	0.0800	0.85	0.220	0.780	43.4	9.8	0.369	37.29	0.78	8.0	36.4
88	1.590	0.0099	0.320	0.860	0.0800	0.85	0.220	0.780	20.7	13.0	0.176	17.82	1.04	8.0	36.4
89	4.420	0.0356	1.800	0.200	0.0800	0.85	0.220	0.780	243.9	55.2	1.737	48.78	4.41	45.0	204.5
90	1.590	0.0356	1.800	0.200	0.0800	0.85	0.220	0.780	116.6	73.3	0.830	23.31	5.86	45.0	204.5
91	4.420	0.0099	1.800	0.200	0.0800	0.85	0.220	0.780	243.9	55.2	0.483	48.78	4.41	45.0	204.5
92	1.590	0.0099	1.800	0.200	0.0800	0.85	0.220	0.780	116.6	73.3	0.231	23.31	5.86	45.0	204.5
93	4.420	0.0356	0.320	0.200	0.0800	0.85	0.220	0.780	43.4	9.8	0.309	8.67	0.78	8.0	36.4
94	1.590	0.0356	0.320	0.200	0.0800	0.85	0.220	0.780	20.7	13.0	0.148	4.14	1.04	8.0	36.4
95	4.420	0.0099	0.320	0.200	0.0800	0.85	0.220	0.780	43.4	9.8	0.086	8.67	0.78	8.0	36.4
96	1.590	0.0099	0.320	0.200	0.0800	0.85	0.220	0.780	20.7	13.0	0.041	4.14	1.04	8.0	36.4
97	4.420	0.0356	1.800	0.860	0.4280	0.45	0.220	0.780	243.9	55.2	7.467	209.75	23.62	45.0	204.5
98	1.590	0.0356	1.800	0.860	0.4280	0.45	0.220	0.780	116.6	73.3	3.568	100.23	31.37	45.0	204.5
99	4.420	0.0099	1.800	0.860	0.4280	0.45	0.220	0.780	243.9	55.2	2.077	209.75	23.62	45.0	204.5
100	1.590	0.0099	1.800	0.860	0.4280	0.45	0.220	0.780	116.6	73.3	0.992	100.23	31.37	45.0	204.5
101	4.420	0.0356	0.320	0.860	0.4280	0.45	0.220	0.780	43.4	9.8	1.328	37.29	4.20	8.0	36.4
102	1.590	0.0356	0.320	0.860	0.4280	0.45	0.220	0.780	20.7	13.0	0.634	17.82	5.58	8.0	36.4
103	4.420	0.0099	0.320	0.860	0.4280	0.45	0.220	0.780	43.4	9.8	0.369	37.29	4.20	8.0	36.4
104	1.590	0.0099	0.320	0.860	0.4280	0.45	0.220	0.780	20.7	13.0	0.176	17.82	5.58	8.0	36.4
105	4.420	0.0356	1.800	0.200	0.4280	0.45	0.220	0.780	243.9	55.2	1.737	48.78	23.62	45.0	204.5
106	1.590	0.0356	1.800	0.200	0.4280	0.45	0.220	0.780	116.6	73.3	0.830	23.31	31.37	45.0	204.5
107	4.420	0.0099	1.800	0.200	0.4280	0.45	0.220	0.780	243.9	55.2	0.483	48.78	23.62	45.0	204.5
108	1.590	0.0099	1.800	0.200	0.4280	0.45	0.220	0.780	116.6	73.3	0.231	23.31	31.37	45.0	204.5
109	4.420	0.0356	0.320	0.200	0.4280	0.45	0.220	0.780	43.4	9.8	0.309	8.67	4.20	8.0	36.4
110	1.590	0.0356	0.320	0.200	0.4280	0.45	0.220	0.780	20.7	13.0	0.148	4.14	5.58	8.0	36.4
111	4.420	0.0099	0.320	0.200	0.4280	0.45	0.220	0.780	43.4	9.8	0.086	8.67	4.20	8.0	36.4
112	1.590	0.0099	0.320	0.200	0.4280	0.45	0.220	0.780	20.7	13.0	0.041	4.14	5.58	8.0	36.4
113	4.420	0.0356	1.800	0.860	0.0800	0.45	0.220	0.780	243.9	55.2	7.467	209.75	4.41	45.0	204.5
114	1.590	0.0356	1.800	0.860	0.0800	0.45	0.220	0.780	116.6	73.3	3.568	100.23	5.86	45.0	204.5
115	4.420	0.0099	1.800	0.860	0.0800	0.45	0.220	0.780	243.9	55.2	2.077	209.75	4.41	45.0	204.5
116	1.590	0.0099	1.800	0.860	0.0800	0.45	0.220	0.780	116.6	73.3	0.992	100.23	5.86	45.0	204.5

APPENDIX K: Dimensionless Parameters and Variables for CCD Analysis

Case	A	B	C	D	E	F	G	J	Computed Values for Variables						
	W/H	r/l	kPL/Q	x/W	y/H	p	z/L	Af	W	H	r	l	y	z	L
117	4.420	0.0356	0.320	0.860	0.0800	0.45	0.220	0.780	43.4	9.8	1.328	37.29	0.78	8.0	36.4
118	1.590	0.0356	0.320	0.860	0.0800	0.45	0.220	0.780	20.7	13.0	0.634	17.82	1.04	8.0	36.4
119	4.420	0.0099	0.320	0.860	0.0800	0.45	0.220	0.780	43.4	9.8	0.369	37.29	0.78	8.0	36.4
120	1.590	0.0099	0.320	0.860	0.0800	0.45	0.220	0.780	20.7	13.0	0.176	17.82	1.04	8.0	36.4
121	4.420	0.0356	1.800	0.200	0.0800	0.45	0.220	0.780	243.9	55.2	1.737	48.78	4.41	45.0	204.5
122	1.590	0.0356	1.800	0.200	0.0800	0.45	0.220	0.780	116.6	73.3	0.830	23.31	5.86	45.0	204.5
123	4.420	0.0099	1.800	0.200	0.0800	0.45	0.220	0.780	243.9	55.2	0.483	48.78	4.41	45.0	204.5
124	1.590	0.0099	1.800	0.200	0.0800	0.45	0.220	0.780	116.6	73.3	0.231	23.31	5.86	45.0	204.5
125	4.420	0.0356	0.320	0.200	0.0800	0.45	0.220	0.780	43.4	9.8	0.309	8.67	0.78	8.0	36.4
126	1.590	0.0356	0.320	0.200	0.0800	0.45	0.220	0.780	20.7	13.0	0.148	4.14	1.04	8.0	36.4
127	4.420	0.0099	0.320	0.200	0.0800	0.45	0.220	0.780	43.4	9.8	0.086	8.67	0.78	8.0	36.4
128	1.590	0.0099	0.320	0.200	0.0800	0.45	0.220	0.780	20.7	13.0	0.041	4.14	1.04	8.0	36.4
129	4.420	0.0356	1.800	0.860	0.4280	0.85	0.780	0.220	864.7	195.6	26.475	743.67	83.73	159.5	204.5
130	1.590	0.0356	1.800	0.860	0.4280	0.85	0.780	0.220	413.2	259.9	12.651	355.37	111.23	159.5	204.5
131	4.420	0.0099	1.800	0.860	0.4280	0.85	0.780	0.220	864.7	195.6	7.362	743.67	83.73	159.5	204.5
132	1.590	0.0099	1.800	0.860	0.4280	0.85	0.780	0.220	413.2	259.9	3.518	355.37	111.23	159.5	204.5
133	4.420	0.0356	0.320	0.860	0.4280	0.85	0.780	0.220	153.7	34.8	4.707	132.21	14.89	28.4	36.4
134	1.590	0.0356	0.320	0.860	0.4280	0.85	0.780	0.220	73.5	46.2	2.249	63.18	19.77	28.4	36.4
135	4.420	0.0099	0.320	0.860	0.4280	0.85	0.780	0.220	153.7	34.8	1.309	132.21	14.89	28.4	36.4
136	1.590	0.0099	0.320	0.860	0.4280	0.85	0.780	0.220	73.5	46.2	0.625	63.18	19.77	28.4	36.4
137	4.420	0.0356	1.800	0.200	0.4280	0.85	0.780	0.220	864.7	195.6	6.157	172.95	83.73	159.5	204.5
138	1.590	0.0356	1.800	0.200	0.4280	0.85	0.780	0.220	413.2	259.9	2.942	82.64	111.23	159.5	204.5
139	4.420	0.0099	1.800	0.200	0.4280	0.85	0.780	0.220	864.7	195.6	1.712	172.95	83.73	159.5	204.5
140	1.590	0.0099	1.800	0.200	0.4280	0.85	0.780	0.220	413.2	259.9	0.818	82.64	111.23	159.5	204.5
141	4.420	0.0356	0.320	0.200	0.4280	0.85	0.780	0.220	153.7	34.8	1.095	30.75	14.89	28.4	36.4
142	1.590	0.0356	0.320	0.200	0.4280	0.85	0.780	0.220	73.5	46.2	0.523	14.69	19.77	28.4	36.4
143	4.420	0.0099	0.320	0.200	0.4280	0.85	0.780	0.220	153.7	34.8	0.304	30.75	14.89	28.4	36.4
144	1.590	0.0099	0.320	0.200	0.4280	0.85	0.780	0.220	73.5	46.2	0.145	14.69	19.77	28.4	36.4
145	4.420	0.0356	1.800	0.860	0.0800	0.85	0.780	0.220	864.7	195.6	26.475	743.67	15.65	159.5	204.5
146	1.590	0.0356	1.800	0.860	0.0800	0.85	0.780	0.220	413.2	259.9	12.651	355.37	20.79	159.5	204.5
147	4.420	0.0099	1.800	0.860	0.0800	0.85	0.780	0.220	864.7	195.6	7.362	743.67	15.65	159.5	204.5
148	1.590	0.0099	1.800	0.860	0.0800	0.85	0.780	0.220	413.2	259.9	3.518	355.37	20.79	159.5	204.5
149	4.420	0.0356	0.320	0.860	0.0800	0.85	0.780	0.220	153.7	34.8	4.707	132.21	2.78	28.4	36.4
150	1.590	0.0356	0.320	0.860	0.0800	0.85	0.780	0.220	73.5	46.2	2.249	63.18	3.70	28.4	36.4
151	4.420	0.0099	0.320	0.860	0.0800	0.85	0.780	0.220	153.7	34.8	1.309	132.21	2.78	28.4	36.4
152	1.590	0.0099	0.320	0.860	0.0800	0.85	0.780	0.220	73.5	46.2	0.625	63.18	3.70	28.4	36.4
153	4.420	0.0356	1.800	0.200	0.0800	0.85	0.780	0.220	864.7	195.6	6.157	172.95	15.65	159.5	204.5
154	1.590	0.0356	1.800	0.200	0.0800	0.85	0.780	0.220	413.2	259.9	2.942	82.64	20.79	159.5	204.5
155	4.420	0.0099	1.800	0.200	0.0800	0.85	0.780	0.220	864.7	195.6	1.712	172.95	15.65	159.5	204.5
156	1.590	0.0099	1.800	0.200	0.0800	0.85	0.780	0.220	413.2	259.9	0.818	82.64	20.79	159.5	204.5
157	4.420	0.0356	0.320	0.200	0.0800	0.85	0.780	0.220	153.7	34.8	1.095	30.75	2.78	28.4	36.4
158	1.590	0.0356	0.320	0.200	0.0800	0.85	0.780	0.220	73.5	46.2	0.523	14.69	3.70	28.4	36.4
159	4.420	0.0099	0.320	0.200	0.0800	0.85	0.780	0.220	153.7	34.8	0.304	30.75	2.78	28.4	36.4
160	1.590	0.0099	0.320	0.200	0.0800	0.85	0.780	0.220	73.5	46.2	0.145	14.69	3.70	28.4	36.4
161	4.420	0.0356	1.800	0.860	0.4280	0.45	0.780	0.220	864.7	195.6	26.475	743.67	83.73	159.5	204.5
162	1.590	0.0356	1.800	0.860	0.4280	0.45	0.780	0.220	413.2	259.9	12.651	355.37	111.23	159.5	204.5
163	4.420	0.0099	1.800	0.860	0.4280	0.45	0.780	0.220	864.7	195.6	7.362	743.67	83.73	159.5	204.5
164	1.590	0.0099	1.800	0.860	0.4280	0.45	0.780	0.220	413.2	259.9	3.518	355.37	111.23	159.5	204.5
165	4.420	0.0356	0.320	0.860	0.4280	0.45	0.780	0.220	153.7	34.8	4.707	132.21	14.89	28.4	36.4
166	1.590	0.0356	0.320	0.860	0.4280	0.45	0.780	0.220	73.5	46.2	2.249	63.18	19.77	28.4	36.4
167	4.420	0.0099	0.320	0.860	0.4280	0.45	0.780	0.220	153.7	34.8	1.309	132.21	14.89	28.4	36.4
168	1.590	0.0099	0.320	0.860	0.4280	0.45	0.780	0.220	73.5	46.2	0.625	63.18	19.77	28.4	36.4
169	4.420	0.0356	1.800	0.200	0.4280	0.45	0.780	0.220	864.7	195.6	6.157	172.95	83.73	159.5	204.5
170	1.590	0.0356	1.800	0.200	0.4280	0.45	0.780	0.220	413.2	259.9	2.942	82.64	111.23	159.5	204.5
171	4.420	0.0099	1.800	0.200	0.4280	0.45	0.780	0.220	864.7	195.6	1.712	172.95	83.73	159.5	204.5
172	1.590	0.0099	1.800	0.200	0.4280	0.45	0.780	0.220	413.2	259.9	0.818	82.64	111.23	159.5	204.5
173	4.420	0.0356	0.320	0.200	0.4280	0.45	0.780	0.220	153.7	34.8	1.095	30.75	14.89	28.4	36.4
174	1.590	0.0356	0.320	0.200	0.4280	0.45	0.780	0.220	73.5	46.2	0.523	14.69	19.77	28.4	36.4

APPENDIX K: Dimensionless Parameters and Variables for CCD Analysis

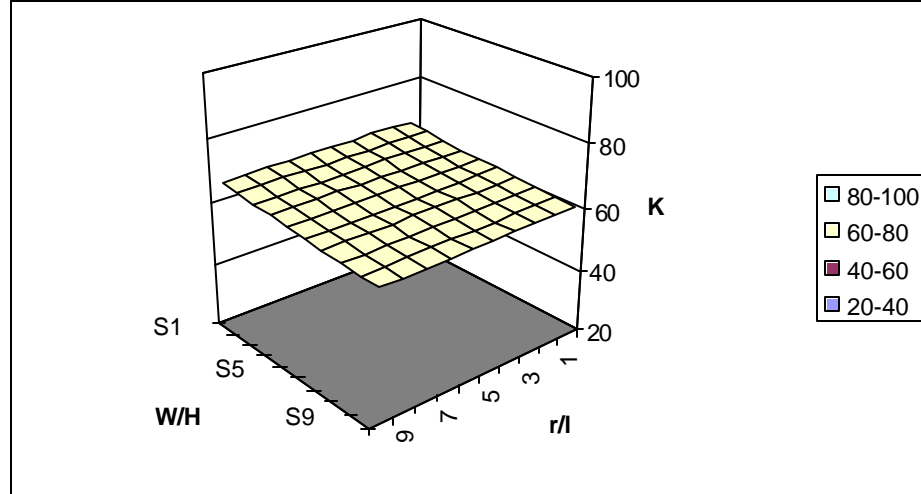
Case	A	B	C	D	E	F	G	J	Computed Values for Variables						
	W/H	r/l	kPL/Q	x/W	y/H	p	z/L	Af	W	H	r	l	y	z	L
175	4.420	0.0099	0.320	0.200	0.4280	0.45	0.780	0.220	153.7	34.8	0.304	30.75	14.89	28.4	36.4
176	1.590	0.0099	0.320	0.200	0.4280	0.45	0.780	0.220	73.5	46.2	0.145	14.69	19.77	28.4	36.4
177	4.420	0.0356	1.800	0.860	0.0800	0.45	0.780	0.220	864.7	195.6	26.475	743.67	15.65	159.5	204.5
178	1.590	0.0356	1.800	0.860	0.0800	0.45	0.780	0.220	413.2	259.9	12.651	355.37	20.79	159.5	204.5
179	4.420	0.0099	1.800	0.860	0.0800	0.45	0.780	0.220	864.7	195.6	7.362	743.67	15.65	159.5	204.5
180	1.590	0.0099	1.800	0.860	0.0800	0.45	0.780	0.220	413.2	259.9	3.518	355.37	20.79	159.5	204.5
181	4.420	0.0356	0.320	0.860	0.0800	0.45	0.780	0.220	153.7	34.8	4.707	132.21	2.78	28.4	36.4
182	1.590	0.0356	0.320	0.860	0.0800	0.45	0.780	0.220	73.5	46.2	2.249	63.18	3.70	28.4	36.4
183	4.420	0.0099	0.320	0.860	0.0800	0.45	0.780	0.220	153.7	34.8	1.309	132.21	2.78	28.4	36.4
184	1.590	0.0099	0.320	0.860	0.0800	0.45	0.780	0.220	73.5	46.2	0.625	63.18	3.70	28.4	36.4
185	4.420	0.0356	1.800	0.200	0.0800	0.45	0.780	0.220	864.7	195.6	6.157	172.95	15.65	159.5	204.5
186	1.590	0.0356	1.800	0.200	0.0800	0.45	0.780	0.220	413.2	259.9	2.942	82.64	20.79	159.5	204.5
187	4.420	0.0099	1.800	0.200	0.0800	0.45	0.780	0.220	864.7	195.6	1.712	172.95	15.65	159.5	204.5
188	1.590	0.0099	1.800	0.200	0.0800	0.45	0.780	0.220	413.2	259.9	0.818	82.64	20.79	159.5	204.5
189	4.420	0.0356	0.320	0.200	0.0800	0.45	0.780	0.220	153.7	34.8	1.095	30.75	2.78	28.4	36.4
190	1.590	0.0356	0.320	0.200	0.0800	0.45	0.780	0.220	73.5	46.2	0.523	14.69	3.70	28.4	36.4
191	4.420	0.0099	0.320	0.200	0.0800	0.45	0.780	0.220	153.7	34.8	0.304	30.75	2.78	28.4	36.4
192	1.590	0.0099	0.320	0.200	0.0800	0.45	0.780	0.220	73.5	46.2	0.145	14.69	3.70	28.4	36.4
193	4.420	0.0356	1.800	0.860	0.4280	0.85	0.220	0.220	864.7	195.6	26.475	743.67	83.73	45.0	204.5
194	1.590	0.0356	1.800	0.860	0.4280	0.85	0.220	0.220	413.2	259.9	12.651	355.37	111.23	45.0	204.5
195	4.420	0.0099	1.800	0.860	0.4280	0.85	0.220	0.220	864.7	195.6	7.362	743.67	83.73	45.0	204.5
196	1.590	0.0099	1.800	0.860	0.4280	0.85	0.220	0.220	413.2	259.9	3.518	355.37	111.23	45.0	204.5
197	4.420	0.0356	0.320	0.860	0.4280	0.85	0.220	0.220	153.7	34.8	4.707	132.21	14.89	8.0	36.4
198	1.590	0.0356	0.320	0.860	0.4280	0.85	0.220	0.220	73.5	46.2	2.249	63.18	19.77	8.0	36.4
199	4.420	0.0099	0.320	0.860	0.4280	0.85	0.220	0.220	153.7	34.8	1.309	132.21	14.89	8.0	36.4
200	1.590	0.0099	0.320	0.860	0.4280	0.85	0.220	0.220	73.5	46.2	0.625	63.18	19.77	8.0	36.4
201	4.420	0.0356	1.800	0.200	0.4280	0.85	0.220	0.220	864.7	195.6	6.157	172.95	83.73	45.0	204.5
202	1.590	0.0356	1.800	0.200	0.4280	0.85	0.220	0.220	413.2	259.9	2.942	82.64	111.23	45.0	204.5
203	4.420	0.0099	1.800	0.200	0.4280	0.85	0.220	0.220	864.7	195.6	1.712	172.95	83.73	45.0	204.5
204	1.590	0.0099	1.800	0.200	0.4280	0.85	0.220	0.220	413.2	259.9	0.818	82.64	111.23	45.0	204.5
205	4.420	0.0356	0.320	0.200	0.4280	0.85	0.220	0.220	153.7	34.8	1.095	30.75	14.89	8.0	36.4
206	1.590	0.0356	0.320	0.200	0.4280	0.85	0.220	0.220	73.5	46.2	0.523	14.69	19.77	8.0	36.4
207	4.420	0.0099	0.320	0.200	0.4280	0.85	0.220	0.220	153.7	34.8	0.304	30.75	14.89	8.0	36.4
208	1.590	0.0099	0.320	0.200	0.4280	0.85	0.220	0.220	73.5	46.2	0.145	14.69	19.77	8.0	36.4
209	4.420	0.0356	1.800	0.860	0.0800	0.85	0.220	0.220	864.7	195.6	26.475	743.67	15.65	45.0	204.5
210	1.590	0.0356	1.800	0.860	0.0800	0.85	0.220	0.220	413.2	259.9	12.651	355.37	20.79	45.0	204.5
211	4.420	0.0099	1.800	0.860	0.0800	0.85	0.220	0.220	864.7	195.6	7.362	743.67	15.65	45.0	204.5
212	1.590	0.0099	1.800	0.860	0.0800	0.85	0.220	0.220	413.2	259.9	3.518	355.37	20.79	45.0	204.5
213	4.420	0.0356	0.320	0.860	0.0800	0.85	0.220	0.220	153.7	34.8	4.707	132.21	2.78	8.0	36.4
214	1.590	0.0356	0.320	0.860	0.0800	0.85	0.220	0.220	73.5	46.2	2.249	63.18	3.70	8.0	36.4
215	4.420	0.0099	0.320	0.860	0.0800	0.85	0.220	0.220	153.7	34.8	1.309	132.21	2.78	8.0	36.4
216	1.590	0.0099	0.320	0.860	0.0800	0.85	0.220	0.220	73.5	46.2	0.625	63.18	3.70	8.0	36.4
217	4.420	0.0356	1.800	0.200	0.0800	0.85	0.220	0.220	864.7	195.6	6.157	172.95	15.65	45.0	204.5
218	1.590	0.0356	1.800	0.200	0.0800	0.85	0.220	0.220	413.2	259.9	2.942	82.64	20.79	45.0	204.5
219	4.420	0.0099	1.800	0.200	0.0800	0.85	0.220	0.220	864.7	195.6	1.712	172.95	15.65	45.0	204.5
220	1.590	0.0099	1.800	0.200	0.0800	0.85	0.220	0.220	413.2	259.9	0.818	82.64	20.79	45.0	204.5
221	4.420	0.0356	0.320	0.200	0.0800	0.85	0.220	0.220	153.7	34.8	1.095	30.75	2.78	8.0	36.4
222	1.590	0.0356	0.320	0.200	0.0800	0.85	0.220	0.220	73.5	46.2	0.523	14.69	3.70	8.0	36.4
223	4.420	0.0099	0.320	0.200	0.0800	0.85	0.220	0.220	153.7	34.8	0.304	30.75	2.78	8.0	36.4
224	1.590	0.0099	0.320	0.200	0.0800	0.85	0.220	0.220	73.5	46.2	0.145	14.69	3.70	8.0	36.4
225	4.420	0.0356	1.800	0.860	0.4280	0.45	0.220	0.220	864.7	195.6	26.475	743.67	83.73	45.0	204.5
226	1.590	0.0356	1.800	0.860	0.4280	0.45	0.220	0.220	413.2	259.9	12.651	355.37	111.23	45.0	204.5
227	4.420	0.0099	1.800	0.860	0.4280	0.45	0.220	0.220	864.7	195.6	7.362	743.67	83.73	45.0	204.5
228	1.590	0.0099	1.800	0.860	0.4280	0.45	0.220	0.220	413.2	259.9	3.518	355.37	111.23	45.0	204.5
229	4.420	0.0356	0.320	0.860	0.4280	0.45	0.220	0.220	153.7	34.8	4.707	132.21	14.89	8.0	36.4
230	1.590	0.0356	0.320	0.860	0.4280	0.45	0.220	0.220	73.5	46.2	2.249	63.18	19.77	8.0	36.4
231	4.420	0.0099	0.320	0.860	0.4280	0.45	0.220	0.220	153.7	34.8	1.309	132.21	14.89	8.0	36.4
232	1.590	0.0099	0.320	0.860	0.4280	0.45	0.220	0.220	73.5	46.2	0.625	63.18	19.77	8.0	36.4

APPENDIX K: Dimensionless Parameters and Variables for CCD Analysis

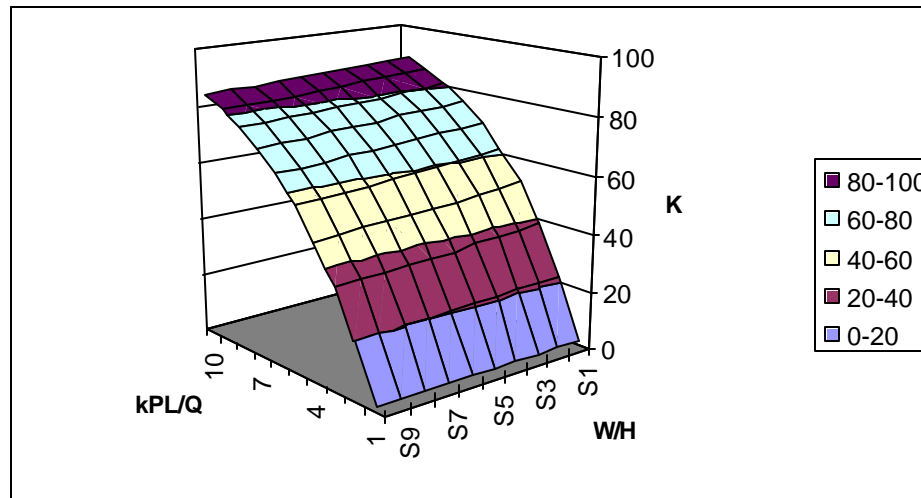
Case	A	B	C	D	E	F	G	J	Computed Values for Variables						
	W/H	r/l	kPL/Q	x/W	y/H	ρ	z/L	Af	W	H	r	l	y	z	L
233	4.420	0.0356	1.800	0.200	0.4280	0.45	0.220	0.220	864.7	195.6	6.157	172.95	83.73	45.0	204.5
234	1.590	0.0356	1.800	0.200	0.4280	0.45	0.220	0.220	413.2	259.9	2.942	82.64	111.23	45.0	204.5
235	4.420	0.0099	1.800	0.200	0.4280	0.45	0.220	0.220	864.7	195.6	1.712	172.95	83.73	45.0	204.5
236	1.590	0.0099	1.800	0.200	0.4280	0.45	0.220	0.220	413.2	259.9	0.818	82.64	111.23	45.0	204.5
237	4.420	0.0356	0.320	0.200	0.4280	0.45	0.220	0.220	153.7	34.8	1.095	30.75	14.89	8.0	36.4
238	1.590	0.0356	0.320	0.200	0.4280	0.45	0.220	0.220	73.5	46.2	0.523	14.69	19.77	8.0	36.4
239	4.420	0.0099	0.320	0.200	0.4280	0.45	0.220	0.220	153.7	34.8	0.304	30.75	14.89	8.0	36.4
240	1.590	0.0099	0.320	0.200	0.4280	0.45	0.220	0.220	73.5	46.2	0.145	14.69	19.77	8.0	36.4
241	4.420	0.0356	1.800	0.860	0.0800	0.45	0.220	0.220	864.7	195.6	26.475	743.67	15.65	45.0	204.5
242	1.590	0.0356	1.800	0.860	0.0800	0.45	0.220	0.220	413.2	259.9	12.651	355.37	20.79	45.0	204.5
243	4.420	0.0099	1.800	0.860	0.0800	0.45	0.220	0.220	864.7	195.6	7.362	743.67	15.65	45.0	204.5
244	1.590	0.0099	1.800	0.860	0.0800	0.45	0.220	0.220	413.2	259.9	3.518	355.37	20.79	45.0	204.5
245	4.420	0.0356	0.320	0.860	0.0800	0.45	0.220	0.220	153.7	34.8	4.707	132.21	2.78	8.0	36.4
246	1.590	0.0356	0.320	0.860	0.0800	0.45	0.220	0.220	73.5	46.2	2.249	63.18	3.70	8.0	36.4
247	4.420	0.0099	0.320	0.860	0.0800	0.45	0.220	0.220	153.7	34.8	1.309	132.21	2.78	8.0	36.4
248	1.590	0.0099	0.320	0.860	0.0800	0.45	0.220	0.220	73.5	46.2	0.625	63.18	3.70	8.0	36.4
249	4.420	0.0356	1.800	0.200	0.0800	0.45	0.220	0.220	864.7	195.6	6.157	172.95	15.65	45.0	204.5
250	1.590	0.0356	1.800	0.200	0.0800	0.45	0.220	0.220	413.2	259.9	2.942	82.64	20.79	45.0	204.5
251	4.420	0.0099	1.800	0.200	0.0800	0.45	0.220	0.220	864.7	195.6	1.712	172.95	15.65	45.0	204.5
252	1.590	0.0099	1.800	0.200	0.0800	0.45	0.220	0.220	413.2	259.9	0.818	82.64	20.79	45.0	204.5
253	4.420	0.0356	0.320	0.200	0.0800	0.45	0.220	0.220	153.7	34.8	1.095	30.75	2.78	8.0	36.4
254	1.590	0.0356	0.320	0.200	0.0800	0.45	0.220	0.220	73.5	46.2	0.523	14.69	3.70	8.0	36.4
255	4.420	0.0099	0.320	0.200	0.0800	0.45	0.220	0.220	153.7	34.8	0.304	30.75	2.78	8.0	36.4
256	1.590	0.0099	0.320	0.200	0.0800	0.45	0.220	0.220	73.5	46.2	0.145	14.69	3.70	8.0	36.4
257	1.004	0.0228	1.060	0.530	0.2540	0.65	0.220	0.220	188.3	187.5	2.270	99.79	47.63	26.5	120.5
258	5.006	0.0228	1.060	0.530	0.2540	0.65	0.220	0.220	564.3	112.7	6.804	299.07	28.63	26.5	120.5
259	3.005	0.0046	1.060	0.530	0.2540	0.65	0.220	0.220	376.3	125.2	0.913	199.43	31.81	26.5	120.5
260	3.005	0.0409	1.060	0.530	0.2540	0.65	0.220	0.220	376.3	125.2	8.161	199.43	31.81	26.5	120.5
261	3.005	0.0228	0.014	0.530	0.2540	0.65	0.220	0.220	4.8	1.6	0.058	2.55	0.41	0.3	1.5
262	3.005	0.0228	2.106	0.530	0.2540	0.65	0.220	0.220	747.8	248.8	9.016	396.31	63.21	52.7	239.4
263	3.005	0.0228	1.060	0.063	0.2540	0.65	0.220	0.220	376.3	125.2	0.542	23.84	31.81	26.5	120.5
264	3.005	0.0228	1.060	0.997	0.2540	0.65	0.220	0.220	376.3	125.2	8.532	375.03	31.81	26.5	120.5
265	3.005	0.0228	1.060	0.530	0.0079	0.65	0.220	0.220	376.3	125.2	4.537	199.43	1.00	26.5	120.5
266	3.005	0.0228	1.060	0.530	0.5001	0.65	0.220	0.220	376.3	125.2	4.537	199.43	62.62	26.5	120.5
267	3.005	0.0228	1.060	0.530	0.2540	0.37	0.220	0.220	376.3	125.2	4.537	199.43	31.81	26.5	120.5
268	3.005	0.0228	1.060	0.530	0.2540	0.93	0.220	0.220	376.3	125.2	4.537	199.43	31.81	26.5	120.5
269	3.005	0.0228	1.060	0.530	0.2540	0.65	0.104	0.220	376.3	125.2	4.537	199.43	31.81	12.6	120.5
270	3.005	0.0228	1.060	0.530	0.2540	0.65	0.896	0.220	376.3	125.2	4.537	199.43	31.81	107.9	120.5
271	3.005	0.0228	1.060	0.530	0.2540	0.65	0.220	0.104	432.2	143.8	5.211	229.04	36.53	26.5	120.5
272	3.005	0.0228	1.060	0.530	0.2540	0.65	0.220	0.896	50.3	16.7	0.606	26.64	4.25	26.5	120.5
273	3.005	0.0228	1.060	0.530	0.2540	0.65	0.220	0.220	376.3	125.2	4.537	199.43	31.81	26.5	120.5

APPENDIX L: Response Surfaces for Dimensionless Parameters -- Mixed Air

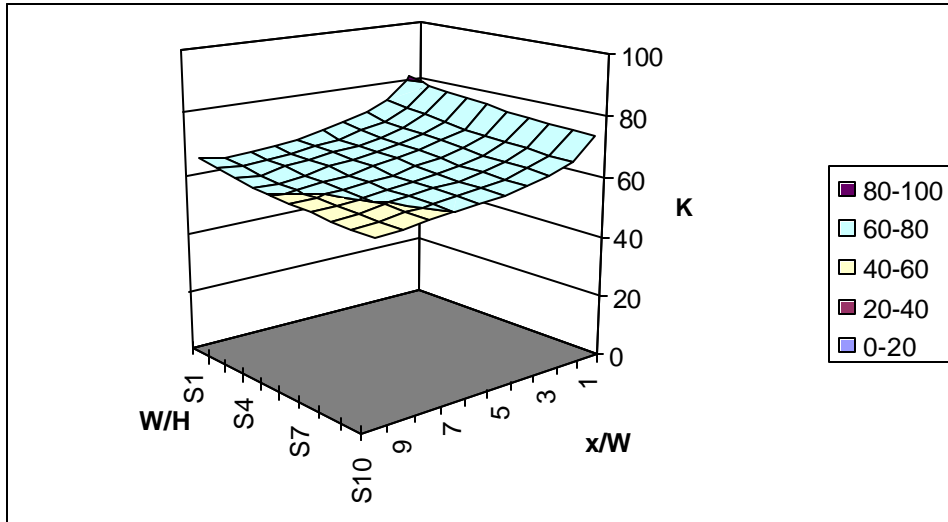
AB	MIXED AIR										
r/l	1.004049	1.448704	1.89336	2.338016	2.782672	3.227328	3.671984	4.11664	4.561296	5.005952	
0.004579	66.0691	65.3482	64.747	64.1284	63.6515	63.204	62.7816	62.3864	62.0506	61.7548	
0.008617	66.1023	65.3075	64.6644	64.0233	63.5872	63.1262	62.7186	62.2753	61.9317	61.6428	
0.012655	66.04	65.2687	64.6476	63.9772	63.498	62.9915	62.5869	62.1576	61.8133	61.5247	
0.016693	66.0171	65.2686	64.5821	63.8805	63.424	62.9238	62.4943	62.0462	61.686	61.3935	
0.020731	66.0182	65.2264	64.5376	63.8404	63.3598	62.8177	62.384	61.9548	61.5731	61.2714	
0.024769	65.9065	65.1627	64.5041	63.7648	63.2827	62.7336	62.3055	61.8504	61.4334	61.1442	
0.028807	65.8457	65.13	64.4094	63.708	63.2128	62.6372	62.1972	61.7363	61.3157	60.9987	
0.032845	65.8345	65.0885	64.3565	63.6558	63.1155	62.5565	62.0857	61.6247	61.192	60.8653	
0.036883	65.8142	65.0036	64.3013	63.5875	63.0535	62.4664	61.9846	61.5136	61.0574	60.743	
0.040921	65.7682	64.9382	64.2569	63.5189	62.9644	62.3683	61.8841	61.3969	60.9318	60.6021	



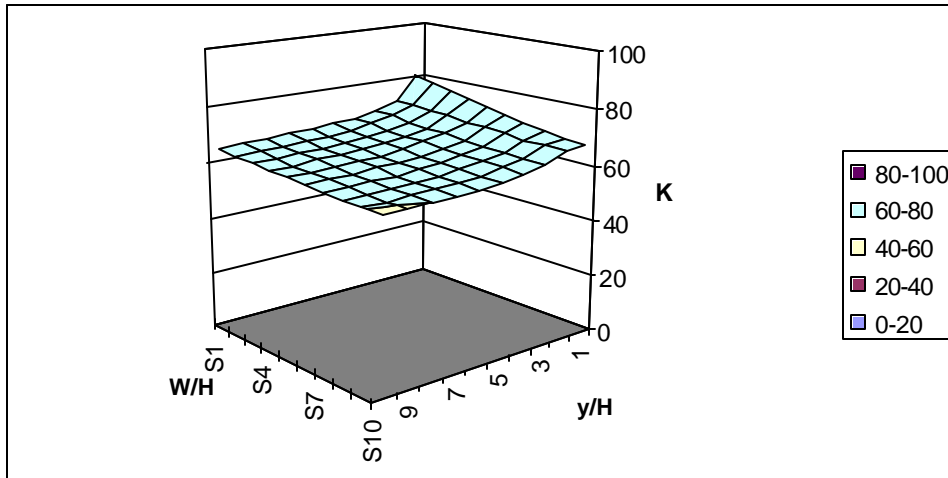
AC	W/H										
kPL/Q	1.004049	1.448704	1.89336	2.338016	2.782672	3.227328	3.671984	4.11664	4.561296	5.005952	
0.013566	1.3337	1.31503	1.28737	1.27116	1.24766	1.23335	1.21669	1.20446	1.18847	1.17622	
0.246107	22.1661	21.7355	21.3962	21.0957	20.8091	20.5529	20.3035	20.0962	19.9158	19.7391	
0.478648	38.511	37.8858	37.3807	36.8843	36.4516	36.0122	35.6339	35.298	35.057	34.7618	
0.711189	51.4363	50.6646	49.9699	49.5245	48.8799	48.4651	48.0884	47.6643	47.3137	46.9756	
0.94373	61.7279	60.8295	60.2428	59.5702	59.0478	58.552	58.0193	57.5966	57.2544	56.8912	
1.17627	69.7024	68.9512	68.1734	67.7139	67.115	66.5181	66.1467	65.7347	65.3376	64.997	
1.408811	76.0634	75.3205	74.6309	74.1451	73.6219	73.0938	72.6683	72.2671	71.9132	71.5318	
1.641352	81.1341	80.4608	79.8075	79.3418	78.7364	78.3388	77.8578	77.5478	77.1073	76.8453	
1.873893	85.1009	84.4667	83.9532	83.488	83.0031	82.5489	82.1937	81.8222	81.4966	81.1082	
2.106434	88.204	87.6553	87.1526	86.7672	86.3392	85.9961	85.6504	85.3206	84.9865	84.7358	



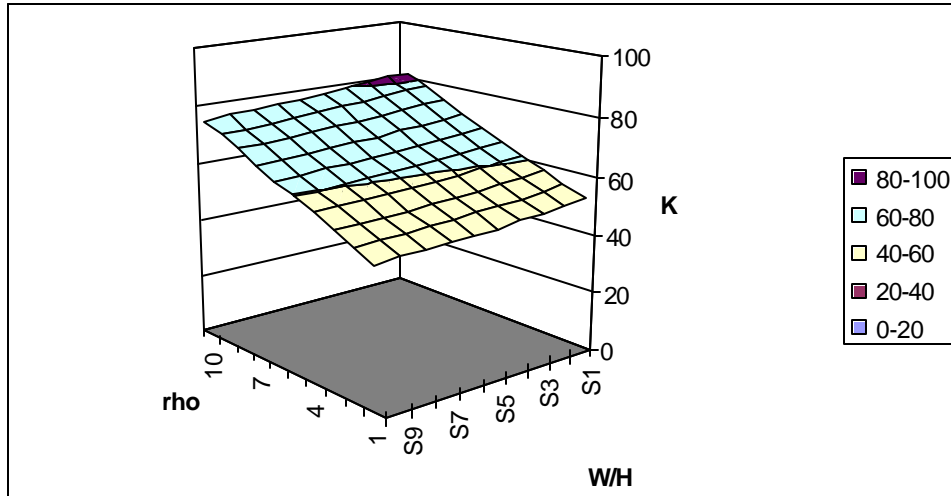
AD	W/H										MIXED AIR
x/W	1.004049	1.448704	1.89336	2.338016	2.782672	3.227328	3.671984	4.11664	4.561296	5.005952	
0.063347	80.8859	79.6305	78.4821	77.4171	76.7364	76.0863	75.5509	75.1048	74.5913	74.2566	
0.167048	73.9963	72.7389	71.5428	70.5499	69.9467	69.4078	68.8501	68.4392	68.0357	67.613	
0.270748	70.3874	69.2763	68.4002	67.5634	67.0115	66.3845	65.8611	65.4368	65.0486	64.5979	
0.374449	68.1595	67.2572	66.4166	65.687	65.131	64.5867	64.1129	63.6736	63.1897	62.8265	
0.47815	66.6261	65.6953	65.0072	64.3645	63.8625	63.3268	62.7988	62.3854	61.9697	61.6272	
0.58185	65.3785	64.6233	63.961	63.2662	62.8568	62.3124	61.8386	61.4715	61.0906	60.7668	
0.685551	64.4343	63.6665	63.0002	62.3569	61.9036	61.4301	61.0191	60.625	60.265	59.9817	
0.789252	63.7529	62.8974	62.145	61.5055	61.0208	60.6056	60.1998	59.8136	59.4737	59.1606	
0.892952	63.4272	62.2559	61.3724	60.6488	60.1513	59.6622	59.2531	58.874	58.532	58.2256	
0.996653	64.2576	62.7391	61.5158	60.6006	59.8304	59.2083	58.6176	58.1408	57.692	57.3083	



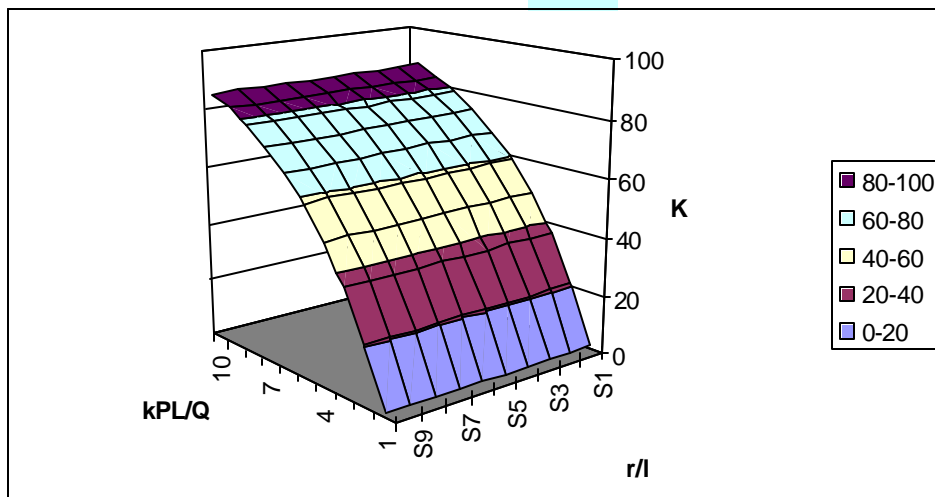
AE	W/H										
y/H	1.004049	1.448704	1.89336	2.338016	2.782672	3.227328	3.671984	4.11664	4.561296	5.005952	
0.007947	80.4015	78.5493	76.8043	75.3201	73.681	72.3575	71.1099	69.9939	68.918	68.1032	
0.062625	71.5333	71.2508	70.8411	70.2321	69.6854	69.1352	68.6405	68.1497	67.7377	67.3723	
0.117304	68.6631	68.1829	67.6624	67.0471	66.5492	66.0106	65.5579	65.1088	64.7066	64.365	
0.171982	67.2659	66.5033	65.9408	65.299	64.8027	64.2798	63.8214	63.3916	63.009	62.6673	
0.226661	66.3329	65.4907	64.8823	64.2528	63.6969	63.1948	62.7329	62.2813	61.9227	61.5779	
0.281339	65.6678	64.8978	64.1789	63.4806	62.9894	62.481	62.0012	61.5701	61.1716	60.8437	
0.336018	65.3441	64.3867	63.7083	62.9412	62.4867	61.9868	61.5284	61.0635	60.6686	60.3552	
0.390696	65.1556	64.0789	63.3652	62.6944	62.1285	61.6422	61.1839	60.7437	60.3525	60.0302	
0.445375	64.8814	63.8287	63.182	62.4136	61.9153	61.4324	60.9744	60.556	60.1605	59.8328	
0.500053	64.6493	63.7159	63.0584	62.2579	61.8307	61.3363	60.8515	60.4445	60.0588	59.7626	



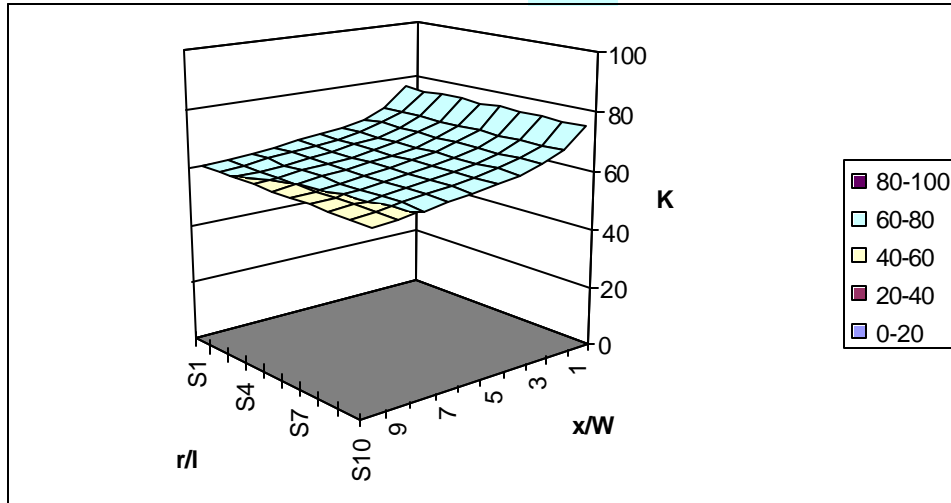
AF	W/H MIXED AIR										
r	1.004049	1.448704	1.89336	2.338016	2.782672	3.227328	3.671984	4.11664	4.561296	5.005952	
0.36718	51.8645	50.8673	50.1113	49.4936	49.0323	48.5915	48.2519	47.9047	47.6087	47.3748	
0.430029	54.6712	53.7293	52.9924	52.3659	51.9071	51.4535	51.1041	50.7407	50.4319	50.1895	
0.492878	57.5903	56.7084	55.9894	55.3498	54.89	54.4197	54.0561	53.6732	53.3482	53.094	
0.555727	61.138	60.3304	59.6284	58.9662	58.4988	58.0026	57.6158	57.2052	56.8566	56.584	
0.618576	64.2981	63.5561	62.8631	62.1738	61.6928	61.1677	60.7546	60.3156	59.9423	59.6494	
0.681424	67.5621	66.8859	66.1948	65.4698	64.967	64.4064	63.9605	63.4884	63.0862	62.7687	
0.744273	70.9198	70.3072	69.609	68.8393	68.3055	67.7024	67.2169	66.7071	66.2718	65.9256	
0.807122	74.9325	74.3889	73.6693	72.8359	72.2534	71.5922	71.0526	70.4937	70.015	69.6305	
0.869971	78.4238	77.9323	77.1827	76.2864	75.6519	74.9349	74.3432	73.739	73.2199	72.7994	
0.93282	81.9224	81.4744	80.6857	79.722	79.0279	78.252	77.6048	76.9541	76.3933	75.9349	



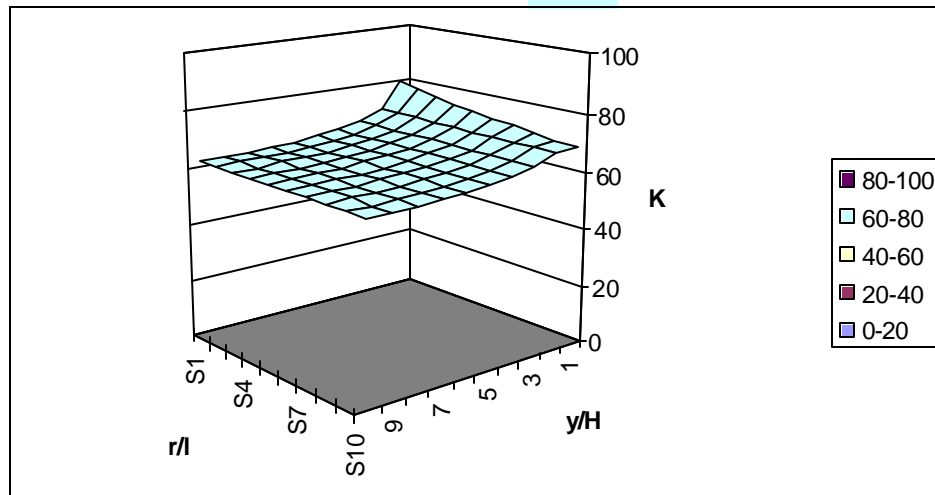
BC	r/l										
kPL/Q	0.004579	0.008617	0.012655	0.016693	0.020731	0.024769	0.028807	0.032845	0.036883	0.040921	
0.013566	1.25284	1.25176	1.24855	1.24663	1.24432	1.24175	1.23959	1.23727	1.23505	1.23256	
0.246107	20.8454	20.8145	20.7691	20.727	20.6932	20.6462	20.6064	20.5617	20.5241	20.4858	
0.478648	36.5055	36.4573	36.3941	36.3312	36.2596	36.1894	36.1244	36.052	35.9803	35.913	
0.711189	49.053	48.9982	48.9096	48.8154	48.752	48.6535	48.5651	48.49	48.4014	48.3246	
0.94373	59.1495	59.0885	59.0193	58.9224	58.8477	58.7457	58.6776	58.5897	58.5016	58.4131	
1.17627	67.2256	67.1716	67.0574	66.9728	66.8954	66.8012	66.7232	66.6271	66.5262	66.4505	
1.408811	73.628	73.5779	73.5003	73.4122	73.3331	73.23	73.1695	73.0876	73.0118	72.9219	
1.641352	78.8988	78.8538	78.7816	78.6994	78.6257	78.5638	78.4878	78.41	78.3198	78.2363	
1.873893	83.0997	83.0496	82.9779	82.9107	82.8298	82.7547	82.6939	82.6163	82.5502	82.4775	
2.106434	86.4515	86.4063	86.3148	86.2394	86.1911	86.1123	86.0417	85.9764	85.9207	85.867	



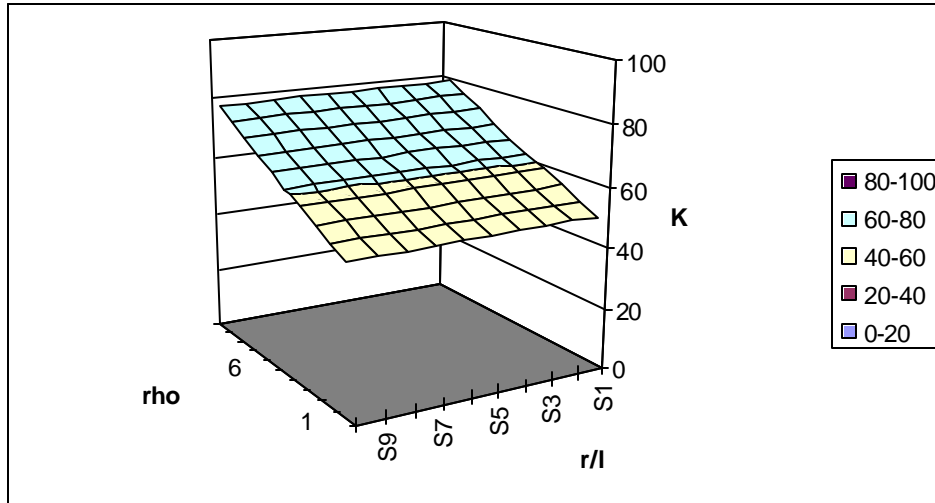
BD	r/l									
MIXED AIR										
x/w	0.004579	0.008617	0.012655	0.016693	0.020731	0.024769	0.028807	0.032845	0.036883	0.040921
0.063347	76.2855	76.3097	76.3336	76.3578	76.3821	76.406	76.4303	76.289	76.2681	76.2572
0.167048	69.7156	69.7456	69.6869	69.6477	69.6377	69.6423	69.5985	69.5969	69.5395	69.5359
0.270748	66.848	66.8399	66.7945	66.7868	66.7005	66.674	66.6192	66.5808	66.5726	66.5332
0.374449	65.142	65.0417	64.9993	64.9364	64.8755	64.8484	64.7605	64.6733	64.6081	64.5438
0.47815	63.9061	63.8363	63.7514	63.6774	63.6129	63.5052	63.4491	63.382	63.326	63.2495
0.58185	62.9607	62.892	62.7572	62.6964	62.588	62.5145	62.4085	62.3282	62.2439	62.1358
0.685551	62.1383	62.0288	61.9124	61.8022	61.7051	61.5968	61.482	61.3596	61.2496	61.1392
0.789252	61.3505	61.2152	61.1182	60.989	60.8741	60.7543	60.6308	60.5116	60.3874	60.2554
0.892952	60.5541	60.4023	60.2605	60.1346	59.9824	59.8372	59.6853	59.5381	59.3846	59.2479
0.996653	60.3299	60.1487	59.9527	59.769	59.6002	59.4171	59.2384	59.05	58.8594	58.6713



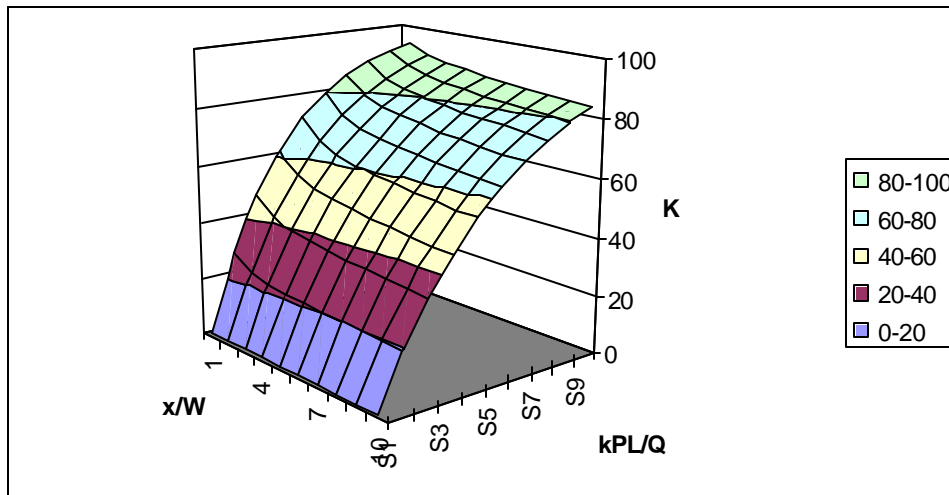
BE	r/l									
y/H	0.004579	0.008617	0.012655	0.016693	0.020731	0.024769	0.028807	0.032845	0.036883	0.040921
0.007947	79.7073	77.8872	76.2997	74.8465	73.6571	72.5573	71.7334	70.8512	70.1232	69.3972
0.062625	69.7244	69.6789	69.5946	69.5033	69.4447	69.3738	69.2875	69.216	69.1623	68.9473
0.117304	66.5773	66.5322	66.4459	66.3815	66.3163	66.24	66.1611	66.0849	66.0384	65.9444
0.171982	64.8873	64.8178	64.744	64.6833	64.5918	64.514	64.4459	64.3705	64.2964	64.2269
0.226661	63.8051	63.748	63.6827	63.6026	63.5085	63.4179	63.3362	63.2546	63.1763	63.1078
0.281339	63.0757	63.019	62.9334	62.836	62.7746	62.6835	62.5965	62.494	62.4388	62.3241
0.336018	62.5989	62.5401	62.4267	62.3278	62.2635	62.1688	62.1	62.0092	61.9286	61.8306
0.390696	62.2943	62.2216	62.0996	62.0343	61.9453	61.8623	61.7818	61.6943	61.5921	61.5151
0.445375	62.1079	62.041	61.933	61.8355	61.7556	61.6601	61.5865	61.4756	61.3829	61.2882
0.500053	61.9976	61.9305	61.8042	61.6999	61.6248	61.5419	61.4409	61.3494	61.297	61.1617



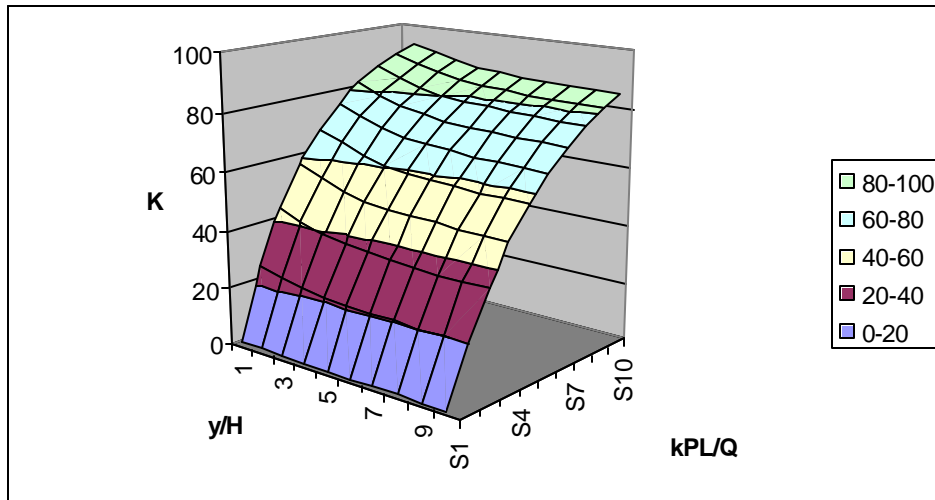
BF	r/l									
MIXED AIR										
r	0.004579	0.008617	0.012655	0.016693	0.020731	0.024769	0.028807	0.032845	0.036883	0.040921
0.36718	49.2768	49.1928	49.0626	48.952	48.8451	48.7487	48.6576	48.5476	48.4477	48.3371
0.430029	52.1271	52.0487	51.9204	51.8142	51.7099	51.6196	51.5334	51.4276	51.3326	51.2256
0.492878	55.0811	55.0085	54.883	54.7818	54.6807	54.5969	54.516	54.415	54.3254	54.2225
0.555727	58.65	58.5846	58.4633	58.3686	58.2721	58.1963	58.1222	58.0274	57.9447	57.8475
0.618576	61.8036	61.7447	61.6281	61.5395	61.4478	61.379	61.3112	61.2224	61.146	61.0544
0.681424	65.0317	64.9794	64.8684	64.7865	64.7002	64.6389	64.5775	64.4953	64.4257	64.3403
0.744273	68.3182	68.2726	68.1682	68.0935	68.0133	67.9595	67.905	67.8299	67.7674	67.6889
0.807122	72.1984	72.1609	72.0653	71.9995	71.9273	71.8825	71.8362	71.77	71.7162	71.6464
0.869971	75.5339	75.5031	75.4162	75.3585	75.2937	75.2566	75.2175	75.1593	75.1132	75.0514
0.93282	78.844	78.8199	78.7424	78.693	78.6363	78.6067	78.5747	78.5249	78.4865	78.4331



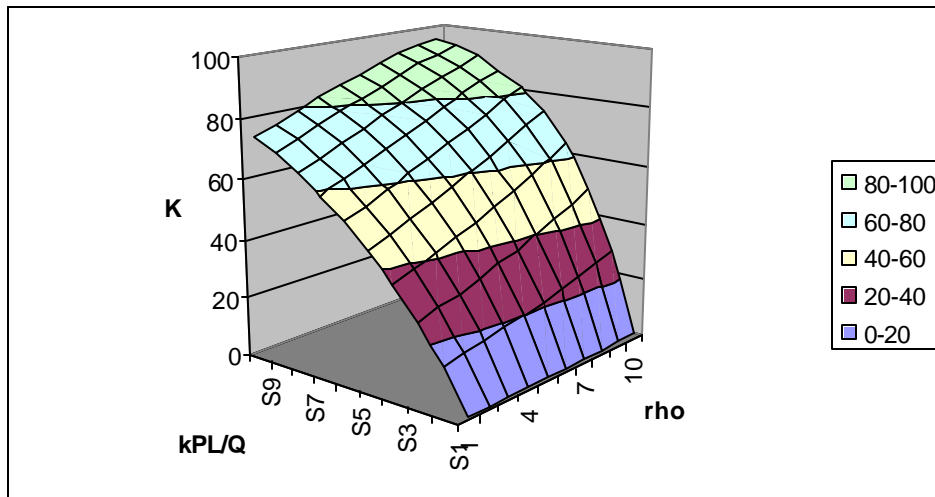
CD	kPL/Q									
x/W	0.013566	0.0246107	0.478648	0.711189	0.94373	1.17627	1.408811	1.641352	1.873893	2.106434
0.063347	1.78381	28.4806	47.8946	62.0267	72.3289	79.8443	85.2079	89.298	92.2008	94.3225
0.167048	1.48668	24.2124	41.6407	55.1008	65.3831	73.4156	79.4108	84.1889	87.874	90.6717
0.270748	1.37025	22.5456	39.1349	52.111	62.37	70.4031	76.6427	81.7233	85.6569	88.733
0.374449	1.30509	21.5829	37.6286	50.4645	60.5719	68.6656	75.0235	80.1672	84.2424	87.4769
0.47815	1.26048	20.952	36.6058	49.1984	59.2798	67.3928	73.7727	79.031	83.2017	86.5804
0.58185	1.22711	20.4264	35.8514	48.2676	58.2634	66.3714	72.8285	78.1562	82.3888	85.7961
0.685551	1.19795	19.9914	35.1583	47.4569	57.3781	65.4967	71.9859	77.2939	81.6315	85.1416
0.789252	1.17049	19.5623	34.4935	46.6452	56.5281	64.6161	71.1473	76.5341	80.8881	84.4427
0.892952	1.14222	19.1416	33.8211	45.8072	55.6708	63.7431	70.2504	75.6828	80.1091	83.7313
0.996653	1.1279	18.9574	33.5326	45.4645	55.2619	63.3181	69.851	75.3185	79.7697	83.4185



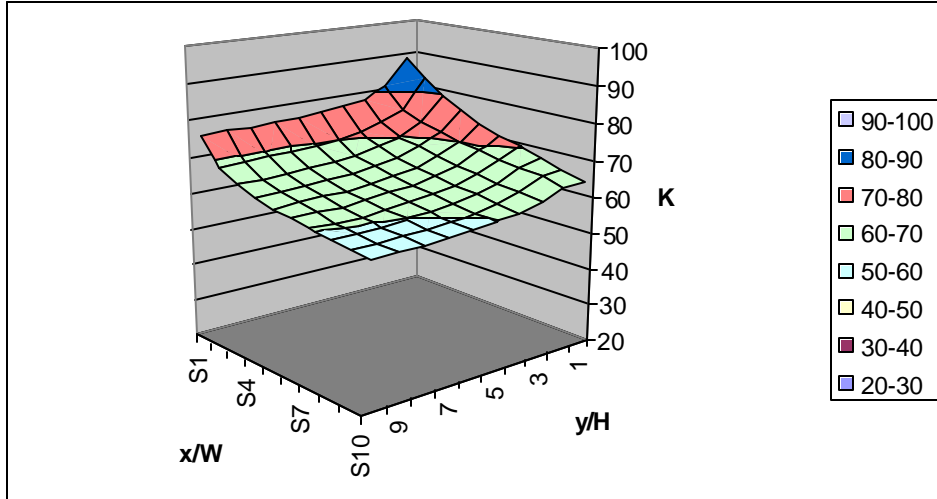
CE	kPL/Q									
	MIXED AIR									
y/H	0.013566	0.246107	0.478648	0.711189	0.94373	1.17627	1.408811	1.641352	1.873893	2.106434
0.007947	1.6436	26.2886	44.7001	58.392	68.8482	76.5931	82.4233	86.8949	90.1594	92.6178
0.062625	1.49378	24.0838	41.4736	54.7972	65.173	73.1261	79.2237	84.029	87.6346	90.481
0.117304	1.35787	22.3505	38.8012	51.7845	62.0035	70.1023	76.3665	81.4271	85.3855	88.4891
0.171982	1.29127	21.4116	37.3611	50.081	60.2499	68.3194	74.6967	79.8865	83.9582	87.2575
0.226661	1.25772	20.8746	36.5306	49.1019	59.1597	67.2618	73.6494	78.9272	83.1302	86.4484
0.281339	1.23127	20.5145	35.9723	48.3914	58.4485	66.5498	72.9564	78.3228	82.5155	85.9241
0.336018	1.21412	20.262	35.5914	47.9235	57.9599	66.0473	72.4725	77.8579	82.1045	85.5683
0.390696	1.20444	20.097	35.3581	47.609	57.6738	65.674	72.1238	77.5567	81.8172	85.282
0.445375	1.19767	20.019	35.1394	47.4387	57.4085	65.5236	71.9488	77.3393	81.6535	85.1072
0.500053	1.19457	19.9557	35.1122	47.3136	57.3107	65.4022	71.8214	77.2993	81.5696	85.0396



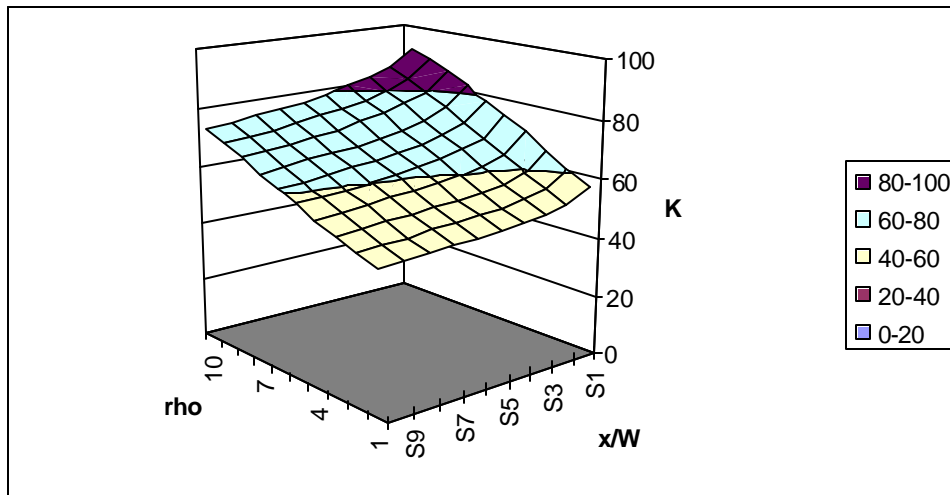
CF	kPL/Q									
r	0.013566	0.246107	0.478648	0.711189	0.94373	1.17627	1.408811	1.641352	1.873893	2.106434
0.36718	0.840356	14.4155	26.0953	36.1697	44.9112	52.4133	58.8899	64.5429	69.3763	73.5425
0.430029	0.91177	15.5569	27.9958	38.5898	47.6703	55.3609	61.9107	67.5731	72.3441	76.404
0.492878	0.990372	16.7967	30.033	41.15	50.5502	58.3974	64.9812	70.6125	75.2819	79.1996
0.555727	1.09249	18.3817	32.5961	44.3203	54.0592	62.0393	68.6053	74.1427	78.6404	82.3458
0.618576	1.19031	19.8728	34.9652	47.1994	57.1892	65.2313	71.726	77.1282	81.4309	84.9143
0.681424	1.29916	21.501	37.5052	50.2305	60.424	68.4708	74.8362	80.0487	84.1113	87.3372
0.744273	1.42082	23.2824	40.2282	53.4144	63.7525	71.7373	77.91	82.8751	86.6531	89.5889
0.807122	1.58186	25.5794	43.6526	57.32	67.7336	75.5485	81.4098	86.0116	89.4047	91.9669
0.869971	1.73941	27.7608	46.8141	60.8254	71.2062	78.7805	84.297	88.5243	91.5475	93.7675
0.93282	1.91867	30.1652	50.1965	64.4657	74.7053	81.942	87.0405	90.8392	93.464	95.331



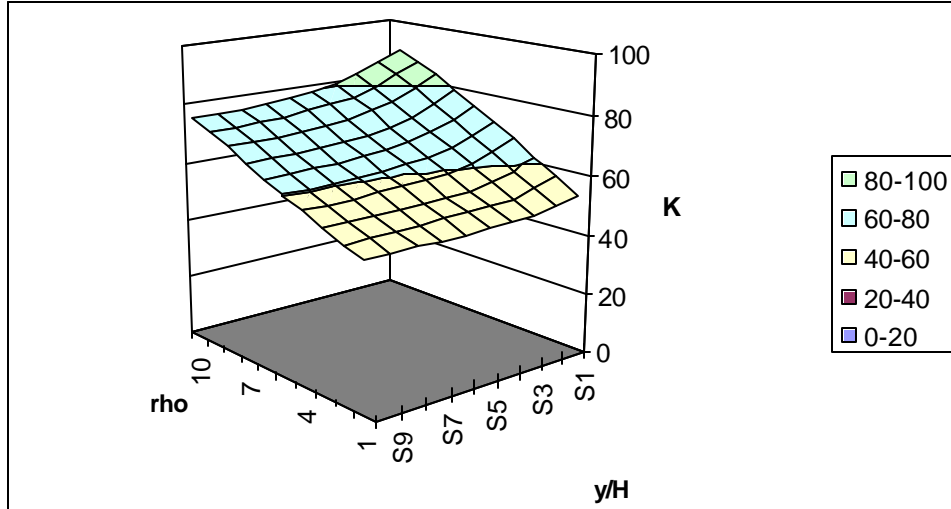
DE	x/w										MIXED AIR									
y/H	0.063347	0.167048	0.270748	0.374449	0.47815	0.58185	0.685551	0.789252	0.892952	0.996653										
0.007947	88.7388	83.6134	79.6896	76.5042	74.1157	72.0701	70.2711	68.4259	66.7204	64.8801										
0.062625	81.3318	75.6996	73.0616	71.2519	69.927	68.8983	67.9811	67.0845	66.0919	64.8774										
0.117304	78.4889	72.686	69.9114	68.1284	66.7979	65.8026	64.879	63.9808	63.0666	62.2551										
0.171982	77.1278	71.0603	68.1011	66.3495	65.0671	64.027	63.1634	62.266	61.3495	60.7423										
0.226661	76.5664	70.0038	67.0486	65.2767	63.9902	62.9564	62.0501	61.2114	60.295	59.8516										
0.281339	76.2383	69.33	66.3638	64.5454	63.2409	62.2256	61.3527	60.4997	59.5811	59.2394										
0.336018	76.0373	68.8961	65.8755	63.986	62.7627	61.7221	60.8376	59.9942	59.1369	58.8406										
0.390696	75.7544	68.6246	65.5227	63.6995	62.4046	61.4249	60.5216	59.69	58.799	58.5917										
0.445375	75.7893	68.379	65.2588	63.455	62.2399	61.1879	60.3024	59.4727	58.6245	58.4359										
0.500053	75.7706	68.2843	65.1651	63.3154	62.0906	61.1022	60.206	59.3762	58.539	58.3381										



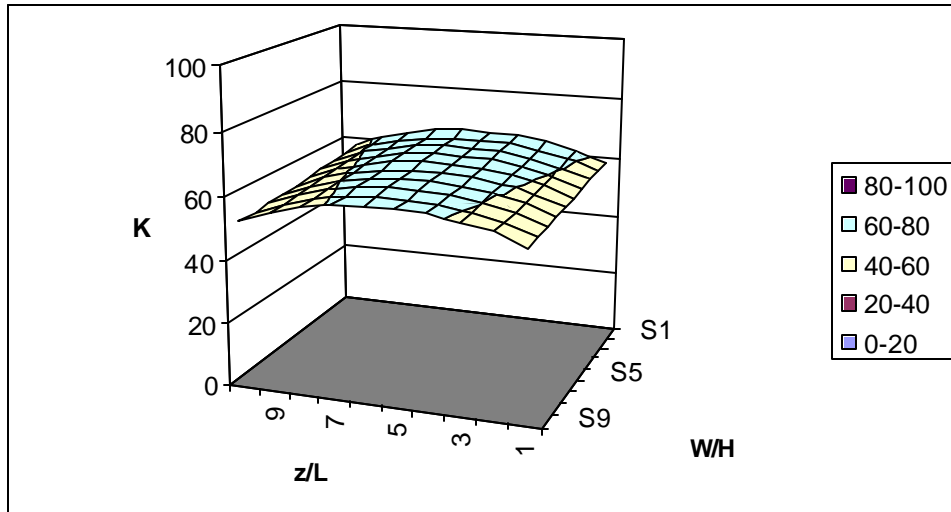
DF	x/W									
r	0.063347	0.167048	0.270748	0.374449	0.47815	0.58185	0.685551	0.789252	0.892952	0.996653
0.36718	56.4115	51.8706	50.3882	49.5722	49.0034	48.5881	48.156	47.719	47.1519	46.7257
0.430029	60.9169	55.5975	53.7242	52.6703	51.9352	51.3982	50.8678	50.3504	49.7097	49.2922
0.492878	65.3328	59.3908	57.1603	55.8761	54.9746	54.3131	53.6814	53.0808	52.365	51.9534
0.555727	70.3238	63.8688	61.2751	59.7381	58.6467	57.8389	57.0876	56.3881	55.5846	55.1767
0.618576	74.4211	67.7197	64.8708	63.137	61.8903	60.9593	60.1063	59.3223	58.4453	58.0385
0.681424	78.3105	71.5472	68.5044	66.5987	65.2081	64.1588	63.2076	62.3414	61.3943	60.9873
0.744273	81.9529	75.3129	72.146	70.1	68.5819	67.4231	66.3798	65.4361	64.4244	64.0165
0.807122	85.8398	79.5698	76.357	74.1969	72.558	71.2878	70.1494	69.1252	68.0485	67.6396
0.869971	88.8211	83.0462	79.8857	77.6786	75.9672	74.6211	73.4163	72.3349	71.2147	70.8065
0.93282	91.4481	86.3084	83.2884	81.0885	79.3398	77.9415	76.6887	75.5653	74.4161	74.0109



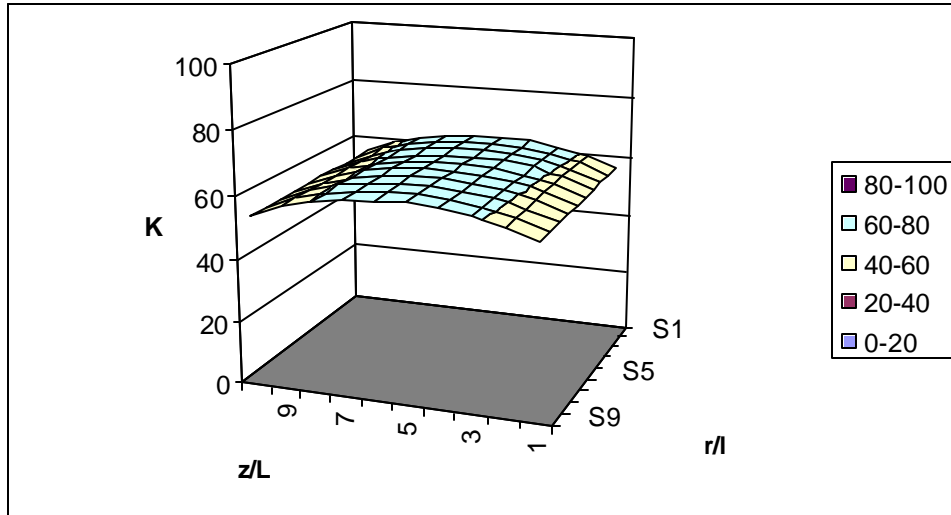
EF	y/H										
MIXED AIR											
r	0.007947	0.062625	0.117304	0.171982	0.226661	0.281339	0.336018	0.390696	0.445375	0.500053	
0.36718	52.7099	51.0332	49.6532	49.1074	48.8844	48.7795	48.7103	48.6917	48.6853	48.6425	
0.430029	57.1431	54.9146	53.0828	52.2499	51.831	51.5862	51.4154	51.3306	51.2857	51.2251	
0.492878	61.5715	58.8525	56.6016	55.4928	54.8824	54.4995	54.2281	54.077	53.9936	53.9156	
0.555727	66.6819	63.4845	60.7982	59.3889	58.5647	58.0256	57.6396	57.4126	57.2847	57.1871	
0.618576	70.9666	67.453	64.4511	62.809	61.814	61.1479	60.668	60.378	60.2128	60.0991	
0.681424	75.1145	71.3831	68.1298	66.2847	65.1345	64.3507	63.7826	63.4326	63.2318	63.1031	
0.744273	79.0766	75.2349	71.8047	69.7935	68.5083	67.6189	66.9708	66.5652	66.3309	66.1883	
0.807122	83.3957	79.5703	76.0408	73.8919	72.4813	71.4888	70.7605	70.2977	70.0282	69.8714	
0.869971	86.7793	83.0945	79.581	77.3701	75.8856	74.8263	74.0437	73.5403	73.2451	73.0783	
0.93282	89.8175	86.3868	82.9883	80.7741	79.252	78.1498	77.3294	76.7952	76.4796	76.3052	



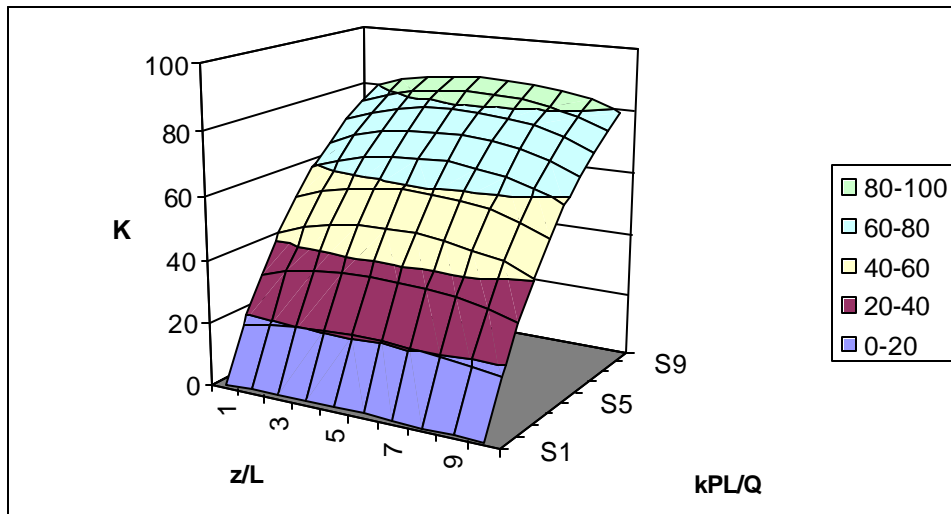
AG	W/H										
MIXED AIR											
z/L	1.004049	1.448704	1.89336	2.338016	2.782672	3.227328	3.671984	4.11664	4.561296	5.005952	
0.1042	58.339	57.4754	56.8309	56.1905	55.7408	55.2773	54.8284	54.4475	54.0597	53.765	
0.192156	61.836	60.9159	60.3224	59.6929	59.1818	58.7283	58.267	57.8581	57.4793	57.1692	
0.280111	64.0297	63.1854	62.5326	61.9308	61.3894	60.894	60.44	60.0254	59.658	59.3284	
0.368067	65.3315	64.4738	63.8695	63.188	62.7186	62.1722	61.7146	61.3155	60.9474	60.5926	
0.456022	65.9041	65.0834	64.4272	63.7254	63.2837	62.7377	62.2869	61.8391	61.4474	61.1761	
0.543978	65.8696	64.9972	64.3595	63.7113	63.2163	62.6471	62.2194	61.7745	61.389	61.0584	
0.631933	65.1778	64.2413	63.6194	62.9776	62.4471	61.9104	61.4492	61.0382	60.6442	60.3243	
0.719889	63.5979	62.771	62.1412	61.4445	60.9205	60.454	60.0113	59.5731	59.1692	58.8978	
0.807844	61.1666	60.3751	59.6651	59.0619	58.5473	58.0549	57.6211	57.2248	56.8404	56.5531	
0.8958	57.5027	56.6256	55.9709	55.3279	54.8774	54.4152	53.9691	53.5891	53.2043	52.9192	



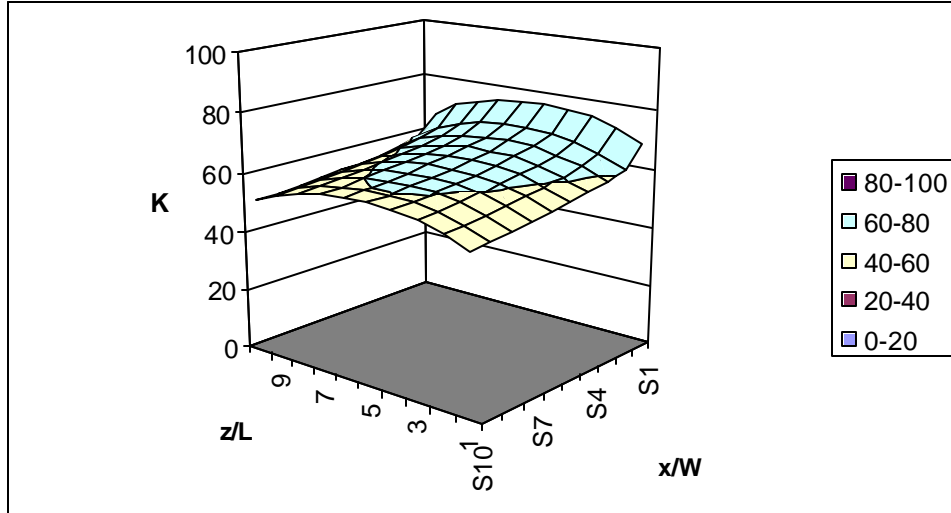
BG	r/l									
MIXED AIR										
z/L	0.004579	0.008617	0.012655	0.020731	0.024769	0.028807	0.032845	0.036883	0.040921	0.004579
0.1042	55.9708	55.8723	55.7822	55.6883	55.569	55.4395	55.3336	55.2305	55.141	55.0334
0.192156	59.3695	59.305	59.1545	59.081	59.0005	58.9038	58.8189	58.7105	58.5963	58.5133
0.280111	61.5403	61.4804	61.3943	61.2974	61.2105	61.1167	61.0378	60.9394	60.8353	60.7392
0.368067	62.8266	62.7416	62.6245	62.5749	62.475	62.391	62.3309	62.2541	62.159	62.0873
0.456022	63.3962	63.3153	63.2286	63.154	63.069	62.9683	62.8884	62.8087	62.7224	62.6574
0.543978	63.3134	63.227	63.1407	63.0625	62.9909	62.9051	62.8225	62.7403	62.6577	62.5852
0.631933	62.5506	62.4931	62.3705	62.3008	62.2268	62.1559	62.0683	61.9666	61.8797	61.7965
0.719889	61.084	61.0234	60.9199	60.8263	60.7409	60.6673	60.5869	60.5095	60.4032	60.3097
0.807844	58.7293	58.6539	58.5406	58.4508	58.3517	58.2487	58.1789	58.0935	57.9891	57.8962
0.8958	55.1041	55.0076	54.9169	54.8235	54.7052	54.5777	54.4717	54.3693	54.2725	54.1715



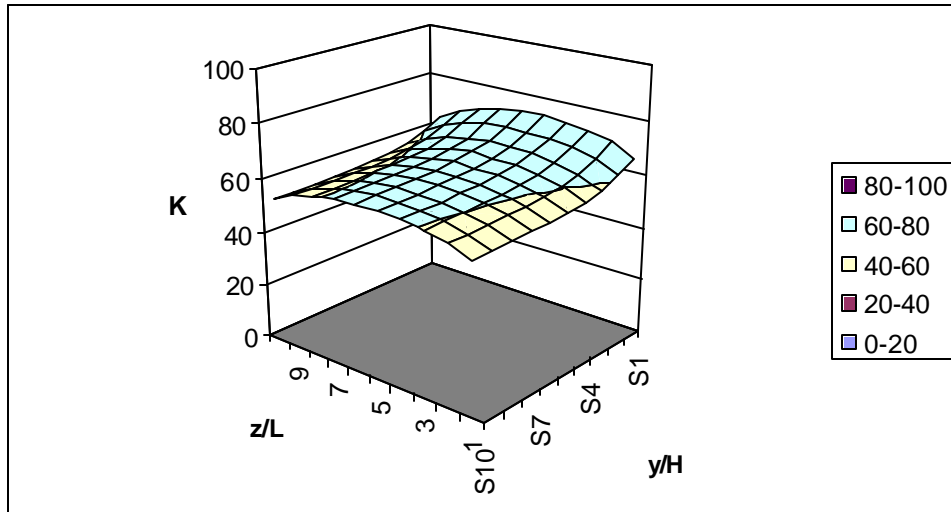
CG	kPL/Q									
MIXED AIR										
z/L	0.013566	0.246107	0.478648	0.711189	0.94373	1.17627	1.408811	1.641352	1.873893	2.106434
0.1042	1.05365	17.1486	30.6329	41.8666	51.3804	59.2632	65.7943	71.4093	76.055	79.9312
0.192156	1.12381	18.7287	33.1616	44.9695	54.7339	62.7707	69.3152	74.8	79.2915	82.9742
0.280111	1.17598	19.7305	34.7629	46.9516	56.9066	64.9711	71.459	76.8939	81.1687	84.7224
0.368067	1.23537	20.3767	35.7435	48.15	58.1801	66.2443	72.6919	78.0672	82.2884	85.7082
0.456022	1.24556	20.6574	36.1815	48.6858	58.7534	66.8252	73.2629	78.5804	82.7438	86.1536
0.543978	1.24326	20.6121	36.109	48.577	58.6615	66.7232	73.1639	78.4668	82.6674	86.0845
0.631933	1.20127	20.2379	35.526	47.8892	57.8919	65.9638	72.421	77.7979	82.0583	85.4949
0.719889	1.16041	19.544	34.4022	46.517	56.4372	64.5213	70.9682	76.4538	80.7604	84.3641
0.807844	1.10444	18.42	32.6683	44.3652	54.0738	62.0928	68.6475	74.1573	78.6868	82.4143
0.8958	0.935592	16.7758	30.0294	41.1139	50.4564	58.3931	64.9154	70.5472	75.2277	79.2293



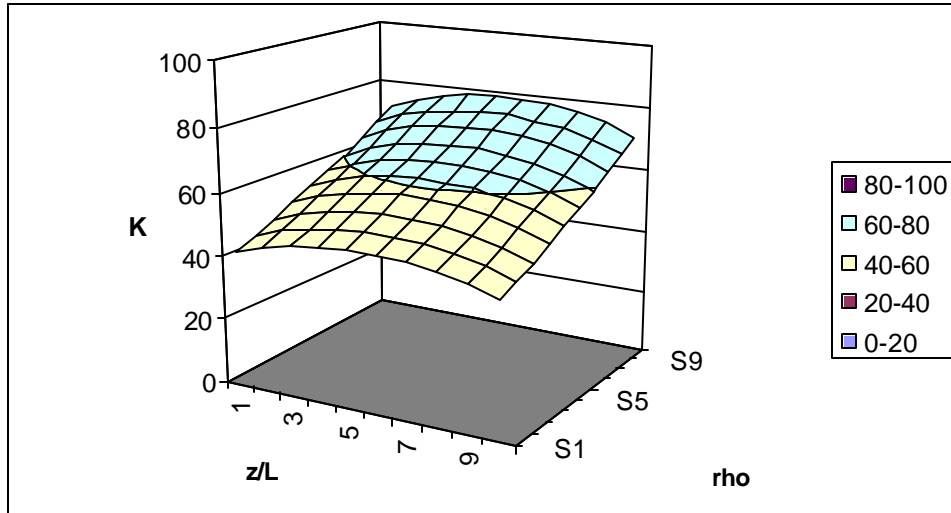
DG	x/W									
z/L	0.063347	0.167048	0.270748	0.374449	0.47815	0.58185	0.685551	0.789252	0.892952	0.996653
0.1042	68.0712	61.3308	58.6958	57.1342	56.0054	55.0655	54.2228	53.4054	52.5452	52.0742
0.192156	72.2395	65.2787	62.378	60.659	59.4703	58.4812	57.6088	56.7668	55.9034	55.4646
0.280111	74.6052	67.6721	64.7615	62.9179	61.677	60.6672	59.7887	58.9428	58.0463	57.6395
0.368067	75.8269	69.0511	66.0141	64.2604	62.9974	61.9351	61.0618	60.2213	59.3192	58.9081
0.456022	76.2939	69.579	66.6449	64.8378	63.5489	62.5262	61.6332	60.7657	59.861	59.4582
0.543978	76.1689	69.4591	66.5084	64.7742	63.4695	62.4204	61.5297	60.688	59.7783	59.3934
0.631933	75.4267	68.6714	65.6889	63.9586	62.6833	61.6948	60.8331	59.9553	59.0809	58.6683
0.719889	73.8402	67.0261	64.1685	62.4471	61.229	60.2034	59.3475	58.5344	57.6549	57.2233
0.807844	71.0111	64.3922	61.6244	59.9566	58.788	57.8612	57.019	56.2177	55.3569	54.916
0.8958	66.2292	59.9924	57.5882	56.1568	55.1096	54.2294	53.4258	52.6555	51.8207	51.3328



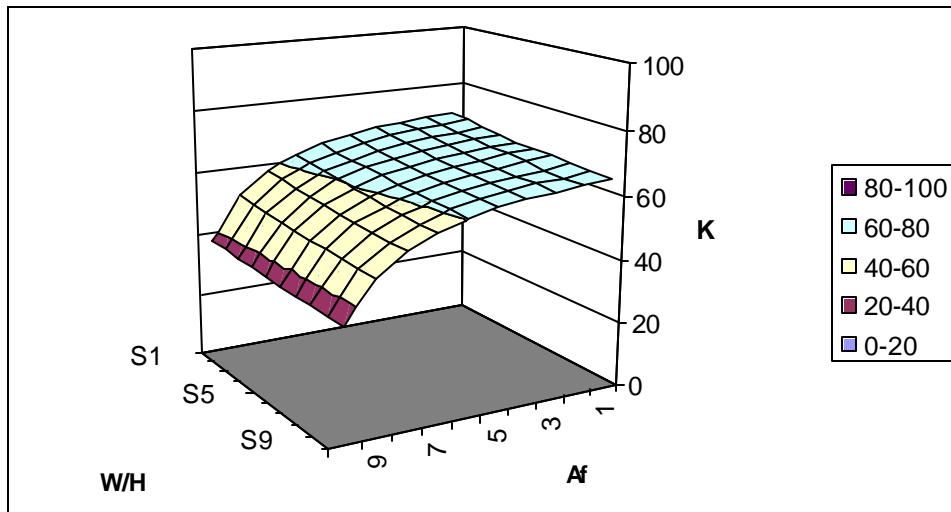
EG	y/H									
MIXED AIR										
z/L	0.007947	0.062625	0.117304	0.171982	0.226661	0.281339	0.336018	0.390696	0.445375	0.500053
0.1042	65.4191	61.5715	58.4787	56.8266	55.8393	55.2401	54.8631	54.5763	54.4598	54.3833
0.192156	69.0841	65.3846	62.1949	60.4447	59.3622	58.6318	58.2042	57.855	57.7546	57.5684
0.280111	71.2339	67.6497	64.4506	62.6377	61.5254	60.882	60.3623	60.0471	59.8023	59.7153
0.368067	72.5343	68.8912	65.715	63.9271	62.8513	62.1257	61.6226	61.2922	61.1296	61.0021
0.456022	73.0758	69.395	66.2974	64.5419	63.4042	62.7109	62.1771	61.8589	61.6619	61.5455
0.543978	73.0441	69.2919	66.1673	64.4405	63.3016	62.5932	62.127	61.7811	61.5755	61.5239
0.631933	72.1046	68.4765	65.4136	63.6166	62.5671	61.8954	61.3765	61.0337	60.8568	60.7774
0.719889	70.5046	66.9098	63.8423	62.0784	61.0963	60.39	59.9196	59.6029	59.4354	59.331
0.807844	67.9271	64.2879	61.2849	59.6744	58.6903	58.0541	57.6008	57.3504	57.1696	57.11
0.8958	63.4753	59.9678	57.2032	55.7669	54.9231	54.4204	54.108	53.8672	53.7741	53.7076



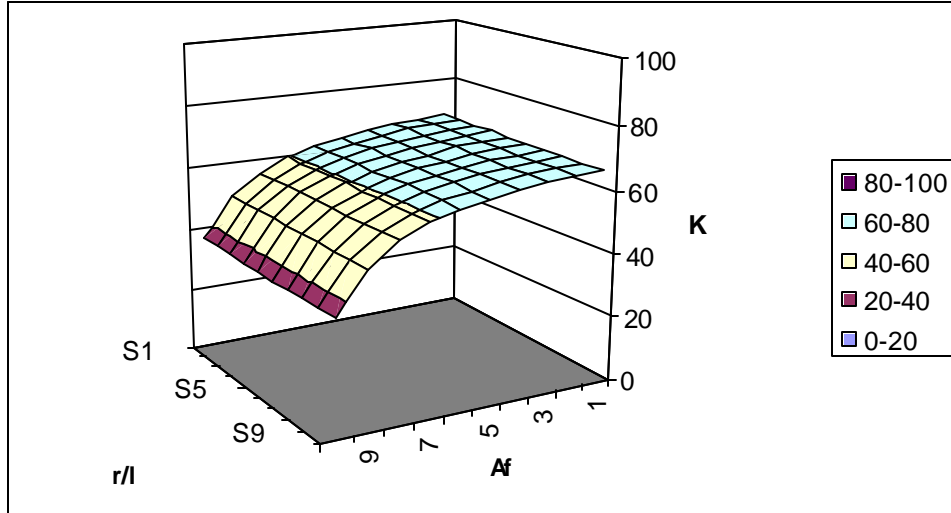
FG	r									
MIXED AIR										
z/L	0.36718	0.430029	0.492878	0.555727	0.618576	0.681424	0.744273	0.807122	0.869971	0.93282
0.1042	42.2776	44.875	47.6002	50.9421	53.9448	57.0717	60.3169	64.2399	67.7034	71.2388
0.192156	45.2601	47.979	50.8174	54.2769	57.364	60.5561	63.8427	67.777	71.2121	74.6775
0.280111	47.1543	49.9569	52.8723	56.41	59.5513	62.7827	66.0906	70.0223	73.4274	76.8333
0.368067	48.2562	51.1058	54.0638	57.6438	60.8134	64.0639	67.3798	71.3043	74.6867	78.0524
0.456022	48.7683	51.6384	54.6146	58.2123	61.3932	64.6508	67.9688	71.8882	75.2588	78.605
0.543978	48.7288	51.5914	54.5605	58.1508	61.3263	64.5797	67.895	71.8134	75.1854	78.5353
0.631933	48.1195	50.945	53.8802	57.4362	60.5884	63.8254	67.1324	71.0537	74.4404	77.8176
0.719889	46.887	49.6443	52.5167	56.0091	59.1172	62.3222	65.6121	69.5355	72.9463	76.3709
0.807844	44.8801	47.5338	50.31	53.7028	56.7399	59.8907	63.147	67.063	70.4997	73.9849
0.8958	41.7705	44.2835	46.9272	50.18	53.1138	56.1814	59.3796	63.2673	66.7212	70.2692



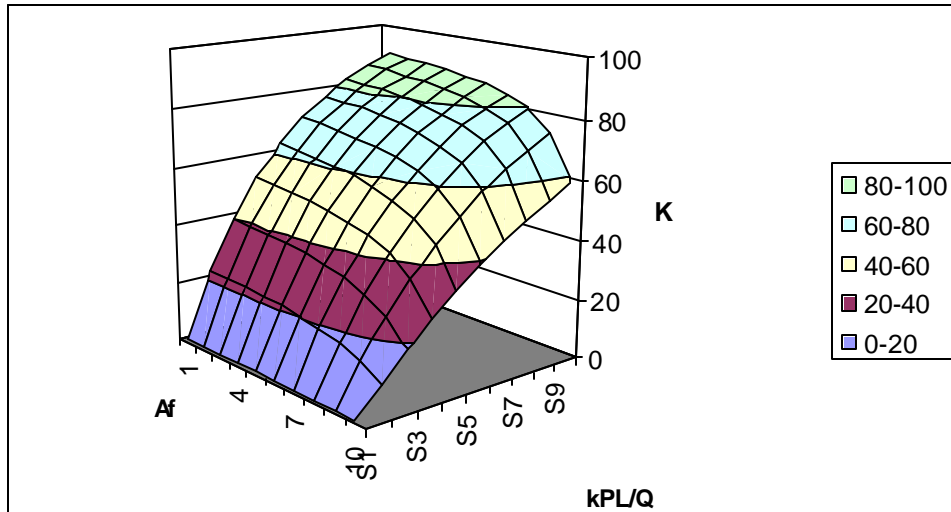
AJ	W/H									
MIXED AIR										
Af	1.004049	1.448704	1.89336	2.338016	2.782672	3.227328	3.671984	4.11664	4.561296	5.005952
0.1042	70.5113	69.6282	68.9443	68.3178	67.7165	67.2422	66.7878	66.3806	65.988	65.6408
0.192156	69.9284	68.9621	68.3223	67.671	67.1782	66.5667	66.1945	65.7586	65.2979	65.0429
0.280111	69.0696	68.2058	67.5453	66.8716	66.3022	65.8415	65.4313	64.9224	64.6556	64.1932
0.368067	68.115	67.2574	66.5399	65.9115	65.4354	64.8273	64.4665	64.0591	63.6362	63.2794
0.456022	66.795	65.9886	65.2414	64.6562	64.1148	63.6078	63.1499	62.6961	62.3589	62.0013
0.543978	65.0677	64.1548	63.4852	62.881	62.3422	61.8351	61.3761	60.9223	60.5314	60.1782
0.631933	62.3362	61.5047	60.8284	60.2437	59.7272	59.16	58.7372	58.2439	57.8871	57.5036
0.719889	58.1728	57.4206	56.7969	56.2364	55.6851	55.1962	54.7727	54.3887	54.0233	53.5997
0.807844	51.1372	50.4116	49.8361	49.3679	48.9327	48.4353	48.1151	47.6946	47.4324	47.0511
0.8958	37.6253	37.0437	36.6117	36.3304	36.0157	35.7482	35.4321	35.2383	35.0519	34.944



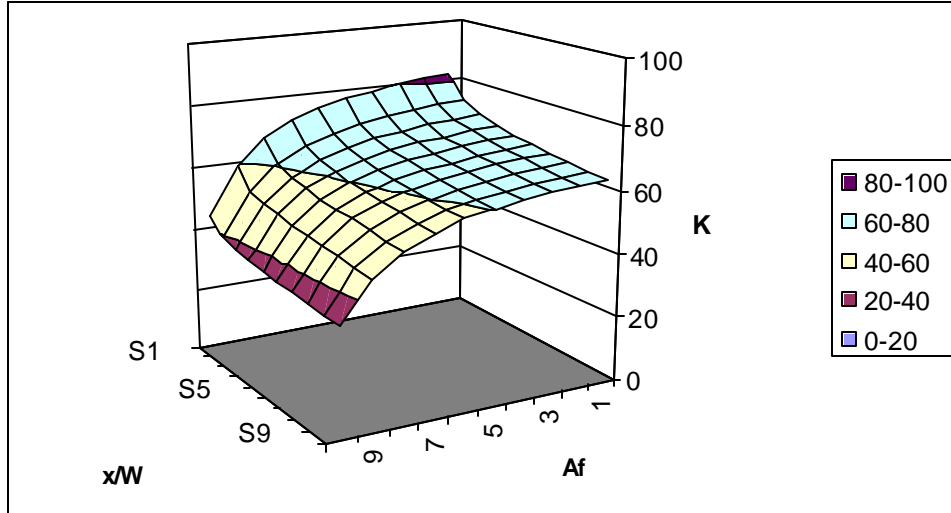
BJ		r/l									
		MIXED AIR									
Af		0.004579	0.008617	0.012655	0.020731	0.024769	0.028807	0.032845	0.036883	0.040921	0.004579
0.1042		68.0981	67.9641	67.8252	67.7072	67.5679	67.4111	67.2683	67.1254	66.9794	66.8382
0.192156		67.4462	67.3243	67.1842	67.0851	66.9583	66.8143	66.7109	66.5723	66.4402	66.3262
0.280111		66.639	66.5497	66.4217	66.3413	66.2489	66.1241	66.0051	65.8851	65.7517	65.655
0.368067		65.5613	65.4806	65.3193	65.2354	65.1524	65.0219	64.9331	64.8066	64.7121	64.6126
0.456022		64.2065	64.1478	64.016	63.941	63.8255	63.73	63.635	63.5654	63.4445	63.3496
0.543978		62.4344	62.3697	62.3121	62.2038	62.1477	62.0597	61.9921	61.8813	61.8193	61.7541
0.631933		59.6815	59.6115	59.5579	59.5013	59.4564	59.3946	59.3242	59.2582	59.1892	59.1259
0.719889		55.7099	55.6248	55.5777	55.5383	55.4638	55.4071	55.3606	55.3331	55.2561	55.2064
0.807844		48.9475	48.8368	48.7556	48.7388	48.7289	48.7104	48.6695	48.6456	48.6125	48.5856
0.8958		36.2454	36.0853	35.9735	35.9181	35.8863	35.8511	35.8434	35.8262	35.8261	35.8313



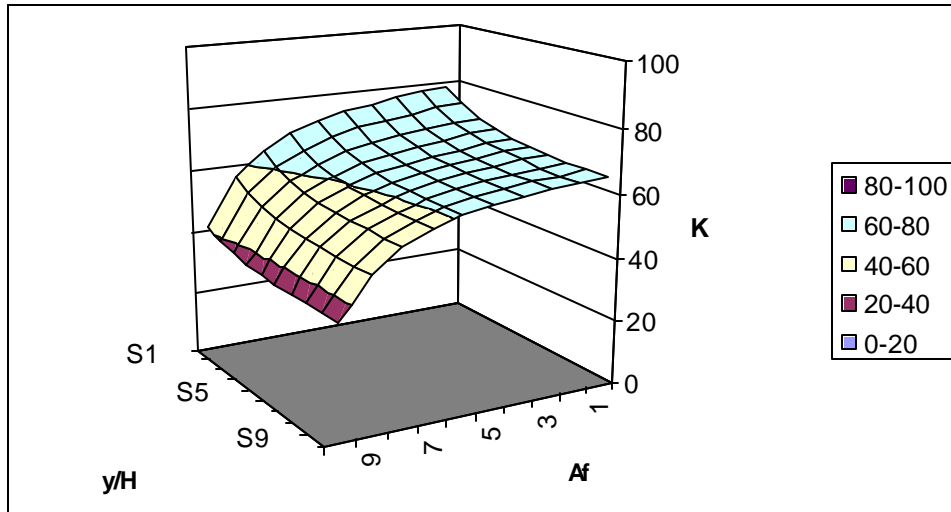
CJ		kPL/Q									
		MIXED AIR									
Af		0.013566	0.246107	0.478648	0.711189	0.94373	1.17627	1.408811	1.641352	1.873893	2.106434
0.1042		1.39145	22.9781	39.7802	52.8729	63.2076	71.2192	77.5066	82.3695	86.2538	89.2902
0.192156		1.37285	22.6708	39.2885	52.3713	62.6061	70.651	76.9394	81.8943	85.7645	88.8639
0.280111		1.34349	22.2507	38.5996	51.6391	61.7663	69.9071	76.2755	81.2929	85.2251	88.2958
0.368067		1.31291	21.7372	37.8932	50.6821	60.8685	68.8791	75.3905	80.4475	84.4739	87.6908
0.456022		1.27346	21.0841	36.8458	49.4215	59.5653	67.7075	74.0854	79.3534	83.4614	86.7418
0.543978		1.20688	20.1828	35.4765	47.8253	57.8256	65.8437	72.321	77.6952	81.964	85.4411
0.631933		1.13478	18.9085	33.5089	45.4222	55.1976	63.2846	69.899	75.2715	79.7209	83.3345
0.719889		1.01203	17.1039	30.5363	41.8896	51.2377	59.1162	65.8593	71.4143	76.0207	79.9569
0.807844		0.835234	14.374	25.9885	36.1104	44.8119	52.3328	58.8197	64.4229	69.3017	73.4548
0.8958		0.548273	9.80664	18.1834	25.7611	32.689	38.9113	44.4714	49.6211	54.4003	58.6588



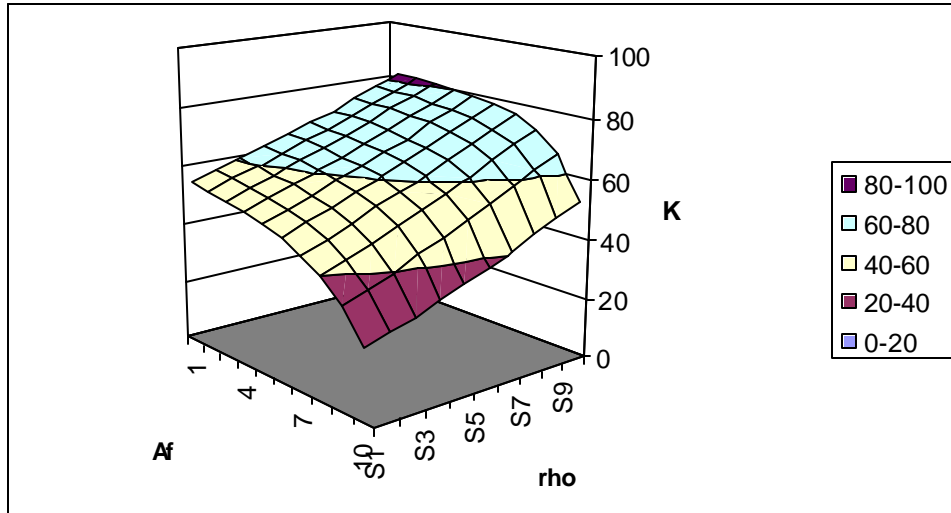
DJ	x/W										MIXED AIR
Af	0.063347	0.167048	0.270748	0.374449	0.47815	0.58185	0.685551	0.789252	0.892952	0.996653	
0.1042	82.2104	74.7387	71.4067	69.4391	68.0136	66.9648	66.0576	65.2115	64.3652	63.9534	
0.192156	81.4257	74.0616	70.7692	68.7945	67.4359	66.3794	65.4743	64.647	63.725	63.3482	
0.280111	80.4325	73.3458	70.0092	68.0031	66.704	65.6372	64.7467	63.8575	62.995	62.5706	
0.368067	79.0325	72.0085	68.8147	66.9748	65.5969	64.5584	63.736	62.8502	61.9444	61.5368	
0.456022	77.3286	70.5287	67.4297	65.6885	64.2995	63.3033	62.3962	61.5767	60.6815	60.2629	
0.543978	75.1426	68.549	65.5944	63.8646	62.5995	61.5452	60.6992	59.8107	58.9207	58.5801	
0.631933	71.7066	65.2996	62.6545	61.0412	59.8691	58.9759	58.0666	57.2038	56.3296	55.9334	
0.719889	66.8736	60.8681	58.4248	57.0204	55.9189	55.021	54.23	53.3599	52.5026	52.079	
0.807844	58.7933	53.2403	51.1095	49.9751	49.0797	48.3718	47.6137	46.8153	46.0052	45.6357	
0.8958	43.9191	39.2278	37.6488	36.7975	36.1726	35.5992	35.079	34.5025	33.8965	33.5862	



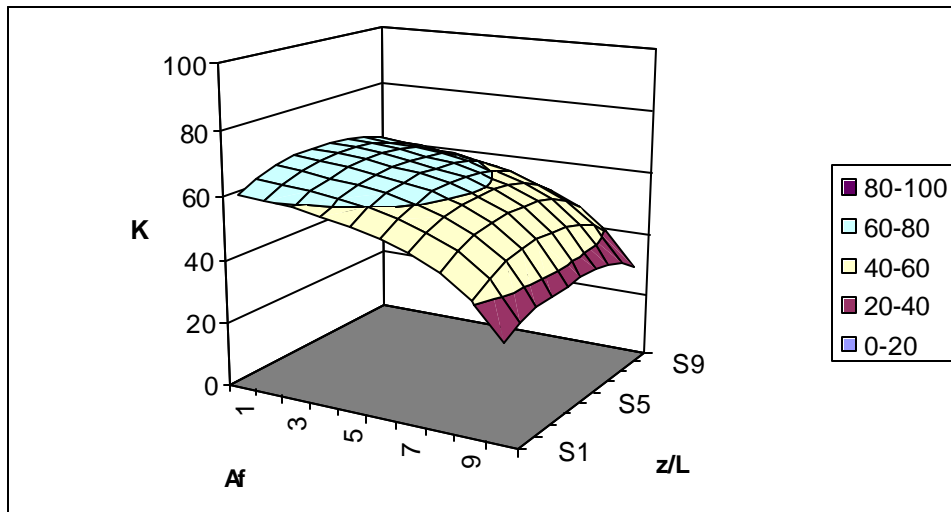
EJ	y/H										MIXED AIR
Af	0.007947	0.062625	0.117304	0.171982	0.226661	0.281339	0.336018	0.390696	0.445375	0.500053	
0.1042	78.646	74.7295	71.1939	69.1789	67.9276	67.0867	66.5871	66.1543	65.8939	65.8208	
0.192156	77.881	74.001	70.5308	68.5999	67.3584	66.5404	65.9674	65.5894	65.3204	65.2585	
0.280111	76.9389	73.0598	69.7145	67.7863	66.5884	65.8041	65.2548	64.8484	64.634	64.5467	
0.368067	75.6884	71.8933	68.5683	66.6599	65.5078	64.7069	64.1825	63.8499	63.589	63.4685	
0.456022	74.0091	70.3099	67.1465	65.3275	64.1804	63.4237	62.9016	62.5508	62.3937	62.2447	
0.543978	71.8385	68.2686	65.2382	63.5304	62.4249	61.7567	61.2822	60.9433	60.7664	60.7238	
0.631933	68.7355	65.2252	62.361	60.767	59.7841	59.0999	58.6671	58.3873	58.1459	58.063	
0.719889	63.8962	60.7221	58.1192	56.6547	55.7799	55.1603	54.7578	54.538	54.4003	54.3158	
0.807844	56.2999	53.2967	50.9555	49.7359	48.9667	48.5109	48.1616	47.9652	47.8566	47.8167	
0.8958	41.0312	39.1814	37.4988	36.5787	36.0763	35.7479	35.4855	35.3367	35.2676	35.2585	



FJ	r									
MIXED AIR										
Af	0.36718	0.430029	0.492878	0.555727	0.618576	0.681424	0.744273	0.807122	0.869971	0.93282
0.1042	55.6506	58.0077	60.4556	63.4346	66.1003	68.875	71.7615	75.2701	78.3909	81.5999
0.192156	54.5831	57.0467	59.6027	62.7066	65.4748	68.3434	71.3108	74.89	78.0445	81.2564
0.280111	53.3307	55.9075	58.5789	61.8164	64.6943	67.6641	70.7197	74.3786	77.5758	80.802
0.368067	51.7536	54.4344	57.2124	60.574	63.5546	66.62	69.7603	73.4992	76.7446	79.9975
0.456022	49.8857	52.6868	55.5898	59.0992	62.2042	65.3879	68.6365	72.4835	75.8019	79.1067
0.543978	47.5756	50.5033	53.5407	57.2128	60.458	63.7787	67.1568	71.1405	74.5597	77.9475
0.631933	44.4181	47.4301	50.5627	54.3566	57.7131	61.149	64.6441	68.7637	72.2973	75.797
0.719889	40.0919	43.1432	46.3342	50.2191	53.6719	57.2197	60.8411	65.125	68.8129	72.479
0.807844	33.7211	36.6516	39.7457	43.5515	46.969	50.5147	54.1708	58.5463	62.3609	66.2018
0.8958	23.2976	25.6631	28.206	31.3988	34.3291	37.436	40.7151	44.7488	48.3728	52.1353



GJ	z/L									
MIXED AIR										
Af	0.1042	0.192156	0.280111	0.368067	0.456022	0.543978	0.631933	0.719889	0.807844	0.8958
0.1042	61.2007	64.0081	65.8145	66.9249	67.4266	67.397	66.7779	65.6158	63.7093	60.7678
0.192156	60.3738	63.2934	65.1962	66.3222	66.8384	66.7873	66.1921	64.9334	62.9395	59.8946
0.280111	59.3627	62.4047	64.3996	65.5894	66.1197	66.0269	65.3938	64.1017	62.0246	58.8239
0.368067	57.9964	61.2119	63.2781	64.49	65.058	64.9537	64.2824	62.9186	60.7395	57.3427
0.456022	56.395	59.7793	61.9228	63.1342	63.7239	63.6698	62.9441	61.5054	59.1933	55.6128
0.543978	54.3771	57.9144	60.1624	61.4738	62.0529	61.9332	61.1668	59.6799	57.1675	53.4228
0.631933	51.3674	55.1648	57.482	58.8016	59.3539	59.2842	58.4891	56.8624	54.2706	50.1926
0.719889	47.311	51.1725	53.516	54.8422	55.4686	55.3064	54.4609	52.8037	50.082	45.8402
0.807844	40.9441	44.7292	46.9874	48.1935	48.6888	48.5623	47.7643	46.1755	43.4936	39.1358
0.8958	30.3987	33.2477	34.8066	35.5943	35.9356	35.8304	35.2526	34.1806	32.149	28.4328



Appendix M: General Linear Model for LnK (Mixed Air Kill rate)

General Linear Model: LnK versus A, B, C, D, E, F, G, J

Factor	Type	Levels	Values
A	fixed	2	1.59 4.42
B	fixed	2	0.0099 0.0356
C	fixed	2	0.32 1.80
D	fixed	2	0.20 0.86
E	fixed	2	0.080 0.428
F	fixed	2	0.45 0.85
G	fixed	2	0.22 0.78
J	fixed	2	0.22 0.78

Analysis of Variance for LnK, using Adjusted SS for Tests

Source	DF	Seq SS	Adj SS	Adj MS	F	P
A	1	0.3034	0.3034	0.3034	4.0E+04	0.000
B	1	0.0169	0.0169	0.0169	2228.23	0.000
C	1	87.6581	87.6581	87.6581	1.2E+07	0.000
D	1	1.1371	1.1371	1.1371	1.5E+05	0.000
E	1	0.4404	0.4404	0.4404	5.8E+04	0.000
F	1	11.6569	11.6569	11.6569	1.5E+06	0.000
G	1	0.0133	0.0133	0.0133	1746.61	0.000
J	1	6.7387	6.7387	6.7387	8.9E+05	0.000
A*B	1	0.0050	0.0050	0.0050	662.47	0.000
A*C	1	0.0413	0.0413	0.0413	5443.12	0.000
A*D	1	0.0013	0.0013	0.0013	171.55	0.000
A*E	1	0.0004	0.0004	0.0004	56.47	0.000
A*F	1	0.0043	0.0043	0.0043	571.07	0.000
A*G	1	0.0000	0.0000	0.0000	2.85	0.095
A*J	1	0.0009	0.0009	0.0009	115.01	0.000
B*C	1	0.0018	0.0018	0.0018	239.18	0.000
B*D	1	0.0074	0.0074	0.0074	974.49	0.000
B*E	1	0.0014	0.0014	0.0014	188.83	0.000
B*F	1	0.0008	0.0008	0.0008	101.32	0.000
B*G	1	0.0000	0.0000	0.0000	0.05	0.827
B*J	1	0.0009	0.0009	0.0009	112.81	0.000
C*D	1	0.1790	0.1790	0.1790	2.4E+04	0.000
C*E	1	0.0802	0.0802	0.0802	1.1E+04	0.000
C*F	1	1.3727	1.3727	1.3727	1.8E+05	0.000
C*G	1	0.0014	0.0014	0.0014	188.33	0.000
C*J	1	0.7461	0.7461	0.7461	9.8E+04	0.000
D*E	1	0.0000	0.0000	0.0000	4.42	0.038
D*F	1	0.0522	0.0522	0.0522	6873.78	0.000
D*G	1	0.0001	0.0001	0.0001	11.32	0.001
D*J	1	0.0011	0.0011	0.0011	149.90	0.000
E*F	1	0.0839	0.0839	0.0839	1.1E+04	0.000
E*G	1	0.0002	0.0002	0.0002	22.35	0.000
E*J	1	0.0022	0.0022	0.0022	289.64	0.000
F*G	1	0.0000	0.0000	0.0000	0.10	0.750
F*J	1	0.3804	0.3804	0.3804	5.0E+04	0.000
G*J	1	0.0035	0.0035	0.0035	454.96	0.000
A*B*C	1	0.0005	0.0005	0.0005	69.53	0.000
A*B*D	1	0.0045	0.0045	0.0045	586.32	0.000
A*B*E	1	0.0008	0.0008	0.0008	101.01	0.000
A*B*F	1	0.0001	0.0001	0.0001	12.06	0.001
A*B*G	1	0.0000	0.0000	0.0000	0.00	0.964
A*B*J	1	0.0003	0.0003	0.0003	42.10	0.000
A*C*D	1	0.0001	0.0001	0.0001	8.99	0.003
A*C*E	1	0.0001	0.0001	0.0001	11.97	0.001
A*C*F	1	0.0070	0.0070	0.0070	919.46	0.000

A*C*G	1	0.0000	0.0000	0.0000	0.00	0.976
A*C*J	1	0.0012	0.0012	0.0012	162.12	0.000
A*D*E	1	0.0039	0.0039	0.0039	512.41	0.000
A*D*F	1	0.0000	0.0000	0.0000	1.09	0.298
A*D*G	1	0.0000	0.0000	0.0000	0.13	0.724
A*D*J	1	0.0001	0.0001	0.0001	11.47	0.001
A*E*F	1	0.0002	0.0002	0.0002	32.92	0.000
A*E*G	1	0.0000	0.0000	0.0000	0.55	0.458
A*E*J	1	0.0000	0.0000	0.0000	0.10	0.749
A*F*G	1	0.0000	0.0000	0.0000	3.97	0.049
A*F*J	1	0.0011	0.0011	0.0011	147.42	0.000
A*G*J	1	0.0000	0.0000	0.0000	0.59	0.445
B*C*D	1	0.0008	0.0008	0.0008	109.55	0.000
B*C*E	1	0.0002	0.0002	0.0002	32.20	0.000
B*C*F	1	0.0000	0.0000	0.0000	1.91	0.170
B*C*G	1	0.0000	0.0000	0.0000	0.01	0.942
B*C*J	1	0.0003	0.0003	0.0003	44.73	0.000
B*D*E	1	0.0004	0.0004	0.0004	55.86	0.000
B*D*F	1	0.0002	0.0002	0.0002	20.24	0.000
B*D*G	1	0.0000	0.0000	0.0000	0.00	0.998
B*D*J	1	0.0010	0.0010	0.0010	131.98	0.000
B*E*F	1	0.0000	0.0000	0.0000	0.35	0.553
B*E*G	1	0.0000	0.0000	0.0000	0.00	0.961
B*E*J	1	0.0000	0.0000	0.0000	0.30	0.584
B*F*G	1	0.0000	0.0000	0.0000	0.00	0.997
B*F*J	1	0.0000	0.0000	0.0000	3.73	0.057
B*G*J	1	0.0000	0.0000	0.0000	0.02	0.878
C*D*E	1	0.0013	0.0013	0.0013	173.65	0.000
C*D*F	1	0.0431	0.0431	0.0431	5670.85	0.000
C*D*G	1	0.0000	0.0000	0.0000	5.94	0.017
C*D*J	1	0.0114	0.0114	0.0114	1496.12	0.000
C*E*F	1	0.0352	0.0352	0.0352	4636.32	0.000
C*E*G	1	0.0000	0.0000	0.0000	6.36	0.013
C*E*J	1	0.0071	0.0071	0.0071	935.77	0.000
C*F*G	1	0.0001	0.0001	0.0001	18.54	0.000
C*F*J	1	0.0071	0.0071	0.0071	939.13	0.000
C*G*J	1	0.0001	0.0001	0.0001	18.34	0.000
D*E*F	1	0.0002	0.0002	0.0002	21.40	0.000
D*E*G	1	0.0000	0.0000	0.0000	2.03	0.158
D*E*J	1	0.0000	0.0000	0.0000	0.68	0.412
D*F*G	1	0.0000	0.0000	0.0000	5.62	0.020
D*F*J	1	0.0000	0.0000	0.0000	1.52	0.221
D*G*J	1	0.0000	0.0000	0.0000	0.12	0.734
E*F*G	1	0.0000	0.0000	0.0000	5.36	0.023
E*F*J	1	0.0019	0.0019	0.0019	249.50	0.000
E*G*J	1	0.0000	0.0000	0.0000	2.57	0.112
F*G*J	1	0.0000	0.0000	0.0000	1.35	0.249
A*B*C*D	1	0.0004	0.0004	0.0004	56.83	0.000
A*B*C*E	1	0.0001	0.0001	0.0001	13.27	0.000
A*B*C*F	1	0.0000	0.0000	0.0000	1.54	0.217
A*B*C*G	1	0.0000	0.0000	0.0000	0.00	0.945
A*B*C*J	1	0.0001	0.0001	0.0001	15.27	0.000
A*B*D*E	1	0.0021	0.0021	0.0021	279.73	0.000
A*B*D*F	1	0.0001	0.0001	0.0001	6.67	0.011
A*B*D*G	1	0.0000	0.0000	0.0000	0.00	0.966
A*B*D*J	1	0.0000	0.0000	0.0000	3.93	0.051
A*B*E*F	1	0.0000	0.0000	0.0000	3.87	0.052
A*B*E*G	1	0.0000	0.0000	0.0000	0.01	0.915
A*B*E*J	1	0.0000	0.0000	0.0000	5.85	0.018
A*B*F*G	1	0.0000	0.0000	0.0000	0.00	0.974
A*B*F*J	1	0.0000	0.0000	0.0000	1.25	0.267
A*B*G*J	1	0.0000	0.0000	0.0000	0.00	0.954
A*C*D*E	1	0.0005	0.0005	0.0005	60.72	0.000

A*C*D*F	1	0.0001	0.0001	0.0001	10.59	0.002
A*C*D*G	1	0.0000	0.0000	0.0000	0.00	0.947
A*C*D*J	1	0.0000	0.0000	0.0000	0.25	0.621
A*C*E*F	1	0.0002	0.0002	0.0002	27.38	0.000
A*C*E*G	1	0.0000	0.0000	0.0000	0.11	0.741
A*C*E*J	1	0.0000	0.0000	0.0000	0.08	0.776
A*C*F*G	1	0.0000	0.0000	0.0000	0.23	0.634
A*C*F*J	1	0.0000	0.0000	0.0000	0.00	0.987
A*C*G*J	1	0.0000	0.0000	0.0000	0.00	0.960
A*D*E*F	1	0.0001	0.0001	0.0001	15.53	0.000
A*D*E*G	1	0.0000	0.0000	0.0000	0.21	0.646
A*D*E*J	1	0.0000	0.0000	0.0000	1.41	0.238
A*D*F*G	1	0.0000	0.0000	0.0000	0.16	0.690
A*D*F*J	1	0.0001	0.0001	0.0001	17.19	0.000
A*D*G*J	1	0.0000	0.0000	0.0000	0.15	0.700
A*E*F*G	1	0.0000	0.0000	0.0000	0.31	0.581
A*E*F*J	1	0.0000	0.0000	0.0000	0.32	0.573
A*E*G*J	1	0.0000	0.0000	0.0000	0.01	0.919
A*F*G*J	1	0.0000	0.0000	0.0000	0.76	0.384
B*C*D*E	1	0.0000	0.0000	0.0000	6.36	0.013
B*C*D*F	1	0.0000	0.0000	0.0000	1.38	0.244
B*C*D*G	1	0.0000	0.0000	0.0000	0.01	0.934
B*C*D*J	1	0.0002	0.0002	0.0002	32.79	0.000
B*C*E*F	1	0.0000	0.0000	0.0000	2.55	0.114
B*C*E*G	1	0.0000	0.0000	0.0000	0.00	0.958
B*C*E*J	1	0.0000	0.0000	0.0000	0.89	0.349
B*C*F*G	1	0.0000	0.0000	0.0000	0.00	0.995
B*C*F*J	1	0.0000	0.0000	0.0000	0.03	0.874
B*C*G*J	1	0.0000	0.0000	0.0000	0.00	0.980
B*D*E*F	1	0.0000	0.0000	0.0000	1.85	0.177
B*D*E*G	1	0.0000	0.0000	0.0000	0.00	0.944
B*D*E*J	1	0.0000	0.0000	0.0000	0.86	0.356
B*D*F*G	1	0.0000	0.0000	0.0000	0.00	0.979
B*D*F*J	1	0.0000	0.0000	0.0000	4.40	0.039
B*D*G*J	1	0.0000	0.0000	0.0000	0.00	0.968
B*E*F*G	1	0.0000	0.0000	0.0000	0.00	0.982
B*E*F*J	1	0.0000	0.0000	0.0000	0.10	0.755
B*E*G*J	1	0.0000	0.0000	0.0000	0.00	0.996
B*F*G*J	1	0.0000	0.0000	0.0000	0.00	0.980
C*D*E*F	1	0.0005	0.0005	0.0005	70.70	0.000
C*D*E*G	1	0.0000	0.0000	0.0000	0.06	0.812
C*D*E*J	1	0.0002	0.0002	0.0002	21.83	0.000
C*D*F*G	1	0.0000	0.0000	0.0000	0.14	0.714
C*D*F*J	1	0.0017	0.0017	0.0017	220.51	0.000
C*D*G*J	1	0.0000	0.0000	0.0000	0.03	0.853
C*E*F*G	1	0.0000	0.0000	0.0000	0.14	0.713
C*E*F*J	1	0.0032	0.0032	0.0032	426.75	0.000
C*E*G*J	1	0.0000	0.0000	0.0000	0.60	0.441
C*F*G*J	1	0.0000	0.0000	0.0000	4.90	0.029
D*E*F*G	1	0.0000	0.0000	0.0000	0.75	0.388
D*E*F*J	1	0.0001	0.0001	0.0001	6.92	0.010
D*E*G*J	1	0.0000	0.0000	0.0000	0.20	0.655
D*F*G*J	1	0.0000	0.0000	0.0000	0.64	0.426
E*F*G*J	1	0.0000	0.0000	0.0000	0.15	0.695
Error	93	0.0007	0.0007	0.0000		
Total	255	111.0749				

Unusual Observations for LnK

Obs	LnK	Fit	SE Fit	Residual	St Resid
44	4.06672	4.06326	0.00220	0.00347	2.09R
48	2.66862	2.67264	0.00220	-0.00402	-2.42R
108	4.08493	4.08123	0.00220	0.00370	2.23R

112	2.69576	2.69980	0.00220	-0.00404	-2.43R
129	4.42616	4.43033	0.00220	-0.00418	-2.52R
133	3.31378	3.30958	0.00220	0.00420	2.53R
145	4.48317	4.47780	0.00220	0.00537	3.24R
149	3.46243	3.46762	0.00220	-0.00520	-3.13R
193	4.42877	4.43305	0.00220	-0.00427	-2.57R
197	3.32006	3.31580	0.00220	0.00425	2.56R
209	4.48790	4.48250	0.00220	0.00540	3.25R
213	3.47641	3.48161	0.00220	-0.00520	-3.13R

R denotes an observation with a large standardized residual.

Appendix N: Minitab Output for Regression Analysis -- LnK

Regression Analysis: LnK versus A, B, ...

The regression equation is

$$\begin{aligned} \text{LnK} = & -1.71 - 0.0495 \text{ A} - 0.631 \text{ B} - 8.27 \text{ C} - 0.350 \text{ D} - 0.312 \text{ E} + 1.81 \text{ F} \\ & + 0.692 \text{ G} + 12.8 \text{ J} + 0.00207 \text{ AA} + 1.64 \text{ CC} + 0.336 \text{ DD} + 1.14 \text{ EE} \\ & - 0.037 \text{ FF} - 0.717 \text{ GG} + 0.0121 \text{ AC} - 0.0643 \text{ CD} - 0.159 \text{ CE} - 0.751 \text{ CF} \\ & + 0.261 \text{ CJ} - 0.498 \text{ DF} - 1.00 \text{ EF} + 0.695 \text{ FJ} + 0.266 \text{ CDF} + 0.455 \text{ CEF} \\ & - 0.165 \text{ CCC} + 12.3 \text{ sqrtC} - 13.7 \text{ atJ} - 3.86 \text{ JJJ} \end{aligned}$$

Predictor	Coef	SE Coef	T	P
Constant	-1.7065	0.2429	-7.03	0.000
A	-0.04954	0.02829	-1.75	0.081
B	-0.63087	0.09948	-6.34	0.000
C	-8.2651	0.7985	-10.35	0.000
D	-0.35026	0.09446	-3.71	0.000
E	-0.3116	0.1638	-1.90	0.058
F	1.8090	0.3073	5.89	0.000
G	0.6916	0.2414	2.87	0.005
J	12.810	3.572	3.59	0.000
AA	0.002068	0.004699	0.44	0.660
CC	1.6350	0.4528	3.61	0.000
DD	0.33575	0.08639	3.89	0.000
EE	1.1366	0.3107	3.66	0.000
FF	-0.0374	0.2353	-0.16	0.874
GG	-0.7171	0.2410	-2.98	0.003
AC	0.012135	0.001230	9.86	0.000
CD	-0.06431	0.01794	-3.59	0.000
CE	-0.15854	0.03402	-4.66	0.000
CF	-0.75118	0.02080	-36.11	0.000
CJ	0.260544	0.006218	41.90	0.000
DF	-0.49783	0.03410	-14.60	0.000
EF	-1.00292	0.06467	-15.51	0.000
FJ	0.69531	0.02283	30.46	0.000
CDF	0.26555	0.02638	10.07	0.000
CEF	0.45538	0.05003	9.10	0.000
CCC	-0.1651	0.1103	-1.50	0.136
sqrtC	12.3326	0.5174	23.84	0.000
atJ	-13.716	3.786	-3.62	0.000
JJJ	-3.8589	0.6870	-5.62	0.000

S = 0.02061 R-Sq = 99.9% R-Sq(adj) = 99.9%

Analysis of Variance

Source	DF	SS	MS	F	P
Regression	28	126.6803	4.5243	10648.29	0.000
Residual Error	244	0.1037	0.0004		
Total	272	126.7839			

Source	DF	Seq SS
A	1	0.3060
B	1	0.0170
C	1	93.3600
D	1	1.1687
E	1	0.4551
F	1	11.7297
G	1	0.0611
J	1	7.4000
AA	1	0.0170
CC	1	4.1408

DD	1	0.7529
EE	1	0.4473
FF	1	0.2066
GG	1	0.0300
AC	1	0.0413
CD	1	0.1790
CE	1	0.0802
CF	1	1.3727
CJ	1	0.4017
DF	1	0.0522
EF	1	0.0839
FJ	1	0.3941
CDF	1	0.0431
CEF	1	0.0352
CCC	1	3.6390
sqrtC	1	0.2227
atJ	1	0.0296
JJJ	1	0.0134

Unusual Observations

Obs	A	LnK	Fit	SE Fit	Residual	St Resid
21	4.42	3.09876	3.16094	0.00560	-0.06219	-3.13R
31	4.42	3.36823	3.41864	0.00560	-0.05040	-2.54R
70	1.59	3.13091	3.09051	0.00560	0.04041	2.04R
85	4.42	3.13201	3.17521	0.00560	-0.04321	-2.18R
119	4.42	2.58256	2.53593	0.00560	0.04662	2.35R
149	4.42	3.46243	3.51553	0.00560	-0.05310	-2.68R
158	1.59	3.89406	3.85103	0.00560	0.04303	2.17R
181	4.42	2.96209	3.01578	0.00560	-0.05369	-2.71R
213	4.42	3.47641	3.52979	0.00560	-0.05339	-2.69R
220	1.59	4.58471	4.63432	0.00560	-0.04961	-2.50R
222	1.59	3.90615	3.86530	0.00560	0.04086	2.06R
245	4.42	2.97357	3.03005	0.00560	-0.05648	-2.85R
257	1.00	4.20093	4.21159	0.01469	-0.01066	-0.74 X
258	5.01	4.12522	4.11456	0.01469	0.01066	0.74 X
259	3.01	4.16405	4.16628	0.01204	-0.00223	-0.13 X
260	3.01	4.14535	4.14338	0.01204	0.00198	0.12 X
261	3.01	0.22050	0.22050	0.02061	-0.00000	* X
262	3.01	4.46232	4.46232	0.02061	0.00000	* X
263	3.01	4.35878	4.32274	0.01469	0.03604	2.49RX
264	3.01	4.09707	4.13311	0.01469	-0.03604	-2.49RX
265	3.01	4.31524	4.28280	0.01469	0.03244	2.24RX
266	3.01	4.13202	4.16446	0.01469	-0.03244	-2.24RX
267	3.01	3.94080	3.90568	0.01479	0.03512	2.45RX
268	3.01	4.36281	4.39793	0.01479	-0.03512	-2.45RX
269	3.01	4.09588	4.10163	0.01469	-0.00575	-0.40 X
270	3.01	4.08721	4.08146	0.01469	0.00575	0.40 X
271	3.01	4.16995	4.16995	0.02061	0.00000	* X
272	3.01	3.52177	3.52177	0.02061	-0.00000	* X
273	3.01	4.15504	4.15479	0.01190	0.00025	0.01 X

R denotes an observation with a large standardized residual

X denotes an observation whose X value gives it large influence.

APPENDIX O: Input Data for Cost Optimization

#	W cm	H cm	r cm	l = x cm	k cm ² /mW-s	P W	Airflow m ³ /min	x cm	y cm	z cm	L cm	ρ	Actual Kill Rate	Work Frac.
1	160	160	1.37	100	0.00275	16.00	390	84.8	40.64	50.00	100.00	73.6	54.29	1
2	160	160	1.37	100	0.00275	21.33	390	84.8	40.64	50.00	100.00	73.6	64.79	1
3	160	160	1.37	100	0.00275	26.67	390	84.8	40.64	50.00	100.00	73.6	72.88	1
4	160	160	1.37	100	0.00275	32.00	390	84.8	40.64	50.00	100.00	73.6	79.11	1
5	160	160	1.37	100	0.00275	37.33	390	84.8	40.64	50.00	100.00	73.6	83.91	1
6	160	160	1.37	100	0.00275	42.67	390	84.8	40.64	50.00	100.00	73.6	87.61	1
7	160	160	1.37	100	0.00275	48.00	390	84.8	40.64	50.00	100.00	73.6	90.45	1
8	160	160	1.37	100	0.00275	53.33	390	84.8	40.64	50.00	100.00	73.6	92.64	1
9	160	160	1.37	100	0.00275	58.67	390	84.8	40.64	50.00	100.00	73.6	94.34	1
10	160	160	1.37	100	0.00275	64.00	390	84.8	40.64	50.00	100.00	73.6	95.64	1
11	160	160	1.37	100	0.00275	16.00	390	84.8	40.64	83.33	166.67	73.6	69.02	1
12	160	160	1.37	100	0.00275	21.33	390	84.8	40.64	83.33	166.67	73.6	79.03	1
13	160	160	1.37	100	0.00275	26.67	390	84.8	40.64	83.33	166.67	73.6	85.82	1
14	160	160	1.37	100	0.00275	32.00	390	84.8	40.64	83.33	166.67	73.6	90.40	1
15	160	160	1.37	100	0.00275	37.33	390	84.8	40.64	83.33	166.67	73.6	93.50	1
16	160	160	1.37	100	0.00275	42.67	390	84.8	40.64	83.33	166.67	73.6	95.61	1
17	160	160	1.37	100	0.00275	48.00	390	84.8	40.64	83.33	166.67	73.6	97.03	1
18	160	160	1.37	100	0.00275	53.33	390	84.8	40.64	83.33	166.67	73.6	97.99	1
19	160	160	1.37	100	0.00275	58.67	390	84.8	40.64	83.33	166.67	73.6	98.64	1
20	160	160	1.37	100	0.00275	64.00	390	84.8	40.64	83.33	166.67	73.6	99.08	1
21	160	160	1.37	100	0.00275	16.00	390	84.8	40.64	116.67	233.33	73.6	77.11	1
22	160	160	1.37	100	0.00275	21.33	390	84.8	40.64	116.67	233.33	73.6	86.00	1
23	160	160	1.37	100	0.00275	26.67	390	84.8	40.64	116.67	233.33	73.6	91.44	1
24	160	160	1.37	100	0.00275	32.00	390	84.8	40.64	116.67	233.33	73.6	94.76	1
25	160	160	1.37	100	0.00275	37.33	390	84.8	40.64	116.67	233.33	73.6	96.79	1
26	160	160	1.37	100	0.00275	42.67	390	84.8	40.64	116.67	233.33	73.6	98.04	1
27	160	160	1.37	100	0.00275	48.00	390	84.8	40.64	116.67	233.33	73.6	98.80	1
28	160	160	1.37	100	0.00275	53.33	390	84.8	40.64	116.67	233.33	73.6	99.27	1
29	160	160	1.37	100	0.00275	58.67	390	84.8	40.64	116.67	233.33	73.6	99.55	1
30	160	160	1.37	100	0.00275	64.00	390	84.8	40.64	116.67	233.33	73.6	99.73	1
31	160	160	1.37	100	0.00275	16.00	390	84.8	40.64	150.00	300.00	73.6	81.94	1
32	160	160	1.37	100	0.00275	21.33	390	84.8	40.64	150.00	300.00	73.6	89.78	1
33	160	160	1.37	100	0.00275	26.67	390	84.8	40.64	150.00	300.00	73.6	94.23	1
34	160	160	1.37	100	0.00275	32.00	390	84.8	40.64	150.00	300.00	73.6	96.74	1
35	160	160	1.37	100	0.00275	37.33	390	84.8	40.64	150.00	300.00	73.6	98.15	1
36	160	160	1.37	100	0.00275	42.67	390	84.8	40.64	150.00	300.00	73.6	98.96	1
37	160	160	1.37	100	0.00275	48.00	390	84.8	40.64	150.00	300.00	73.6	99.41	1
38	160	160	1.37	100	0.00275	53.33	390	84.8	40.64	150.00	300.00	73.6	99.67	1
39	160	160	1.37	100	0.00275	58.67	390	84.8	40.64	150.00	300.00	73.6	99.81	1
40	160	160	1.37	100	0.00275	64.00	390	84.8	40.64	150.00	300.00	73.6	99.89	1
41	160	160	1.37	100	0.00275	16.00	390	84.8	40.64	183.33	366.67	73.6	85.00	1
42	160	160	1.37	100	0.00275	21.33	390	84.8	40.64	183.33	366.67	73.6	92.03	1
43	160	160	1.37	100	0.00275	26.67	390	84.8	40.64	183.33	366.67	73.6	95.77	1
44	160	160	1.37	100	0.00275	32.00	390	84.8	40.64	183.33	366.67	73.6	97.75	1
45	160	160	1.37	100	0.00275	37.33	390	84.8	40.64	183.33	366.67	73.6	98.80	1
46	160	160	1.37	100	0.00275	42.67	390	84.8	40.64	183.33	366.67	73.6	99.37	1
47	160	160	1.37	100	0.00275	48.00	390	84.8	40.64	183.33	366.67	73.6	99.66	1

#	W cm	H cm	r cm	l = x cm	k cm ² /mW-s	P W	Airflow m ³ /min	x cm	y cm	z cm	L cm	p	Actual Kill Rate	Work Frac.
48	160	160	1.37	100	0.00275	53.33	390	84.8	40.64	183.33	366.67	73.6	99.82	1
49	160	160	1.37	100	0.00275	58.67	390	84.8	40.64	183.33	366.67	73.6	99.90	1
50	160	160	1.37	100	0.00275	64.00	390	84.8	40.64	183.33	366.67	73.6	99.95	1
51	160	160	1.37	100	0.00275	16.00	390	84.8	40.64	216.67	433.33	73.6	87.07	1
52	160	160	1.37	100	0.00275	21.33	390	84.8	40.64	216.67	433.33	73.6	93.46	1
53	160	160	1.37	100	0.00275	26.67	390	84.8	40.64	216.67	433.33	73.6	96.69	1
54	160	160	1.37	100	0.00275	32.00	390	84.8	40.64	216.67	433.33	73.6	98.33	1
55	160	160	1.37	100	0.00275	37.33	390	84.8	40.64	216.67	433.33	73.6	99.15	1
56	160	160	1.37	100	0.00275	42.67	390	84.8	40.64	216.67	433.33	73.6	99.57	1
57	160	160	1.37	100	0.00275	48.00	390	84.8	40.64	216.67	433.33	73.6	99.78	1
58	160	160	1.37	100	0.00275	53.33	390	84.8	40.64	216.67	433.33	73.6	99.89	1
59	160	160	1.37	100	0.00275	58.67	390	84.8	40.64	216.67	433.33	73.6	99.94	1
60	160	160	1.37	100	0.00275	64.00	390	84.8	40.64	216.67	433.33	73.6	99.97	1
61	160	160	1.37	100	0.00275	16.00	390	84.8	40.64	250.00	500.00	73.6	88.52	1
62	160	160	1.37	100	0.00275	21.33	390	84.8	40.64	250.00	500.00	73.6	94.42	1
63	160	160	1.37	100	0.00275	26.67	390	84.8	40.64	250.00	500.00	73.6	97.29	1
64	160	160	1.37	100	0.00275	32.00	390	84.8	40.64	250.00	500.00	73.6	98.68	1
65	160	160	1.37	100	0.00275	37.33	390	84.8	40.64	250.00	500.00	73.6	99.36	1
66	160	160	1.37	100	0.00275	42.67	390	84.8	40.64	250.00	500.00	73.6	99.69	1
67	160	160	1.37	100	0.00275	48.00	390	84.8	40.64	250.00	500.00	73.6	99.85	1
68	160	160	1.37	100	0.00275	53.33	390	84.8	40.64	250.00	500.00	73.6	99.93	1
69	160	160	1.37	100	0.00275	58.67	390	84.8	40.64	250.00	500.00	73.6	99.96	1
70	160	160	1.37	100	0.00275	64.00	390	84.8	40.64	250.00	500.00	73.6	99.98	1
71	160	160	1.37	100	0.00275	16.00	390	84.8	40.64	283.33	566.67	73.6	89.58	1
72	160	160	1.37	100	0.00275	21.33	390	84.8	40.64	283.33	566.67	73.6	95.10	1
73	160	160	1.37	100	0.00275	26.67	390	84.8	40.64	283.33	566.67	73.6	97.69	1
74	160	160	1.37	100	0.00275	32.00	390	84.8	40.64	283.33	566.67	73.6	98.91	1
75	160	160	1.37	100	0.00275	37.33	390	84.8	40.64	283.33	566.67	73.6	99.49	1
76	160	160	1.37	100	0.00275	42.67	390	84.8	40.64	283.33	566.67	73.6	99.76	1
77	160	160	1.37	100	0.00275	48.00	390	84.8	40.64	283.33	566.67	73.6	99.89	1
78	160	160	1.37	100	0.00275	53.33	390	84.8	40.64	283.33	566.67	73.6	99.95	1
79	160	160	1.37	100	0.00275	58.67	390	84.8	40.64	283.33	566.67	73.6	99.98	1
80	160	160	1.37	100	0.00275	64.00	390	84.8	40.64	283.33	566.67	73.6	99.99	1
81	160	160	1.37	100	0.00275	16.00	390	84.8	40.64	316.67	633.33	73.6	90.39	1
82	160	160	1.37	100	0.00275	21.33	390	84.8	40.64	316.67	633.33	73.6	95.59	1
83	160	160	1.37	100	0.00275	26.67	390	84.8	40.64	316.67	633.33	73.6	97.98	1
84	160	160	1.37	100	0.00275	32.00	390	84.8	40.64	316.67	633.33	73.6	99.08	1
85	160	160	1.37	100	0.00275	37.33	390	84.8	40.64	316.67	633.33	73.6	99.58	1
86	160	160	1.37	100	0.00275	42.67	390	84.8	40.64	316.67	633.33	73.6	99.81	1
87	160	160	1.37	100	0.00275	48.00	390	84.8	40.64	316.67	633.33	73.6	99.91	1
88	160	160	1.37	100	0.00275	53.33	390	84.8	40.64	316.67	633.33	73.6	99.96	1
89	160	160	1.37	100	0.00275	58.67	390	84.8	40.64	316.67	633.33	73.6	99.98	1
90	160	160	1.37	100	0.00275	64.00	390	84.8	40.64	316.67	633.33	73.6	99.99	1
91	160	160	1.37	100	0.00275	16.00	390	84.8	40.64	350.00	700.00	73.6	91.01	1
92	160	160	1.37	100	0.00275	21.33	390	84.8	40.64	350.00	700.00	73.6	95.97	1
93	160	160	1.37	100	0.00275	26.67	390	84.8	40.64	350.00	700.00	73.6	98.20	1
94	160	160	1.37	100	0.00275	32.00	390	84.8	40.64	350.00	700.00	73.6	99.19	1
95	160	160	1.37	100	0.00275	37.33	390	84.8	40.64	350.00	700.00	73.6	99.64	1

#	W cm	H cm	r cm	l = x cm	k cm ² /mW-s	P W	Airflow m ³ /min	x cm	y cm	z cm	L cm	p	Actual Kill Rate	Work Frac.
96	160	160	1.37	100	0.00275	42.67	390	84.8	40.64	350.00	700.00	73.6	99.84	1
97	160	160	1.37	100	0.00275	48.00	390	84.8	40.64	350.00	700.00	73.6	99.93	1
98	160	160	1.37	100	0.00275	53.33	390	84.8	40.64	350.00	700.00	73.6	99.97	1
99	160	160	1.37	100	0.00275	58.67	390	84.8	40.64	350.00	700.00	73.6	99.99	1
100	160	160	1.37	100	0.00275	64.00	390	84.8	40.64	350.00	700.00	73.6	99.99	1
101	160	160	1.37	100	0.00275	16.00	390	84.8	40.64	120.00	240.00	54.0	67.56	1
102	160	160	1.37	100	0.00275	21.33	390	84.8	40.64	120.00	240.00	54.0	77.70	1
103	160	160	1.37	100	0.00275	26.67	390	84.8	40.64	120.00	240.00	54.0	84.69	1
104	160	160	1.37	100	0.00275	32.00	390	84.8	40.64	120.00	240.00	54.0	89.47	1
105	160	160	1.37	100	0.00275	37.33	390	84.8	40.64	120.00	240.00	54.0	92.77	1
106	160	160	1.37	100	0.00275	42.67	390	84.8	40.64	120.00	240.00	54.0	95.03	1
107	160	160	1.37	100	0.00275	48.00	390	84.8	40.64	120.00	240.00	54.0	96.59	1
108	160	160	1.37	100	0.00275	53.33	390	84.8	40.64	120.00	240.00	54.0	97.65	1
109	160	160	1.37	100	0.00275	58.67	390	84.8	40.64	120.00	240.00	54.0	98.39	1
110	160	160	1.37	100	0.00275	64.00	390	84.8	40.64	120.00	240.00	54.0	98.89	1
111	160	160	1.37	100	0.00275	16.00	390	84.8	40.64	120.00	240.00	58.4	69.84	1
112	160	160	1.37	100	0.00275	21.33	390	84.8	40.64	120.00	240.00	58.4	79.77	1
113	160	160	1.37	100	0.00275	26.67	390	84.8	40.64	120.00	240.00	58.4	86.44	1
114	160	160	1.37	100	0.00275	32.00	390	84.8	40.64	120.00	240.00	58.4	90.91	1
115	160	160	1.37	100	0.00275	37.33	390	84.8	40.64	120.00	240.00	58.4	93.90	1
116	160	160	1.37	100	0.00275	42.67	390	84.8	40.64	120.00	240.00	58.4	95.91	1
117	160	160	1.37	100	0.00275	48.00	390	84.8	40.64	120.00	240.00	58.4	97.26	1
118	160	160	1.37	100	0.00275	53.33	390	84.8	40.64	120.00	240.00	58.4	98.16	1
119	160	160	1.37	100	0.00275	58.67	390	84.8	40.64	120.00	240.00	58.4	98.77	1
120	160	160	1.37	100	0.00275	64.00	390	84.8	40.64	120.00	240.00	58.4	99.17	1
121	160	160	1.37	100	0.00275	16.00	390	84.8	40.64	120.00	240.00	62.7	72.08	1
122	160	160	1.37	100	0.00275	21.33	390	84.8	40.64	120.00	240.00	62.7	81.75	1
123	160	160	1.37	100	0.00275	26.67	390	84.8	40.64	120.00	240.00	62.7	88.08	1
124	160	160	1.37	100	0.00275	32.00	390	84.8	40.64	120.00	240.00	62.7	92.21	1
125	160	160	1.37	100	0.00275	37.33	390	84.8	40.64	120.00	240.00	62.7	94.90	1
126	160	160	1.37	100	0.00275	42.67	390	84.8	40.64	120.00	240.00	62.7	96.67	1
127	160	160	1.37	100	0.00275	48.00	390	84.8	40.64	120.00	240.00	62.7	97.82	1
128	160	160	1.37	100	0.00275	53.33	390	84.8	40.64	120.00	240.00	62.7	98.58	1
129	160	160	1.37	100	0.00275	58.67	390	84.8	40.64	120.00	240.00	62.7	99.07	1
130	160	160	1.37	100	0.00275	64.00	390	84.8	40.64	120.00	240.00	62.7	99.39	1
131	160	160	1.37	100	0.00275	16.00	390	84.8	40.64	120.00	240.00	67.1	74.37	1
132	160	160	1.37	100	0.00275	21.33	390	84.8	40.64	120.00	240.00	67.1	83.71	1
133	160	160	1.37	100	0.00275	26.67	390	84.8	40.64	120.00	240.00	67.1	89.66	1
134	160	160	1.37	100	0.00275	32.00	390	84.8	40.64	120.00	240.00	67.1	93.43	1
135	160	160	1.37	100	0.00275	37.33	390	84.8	40.64	120.00	240.00	67.1	95.83	1
136	160	160	1.37	100	0.00275	42.67	390	84.8	40.64	120.00	240.00	67.1	97.35	1
137	160	160	1.37	100	0.00275	48.00	390	84.8	40.64	120.00	240.00	67.1	98.32	1
138	160	160	1.37	100	0.00275	53.33	390	84.8	40.64	120.00	240.00	67.1	98.93	1
139	160	160	1.37	100	0.00275	58.67	390	84.8	40.64	120.00	240.00	67.1	99.32	1
140	160	160	1.37	100	0.00275	64.00	390	84.8	40.64	120.00	240.00	67.1	99.57	1
141	160	160	1.37	100	0.00275	16.00	390	84.8	40.64	120.00	240.00	71.5	76.64	1
142	160	160	1.37	100	0.00275	21.33	390	84.8	40.64	120.00	240.00	71.5	85.61	1
143	160	160	1.37	100	0.00275	26.67	390	84.8	40.64	120.00	240.00	71.5	91.14	1

#	W cm	H cm	r cm	l = x cm	k cm ² /mW-s	P W	Airflow m ³ /min	x cm	y cm	z cm	L cm	p	Actual Kill Rate	Work Frac.
144	160	160	1.37	100	0.00275	32.00	390	84.8	40.64	120.00	240.00	71.5	94.54	1
145	160	160	1.37	100	0.00275	37.33	390	84.8	40.64	120.00	240.00	71.5	96.64	1
146	160	160	1.37	100	0.00275	42.67	390	84.8	40.64	120.00	240.00	71.5	97.93	1
147	160	160	1.37	100	0.00275	48.00	390	84.8	40.64	120.00	240.00	71.5	98.72	1
148	160	160	1.37	100	0.00275	53.33	390	84.8	40.64	120.00	240.00	71.5	99.21	1
149	160	160	1.37	100	0.00275	58.67	390	84.8	40.64	120.00	240.00	71.5	99.52	1
150	160	160	1.37	100	0.00275	64.00	390	84.8	40.64	120.00	240.00	71.5	99.70	1
151	160	160	1.37	100	0.00275	16.00	390	84.8	40.64	120.00	240.00	75.8	78.83	1
152	160	160	1.37	100	0.00275	21.33	390	84.8	40.64	120.00	240.00	75.8	87.38	1
153	160	160	1.37	100	0.00275	26.67	390	84.8	40.64	120.00	240.00	75.8	92.48	1
154	160	160	1.37	100	0.00275	32.00	390	84.8	40.64	120.00	240.00	75.8	95.52	1
155	160	160	1.37	100	0.00275	37.33	390	84.8	40.64	120.00	240.00	75.8	97.33	1
156	160	160	1.37	100	0.00275	42.67	390	84.8	40.64	120.00	240.00	75.8	98.41	1
157	160	160	1.37	100	0.00275	48.00	390	84.8	40.64	120.00	240.00	75.8	99.05	1
158	160	160	1.37	100	0.00275	53.33	390	84.8	40.64	120.00	240.00	75.8	99.43	1
159	160	160	1.37	100	0.00275	58.67	390	84.8	40.64	120.00	240.00	75.8	99.66	1
160	160	160	1.37	100	0.00275	64.00	390	84.8	40.64	120.00	240.00	75.8	99.80	1
161	160	160	1.37	100	0.00275	16.00	390	84.8	40.64	120.00	240.00	80.2	81.02	1
162	160	160	1.37	100	0.00275	21.33	390	84.8	40.64	120.00	240.00	80.2	89.09	1
163	160	160	1.37	100	0.00275	26.67	390	84.8	40.64	120.00	240.00	80.2	93.74	1
164	160	160	1.37	100	0.00275	32.00	390	84.8	40.64	120.00	240.00	80.2	96.40	1
165	160	160	1.37	100	0.00275	37.33	390	84.8	40.64	120.00	240.00	80.2	97.93	1
166	160	160	1.37	100	0.00275	42.67	390	84.8	40.64	120.00	240.00	80.2	98.81	1
167	160	160	1.37	100	0.00275	48.00	390	84.8	40.64	120.00	240.00	80.2	99.32	1
168	160	160	1.37	100	0.00275	53.33	390	84.8	40.64	120.00	240.00	80.2	99.61	1
169	160	160	1.37	100	0.00275	58.67	390	84.8	40.64	120.00	240.00	80.2	99.77	1
170	160	160	1.37	100	0.00275	64.00	390	84.8	40.64	120.00	240.00	80.2	99.87	1
171	160	160	1.37	100	0.00275	16.00	390	84.8	40.64	120.00	240.00	84.6	83.16	1
172	160	160	1.37	100	0.00275	21.33	390	84.8	40.64	120.00	240.00	84.6	90.70	1
173	160	160	1.37	100	0.00275	26.67	390	84.8	40.64	120.00	240.00	84.6	94.87	1
174	160	160	1.37	100	0.00275	32.00	390	84.8	40.64	120.00	240.00	84.6	97.17	1
175	160	160	1.37	100	0.00275	37.33	390	84.8	40.64	120.00	240.00	84.6	98.43	1
176	160	160	1.37	100	0.00275	42.67	390	84.8	40.64	120.00	240.00	84.6	99.14	1
177	160	160	1.37	100	0.00275	48.00	390	84.8	40.64	120.00	240.00	84.6	99.52	1
178	160	160	1.37	100	0.00275	53.33	390	84.8	40.64	120.00	240.00	84.6	99.74	1
179	160	160	1.37	100	0.00275	58.67	390	84.8	40.64	120.00	240.00	84.6	99.85	1
180	160	160	1.37	100	0.00275	64.00	390	84.8	40.64	120.00	240.00	84.6	99.92	1
181	160	160	1.37	100	0.00275	16.00	390	84.8	40.64	120.00	240.00	88.9	85.19	1
182	160	160	1.37	100	0.00275	21.33	390	84.8	40.64	120.00	240.00	88.9	92.16	1
183	160	160	1.37	100	0.00275	26.67	390	84.8	40.64	120.00	240.00	88.9	95.86	1
184	160	160	1.37	100	0.00275	32.00	390	84.8	40.64	120.00	240.00	88.9	97.81	1
185	160	160	1.37	100	0.00275	37.33	390	84.8	40.64	120.00	240.00	88.9	98.84	1
186	160	160	1.37	100	0.00275	42.67	390	84.8	40.64	120.00	240.00	88.9	99.39	1
187	160	160	1.37	100	0.00275	48.00	390	84.8	40.64	120.00	240.00	88.9	99.68	1
188	160	160	1.37	100	0.00275	53.33	390	84.8	40.64	120.00	240.00	88.9	99.83	1
189	160	160	1.37	100	0.00275	58.67	390	84.8	40.64	120.00	240.00	88.9	99.91	1
190	160	160	1.37	100	0.00275	64.00	390	84.8	40.64	120.00	240.00	88.9	99.95	1
191	160	160	1.37	100	0.00275	16.00	390	84.8	40.64	120.00	240.00	93.3	87.17	1

#	W cm	H cm	r cm	l = x cm	k cm ² /mW-s	P W	Airflow m ³ /min	x cm	y cm	z cm	L cm	p	Actual Kill Rate	Work Frac.
192	160	160	1.37	100	0.00275	21.33	390	84.8	40.64	120.00	240.00	93.3	93.53	1
193	160	160	1.37	100	0.00275	26.67	390	84.8	40.64	120.00	240.00	93.3	96.74	1
194	160	160	1.37	100	0.00275	32.00	390	84.8	40.64	120.00	240.00	93.3	98.35	1
195	160	160	1.37	100	0.00275	37.33	390	84.8	40.64	120.00	240.00	93.3	99.17	1
196	160	160	1.37	100	0.00275	42.67	390	84.8	40.64	120.00	240.00	93.3	99.58	1
197	160	160	1.37	100	0.00275	48.00	390	84.8	40.64	120.00	240.00	93.3	99.79	1
198	160	160	1.37	100	0.00275	53.33	390	84.8	40.64	120.00	240.00	93.3	99.89	1
199	160	160	1.37	100	0.00275	58.67	390	84.8	40.64	120.00	240.00	93.3	99.95	1
200	160	160	1.37	100	0.00275	64.00	390	84.8	40.64	120.00	240.00	93.3	99.97	1
201	160	160	1.37	100	0.00275	40.00	390	84.8	40.64	50.00	100.00	54.0	79.17	1
202	160	160	1.37	100	0.00275	40.00	390	84.8	40.64	83.33	166.67	54.0	89.52	1
203	160	160	1.37	100	0.00275	40.00	390	84.8	40.64	116.67	233.33	54.0	93.73	1
204	160	160	1.37	100	0.00275	40.00	390	84.8	40.64	150.00	300.00	54.0	95.77	1
205	160	160	1.37	100	0.00275	40.00	390	84.8	40.64	183.33	366.67	54.0	96.87	1
206	160	160	1.37	100	0.00275	40.00	390	84.8	40.64	216.67	433.33	54.0	97.53	1
207	160	160	1.37	100	0.00275	40.00	390	84.8	40.64	250.00	500.00	54.0	97.96	1
208	160	160	1.37	100	0.00275	40.00	390	84.8	40.64	283.33	566.67	54.0	98.25	1
209	160	160	1.37	100	0.00275	40.00	390	84.8	40.64	316.67	633.33	54.0	98.46	1
210	160	160	1.37	100	0.00275	40.00	390	84.8	40.64	350.00	700.00	54.0	98.61	1
211	160	160	1.37	100	0.00275	40.00	390	84.8	40.64	50.00	100.00	58.4	80.67	1
212	160	160	1.37	100	0.00275	40.00	390	84.8	40.64	83.33	166.67	58.4	90.80	1
213	160	160	1.37	100	0.00275	40.00	390	84.8	40.64	116.67	233.33	58.4	94.76	1
214	160	160	1.37	100	0.00275	40.00	390	84.8	40.64	150.00	300.00	58.4	96.59	1
215	160	160	1.37	100	0.00275	40.00	390	84.8	40.64	183.33	366.67	58.4	97.56	1
216	160	160	1.37	100	0.00275	40.00	390	84.8	40.64	216.67	433.33	58.4	98.12	1
217	160	160	1.37	100	0.00275	40.00	390	84.8	40.64	250.00	500.00	58.4	98.48	1
218	160	160	1.37	100	0.00275	40.00	390	84.8	40.64	283.33	566.67	58.4	98.72	1
219	160	160	1.37	100	0.00275	40.00	390	84.8	40.64	316.67	633.33	58.4	98.89	1
220	160	160	1.37	100	0.00275	40.00	390	84.8	40.64	350.00	700.00	58.4	99.01	1
221	160	160	1.37	100	0.00275	40.00	390	84.8	40.64	50.00	100.00	62.7	82.14	1
222	160	160	1.37	100	0.00275	40.00	390	84.8	40.64	83.33	166.67	62.7	91.99	1
223	160	160	1.37	100	0.00275	40.00	390	84.8	40.64	116.67	233.33	62.7	95.66	1
224	160	160	1.37	100	0.00275	40.00	390	84.8	40.64	150.00	300.00	62.7	97.29	1
225	160	160	1.37	100	0.00275	40.00	390	84.8	40.64	183.33	366.67	62.7	98.12	1
226	160	160	1.37	100	0.00275	40.00	390	84.8	40.64	216.67	433.33	62.7	98.60	1
227	160	160	1.37	100	0.00275	40.00	390	84.8	40.64	250.00	500.00	62.7	98.89	1
228	160	160	1.37	100	0.00275	40.00	390	84.8	40.64	283.33	566.67	62.7	99.08	1
229	160	160	1.37	100	0.00275	40.00	390	84.8	40.64	316.67	633.33	62.7	99.21	1
230	160	160	1.37	100	0.00275	40.00	390	84.8	40.64	350.00	700.00	62.7	99.31	1
231	160	160	1.37	100	0.00275	40.00	390	84.8	40.64	50.00	100.00	67.1	83.65	1
232	160	160	1.37	100	0.00275	40.00	390	84.8	40.64	83.33	166.67	67.1	93.13	1
233	160	160	1.37	100	0.00275	40.00	390	84.8	40.64	116.67	233.33	67.1	96.47	1
234	160	160	1.37	100	0.00275	40.00	390	84.8	40.64	150.00	300.00	67.1	97.90	1
235	160	160	1.37	100	0.00275	40.00	390	84.8	40.64	183.33	366.67	67.1	98.60	1
236	160	160	1.37	100	0.00275	40.00	390	84.8	40.64	216.67	433.33	67.1	98.98	1
237	160	160	1.37	100	0.00275	40.00	390	84.8	40.64	250.00	500.00	67.1	99.21	1
238	160	160	1.37	100	0.00275	40.00	390	84.8	40.64	283.33	566.67	67.1	99.36	1
239	160	160	1.37	100	0.00275	40.00	390	84.8	40.64	316.67	633.33	67.1	99.46	1

#	W cm	H cm	r cm	l = x cm	k cm ² /mW-s	P W	Airflow m ³ /min	x cm	y cm	z cm	L cm	p	Actual Kill Rate	Work Frac.
240	160	160	1.37	100	0.00275	40.00	390	84.8	40.64	350.00	700.00	67.1	99.53	1
241	160	160	1.37	100	0.00275	40.00	390	84.8	40.64	50.00	100.00	71.5	85.16	1
242	160	160	1.37	100	0.00275	40.00	390	84.8	40.64	83.33	166.67	71.5	94.19	1
243	160	160	1.37	100	0.00275	40.00	390	84.8	40.64	116.67	233.33	71.5	97.19	1
244	160	160	1.37	100	0.00275	40.00	390	84.8	40.64	150.00	300.00	71.5	98.40	1
245	160	160	1.37	100	0.00275	40.00	390	84.8	40.64	183.33	366.67	71.5	98.98	1
246	160	160	1.37	100	0.00275	40.00	390	84.8	40.64	216.67	433.33	71.5	99.28	1
247	160	160	1.37	100	0.00275	40.00	390	84.8	40.64	250.00	500.00	71.5	99.46	1
248	160	160	1.37	100	0.00275	40.00	390	84.8	40.64	283.33	566.67	71.5	99.57	1
249	160	160	1.37	100	0.00275	40.00	390	84.8	40.64	316.67	633.33	71.5	99.65	1
250	160	160	1.37	100	0.00275	40.00	390	84.8	40.64	350.00	700.00	71.5	99.70	1
251	160	160	1.37	100	0.00275	40.00	390	84.8	40.64	50.00	100.00	75.8	86.62	1
252	160	160	1.37	100	0.00275	40.00	390	84.8	40.64	83.33	166.67	75.8	95.13	1
253	160	160	1.37	100	0.00275	40.00	390	84.8	40.64	116.67	233.33	75.8	97.79	1
254	160	160	1.37	100	0.00275	40.00	390	84.8	40.64	150.00	300.00	75.8	98.81	1
255	160	160	1.37	100	0.00275	40.00	390	84.8	40.64	183.33	366.67	75.8	99.27	1
256	160	160	1.37	100	0.00275	40.00	390	84.8	40.64	216.67	433.33	75.8	99.50	1
257	160	160	1.37	100	0.00275	40.00	390	84.8	40.64	250.00	500.00	75.8	99.64	1
258	160	160	1.37	100	0.00275	40.00	390	84.8	40.64	283.33	566.67	75.8	99.72	1
259	160	160	1.37	100	0.00275	40.00	390	84.8	40.64	316.67	633.33	75.8	99.77	1
260	160	160	1.37	100	0.00275	40.00	390	84.8	40.64	350.00	700.00	75.8	99.81	1
261	160	160	1.37	100	0.00275	40.00	390	84.8	40.64	50.00	100.00	80.2	88.11	1
262	160	160	1.37	100	0.00275	40.00	390	84.8	40.64	83.33	166.67	80.2	96.01	1
263	160	160	1.37	100	0.00275	40.00	390	84.8	40.64	116.67	233.33	80.2	98.31	1
264	160	160	1.37	100	0.00275	40.00	390	84.8	40.64	150.00	300.00	80.2	99.14	1
265	160	160	1.37	100	0.00275	40.00	390	84.8	40.64	183.33	366.67	80.2	99.50	1
266	160	160	1.37	100	0.00275	40.00	390	84.8	40.64	216.67	433.33	80.2	99.67	1
267	160	160	1.37	100	0.00275	40.00	390	84.8	40.64	250.00	500.00	80.2	99.77	1
268	160	160	1.37	100	0.00275	40.00	390	84.8	40.64	283.33	566.67	80.2	99.83	1
269	160	160	1.37	100	0.00275	40.00	390	84.8	40.64	316.67	633.33	80.2	99.86	1
270	160	160	1.37	100	0.00275	40.00	390	84.8	40.64	350.00	700.00	80.2	99.89	1
271	160	160	1.37	100	0.00275	40.00	390	84.8	40.64	50.00	100.00	84.6	89.57	1
272	160	160	1.37	100	0.00275	40.00	390	84.8	40.64	83.33	166.67	84.6	96.79	1
273	160	160	1.37	100	0.00275	40.00	390	84.8	40.64	116.67	233.33	84.6	98.74	1
274	160	160	1.37	100	0.00275	40.00	390	84.8	40.64	150.00	300.00	84.6	99.40	1
275	160	160	1.37	100	0.00275	40.00	390	84.8	40.64	183.33	366.67	84.6	99.67	1
276	160	160	1.37	100	0.00275	40.00	390	84.8	40.64	216.67	433.33	84.6	99.79	1
277	160	160	1.37	100	0.00275	40.00	390	84.8	40.64	250.00	500.00	84.6	99.86	1
278	160	160	1.37	100	0.00275	40.00	390	84.8	40.64	283.33	566.67	84.6	99.90	1
279	160	160	1.37	100	0.00275	40.00	390	84.8	40.64	316.67	633.33	84.6	99.92	1
280	160	160	1.37	100	0.00275	40.00	390	84.8	40.64	350.00	700.00	84.6	99.94	1
281	160	160	1.37	100	0.00275	40.00	390	84.8	40.64	50.00	100.00	88.9	90.96	1
282	160	160	1.37	100	0.00275	40.00	390	84.8	40.64	83.33	166.67	88.9	97.46	1
283	160	160	1.37	100	0.00275	40.00	390	84.8	40.64	116.67	233.33	88.9	99.08	1
284	160	160	1.37	100	0.00275	40.00	390	84.8	40.64	150.00	300.00	88.9	99.59	1
285	160	160	1.37	100	0.00275	40.00	390	84.8	40.64	183.33	366.67	88.9	99.78	1
286	160	160	1.37	100	0.00275	40.00	390	84.8	40.64	216.67	433.33	88.9	99.87	1
287	160	160	1.37	100	0.00275	40.00	390	84.8	40.64	250.00	500.00	88.9	99.92	1

#	W cm	H cm	r cm	l = x cm	k cm ² /mW-s	P W	Airflow m ³ /min	x cm	y cm	z cm	L cm	p	Actual Kill Rate	Work Frac.
288	160	160	1.37	100	0.00275	40.00	390	84.8	40.64	283.33	566.67	88.9	99.94	1
289	160	160	1.37	100	0.00275	40.00	390	84.8	40.64	316.67	633.33	88.9	99.96	1
290	160	160	1.37	100	0.00275	40.00	390	84.8	40.64	350.00	700.00	88.9	99.96	1
291	160	160	1.37	100	0.00275	40.00	390	84.8	40.64	50.00	100.00	93.3	92.35	1
292	160	160	1.37	100	0.00275	40.00	390	84.8	40.64	83.33	166.67	93.3	98.05	1
293	160	160	1.37	100	0.00275	40.00	390	84.8	40.64	116.67	233.33	93.3	99.35	1
294	160	160	1.37	100	0.00275	40.00	390	84.8	40.64	150.00	300.00	93.3	99.73	1
295	160	160	1.37	100	0.00275	40.00	390	84.8	40.64	183.33	366.67	93.3	99.87	1
296	160	160	1.37	100	0.00275	40.00	390	84.8	40.64	216.67	433.33	93.3	99.92	1
297	160	160	1.37	100	0.00275	40.00	390	84.8	40.64	250.00	500.00	93.3	99.95	1
298	160	160	1.37	100	0.00275	40.00	390	84.8	40.64	283.33	566.67	93.3	99.97	1
299	160	160	1.37	100	0.00275	40.00	390	84.8	40.64	316.67	633.33	93.3	99.98	1
300	160	160	1.37	100	0.00275	40.00	390	84.8	40.64	350.00	700.00	93.3	99.98	1
301	160	160	1.37	100	0.00275	16.00	100	84.8	40.64	120.00	240.00	73.6	99.71	0.26
302	160	160	1.37	100	0.00275	16.00	164.44	84.8	40.64	120.00	240.00	73.6	97.18	0.42
303	160	160	1.37	100	0.00275	16.00	228.89	84.8	40.64	120.00	240.00	73.6	92.24	0.59
304	160	160	1.37	100	0.00275	16.00	293.33	84.8	40.64	120.00	240.00	73.6	86.44	0.75
305	160	160	1.37	100	0.00275	16.00	357.78	84.8	40.64	120.00	240.00	73.6	80.51	0.92
306	160	160	1.37	100	0.00275	16.00	422.22	84.8	40.64	120.00	240.00	73.6	75.02	1.08
307	160	160	1.37	100	0.00275	16.00	486.67	84.8	40.64	120.00	240.00	73.6	69.94	1.25
308	160	160	1.37	100	0.00275	16.00	551.11	84.8	40.64	120.00	240.00	73.6	65.44	1.41
309	160	160	1.37	100	0.00275	16.00	615.56	84.8	40.64	120.00	240.00	73.6	61.34	1.58
310	160	160	1.37	100	0.00275	16.00	680	84.8	40.64	120.00	240.00	73.6	57.72	1.74
311	160	160	1.37	100	0.00275	21.33	100	84.8	40.64	120.00	240.00	73.6	99.96	0.26
312	160	160	1.37	100	0.00275	21.33	164.44	84.8	40.64	120.00	240.00	73.6	99.14	0.42
313	160	160	1.37	100	0.00275	21.33	228.89	84.8	40.64	120.00	240.00	73.6	96.69	0.59
314	160	160	1.37	100	0.00275	21.33	293.33	84.8	40.64	120.00	240.00	73.6	93.03	0.75
315	160	160	1.37	100	0.00275	21.33	357.78	84.8	40.64	120.00	240.00	73.6	88.70	0.92
316	160	160	1.37	100	0.00275	21.33	422.22	84.8	40.64	120.00	240.00	73.6	84.27	1.08
317	160	160	1.37	100	0.00275	21.33	486.67	84.8	40.64	120.00	240.00	73.6	79.86	1.25
318	160	160	1.37	100	0.00275	21.33	551.11	84.8	40.64	120.00	240.00	73.6	75.74	1.41
319	160	160	1.37	100	0.00275	21.33	615.56	84.8	40.64	120.00	240.00	73.6	71.83	1.58
320	160	160	1.37	100	0.00275	21.33	680	84.8	40.64	120.00	240.00	73.6	68.26	1.74
321	160	160	1.37	100	0.00275	26.67	100	84.8	40.64	120.00	240.00	73.6	99.99	0.26
322	160	160	1.37	100	0.00275	26.67	164.44	84.8	40.64	120.00	240.00	73.6	99.74	0.42
323	160	160	1.37	100	0.00275	26.67	228.89	84.8	40.64	120.00	240.00	73.6	98.59	0.59
324	160	160	1.37	100	0.00275	26.67	293.33	84.8	40.64	120.00	240.00	73.6	96.42	0.75
325	160	160	1.37	100	0.00275	26.67	357.78	84.8	40.64	120.00	240.00	73.6	93.45	0.92
326	160	160	1.37	100	0.00275	26.67	422.22	84.8	40.64	120.00	240.00	73.6	90.10	1.08
327	160	160	1.37	100	0.00275	26.67	486.67	84.8	40.64	120.00	240.00	73.6	86.52	1.25
328	160	160	1.37	100	0.00275	26.67	551.11	84.8	40.64	120.00	240.00	73.6	82.98	1.41
329	160	160	1.37	100	0.00275	26.67	615.56	84.8	40.64	120.00	240.00	73.6	79.49	1.58
330	160	160	1.37	100	0.00275	26.67	680	84.8	40.64	120.00	240.00	73.6	76.19	1.74
331	160	160	1.37	100	0.00275	32.00	100	84.8	40.64	120.00	240.00	73.6	100.00	0.26
332	160	160	1.37	100	0.00275	32.00	164.44	84.8	40.64	120.00	240.00	73.6	99.92	0.42
333	160	160	1.37	100	0.00275	32.00	228.89	84.8	40.64	120.00	240.00	73.6	99.40	0.59
334	160	160	1.37	100	0.00275	32.00	293.33	84.8	40.64	120.00	240.00	73.6	98.16	0.75
335	160	160	1.37	100	0.00275	32.00	357.78	84.8	40.64	120.00	240.00	73.6	96.20	0.92

#	W cm	H cm	r cm	l = x cm	k cm ² /mW-s	P W	Airflow m ³ /min	x cm	y cm	z cm	L cm	p	Actual Kill Rate	Work Frac.
336	160	160	1.37	100	0.00275	32.00	422.22	84.8	40.64	120.00	240.00	73.6	93.76	1.08
337	160	160	1.37	100	0.00275	32.00	486.67	84.8	40.64	120.00	240.00	73.6	90.97	1.25
338	160	160	1.37	100	0.00275	32.00	551.11	84.8	40.64	120.00	240.00	73.6	88.06	1.41
339	160	160	1.37	100	0.00275	32.00	615.56	84.8	40.64	120.00	240.00	73.6	85.05	1.58
340	160	160	1.37	100	0.00275	32.00	680	84.8	40.64	120.00	240.00	73.6	82.13	1.74
341	160	160	1.37	100	0.00275	37.33	100	84.8	40.64	120.00	240.00	73.6	100.00	0.26
342	160	160	1.37	100	0.00275	37.33	164.44	84.8	40.64	120.00	240.00	73.6	99.98	0.42
343	160	160	1.37	100	0.00275	37.33	228.89	84.8	40.64	120.00	240.00	73.6	99.74	0.59
344	160	160	1.37	100	0.00275	37.33	293.33	84.8	40.64	120.00	240.00	73.6	99.05	0.75
345	160	160	1.37	100	0.00275	37.33	357.78	84.8	40.64	120.00	240.00	73.6	97.80	0.92
346	160	160	1.37	100	0.00275	37.33	422.22	84.8	40.64	120.00	240.00	73.6	96.07	1.08
347	160	160	1.37	100	0.00275	37.33	486.67	84.8	40.64	120.00	240.00	73.6	93.95	1.25
348	160	160	1.37	100	0.00275	37.33	551.11	84.8	40.64	120.00	240.00	73.6	91.62	1.41
349	160	160	1.37	100	0.00275	37.33	615.56	84.8	40.64	120.00	240.00	73.6	89.11	1.58
350	160	160	1.37	100	0.00275	37.33	680	84.8	40.64	120.00	240.00	73.6	86.58	1.74
351	160	160	1.37	100	0.00275	42.67	100	84.8	40.64	120.00	240.00	73.6	100.00	0.26
352	160	160	1.37	100	0.00275	42.67	164.44	84.8	40.64	120.00	240.00	73.6	99.99	0.42
353	160	160	1.37	100	0.00275	42.67	228.89	84.8	40.64	120.00	240.00	73.6	99.89	0.59
354	160	160	1.37	100	0.00275	42.67	293.33	84.8	40.64	120.00	240.00	73.6	99.51	0.75
355	160	160	1.37	100	0.00275	42.67	357.78	84.8	40.64	120.00	240.00	73.6	98.72	0.92
356	160	160	1.37	100	0.00275	42.67	422.22	84.8	40.64	120.00	240.00	73.6	97.53	1.08
357	160	160	1.37	100	0.00275	42.67	486.67	84.8	40.64	120.00	240.00	73.6	95.95	1.25
358	160	160	1.37	100	0.00275	42.67	551.11	84.8	40.64	120.00	240.00	73.6	94.12	1.41
359	160	160	1.37	100	0.00275	42.67	615.56	84.8	40.64	120.00	240.00	73.6	92.07	1.58
360	160	160	1.37	100	0.00275	42.67	680	84.8	40.64	120.00	240.00	73.6	89.93	1.74
361	160	160	1.37	100	0.00275	48.00	100	84.8	40.64	120.00	240.00	73.6	100.00	0.26
362	160	160	1.37	100	0.00275	48.00	164.44	84.8	40.64	120.00	240.00	73.6	100.00	0.42
363	160	160	1.37	100	0.00275	48.00	228.89	84.8	40.64	120.00	240.00	73.6	99.95	0.59
364	160	160	1.37	100	0.00275	48.00	293.33	84.8	40.64	120.00	240.00	73.6	99.75	0.75
365	160	160	1.37	100	0.00275	48.00	357.78	84.8	40.64	120.00	240.00	73.6	99.26	0.92
366	160	160	1.37	100	0.00275	48.00	422.22	84.8	40.64	120.00	240.00	73.6	98.44	1.08
367	160	160	1.37	100	0.00275	48.00	486.67	84.8	40.64	120.00	240.00	73.6	97.28	1.25
368	160	160	1.37	100	0.00275	48.00	551.11	84.8	40.64	120.00	240.00	73.6	95.87	1.41
369	160	160	1.37	100	0.00275	48.00	615.56	84.8	40.64	120.00	240.00	73.6	94.22	1.58
370	160	160	1.37	100	0.00275	48.00	680	84.8	40.64	120.00	240.00	73.6	92.44	1.74
371	160	160	1.37	100	0.00275	53.33	100	84.8	40.64	120.00	240.00	73.6	100.00	0.26
372	160	160	1.37	100	0.00275	53.33	164.44	84.8	40.64	120.00	240.00	73.6	100.00	0.42
373	160	160	1.37	100	0.00275	53.33	228.89	84.8	40.64	120.00	240.00	73.6	99.98	0.59
374	160	160	1.37	100	0.00275	53.33	293.33	84.8	40.64	120.00	240.00	73.6	99.87	0.75
375	160	160	1.37	100	0.00275	53.33	357.78	84.8	40.64	120.00	240.00	73.6	99.57	0.92
376	160	160	1.37	100	0.00275	53.33	422.22	84.8	40.64	120.00	240.00	73.6	99.02	1.08
377	160	160	1.37	100	0.00275	53.33	486.67	84.8	40.64	120.00	240.00	73.6	98.18	1.25
378	160	160	1.37	100	0.00275	53.33	551.11	84.8	40.64	120.00	240.00	73.6	97.10	1.41
379	160	160	1.37	100	0.00275	53.33	615.56	84.8	40.64	120.00	240.00	73.6	95.79	1.58
380	160	160	1.37	100	0.00275	53.33	680	84.8	40.64	120.00	240.00	73.6	94.33	1.74
381	160	160	1.37	100	0.00275	58.67	100	84.8	40.64	120.00	240.00	73.6	100.00	0.26
382	160	160	1.37	100	0.00275	58.67	164.44	84.8	40.64	120.00	240.00	73.6	100.00	0.42
383	160	160	1.37	100	0.00275	58.67	228.89	84.8	40.64	120.00	240.00	73.6	99.99	0.59

#	W cm	H cm	r cm	l = x cm	k cm ² /mW-s	P W	Airflow m ³ /min	x cm	y cm	z cm	L cm	p	Actual Kill Rate	Work Frac.
384	160	160	1.37	100	0.00275	58.67	293.33	84.8	40.64	120.00	240.00	73.6	99.93	0.75
385	160	160	1.37	100	0.00275	58.67	357.78	84.8	40.64	120.00	240.00	73.6	99.75	0.92
386	160	160	1.37	100	0.00275	58.67	422.22	84.8	40.64	120.00	240.00	73.6	99.38	1.08
387	160	160	1.37	100	0.00275	58.67	486.67	84.8	40.64	120.00	240.00	73.6	98.78	1.25
388	160	160	1.37	100	0.00275	58.67	551.11	84.8	40.64	120.00	240.00	73.6	97.97	1.41
389	160	160	1.37	100	0.00275	58.67	615.56	84.8	40.64	120.00	240.00	73.6	96.93	1.58
390	160	160	1.37	100	0.00275	58.67	680	84.8	40.64	120.00	240.00	73.6	95.74	1.74
391	160	160	1.37	100	0.00275	64.00	100	84.8	40.64	120.00	240.00	73.6	100.00	0.26
392	160	160	1.37	100	0.00275	64.00	164.44	84.8	40.64	120.00	240.00	73.6	100.00	0.42
393	160	160	1.37	100	0.00275	64.00	228.89	84.8	40.64	120.00	240.00	73.6	100.00	0.59
394	160	160	1.37	100	0.00275	64.00	293.33	84.8	40.64	120.00	240.00	73.6	99.97	0.75
395	160	160	1.37	100	0.00275	64.00	357.78	84.8	40.64	120.00	240.00	73.6	99.86	0.92
396	160	160	1.37	100	0.00275	64.00	422.22	84.8	40.64	120.00	240.00	73.6	99.61	1.08
397	160	160	1.37	100	0.00275	64.00	486.67	84.8	40.64	120.00	240.00	73.6	99.18	1.25
398	160	160	1.37	100	0.00275	64.00	551.11	84.8	40.64	120.00	240.00	73.6	98.57	1.41
399	160	160	1.37	100	0.00275	64.00	615.56	84.8	40.64	120.00	240.00	73.6	97.77	1.58
400	160	160	1.37	100	0.00275	64.00	680	84.8	40.64	120.00	240.00	73.6	96.80	1.74
401	160	160	1.37	100	0.00275	40.00	100	84.8	40.64	50.00	100.00	73.6	99.95	0.26
402	160	160	1.37	100	0.00275	40.00	164.44	84.8	40.64	50.00	100.00	73.6	99.05	0.42
403	160	160	1.37	100	0.00275	40.00	228.89	84.8	40.64	50.00	100.00	73.6	96.43	0.59
404	160	160	1.37	100	0.00275	40.00	293.33	84.8	40.64	50.00	100.00	73.6	92.61	0.75
405	160	160	1.37	100	0.00275	40.00	357.78	84.8	40.64	50.00	100.00	73.6	88.14	0.92
406	160	160	1.37	100	0.00275	40.00	422.22	84.8	40.64	50.00	100.00	73.6	83.62	1.08
407	160	160	1.37	100	0.00275	40.00	486.67	84.8	40.64	50.00	100.00	73.6	79.14	1.25
408	160	160	1.37	100	0.00275	40.00	551.11	84.8	40.64	50.00	100.00	73.6	74.98	1.41
409	160	160	1.37	100	0.00275	40.00	615.56	84.8	40.64	50.00	100.00	73.6	71.04	1.58
410	160	160	1.37	100	0.00275	40.00	680	84.8	40.64	50.00	100.00	73.6	67.46	1.74
411	160	160	1.37	100	0.00275	40.00	100	84.8	40.64	83.33	166.67	73.6	100.00	0.26
412	160	160	1.37	100	0.00275	40.00	164.44	84.8	40.64	83.33	166.67	73.6	99.91	0.42
413	160	160	1.37	100	0.00275	40.00	228.89	84.8	40.64	83.33	166.67	73.6	99.32	0.59
414	160	160	1.37	100	0.00275	40.00	293.33	84.8	40.64	83.33	166.67	73.6	97.97	0.75
415	160	160	1.37	100	0.00275	40.00	357.78	84.8	40.64	83.33	166.67	73.6	95.89	0.92
416	160	160	1.37	100	0.00275	40.00	422.22	84.8	40.64	83.33	166.67	73.6	93.33	1.08
417	160	160	1.37	100	0.00275	40.00	486.67	84.8	40.64	83.33	166.67	73.6	90.43	1.25
418	160	160	1.37	100	0.00275	40.00	551.11	84.8	40.64	83.33	166.67	73.6	87.43	1.41
419	160	160	1.37	100	0.00275	40.00	615.56	84.8	40.64	83.33	166.67	73.6	84.35	1.58
420	160	160	1.37	100	0.00275	40.00	680	84.8	40.64	83.33	166.67	73.6	81.37	1.74
421	160	160	1.37	100	0.00275	40.00	100	84.8	40.64	116.67	233.33	73.6	100.00	0.26
422	160	160	1.37	100	0.00275	40.00	164.44	84.8	40.64	116.67	233.33	73.6	99.98	0.42
423	160	160	1.37	100	0.00275	40.00	228.89	84.8	40.64	116.67	233.33	73.6	99.81	0.59
424	160	160	1.37	100	0.00275	40.00	293.33	84.8	40.64	116.67	233.33	73.6	99.26	0.75
425	160	160	1.37	100	0.00275	40.00	357.78	84.8	40.64	116.67	233.33	73.6	98.20	0.92
426	160	160	1.37	100	0.00275	40.00	422.22	84.8	40.64	116.67	233.33	73.6	96.69	1.08
427	160	160	1.37	100	0.00275	40.00	486.67	84.8	40.64	116.67	233.33	73.6	94.78	1.25
428	160	160	1.37	100	0.00275	40.00	551.11	84.8	40.64	116.67	233.33	73.6	92.64	1.41
429	160	160	1.37	100	0.00275	40.00	615.56	84.8	40.64	116.67	233.33	73.6	90.31	1.58
430	160	160	1.37	100	0.00275	40.00	680	84.8	40.64	116.67	233.33	73.6	87.93	1.74
431	160	160	1.37	100	0.00275	40.00	100	84.8	40.64	150.00	300.00	73.6	100.00	0.26

#	W cm	H cm	r cm	l = x cm	k cm ² /mW-s	P W	Airflow m ³ /min	x cm	y cm	z cm	L cm	p	Actual Kill Rate	Work Frac.
432	160	160	1.37	100	0.00275	40.00	164.44	84.8	40.64	150.00	300.00	73.6	100.00	0.42
433	160	160	1.37	100	0.00275	40.00	228.89	84.8	40.64	150.00	300.00	73.6	99.93	0.59
434	160	160	1.37	100	0.00275	40.00	293.33	84.8	40.64	150.00	300.00	73.6	99.66	0.75
435	160	160	1.37	100	0.00275	40.00	357.78	84.8	40.64	150.00	300.00	73.6	99.05	0.92
436	160	160	1.37	100	0.00275	40.00	422.22	84.8	40.64	150.00	300.00	73.6	98.08	1.08
437	160	160	1.37	100	0.00275	40.00	486.67	84.8	40.64	150.00	300.00	73.6	96.75	1.25
438	160	160	1.37	100	0.00275	40.00	551.11	84.8	40.64	150.00	300.00	73.6	95.16	1.41
439	160	160	1.37	100	0.00275	40.00	615.56	84.8	40.64	150.00	300.00	73.6	93.34	1.58
440	160	160	1.37	100	0.00275	40.00	680	84.8	40.64	150.00	300.00	73.6	91.40	1.74
441	160	160	1.37	100	0.00275	40.00	100	84.8	40.64	183.33	366.67	73.6	100.00	0.26
442	160	160	1.37	100	0.00275	40.00	164.44	84.8	40.64	183.33	366.67	73.6	100.00	0.42
443	160	160	1.37	100	0.00275	40.00	228.89	84.8	40.64	183.33	366.67	73.6	99.97	0.59
444	160	160	1.37	100	0.00275	40.00	293.33	84.8	40.64	183.33	366.67	73.6	99.82	0.75
445	160	160	1.37	100	0.00275	40.00	357.78	84.8	40.64	183.33	366.67	73.6	99.43	0.92
446	160	160	1.37	100	0.00275	40.00	422.22	84.8	40.64	183.33	366.67	73.6	98.75	1.08
447	160	160	1.37	100	0.00275	40.00	486.67	84.8	40.64	183.33	366.67	73.6	97.76	1.25
448	160	160	1.37	100	0.00275	40.00	551.11	84.8	40.64	183.33	366.67	73.6	96.52	1.41
449	160	160	1.37	100	0.00275	40.00	615.56	84.8	40.64	183.33	366.67	73.6	95.04	1.58
450	160	160	1.37	100	0.00275	40.00	680	84.8	40.64	183.33	366.67	73.6	93.42	1.74
451	160	160	1.37	100	0.00275	40.00	100	84.8	40.64	216.67	433.33	73.6	100.00	0.26
452	160	160	1.37	100	0.00275	40.00	164.44	84.8	40.64	216.67	433.33	73.6	100.00	0.42
453	160	160	1.37	100	0.00275	40.00	228.89	84.8	40.64	216.67	433.33	73.6	99.98	0.59
454	160	160	1.37	100	0.00275	40.00	293.33	84.8	40.64	216.67	433.33	73.6	99.89	0.75
455	160	160	1.37	100	0.00275	40.00	357.78	84.8	40.64	216.67	433.33	73.6	99.62	0.92
456	160	160	1.37	100	0.00275	40.00	422.22	84.8	40.64	216.67	433.33	73.6	99.11	1.08
457	160	160	1.37	100	0.00275	40.00	486.67	84.8	40.64	216.67	433.33	73.6	98.33	1.25
458	160	160	1.37	100	0.00275	40.00	551.11	84.8	40.64	216.67	433.33	73.6	97.32	1.41
459	160	160	1.37	100	0.00275	40.00	615.56	84.8	40.64	216.67	433.33	73.6	96.07	1.58
460	160	160	1.37	100	0.00275	40.00	680	84.8	40.64	216.67	433.33	73.6	94.67	1.74
461	160	160	1.37	100	0.00275	40.00	100	84.8	40.64	250.00	500.00	73.6	100.00	0.26
462	160	160	1.37	100	0.00275	40.00	164.44	84.8	40.64	250.00	500.00	73.6	100.00	0.42
463	160	160	1.37	100	0.00275	40.00	228.89	84.8	40.64	250.00	500.00	73.6	99.99	0.59
464	160	160	1.37	100	0.00275	40.00	293.33	84.8	40.64	250.00	500.00	73.6	99.93	0.75
465	160	160	1.37	100	0.00275	40.00	357.78	84.8	40.64	250.00	500.00	73.6	99.72	0.92
466	160	160	1.37	100	0.00275	40.00	422.22	84.8	40.64	250.00	500.00	73.6	99.33	1.08
467	160	160	1.37	100	0.00275	40.00	486.67	84.8	40.64	250.00	500.00	73.6	98.69	1.25
468	160	160	1.37	100	0.00275	40.00	551.11	84.8	40.64	250.00	500.00	73.6	97.83	1.41
469	160	160	1.37	100	0.00275	40.00	615.56	84.8	40.64	250.00	500.00	73.6	96.75	1.58
470	160	160	1.37	100	0.00275	40.00	680	84.8	40.64	250.00	500.00	73.6	95.51	1.74
471	160	160	1.37	100	0.00275	40.00	100	84.8	40.64	283.33	566.67	73.6	100.00	0.26
472	160	160	1.37	100	0.00275	40.00	164.44	84.8	40.64	283.33	566.67	73.6	100.00	0.42
473	160	160	1.37	100	0.00275	40.00	228.89	84.8	40.64	283.33	566.67	73.6	99.99	0.59
474	160	160	1.37	100	0.00275	40.00	293.33	84.8	40.64	283.33	566.67	73.6	99.95	0.75
475	160	160	1.37	100	0.00275	40.00	357.78	84.8	40.64	283.33	566.67	73.6	99.79	0.92
476	160	160	1.37	100	0.00275	40.00	422.22	84.8	40.64	283.33	566.67	73.6	99.46	1.08
477	160	160	1.37	100	0.00275	40.00	486.67	84.8	40.64	283.33	566.67	73.6	98.92	1.25
478	160	160	1.37	100	0.00275	40.00	551.11	84.8	40.64	283.33	566.67	73.6	98.17	1.41
479	160	160	1.37	100	0.00275	40.00	615.56	84.8	40.64	283.33	566.67	73.6	97.21	1.58

#	W cm	H cm	r cm	l = x cm	k cm ² /mW-s	P W	Airflow m ³ /min	x cm	y cm	z cm	L cm	p	Actual Kill Rate	Work Frac.
480	160	160	1.37	100	0.00275	40.00	680	84.8	40.64	283.33	566.67	73.6	96.10	1.74
481	160	160	1.37	100	0.00275	40.00	100	84.8	40.64	316.67	633.33	73.6	100.00	0.26
482	160	160	1.37	100	0.00275	40.00	164.44	84.8	40.64	316.67	633.33	73.6	100.00	0.42
483	160	160	1.37	100	0.00275	40.00	228.89	84.8	40.64	316.67	633.33	73.6	100.00	0.59
484	160	160	1.37	100	0.00275	40.00	293.33	84.8	40.64	316.67	633.33	73.6	99.96	0.75
485	160	160	1.37	100	0.00275	40.00	357.78	84.8	40.64	316.67	633.33	73.6	99.83	0.92
486	160	160	1.37	100	0.00275	40.00	422.22	84.8	40.64	316.67	633.33	73.6	99.55	1.08
487	160	160	1.37	100	0.00275	40.00	486.67	84.8	40.64	316.67	633.33	73.6	99.08	1.25
488	160	160	1.37	100	0.00275	40.00	551.11	84.8	40.64	316.67	633.33	73.6	98.41	1.41
489	160	160	1.37	100	0.00275	40.00	615.56	84.8	40.64	316.67	633.33	73.6	97.54	1.58
490	160	160	1.37	100	0.00275	40.00	680	84.8	40.64	316.67	633.33	73.6	96.52	1.74
491	160	160	1.37	100	0.00275	40.00	100	84.8	40.64	350.00	700.00	73.6	100.00	0.26
492	160	160	1.37	100	0.00275	40.00	164.44	84.8	40.64	350.00	700.00	73.6	100.00	0.42
493	160	160	1.37	100	0.00275	40.00	228.89	84.8	40.64	350.00	700.00	73.6	100.00	0.59
494	160	160	1.37	100	0.00275	40.00	293.33	84.8	40.64	350.00	700.00	73.6	99.97	0.75
495	160	160	1.37	100	0.00275	40.00	357.78	84.8	40.64	350.00	700.00	73.6	99.86	0.92
496	160	160	1.37	100	0.00275	40.00	422.22	84.8	40.64	350.00	700.00	73.6	99.62	1.08
497	160	160	1.37	100	0.00275	40.00	486.67	84.8	40.64	350.00	700.00	73.6	99.20	1.25
498	160	160	1.37	100	0.00275	40.00	551.11	84.8	40.64	350.00	700.00	73.6	98.59	1.41
499	160	160	1.37	100	0.00275	40.00	615.56	84.8	40.64	350.00	700.00	73.6	97.79	1.58
500	160	160	1.37	100	0.00275	40.00	680	84.8	40.64	350.00	700.00	73.6	96.84	1.74
501	160	160	1.37	100	0.00275	40.00	100	84.8	40.64	120.00	240.00	54.0	100.00	0.26
502	160	160	1.37	100	0.00275	40.00	164.44	84.8	40.64	120.00	240.00	54.0	99.88	0.42
503	160	160	1.37	100	0.00275	40.00	228.89	84.8	40.64	120.00	240.00	54.0	99.17	0.59
504	160	160	1.37	100	0.00275	40.00	293.33	84.8	40.64	120.00	240.00	54.0	97.64	0.75
505	160	160	1.37	100	0.00275	40.00	357.78	84.8	40.64	120.00	240.00	54.0	95.34	0.92
506	160	160	1.37	100	0.00275	40.00	422.22	84.8	40.64	120.00	240.00	54.0	92.58	1.08
507	160	160	1.37	100	0.00275	40.00	486.67	84.8	40.64	120.00	240.00	54.0	89.50	1.25
508	160	160	1.37	100	0.00275	40.00	551.11	84.8	40.64	120.00	240.00	54.0	86.36	1.41
509	160	160	1.37	100	0.00275	40.00	615.56	84.8	40.64	120.00	240.00	54.0	83.16	1.58
510	160	160	1.37	100	0.00275	40.00	680	84.8	40.64	120.00	240.00	54.0	80.09	1.74
511	160	160	1.37	100	0.00275	40.00	100	84.8	40.64	120.00	240.00	58.4	100.00	0.26
512	160	160	1.37	100	0.00275	40.00	164.44	84.8	40.64	120.00	240.00	58.4	99.92	0.42
513	160	160	1.37	100	0.00275	40.00	228.89	84.8	40.64	120.00	240.00	58.4	99.39	0.59
514	160	160	1.37	100	0.00275	40.00	293.33	84.8	40.64	120.00	240.00	58.4	98.15	0.75
515	160	160	1.37	100	0.00275	40.00	357.78	84.8	40.64	120.00	240.00	58.4	96.18	0.92
516	160	160	1.37	100	0.00275	40.00	422.22	84.8	40.64	120.00	240.00	58.4	93.73	1.08
517	160	160	1.37	100	0.00275	40.00	486.67	84.8	40.64	120.00	240.00	58.4	90.93	1.25
518	160	160	1.37	100	0.00275	40.00	551.11	84.8	40.64	120.00	240.00	58.4	88.01	1.41
519	160	160	1.37	100	0.00275	40.00	615.56	84.8	40.64	120.00	240.00	58.4	85.00	1.58
520	160	160	1.37	100	0.00275	40.00	680	84.8	40.64	120.00	240.00	58.4	82.07	1.74
521	160	160	1.37	100	0.00275	40.00	100	84.8	40.64	120.00	240.00	62.7	100.00	0.26
522	160	160	1.37	100	0.00275	40.00	164.44	84.8	40.64	120.00	240.00	62.7	99.95	0.42
523	160	160	1.37	100	0.00275	40.00	228.89	84.8	40.64	120.00	240.00	62.7	99.56	0.59
524	160	160	1.37	100	0.00275	40.00	293.33	84.8	40.64	120.00	240.00	62.7	98.57	0.75
525	160	160	1.37	100	0.00275	40.00	357.78	84.8	40.64	120.00	240.00	62.7	96.90	0.92
526	160	160	1.37	100	0.00275	40.00	422.22	84.8	40.64	120.00	240.00	62.7	94.75	1.08
527	160	160	1.37	100	0.00275	40.00	486.67	84.8	40.64	120.00	240.00	62.7	92.23	1.25

#	W cm	H cm	r cm	l = x cm	k cm ² /mW-s	P W	Airflow m ³ /min	x cm	y cm	z cm	L cm	p	Actual Kill Rate	Work Frac.
528	160	160	1.37	100	0.00275	40.00	551.11	84.8	40.64	120.00	240.00	62.7	89.54	1.41
529	160	160	1.37	100	0.00275	40.00	615.56	84.8	40.64	120.00	240.00	62.7	86.73	1.58
530	160	160	1.37	100	0.00275	40.00	680	84.8	40.64	120.00	240.00	62.7	83.95	1.74
531	160	160	1.37	100	0.00275	40.00	100	84.8	40.64	120.00	240.00	67.1	100.00	0.26
532	160	160	1.37	100	0.00275	40.00	164.44	84.8	40.64	120.00	240.00	67.1	99.97	0.42
533	160	160	1.37	100	0.00275	40.00	228.89	84.8	40.64	120.00	240.00	67.1	99.70	0.59
534	160	160	1.37	100	0.00275	40.00	293.33	84.8	40.64	120.00	240.00	67.1	98.92	0.75
535	160	160	1.37	100	0.00275	40.00	357.78	84.8	40.64	120.00	240.00	67.1	97.55	0.92
536	160	160	1.37	100	0.00275	40.00	422.22	84.8	40.64	120.00	240.00	67.1	95.69	1.08
537	160	160	1.37	100	0.00275	40.00	486.67	84.8	40.64	120.00	240.00	67.1	93.45	1.25
538	160	160	1.37	100	0.00275	40.00	551.11	84.8	40.64	120.00	240.00	67.1	91.01	1.41
539	160	160	1.37	100	0.00275	40.00	615.56	84.8	40.64	120.00	240.00	67.1	88.41	1.58
540	160	160	1.37	100	0.00275	40.00	680	84.8	40.64	120.00	240.00	67.1	85.80	1.74
541	160	160	1.37	100	0.00275	40.00	100	84.8	40.64	120.00	240.00	71.5	100.00	0.26
542	160	160	1.37	100	0.00275	40.00	164.44	84.8	40.64	120.00	240.00	71.5	99.98	0.42
543	160	160	1.37	100	0.00275	40.00	228.89	84.8	40.64	120.00	240.00	71.5	99.80	0.59
544	160	160	1.37	100	0.00275	40.00	293.33	84.8	40.64	120.00	240.00	71.5	99.21	0.75
545	160	160	1.37	100	0.00275	40.00	357.78	84.8	40.64	120.00	240.00	71.5	98.09	0.92
546	160	160	1.37	100	0.00275	40.00	422.22	84.8	40.64	120.00	240.00	71.5	96.52	1.08
547	160	160	1.37	100	0.00275	40.00	486.67	84.8	40.64	120.00	240.00	71.5	94.56	1.25
548	160	160	1.37	100	0.00275	40.00	551.11	84.8	40.64	120.00	240.00	71.5	92.37	1.41
549	160	160	1.37	100	0.00275	40.00	615.56	84.8	40.64	120.00	240.00	71.5	89.99	1.58
550	160	160	1.37	100	0.00275	40.00	680	84.8	40.64	120.00	240.00	71.5	87.57	1.74
551	160	160	1.37	100	0.00275	40.00	100	84.8	40.64	120.00	240.00	75.8	100.00	0.26
552	160	160	1.37	100	0.00275	40.00	164.44	84.8	40.64	120.00	240.00	75.8	99.99	0.42
553	160	160	1.37	100	0.00275	40.00	228.89	84.8	40.64	120.00	240.00	75.8	99.87	0.59
554	160	160	1.37	100	0.00275	40.00	293.33	84.8	40.64	120.00	240.00	75.8	99.43	0.75
555	160	160	1.37	100	0.00275	40.00	357.78	84.8	40.64	120.00	240.00	75.8	98.54	0.92
556	160	160	1.37	100	0.00275	40.00	422.22	84.8	40.64	120.00	240.00	75.8	97.23	1.08
557	160	160	1.37	100	0.00275	40.00	486.67	84.8	40.64	120.00	240.00	75.8	95.53	1.25
558	160	160	1.37	100	0.00275	40.00	551.11	84.8	40.64	120.00	240.00	75.8	93.59	1.41
559	160	160	1.37	100	0.00275	40.00	615.56	84.8	40.64	120.00	240.00	75.8	91.43	1.58
560	160	160	1.37	100	0.00275	40.00	680	84.8	40.64	120.00	240.00	75.8	89.20	1.74
561	160	160	1.37	100	0.00275	40.00	100	84.8	40.64	120.00	240.00	80.2	100.00	0.26
562	160	160	1.37	100	0.00275	40.00	164.44	84.8	40.64	120.00	240.00	80.2	99.99	0.42
563	160	160	1.37	100	0.00275	40.00	228.89	84.8	40.64	120.00	240.00	80.2	99.92	0.59
564	160	160	1.37	100	0.00275	40.00	293.33	84.8	40.64	120.00	240.00	80.2	99.60	0.75
565	160	160	1.37	100	0.00275	40.00	357.78	84.8	40.64	120.00	240.00	80.2	98.92	0.92
566	160	160	1.37	100	0.00275	40.00	422.22	84.8	40.64	120.00	240.00	80.2	97.85	1.08
567	160	160	1.37	100	0.00275	40.00	486.67	84.8	40.64	120.00	240.00	80.2	96.41	1.25
568	160	160	1.37	100	0.00275	40.00	551.11	84.8	40.64	120.00	240.00	80.2	94.72	1.41
569	160	160	1.37	100	0.00275	40.00	615.56	84.8	40.64	120.00	240.00	80.2	92.80	1.58
570	160	160	1.37	100	0.00275	40.00	680	84.8	40.64	120.00	240.00	80.2	90.77	1.74
571	160	160	1.37	100	0.00275	40.00	100	84.8	40.64	120.00	240.00	84.6	100.00	0.26
572	160	160	1.37	100	0.00275	40.00	164.44	84.8	40.64	120.00	240.00	84.6	100.00	0.42
573	160	160	1.37	100	0.00275	40.00	228.89	84.8	40.64	120.00	240.00	84.6	99.95	0.59
574	160	160	1.37	100	0.00275	40.00	293.33	84.8	40.64	120.00	240.00	84.6	99.73	0.75
575	160	160	1.37	100	0.00275	40.00	357.78	84.8	40.64	120.00	240.00	84.6	99.22	0.92

#	W cm	H cm	r cm	l = x cm	k cm ² /mW-s	P W	Airflow m ³ /min	x cm	y cm	z cm	L cm	p	Actual Kill Rate	Work Frac.
576	160	160	1.37	100	0.00275	40.00	422.22	84.8	40.64	120.00	240.00	84.6	98.37	1.08
577	160	160	1.37	100	0.00275	40.00	486.67	84.8	40.64	120.00	240.00	84.6	97.18	1.25
578	160	160	1.37	100	0.00275	40.00	551.11	84.8	40.64	120.00	240.00	84.6	95.73	1.41
579	160	160	1.37	100	0.00275	40.00	615.56	84.8	40.64	120.00	240.00	84.6	94.04	1.58
580	160	160	1.37	100	0.00275	40.00	680	84.8	40.64	120.00	240.00	84.6	92.23	1.74
581	160	160	1.37	100	0.00275	40.00	100	84.8	40.64	120.00	240.00	88.9	100.00	0.26
582	160	160	1.37	100	0.00275	40.00	164.44	84.8	40.64	120.00	240.00	88.9	100.00	0.42
583	160	160	1.37	100	0.00275	40.00	228.89	84.8	40.64	120.00	240.00	88.9	99.97	0.59
584	160	160	1.37	100	0.00275	40.00	293.33	84.8	40.64	120.00	240.00	88.9	99.83	0.75
585	160	160	1.37	100	0.00275	40.00	357.78	84.8	40.64	120.00	240.00	88.9	99.45	0.92
586	160	160	1.37	100	0.00275	40.00	422.22	84.8	40.64	120.00	240.00	88.9	98.79	1.08
587	160	160	1.37	100	0.00275	40.00	486.67	84.8	40.64	120.00	240.00	88.9	97.81	1.25
588	160	160	1.37	100	0.00275	40.00	551.11	84.8	40.64	120.00	240.00	88.9	96.59	1.41
589	160	160	1.37	100	0.00275	40.00	615.56	84.8	40.64	120.00	240.00	88.9	95.13	1.58
590	160	160	1.37	100	0.00275	40.00	680	84.8	40.64	120.00	240.00	88.9	93.53	1.74
591	160	160	1.37	100	0.00275	40.00	100	84.8	40.64	120.00	240.00	93.3	100.00	0.26
592	160	160	1.37	100	0.00275	40.00	164.44	84.8	40.64	120.00	240.00	93.3	100.00	0.42
593	160	160	1.37	100	0.00275	40.00	228.89	84.8	40.64	120.00	240.00	93.3	99.98	0.59
594	160	160	1.37	100	0.00275	40.00	293.33	84.8	40.64	120.00	240.00	93.3	99.89	0.75
595	160	160	1.37	100	0.00275	40.00	357.78	84.8	40.64	120.00	240.00	93.3	99.63	0.92
596	160	160	1.37	100	0.00275	40.00	422.22	84.8	40.64	120.00	240.00	93.3	99.13	1.08
597	160	160	1.37	100	0.00275	40.00	486.67	84.8	40.64	120.00	240.00	93.3	98.36	1.25
598	160	160	1.37	100	0.00275	40.00	551.11	84.8	40.64	120.00	240.00	93.3	97.36	1.41
599	160	160	1.37	100	0.00275	40.00	615.56	84.8	40.64	120.00	240.00	93.3	96.12	1.58
600	160	160	1.37	100	0.00275	40.00	680	84.8	40.64	120.00	240.00	93.3	94.74	1.74

NOTE: Work Fraction is the fraction of total airflow compared to the design airflow.

It represents the fractional volume of air disinfected when the airflow is being varied.

APPENDIX P: First Costs for Cost Optimization

#	UV Lamp \$	Duct ft2	Duct Matl, \$	Labor \$	Fan FC \$	Filter FC \$	Reflect Type \$/ft2	Refl Matl, \$	Total FC \$	Annual FC \$
1	594.46	68.89	332.74	494.44	200	275.56	1.667	114.81	2012.00	204.93
2	717.07	68.89	332.73	494.44	200	275.56	1.667	114.81	2134.61	217.41
3	836.88	68.89	332.73	494.44	200	275.56	1.667	114.81	2254.42	229.62
4	953.88	68.89	332.73	494.44	200	275.56	1.667	114.81	2371.42	241.53
5	1068.07	68.89	332.73	494.44	200	275.56	1.667	114.81	2485.61	253.17
6	1179.47	68.89	332.73	494.44	200	275.56	1.667	114.81	2597.01	264.51
7	1288.05	68.89	332.73	494.44	200	275.56	1.667	114.81	2705.59	275.57
8	1393.84	68.89	332.73	494.44	200	275.56	1.667	114.81	2811.38	286.34
9	1496.81	68.89	332.73	494.44	200	275.56	1.667	114.81	2914.35	296.83
10	1596.99	68.89	332.73	494.44	200	275.56	1.667	114.81	3014.53	307.04
11	594.46	114.82	554.56	517.41	200	275.56	1.667	191.34	2333.32	237.65
12	717.07	114.82	554.56	517.41	200	275.56	1.667	191.34	2455.93	250.14
13	836.88	114.82	554.56	517.41	200	275.56	1.667	191.34	2575.74	262.34
14	953.88	114.82	554.56	517.41	200	275.56	1.667	191.34	2692.74	274.26
15	1068.07	114.82	554.56	517.41	200	275.56	1.667	191.34	2806.94	285.89
16	1179.47	114.82	554.56	517.41	200	275.56	1.667	191.34	2918.33	297.24
17	1288.05	114.82	554.56	517.41	200	275.56	1.667	191.34	3026.92	308.30
18	1393.84	114.82	554.56	517.41	200	275.56	1.667	191.34	3132.70	319.07
19	1496.81	114.82	554.56	517.41	200	275.56	1.667	191.34	3235.68	329.56
20	1596.99	114.82	554.56	517.41	200	275.56	1.667	191.34	3335.85	339.76
21	594.46	160.74	776.38	540.37	200	275.56	1.667	267.88	2654.65	270.38
22	717.07	160.74	776.38	540.37	200	275.56	1.667	267.88	2777.26	282.87
23	836.88	160.74	776.38	540.37	200	275.56	1.667	267.88	2897.06	295.07
24	953.88	160.74	776.38	540.37	200	275.56	1.667	267.88	3014.06	306.99
25	1068.07	160.74	776.38	540.37	200	275.56	1.667	267.88	3128.26	318.62
26	1179.47	160.74	776.38	540.37	200	275.56	1.667	267.88	3239.65	329.97
27	1288.05	160.74	776.38	540.37	200	275.56	1.667	267.88	3348.24	341.03
28	1393.84	160.74	776.38	540.37	200	275.56	1.667	267.88	3454.02	351.80
29	1496.81	160.74	776.38	540.37	200	275.56	1.667	267.88	3557.00	362.29
30	1596.99	160.74	776.38	540.37	200	275.56	1.667	267.88	3657.17	372.49
31	594.46	206.67	998.20	563.33	200	275.56	1.667	344.42	2975.97	303.11
32	717.07	206.67	998.20	563.33	200	275.56	1.667	344.42	3098.58	315.60
33	836.88	206.67	998.20	563.33	200	275.56	1.667	344.42	3218.39	327.80
34	953.88	206.67	998.20	563.33	200	275.56	1.667	344.42	3335.39	339.72
35	1068.07	206.67	998.20	563.33	200	275.56	1.667	344.42	3449.58	351.35
36	1179.47	206.67	998.20	563.33	200	275.56	1.667	344.42	3560.98	362.69
37	1288.05	206.67	998.20	563.33	200	275.56	1.667	344.42	3669.56	373.75
38	1393.84	206.67	998.20	563.33	200	275.56	1.667	344.42	3775.35	384.53
39	1496.81	206.67	998.20	563.33	200	275.56	1.667	344.42	3878.32	395.02
40	1596.99	206.67	998.20	563.33	200	275.56	1.667	344.42	3978.50	405.22
41	594.46	252.59	1220.02	586.30	200	275.56	1.667	420.96	3297.29	335.84
42	717.07	252.59	1220.02	586.30	200	275.56	1.667	420.96	3419.90	348.32
43	836.88	252.59	1220.02	586.30	200	275.56	1.667	420.96	3539.71	360.53
44	953.88	252.59	1220.02	586.30	200	275.56	1.667	420.96	3656.71	372.44
45	1068.07	252.59	1220.02	586.30	200	275.56	1.667	420.96	3770.91	384.08
46	1179.47	252.59	1220.02	586.30	200	275.56	1.667	420.96	3882.30	395.42
47	1288.05	252.59	1220.02	586.30	200	275.56	1.667	420.96	3990.89	406.48

#	UV Lamp \$	Duct ft2	Duct Matl, \$	Labor \$	Fan FC \$	Filter FC \$	Reflect Type \$/ft2	Refl Matl, \$	Total FC \$	Annual FC \$
48	1393.84	252.59	1220.02	586.30	200	275.56	1.667	420.96	4096.67	417.25
49	1496.81	252.59	1220.02	586.30	200	275.56	1.667	420.96	4199.65	427.74
50	1596.99	252.59	1220.02	586.30	200	275.56	1.667	420.96	4299.82	437.95
51	594.46	298.52	1441.85	609.26	200	275.56	1.667	497.49	3618.62	368.56
52	717.07	298.52	1441.85	609.26	200	275.56	1.667	497.49	3741.23	381.05
53	836.88	298.52	1441.85	609.26	200	275.56	1.667	497.49	3861.03	393.25
54	953.88	298.52	1441.85	609.26	200	275.56	1.667	497.49	3978.03	405.17
55	1068.07	298.52	1441.85	609.26	200	275.56	1.667	497.49	4092.23	416.80
56	1179.47	298.52	1441.85	609.26	200	275.56	1.667	497.49	4203.62	428.15
57	1288.05	298.52	1441.85	609.26	200	275.56	1.667	497.49	4312.21	439.21
58	1393.84	298.52	1441.85	609.26	200	275.56	1.667	497.49	4417.99	449.98
59	1496.81	298.52	1441.85	609.26	200	275.56	1.667	497.49	4520.97	460.47
60	1596.99	298.52	1441.85	609.26	200	275.56	1.667	497.49	4621.14	470.67
61	594.46	344.45	1663.67	632.22	200	275.56	1.667	574.03	3939.94	401.29
62	717.07	344.45	1663.67	632.22	200	275.56	1.667	574.03	4062.55	413.78
63	836.88	344.45	1663.67	632.22	200	275.56	1.667	574.03	4182.35	425.98
64	953.88	344.45	1663.67	632.22	200	275.56	1.667	574.03	4299.36	437.90
65	1068.07	344.45	1663.67	632.22	200	275.56	1.667	574.03	4413.55	449.53
66	1179.47	344.45	1663.67	632.22	200	275.56	1.667	574.03	4524.94	460.88
67	1288.05	344.45	1663.67	632.22	200	275.56	1.667	574.03	4633.53	471.94
68	1393.84	344.45	1663.67	632.22	200	275.56	1.667	574.03	4739.31	482.71
69	1496.81	344.45	1663.67	632.22	200	275.56	1.667	574.03	4842.29	493.20
70	1596.99	344.45	1663.67	632.22	200	275.56	1.667	574.03	4942.47	503.40
71	594.46	390.37	1885.49	655.19	200	275.56	1.667	650.57	4261.26	434.02
72	717.07	390.37	1885.49	655.19	200	275.56	1.667	650.57	4383.87	446.51
73	836.88	390.37	1885.49	655.19	200	275.56	1.667	650.57	4503.68	458.71
74	953.88	390.37	1885.49	655.19	200	275.56	1.667	650.57	4620.68	470.63
75	1068.07	390.37	1885.49	655.19	200	275.56	1.667	650.57	4734.88	482.26
76	1179.47	390.37	1885.49	655.19	200	275.56	1.667	650.57	4846.27	493.60
77	1288.05	390.37	1885.49	655.19	200	275.56	1.667	650.57	4954.85	504.66
78	1393.84	390.37	1885.49	655.19	200	275.56	1.667	650.57	5060.64	515.44
79	1496.81	390.37	1885.49	655.19	200	275.56	1.667	650.57	5163.62	525.93
80	1596.99	390.37	1885.49	655.19	200	275.56	1.667	650.57	5263.79	536.13
81	594.46	436.30	2107.32	678.15	200	275.56	1.667	727.11	4582.58	466.75
82	717.07	436.30	2107.32	678.15	200	275.56	1.667	727.11	4705.19	479.23
83	836.88	436.30	2107.32	678.15	200	275.56	1.667	727.11	4825.00	491.44
84	953.88	436.30	2107.32	678.15	200	275.56	1.667	727.11	4942.00	503.35
85	1068.07	436.30	2107.32	678.15	200	275.56	1.667	727.11	5056.20	514.98
86	1179.47	436.30	2107.32	678.15	200	275.56	1.667	727.11	5167.59	526.33
87	1288.05	436.30	2107.32	678.15	200	275.56	1.667	727.11	5276.18	537.39
88	1393.84	436.30	2107.32	678.15	200	275.56	1.667	727.11	5381.96	548.16
89	1496.81	436.30	2107.32	678.15	200	275.56	1.667	727.11	5484.94	558.65
90	1596.99	436.30	2107.32	678.15	200	275.56	1.667	727.11	5585.11	568.86
91	594.46	482.22	2329.14	701.11	200	275.56	1.667	803.64	4903.91	499.47
92	717.07	482.22	2329.14	701.11	200	275.56	1.667	803.64	5026.52	511.96
93	836.88	482.22	2329.14	701.11	200	275.56	1.667	803.64	5146.32	524.16
94	953.88	482.22	2329.14	701.11	200	275.56	1.667	803.64	5263.33	536.08
95	1068.07	482.22	2329.14	701.11	200	275.56	1.667	803.64	5377.52	547.71

#	UV Lamp \$	Duct ft2	Duct Matl, \$	Labor \$	Fan FC \$	Filter FC \$	Reflect Type \$/ft2	Refl Matl, \$	Total FC \$	Annual FC \$
96	1179.47	482.22	2329.14	701.11	200	275.56	1.667	803.64	5488.91	559.06
97	1288.05	482.22	2329.14	701.11	200	275.56	1.667	803.64	5597.50	570.12
98	1393.84	482.22	2329.14	701.11	200	275.56	1.667	803.64	5703.28	580.89
99	1496.81	482.22	2329.14	701.11	200	275.56	1.667	803.64	5806.26	591.38
100	1596.99	482.22	2329.14	701.11	200	275.56	1.667	803.64	5906.44	601.58
101	594.46	165.33	798.56	542.67	200	275.56	0.000	0.00	2411.24	245.59
102	717.07	165.33	798.56	542.67	200	275.56	0.000	0.00	2533.85	258.08
103	836.88	165.33	798.56	542.67	200	275.56	0.000	0.00	2653.66	270.28
104	953.88	165.33	798.56	542.67	200	275.56	0.000	0.00	2770.66	282.20
105	1068.07	165.33	798.56	542.67	200	275.56	0.000	0.00	2884.86	293.83
106	1179.47	165.33	798.56	542.67	200	275.56	0.000	0.00	2996.25	305.17
107	1288.05	165.33	798.56	542.67	200	275.56	0.000	0.00	3104.84	316.23
108	1393.84	165.33	798.56	542.67	200	275.56	0.000	0.00	3210.62	327.01
109	1496.81	165.33	798.56	542.67	200	275.56	0.000	0.00	3313.60	337.50
110	1596.99	165.33	798.56	542.67	200	275.56	0.000	0.00	3413.77	347.70
111	594.46	165.33	798.56	542.67	200	275.56	0.319	52.77	2464.01	250.97
112	717.07	165.33	798.56	542.67	200	275.56	0.319	52.77	2586.62	263.45
113	836.88	165.33	798.56	542.67	200	275.56	0.319	52.77	2706.43	275.66
114	953.88	165.33	798.56	542.67	200	275.56	0.319	52.77	2823.43	287.57
115	1068.07	165.33	798.56	542.67	200	275.56	0.319	52.77	2937.63	299.20
116	1179.47	165.33	798.56	542.67	200	275.56	0.319	52.77	3049.02	310.55
117	1288.05	165.33	798.56	542.67	200	275.56	0.319	52.77	3157.61	321.61
118	1393.84	165.33	798.56	542.67	200	275.56	0.319	52.77	3263.39	332.38
119	1496.81	165.33	798.56	542.67	200	275.56	0.319	52.77	3366.37	342.87
120	1596.99	165.33	798.56	542.67	200	275.56	0.319	52.77	3466.54	353.07
121	594.46	165.33	798.56	542.67	200	275.56	0.704	116.42	2527.66	257.45
122	717.07	165.33	798.56	542.67	200	275.56	0.704	116.42	2650.27	269.94
123	836.88	165.33	798.56	542.67	200	275.56	0.704	116.42	2770.08	282.14
124	953.88	165.33	798.56	542.67	200	275.56	0.704	116.42	2887.08	294.06
125	1068.07	165.33	798.56	542.67	200	275.56	0.704	116.42	3001.27	305.69
126	1179.47	165.33	798.56	542.67	200	275.56	0.704	116.42	3112.67	317.03
127	1288.05	165.33	798.56	542.67	200	275.56	0.704	116.42	3221.25	328.09
128	1393.84	165.33	798.56	542.67	200	275.56	0.704	116.42	3327.04	338.87
129	1496.81	165.33	798.56	542.67	200	275.56	0.704	116.42	3430.01	349.35
130	1596.99	165.33	798.56	542.67	200	275.56	0.704	116.42	3530.19	359.56
131	594.46	165.33	798.56	542.67	200	275.56	1.089	180.06	2591.31	263.93
132	717.07	165.33	798.56	542.67	200	275.56	1.089	180.06	2713.92	276.42
133	836.88	165.33	798.56	542.67	200	275.56	1.089	180.06	2833.72	288.62
134	953.88	165.33	798.56	542.67	200	275.56	1.089	180.06	2950.72	300.54
135	1068.07	165.33	798.56	542.67	200	275.56	1.089	180.06	3064.92	312.17
136	1179.47	165.33	798.56	542.67	200	275.56	1.089	180.06	3176.31	323.51
137	1288.05	165.33	798.56	542.67	200	275.56	1.089	180.06	3284.90	334.57
138	1393.84	165.33	798.56	542.67	200	275.56	1.089	180.06	3390.68	345.35
139	1496.81	165.33	798.56	542.67	200	275.56	1.089	180.06	3493.66	355.84
140	1596.99	165.33	798.56	542.67	200	275.56	1.089	180.06	3593.84	366.04
141	594.46	165.33	798.56	542.67	200	275.56	1.474	243.71	2654.95	270.41
142	717.07	165.33	798.56	542.67	200	275.56	1.474	243.71	2777.57	282.90
143	836.88	165.33	798.56	542.67	200	275.56	1.474	243.71	2897.37	295.10

#	UV Lamp \$	Duct ft2	Duct Matl, \$	Labor \$	Fan FC \$	Filter FC \$	Reflect Type \$/ft2	Refl Matl, \$	Total FC \$	Annual FC \$
144	953.88	165.33	798.56	542.67	200	275.56	1.474	243.71	3014.37	307.02
145	1068.07	165.33	798.56	542.67	200	275.56	1.474	243.71	3128.57	318.65
146	1179.47	165.33	798.56	542.67	200	275.56	1.474	243.71	3239.96	330.00
147	1288.05	165.33	798.56	542.67	200	275.56	1.474	243.71	3348.55	341.06
148	1393.84	165.33	798.56	542.67	200	275.56	1.474	243.71	3454.33	351.83
149	1496.81	165.33	798.56	542.67	200	275.56	1.474	243.71	3557.31	362.32
150	1596.99	165.33	798.56	542.67	200	275.56	1.474	243.71	3657.48	372.52
151	594.46	165.33	798.56	542.67	200	275.56	1.859	307.36	2718.60	276.90
152	717.07	165.33	798.56	542.67	200	275.56	1.859	307.36	2841.21	289.38
153	836.88	165.33	798.56	542.67	200	275.56	1.859	307.36	2961.02	301.59
154	953.88	165.33	798.56	542.67	200	275.56	1.859	307.36	3078.02	313.50
155	1068.07	165.33	798.56	542.67	200	275.56	1.859	307.36	3192.22	325.13
156	1179.47	165.33	798.56	542.67	200	275.56	1.859	307.36	3303.61	336.48
157	1288.05	165.33	798.56	542.67	200	275.56	1.859	307.36	3412.20	347.54
158	1393.84	165.33	798.56	542.67	200	275.56	1.859	307.36	3517.98	358.31
159	1496.81	165.33	798.56	542.67	200	275.56	1.859	307.36	3620.96	368.80
160	1596.99	165.33	798.56	542.67	200	275.56	1.859	307.36	3721.13	379.01
161	594.46	165.33	798.56	542.67	200	275.56	2.244	371.01	2782.25	283.38
162	717.07	165.33	798.56	542.67	200	275.56	2.244	371.01	2904.86	295.87
163	836.88	165.33	798.56	542.67	200	275.56	2.244	371.01	3024.67	308.07
164	953.88	165.33	798.56	542.67	200	275.56	2.244	371.01	3141.67	319.99
165	1068.07	165.33	798.56	542.67	200	275.56	2.244	371.01	3255.86	331.62
166	1179.47	165.33	798.56	542.67	200	275.56	2.244	371.01	3367.26	342.96
167	1288.05	165.33	798.56	542.67	200	275.56	2.244	371.01	3475.84	354.02
168	1393.84	165.33	798.56	542.67	200	275.56	2.244	371.01	3581.63	364.80
169	1496.81	165.33	798.56	542.67	200	275.56	2.244	371.01	3684.60	375.29
170	1596.99	165.33	798.56	542.67	200	275.56	2.244	371.01	3784.78	385.49
171	594.46	165.33	798.56	542.67	200	275.56	2.629	434.65	2845.90	289.86
172	717.07	165.33	798.56	542.67	200	275.56	2.629	434.65	2968.51	302.35
173	836.88	165.33	798.56	542.67	200	275.56	2.629	434.65	3088.31	314.55
174	953.88	165.33	798.56	542.67	200	275.56	2.629	434.65	3205.31	326.47
175	1068.07	165.33	798.56	542.67	200	275.56	2.629	434.65	3319.51	338.10
176	1179.47	165.33	798.56	542.67	200	275.56	2.629	434.65	3430.90	349.45
177	1288.05	165.33	798.56	542.67	200	275.56	2.629	434.65	3539.49	360.50
178	1393.84	165.33	798.56	542.67	200	275.56	2.629	434.65	3645.27	371.28
179	1496.81	165.33	798.56	542.67	200	275.56	2.629	434.65	3748.25	381.77
180	1596.99	165.33	798.56	542.67	200	275.56	2.629	434.65	3848.42	391.97
181	594.46	165.33	798.56	542.67	200	275.56	3.014	498.30	2909.54	296.34
182	717.07	165.33	798.56	542.67	200	275.56	3.014	498.30	3032.15	308.83
183	836.88	165.33	798.56	542.67	200	275.56	3.014	498.30	3151.96	321.03
184	953.88	165.33	798.56	542.67	200	275.56	3.014	498.30	3268.96	332.95
185	1068.07	165.33	798.56	542.67	200	275.56	3.014	498.30	3383.16	344.58
186	1179.47	165.33	798.56	542.67	200	275.56	3.014	498.30	3494.55	355.93
187	1288.05	165.33	798.56	542.67	200	275.56	3.014	498.30	3603.14	366.99
188	1393.84	165.33	798.56	542.67	200	275.56	3.014	498.30	3708.92	377.76
189	1496.81	165.33	798.56	542.67	200	275.56	3.014	498.30	3811.90	388.25
190	1596.99	165.33	798.56	542.67	200	275.56	3.014	498.30	3912.07	398.45
191	594.46	165.33	798.56	542.67	200	275.56	3.399	561.95	2973.19	302.83

#	UV Lamp \$	Duct ft2	Duct Matl, \$	Labor \$	Fan FC \$	Filter FC \$	Reflect Type \$/ft2	Refl Matl, \$	Total FC \$	Annual FC \$
192	717.07	165.33	798.56	542.67	200	275.56	3.399	561.95	3095.80	315.31
193	836.88	165.33	798.56	542.67	200	275.56	3.399	561.95	3215.61	327.52
194	953.88	165.33	798.56	542.67	200	275.56	3.399	561.95	3332.61	339.43
195	1068.07	165.33	798.56	542.67	200	275.56	3.399	561.95	3446.81	351.06
196	1179.47	165.33	798.56	542.67	200	275.56	3.399	561.95	3558.20	362.41
197	1288.05	165.33	798.56	542.67	200	275.56	3.399	561.95	3666.79	373.47
198	1393.84	165.33	798.56	542.67	200	275.56	3.399	561.95	3772.57	384.24
199	1496.81	165.33	798.56	542.67	200	275.56	3.399	561.95	3875.55	394.73
200	1596.99	165.33	798.56	542.67	200	275.56	3.399	561.95	3975.72	404.94
201	1124.12	68.89	332.73	494.44	200	275.56	0.000	0.00	2426.85	247.18
202	1124.12	114.82	554.56	517.41	200	275.56	0.000	0.00	2671.64	272.11
203	1124.12	160.74	776.38	540.37	200	275.56	0.000	0.00	2916.43	297.04
204	1124.12	206.67	998.20	563.33	200	275.56	0.000	0.00	3161.21	321.98
205	1124.12	252.59	1220.02	586.30	200	275.56	0.000	0.00	3406.00	346.91
206	1124.12	298.52	1441.85	609.26	200	275.56	0.000	0.00	3650.78	371.84
207	1124.12	344.45	1663.67	632.22	200	275.56	0.000	0.00	3895.57	396.77
208	1124.12	390.37	1885.49	655.19	200	275.56	0.000	0.00	4140.35	421.70
209	1124.12	436.30	2107.32	678.15	200	275.56	0.000	0.00	4385.14	446.64
210	1124.12	482.22	2329.14	701.11	200	275.56	0.000	0.00	4629.93	471.57
211	1124.12	68.89	332.73	494.44	200	275.56	0.319	21.99	2448.84	249.42
212	1124.12	114.82	554.56	517.41	200	275.56	0.319	36.64	2708.29	275.84
213	1124.12	160.74	776.38	540.37	200	275.56	0.319	51.30	2967.73	302.27
214	1124.12	206.67	998.20	563.33	200	275.56	0.319	65.96	3227.17	328.69
215	1124.12	252.59	1220.02	586.30	200	275.56	0.319	80.62	3486.62	355.12
216	1124.12	298.52	1441.85	609.26	200	275.56	0.319	95.28	3746.06	381.54
217	1124.12	344.45	1663.67	632.22	200	275.56	0.319	109.93	4005.50	407.97
218	1124.12	390.37	1885.49	655.19	200	275.56	0.319	124.59	4264.95	434.39
219	1124.12	436.30	2107.32	678.15	200	275.56	0.319	139.25	4524.39	460.82
220	1124.12	482.22	2329.14	701.11	200	275.56	0.319	153.91	4783.83	487.24
221	1124.12	68.89	332.73	494.44	200	275.56	0.704	48.51	2475.36	252.12
222	1124.12	114.82	554.56	517.41	200	275.56	0.704	80.84	2752.48	280.35
223	1124.12	160.74	776.38	540.37	200	275.56	0.704	113.18	3029.61	308.57
224	1124.12	206.67	998.20	563.33	200	275.56	0.704	145.52	3306.73	336.80
225	1124.12	252.59	1220.02	586.30	200	275.56	0.704	177.86	3583.86	365.02
226	1124.12	298.52	1441.85	609.26	200	275.56	0.704	210.20	3860.98	393.25
227	1124.12	344.45	1663.67	632.22	200	275.56	0.704	242.53	4138.10	421.47
228	1124.12	390.37	1885.49	655.19	200	275.56	0.704	274.87	4415.23	449.70
229	1124.12	436.30	2107.32	678.15	200	275.56	0.704	307.21	4692.35	477.93
230	1124.12	482.22	2329.14	701.11	200	275.56	0.704	339.55	4969.47	506.15
231	1124.12	68.89	332.73	494.44	200	275.56	1.089	75.03	2501.88	254.82
232	1124.12	114.82	554.56	517.41	200	275.56	1.089	125.04	2796.68	284.85
233	1124.12	160.74	776.38	540.37	200	275.56	1.089	175.06	3091.49	314.87
234	1124.12	206.67	998.20	563.33	200	275.56	1.089	225.08	3386.29	344.90
235	1124.12	252.59	1220.02	586.30	200	275.56	1.089	275.10	3681.09	374.93
236	1124.12	298.52	1441.85	609.26	200	275.56	1.089	325.11	3975.90	404.95
237	1124.12	344.45	1663.67	632.22	200	275.56	1.089	375.13	4270.70	434.98
238	1124.12	390.37	1885.49	655.19	200	275.56	1.089	425.15	4565.50	465.01
239	1124.12	436.30	2107.32	678.15	200	275.56	1.089	475.17	4860.31	495.03

#	UV Lamp \$	Duct ft2	Duct Matl, \$	Labor \$	Fan FC \$	Filter FC \$	Reflect Type \$/ft2	Refl Matl, \$	Total FC \$	Annual FC \$
240	1124.12	482.22	2329.14	701.11	200	275.56	1.089	525.18	5155.11	525.06
241	1124.12	68.89	332.73	494.44	200	275.56	1.474	101.55	2528.40	257.52
242	1124.12	114.82	554.56	517.41	200	275.56	1.474	169.24	2840.88	289.35
243	1124.12	160.74	776.38	540.37	200	275.56	1.474	236.94	3153.37	321.18
244	1124.12	206.67	998.20	563.33	200	275.56	1.474	304.64	3465.85	353.00
245	1124.12	252.59	1220.02	586.30	200	275.56	1.474	372.34	3778.33	384.83
246	1124.12	298.52	1441.85	609.26	200	275.56	1.474	440.03	4090.82	416.66
247	1124.12	344.45	1663.67	632.22	200	275.56	1.474	507.73	4403.30	448.49
248	1124.12	390.37	1885.49	655.19	200	275.56	1.474	575.43	4715.78	480.31
249	1124.12	436.30	2107.32	678.15	200	275.56	1.474	643.13	5028.27	512.14
250	1124.12	482.22	2329.14	701.11	200	275.56	1.474	710.82	5340.75	543.97
251	1124.12	68.89	332.73	494.44	200	275.56	1.859	128.07	2554.92	260.22
252	1124.12	114.82	554.56	517.41	200	275.56	1.859	213.44	2885.08	293.85
253	1124.12	160.74	776.38	540.37	200	275.56	1.859	298.82	3215.25	327.48
254	1124.12	206.67	998.20	563.33	200	275.56	1.859	384.20	3545.41	361.11
255	1124.12	252.59	1220.02	586.30	200	275.56	1.859	469.58	3875.57	394.74
256	1124.12	298.52	1441.85	609.26	200	275.56	1.859	554.95	4205.74	428.36
257	1124.12	344.45	1663.67	632.22	200	275.56	1.859	640.33	4535.90	461.99
258	1124.12	390.37	1885.49	655.19	200	275.56	1.859	725.71	4866.06	495.62
259	1124.12	436.30	2107.32	678.15	200	275.56	1.859	811.08	5196.22	529.25
260	1124.12	482.22	2329.14	701.11	200	275.56	1.859	896.46	5526.39	562.87
261	1124.12	68.89	332.73	494.44	200	275.56	2.244	154.59	2581.44	262.93
262	1124.12	114.82	554.56	517.41	200	275.56	2.244	257.64	2929.28	298.35
263	1124.12	160.74	776.38	540.37	200	275.56	2.244	360.70	3277.13	333.78
264	1124.12	206.67	998.20	563.33	200	275.56	2.244	463.76	3624.97	369.21
265	1124.12	252.59	1220.02	586.30	200	275.56	2.244	566.81	3972.81	404.64
266	1124.12	298.52	1441.85	609.26	200	275.56	2.244	669.87	4320.65	440.07
267	1124.12	344.45	1663.67	632.22	200	275.56	2.244	772.93	4668.50	475.50
268	1124.12	390.37	1885.49	655.19	200	275.56	2.244	875.99	5016.34	510.93
269	1124.12	436.30	2107.32	678.15	200	275.56	2.244	979.04	5364.18	546.35
270	1124.12	482.22	2329.14	701.11	200	275.56	2.244	1082.10	5712.03	581.78
271	1124.12	68.89	332.73	494.44	200	275.56	2.629	181.11	2607.96	265.63
272	1124.12	114.82	554.56	517.41	200	275.56	2.629	301.84	2973.48	302.86
273	1124.12	160.74	776.38	540.37	200	275.56	2.629	422.58	3339.01	340.09
274	1124.12	206.67	998.20	563.33	200	275.56	2.629	543.32	3704.53	377.31
275	1124.12	252.59	1220.02	586.30	200	275.56	2.629	664.05	4070.05	414.54
276	1124.12	298.52	1441.85	609.26	200	275.56	2.629	784.79	4435.57	451.77
277	1124.12	344.45	1663.67	632.22	200	275.56	2.629	905.53	4801.10	489.00
278	1124.12	390.37	1885.49	655.19	200	275.56	2.629	1026.26	5166.62	526.23
279	1124.12	436.30	2107.32	678.15	200	275.56	2.629	1147.00	5532.14	563.46
280	1124.12	482.22	2329.14	701.11	200	275.56	2.629	1267.74	5897.66	600.69
281	1124.12	68.89	332.73	494.44	200	275.56	3.014	207.63	2634.48	268.33
282	1124.12	114.82	554.56	517.41	200	275.56	3.014	346.04	3017.68	307.36
283	1124.12	160.74	776.38	540.37	200	275.56	3.014	484.46	3400.88	346.39
284	1124.12	206.67	998.20	563.33	200	275.56	3.014	622.88	3784.09	385.42
285	1124.12	252.59	1220.02	586.30	200	275.56	3.014	761.29	4167.29	424.45
286	1124.12	298.52	1441.85	609.26	200	275.56	3.014	899.71	4550.49	463.48
287	1124.12	344.45	1663.67	632.22	200	275.56	3.014	1038.13	4933.70	502.51

#	UV Lamp \$	Duct ft2	Duct Matl, \$	Labor \$	Fan FC \$	Filter FC \$	Reflect Type \$/ft2	Refl Matl, \$	Total FC \$	Annual FC \$
288	1124.12	390.37	1885.49	655.19	200	275.56	3.014	1176.54	5316.90	541.54
289	1124.12	436.30	2107.32	678.15	200	275.56	3.014	1314.96	5700.10	580.57
290	1124.12	482.22	2329.14	701.11	200	275.56	3.014	1453.38	6083.30	619.60
291	1124.12	68.89	332.73	494.44	200	275.56	3.399	234.15	2661.00	271.03
292	1124.12	114.82	554.56	517.41	200	275.56	3.399	390.24	3061.88	311.86
293	1124.12	160.74	776.38	540.37	200	275.56	3.399	546.34	3462.76	352.69
294	1124.12	206.67	998.20	563.33	200	275.56	3.399	702.44	3863.65	393.52
295	1124.12	252.59	1220.02	586.30	200	275.56	3.399	858.53	4264.53	434.35
296	1124.12	298.52	1441.85	609.26	200	275.56	3.399	1014.63	4665.41	475.18
297	1124.12	344.45	1663.67	632.22	200	275.56	3.399	1170.73	5066.29	516.01
298	1124.12	390.37	1885.49	655.19	200	275.56	3.399	1326.82	5467.18	556.84
299	1124.12	436.30	2107.32	678.15	200	275.56	3.399	1482.92	5868.06	597.67
300	1124.12	482.22	2329.14	701.11	200	275.56	3.399	1639.02	6268.94	638.51
301	594.46	165.33	798.56	542.67	51.281	275.56	1.667	275.53	2538.06	258.51
302	594.46	165.33	798.56	542.67	84.33	275.56	1.667	275.53	2571.11	261.87
303	594.46	165.33	798.56	542.67	117.38	275.56	1.667	275.53	2604.16	265.24
304	594.46	165.33	798.56	542.67	150.43	275.56	1.667	275.53	2637.21	268.61
305	594.46	165.33	798.56	542.67	183.47	275.56	1.667	275.53	2670.25	271.97
306	594.46	165.33	798.56	542.67	216.52	275.56	1.667	275.53	2703.30	275.34
307	594.46	165.33	798.56	542.67	249.57	275.56	1.667	275.53	2736.35	278.70
308	594.46	165.33	798.56	542.67	282.62	275.56	1.667	275.53	2769.40	282.07
309	594.46	165.33	798.56	542.67	315.67	275.56	1.667	275.53	2802.45	285.44
310	594.46	165.33	798.56	542.67	348.71	275.56	1.667	275.53	2835.49	288.80
311	717.07	165.33	798.56	542.67	51.281	275.56	1.667	275.53	2660.67	271.00
312	717.07	165.33	798.56	542.67	84.33	275.56	1.667	275.53	2693.72	274.36
313	717.07	165.33	798.56	542.67	117.38	275.56	1.667	275.53	2726.77	277.73
314	717.07	165.33	798.56	542.67	150.43	275.56	1.667	275.53	2759.82	281.09
315	717.07	165.33	798.56	542.67	183.47	275.56	1.667	275.53	2792.86	284.46
316	717.07	165.33	798.56	542.67	216.52	275.56	1.667	275.53	2825.91	287.83
317	717.07	165.33	798.56	542.67	249.57	275.56	1.667	275.53	2858.96	291.19
318	717.07	165.33	798.56	542.67	282.62	275.56	1.667	275.53	2892.01	294.56
319	717.07	165.33	798.56	542.67	315.67	275.56	1.667	275.53	2925.06	297.92
320	717.07	165.33	798.56	542.67	348.71	275.56	1.667	275.53	2958.11	301.29
321	836.88	165.33	798.56	542.67	51.281	275.56	1.667	275.53	2780.48	283.20
322	836.88	165.33	798.56	542.67	84.33	275.56	1.667	275.53	2813.53	286.56
323	836.88	165.33	798.56	542.67	117.38	275.56	1.667	275.53	2846.57	289.93
324	836.88	165.33	798.56	542.67	150.43	275.56	1.667	275.53	2879.62	293.30
325	836.88	165.33	798.56	542.67	183.47	275.56	1.667	275.53	2912.67	296.66
326	836.88	165.33	798.56	542.67	216.52	275.56	1.667	275.53	2945.72	300.03
327	836.88	165.33	798.56	542.67	249.57	275.56	1.667	275.53	2978.77	303.39
328	836.88	165.33	798.56	542.67	282.62	275.56	1.667	275.53	3011.81	306.76
329	836.88	165.33	798.56	542.67	315.67	275.56	1.667	275.53	3044.86	310.13
330	836.88	165.33	798.56	542.67	348.71	275.56	1.667	275.53	3077.91	313.49
331	953.88	165.33	798.56	542.67	51.281	275.56	1.667	275.53	2897.48	295.11
332	953.88	165.33	798.56	542.67	84.33	275.56	1.667	275.53	2930.53	298.48
333	953.88	165.33	798.56	542.67	117.38	275.56	1.667	275.53	2963.58	301.85
334	953.88	165.33	798.56	542.67	150.43	275.56	1.667	275.53	2996.62	305.21
335	953.88	165.33	798.56	542.67	183.47	275.56	1.667	275.53	3029.67	308.58

#	UV Lamp \$	Duct ft2	Duct Matl, \$	Labor \$	Fan FC \$	Filter FC \$	Reflect Type \$/ft2	Refl Matl, \$	Total FC \$	Annual FC \$
336	953.88	165.33	798.56	542.67	216.52	275.56	1.667	275.53	3062.72	311.94
337	953.88	165.33	798.56	542.67	249.57	275.56	1.667	275.53	3095.77	315.31
338	953.88	165.33	798.56	542.67	282.62	275.56	1.667	275.53	3128.82	318.68
339	953.88	165.33	798.56	542.67	315.67	275.56	1.667	275.53	3161.86	322.04
340	953.88	165.33	798.56	542.67	348.71	275.56	1.667	275.53	3194.91	325.41
341	1068.07	165.33	798.56	542.67	51.281	275.56	1.667	275.53	3011.68	306.75
342	1068.07	165.33	798.56	542.67	84.33	275.56	1.667	275.53	3044.72	310.11
343	1068.07	165.33	798.56	542.67	117.38	275.56	1.667	275.53	3077.77	313.48
344	1068.07	165.33	798.56	542.67	150.43	275.56	1.667	275.53	3110.82	316.84
345	1068.07	165.33	798.56	542.67	183.47	275.56	1.667	275.53	3143.87	320.21
346	1068.07	165.33	798.56	542.67	216.52	275.56	1.667	275.53	3176.92	323.58
347	1068.07	165.33	798.56	542.67	249.57	275.56	1.667	275.53	3209.96	326.94
348	1068.07	165.33	798.56	542.67	282.62	275.56	1.667	275.53	3243.01	330.31
349	1068.07	165.33	798.56	542.67	315.67	275.56	1.667	275.53	3276.06	333.67
350	1068.07	165.33	798.56	542.67	348.71	275.56	1.667	275.53	3309.11	337.04
351	1179.47	165.33	798.56	542.67	51.281	275.56	1.667	275.53	3123.07	318.09
352	1179.47	165.33	798.56	542.67	84.33	275.56	1.667	275.53	3156.12	321.46
353	1179.47	165.33	798.56	542.67	117.38	275.56	1.667	275.53	3189.16	324.82
354	1179.47	165.33	798.56	542.67	150.43	275.56	1.667	275.53	3222.21	328.19
355	1179.47	165.33	798.56	542.67	183.47	275.56	1.667	275.53	3255.26	331.56
356	1179.47	165.33	798.56	542.67	216.52	275.56	1.667	275.53	3288.31	334.92
357	1179.47	165.33	798.56	542.67	249.57	275.56	1.667	275.53	3321.36	338.29
358	1179.47	165.33	798.56	542.67	282.62	275.56	1.667	275.53	3354.40	341.65
359	1179.47	165.33	798.56	542.67	315.67	275.56	1.667	275.53	3387.45	345.02
360	1179.47	165.33	798.56	542.67	348.71	275.56	1.667	275.53	3420.50	348.39
361	1288.05	165.33	798.56	542.67	51.281	275.56	1.667	275.53	3231.66	329.15
362	1288.05	165.33	798.56	542.67	84.33	275.56	1.667	275.53	3264.70	332.52
363	1288.05	165.33	798.56	542.67	117.38	275.56	1.667	275.53	3297.75	335.88
364	1288.05	165.33	798.56	542.67	150.43	275.56	1.667	275.53	3330.80	339.25
365	1288.05	165.33	798.56	542.67	183.47	275.56	1.667	275.53	3363.85	342.62
366	1288.05	165.33	798.56	542.67	216.52	275.56	1.667	275.53	3396.90	345.98
367	1288.05	165.33	798.56	542.67	249.57	275.56	1.667	275.53	3429.94	349.35
368	1288.05	165.33	798.56	542.67	282.62	275.56	1.667	275.53	3462.99	352.71
369	1288.05	165.33	798.56	542.67	315.67	275.56	1.667	275.53	3496.04	356.08
370	1288.05	165.33	798.56	542.67	348.71	275.56	1.667	275.53	3529.09	359.45
371	1393.84	165.33	798.56	542.67	51.281	275.56	1.667	275.53	3337.44	339.93
372	1393.84	165.33	798.56	542.67	84.33	275.56	1.667	275.53	3370.49	343.29
373	1393.84	165.33	798.56	542.67	117.38	275.56	1.667	275.53	3403.53	346.66
374	1393.84	165.33	798.56	542.67	150.43	275.56	1.667	275.53	3436.58	350.02
375	1393.84	165.33	798.56	542.67	183.47	275.56	1.667	275.53	3469.63	353.39
376	1393.84	165.33	798.56	542.67	216.52	275.56	1.667	275.53	3502.68	356.76
377	1393.84	165.33	798.56	542.67	249.57	275.56	1.667	275.53	3535.73	360.12
378	1393.84	165.33	798.56	542.67	282.62	275.56	1.667	275.53	3568.77	363.49
379	1393.84	165.33	798.56	542.67	315.67	275.56	1.667	275.53	3601.82	366.85
380	1393.84	165.33	798.56	542.67	348.71	275.56	1.667	275.53	3634.87	370.22
381	1496.81	165.33	798.56	542.67	51.281	275.56	1.667	275.53	3440.42	350.41
382	1496.81	165.33	798.56	542.67	84.33	275.56	1.667	275.53	3473.46	353.78
383	1496.81	165.33	798.56	542.67	117.38	275.56	1.667	275.53	3506.51	357.15

#	UV Lamp \$	Duct ft2	Duct Matl, \$	Labor \$	Fan FC \$	Filter FC \$	Reflect Type \$/ft2	Refl Matl, \$	Total FC \$	Annual FC \$
384	1496.81	165.33	798.56	542.67	150.43	275.56	1.667	275.53	3539.56	360.51
385	1496.81	165.33	798.56	542.67	183.47	275.56	1.667	275.53	3572.61	363.88
386	1496.81	165.33	798.56	542.67	216.52	275.56	1.667	275.53	3605.66	367.24
387	1496.81	165.33	798.56	542.67	249.57	275.56	1.667	275.53	3638.70	370.61
388	1496.81	165.33	798.56	542.67	282.62	275.56	1.667	275.53	3671.75	373.98
389	1496.81	165.33	798.56	542.67	315.67	275.56	1.667	275.53	3704.80	377.34
390	1496.81	165.33	798.56	542.67	348.71	275.56	1.667	275.53	3737.85	380.71
391	1596.99	165.33	798.56	542.67	51.281	275.56	1.667	275.53	3540.59	360.62
392	1596.99	165.33	798.56	542.67	84.33	275.56	1.667	275.53	3573.64	363.98
393	1596.99	165.33	798.56	542.67	117.38	275.56	1.667	275.53	3606.69	367.35
394	1596.99	165.33	798.56	542.67	150.43	275.56	1.667	275.53	3639.73	370.71
395	1596.99	165.33	798.56	542.67	183.47	275.56	1.667	275.53	3672.78	374.08
396	1596.99	165.33	798.56	542.67	216.52	275.56	1.667	275.53	3705.83	377.45
397	1596.99	165.33	798.56	542.67	249.57	275.56	1.667	275.53	3738.88	380.81
398	1596.99	165.33	798.56	542.67	282.62	275.56	1.667	275.53	3771.93	384.18
399	1596.99	165.33	798.56	542.67	315.67	275.56	1.667	275.53	3804.97	387.55
400	1596.99	165.33	798.56	542.67	348.71	275.56	1.667	275.53	3838.02	390.91
401	1124.12	68.89	332.73	494.44	51.281	275.56	1.667	114.81	2392.94	243.73
402	1124.12	68.89	332.73	494.44	84.33	275.56	1.667	114.81	2425.99	247.09
403	1124.12	68.89	332.73	494.44	117.38	275.56	1.667	114.81	2459.04	250.46
404	1124.12	68.89	332.73	494.44	150.43	275.56	1.667	114.81	2492.09	253.82
405	1124.12	68.89	332.73	494.44	183.47	275.56	1.667	114.81	2525.14	257.19
406	1124.12	68.89	332.73	494.44	216.52	275.56	1.667	114.81	2558.18	260.56
407	1124.12	68.89	332.73	494.44	249.57	275.56	1.667	114.81	2591.23	263.92
408	1124.12	68.89	332.73	494.44	282.62	275.56	1.667	114.81	2624.28	267.29
409	1124.12	68.89	332.73	494.44	315.67	275.56	1.667	114.81	2657.33	270.65
410	1124.12	68.89	332.73	494.44	348.71	275.56	1.667	114.81	2690.38	274.02
411	1124.12	114.82	554.56	517.41	51.281	275.56	1.667	191.34	2714.27	276.45
412	1124.12	114.82	554.56	517.41	84.33	275.56	1.667	191.34	2747.32	279.82
413	1124.12	114.82	554.56	517.41	117.38	275.56	1.667	191.34	2780.36	283.19
414	1124.12	114.82	554.56	517.41	150.43	275.56	1.667	191.34	2813.41	286.55
415	1124.12	114.82	554.56	517.41	183.47	275.56	1.667	191.34	2846.46	289.92
416	1124.12	114.82	554.56	517.41	216.52	275.56	1.667	191.34	2879.51	293.28
417	1124.12	114.82	554.56	517.41	249.57	275.56	1.667	191.34	2912.56	296.65
418	1124.12	114.82	554.56	517.41	282.62	275.56	1.667	191.34	2945.60	300.02
419	1124.12	114.82	554.56	517.41	315.67	275.56	1.667	191.34	2978.65	303.38
420	1124.12	114.82	554.56	517.41	348.71	275.56	1.667	191.34	3011.70	306.75
421	1124.12	160.74	776.38	540.37	51.281	275.56	1.667	267.88	3035.59	309.18
422	1124.12	160.74	776.38	540.37	84.33	275.56	1.667	267.88	3068.64	312.55
423	1124.12	160.74	776.38	540.37	117.38	275.56	1.667	267.88	3101.69	315.91
424	1124.12	160.74	776.38	540.37	150.43	275.56	1.667	267.88	3134.73	319.28
425	1124.12	160.74	776.38	540.37	183.47	275.56	1.667	267.88	3167.78	322.65
426	1124.12	160.74	776.38	540.37	216.52	275.56	1.667	267.88	3200.83	326.01
427	1124.12	160.74	776.38	540.37	249.57	275.56	1.667	267.88	3233.88	329.38
428	1124.12	160.74	776.38	540.37	282.62	275.56	1.667	267.88	3266.93	332.74
429	1124.12	160.74	776.38	540.37	315.67	275.56	1.667	267.88	3299.98	336.11
430	1124.12	160.74	776.38	540.37	348.71	275.56	1.667	267.88	3333.02	339.48
431	1124.12	206.67	998.20	563.33	51.281	275.56	1.667	344.42	3356.91	341.91

#	UV Lamp \$	Duct ft2	Duct Matl, \$	Labor \$	Fan FC \$	Filter FC \$	Reflect Type \$/ft2	Refl Matl, \$	Total FC \$	Annual FC \$
432	1124.12	206.67	998.20	563.33	84.33	275.56	1.667	344.42	3389.96	345.28
433	1124.12	206.67	998.20	563.33	117.38	275.56	1.667	344.42	3423.01	348.64
434	1124.12	206.67	998.20	563.33	150.43	275.56	1.667	344.42	3456.06	352.01
435	1124.12	206.67	998.20	563.33	183.47	275.56	1.667	344.42	3489.11	355.37
436	1124.12	206.67	998.20	563.33	216.52	275.56	1.667	344.42	3522.15	358.74
437	1124.12	206.67	998.20	563.33	249.57	275.56	1.667	344.42	3555.20	362.11
438	1124.12	206.67	998.20	563.33	282.62	275.56	1.667	344.42	3588.25	365.47
439	1124.12	206.67	998.20	563.33	315.67	275.56	1.667	344.42	3621.30	368.84
440	1124.12	206.67	998.20	563.33	348.71	275.56	1.667	344.42	3654.35	372.20
441	1124.12	252.59	1220.02	586.30	51.281	275.56	1.667	420.96	3678.24	374.64
442	1124.12	252.59	1220.02	586.30	84.33	275.56	1.667	420.96	3711.28	378.00
443	1124.12	252.59	1220.02	586.30	117.38	275.56	1.667	420.96	3744.33	381.37
444	1124.12	252.59	1220.02	586.30	150.43	275.56	1.667	420.96	3777.38	384.73
445	1124.12	252.59	1220.02	586.30	183.47	275.56	1.667	420.96	3810.43	388.10
446	1124.12	252.59	1220.02	586.30	216.52	275.56	1.667	420.96	3843.48	391.47
447	1124.12	252.59	1220.02	586.30	249.57	275.56	1.667	420.96	3876.53	394.83
448	1124.12	252.59	1220.02	586.30	282.62	275.56	1.667	420.96	3909.57	398.20
449	1124.12	252.59	1220.02	586.30	315.67	275.56	1.667	420.96	3942.62	401.56
450	1124.12	252.59	1220.02	586.30	348.71	275.56	1.667	420.96	3975.67	404.93
451	1124.12	298.52	1441.85	609.26	51.281	275.56	1.667	497.49	3999.56	407.36
452	1124.12	298.52	1441.85	609.26	84.33	275.56	1.667	497.49	4032.61	410.73
453	1124.12	298.52	1441.85	609.26	117.38	275.56	1.667	497.49	4065.66	414.10
454	1124.12	298.52	1441.85	609.26	150.43	275.56	1.667	497.49	4098.70	417.46
455	1124.12	298.52	1441.85	609.26	183.47	275.56	1.667	497.49	4131.75	420.83
456	1124.12	298.52	1441.85	609.26	216.52	275.56	1.667	497.49	4164.80	424.19
457	1124.12	298.52	1441.85	609.26	249.57	275.56	1.667	497.49	4197.85	427.56
458	1124.12	298.52	1441.85	609.26	282.62	275.56	1.667	497.49	4230.90	430.93
459	1124.12	298.52	1441.85	609.26	315.67	275.56	1.667	497.49	4263.94	434.29
460	1124.12	298.52	1441.85	609.26	348.71	275.56	1.667	497.49	4296.99	437.66
461	1124.12	344.45	1663.67	632.22	51.281	275.56	1.667	574.03	4320.88	440.09
462	1124.12	344.45	1663.67	632.22	84.33	275.56	1.667	574.03	4353.93	443.46
463	1124.12	344.45	1663.67	632.22	117.38	275.56	1.667	574.03	4386.98	446.82
464	1124.12	344.45	1663.67	632.22	150.43	275.56	1.667	574.03	4420.03	450.19
465	1124.12	344.45	1663.67	632.22	183.47	275.56	1.667	574.03	4453.08	453.56
466	1124.12	344.45	1663.67	632.22	216.52	275.56	1.667	574.03	4486.12	456.92
467	1124.12	344.45	1663.67	632.22	249.57	275.56	1.667	574.03	4519.17	460.29
468	1124.12	344.45	1663.67	632.22	282.62	275.56	1.667	574.03	4552.22	463.65
469	1124.12	344.45	1663.67	632.22	315.67	275.56	1.667	574.03	4585.27	467.02
470	1124.12	344.45	1663.67	632.22	348.71	275.56	1.667	574.03	4618.32	470.39
471	1124.12	390.37	1885.49	655.19	51.281	275.56	1.667	650.57	4642.21	472.82
472	1124.12	390.37	1885.49	655.19	84.33	275.56	1.667	650.57	4675.25	476.18
473	1124.12	390.37	1885.49	655.19	117.38	275.56	1.667	650.57	4708.30	479.55
474	1124.12	390.37	1885.49	655.19	150.43	275.56	1.667	650.57	4741.35	482.92
475	1124.12	390.37	1885.49	655.19	183.47	275.56	1.667	650.57	4774.40	486.28
476	1124.12	390.37	1885.49	655.19	216.52	275.56	1.667	650.57	4807.45	489.65
477	1124.12	390.37	1885.49	655.19	249.57	275.56	1.667	650.57	4840.49	493.02
478	1124.12	390.37	1885.49	655.19	282.62	275.56	1.667	650.57	4873.54	496.38
479	1124.12	390.37	1885.49	655.19	315.67	275.56	1.667	650.57	4906.59	499.75

#	UV Lamp \$	Duct ft2	Duct Matl, \$	Labor \$	Fan FC \$	Filter FC \$	Reflect Type \$/ft2	Refl Matl, \$	Total FC \$	Annual FC \$
480	1124.12	390.37	1885.49	655.19	348.71	275.56	1.667	650.57	4939.64	503.11
481	1124.12	436.30	2107.32	678.15	51.281	275.56	1.667	727.11	4963.53	505.55
482	1124.12	436.30	2107.32	678.15	84.33	275.56	1.667	727.11	4996.58	508.91
483	1124.12	436.30	2107.32	678.15	117.38	275.56	1.667	727.11	5029.62	512.28
484	1124.12	436.30	2107.32	678.15	150.43	275.56	1.667	727.11	5062.67	515.64
485	1124.12	436.30	2107.32	678.15	183.47	275.56	1.667	727.11	5095.72	519.01
486	1124.12	436.30	2107.32	678.15	216.52	275.56	1.667	727.11	5128.77	522.38
487	1124.12	436.30	2107.32	678.15	249.57	275.56	1.667	727.11	5161.82	525.74
488	1124.12	436.30	2107.32	678.15	282.62	275.56	1.667	727.11	5194.87	529.11
489	1124.12	436.30	2107.32	678.15	315.67	275.56	1.667	727.11	5227.91	532.47
490	1124.12	436.30	2107.32	678.15	348.71	275.56	1.667	727.11	5260.96	535.84
491	1124.12	482.22	2329.14	701.11	51.281	275.56	1.667	803.64	5284.85	538.27
492	1124.12	482.22	2329.14	701.11	84.33	275.56	1.667	803.64	5317.90	541.64
493	1124.12	482.22	2329.14	701.11	117.38	275.56	1.667	803.64	5350.95	545.01
494	1124.12	482.22	2329.14	701.11	150.43	275.56	1.667	803.64	5384.00	548.37
495	1124.12	482.22	2329.14	701.11	183.47	275.56	1.667	803.64	5417.04	551.74
496	1124.12	482.22	2329.14	701.11	216.52	275.56	1.667	803.64	5450.09	555.10
497	1124.12	482.22	2329.14	701.11	249.57	275.56	1.667	803.64	5483.14	558.47
498	1124.12	482.22	2329.14	701.11	282.62	275.56	1.667	803.64	5516.19	561.84
499	1124.12	482.22	2329.14	701.11	315.67	275.56	1.667	803.64	5549.24	565.20
500	1124.12	482.22	2329.14	701.11	348.71	275.56	1.667	803.64	5582.28	568.57
501	1124.12	165.33	798.56	542.67	51.281	275.56	0.000	0.00	2792.19	284.39
502	1124.12	165.33	798.56	542.67	84.33	275.56	0.000	0.00	2825.24	287.76
503	1124.12	165.33	798.56	542.67	117.38	275.56	0.000	0.00	2858.28	291.12
504	1124.12	165.33	798.56	542.67	150.43	275.56	0.000	0.00	2891.33	294.49
505	1124.12	165.33	798.56	542.67	183.47	275.56	0.000	0.00	2924.38	297.85
506	1124.12	165.33	798.56	542.67	216.52	275.56	0.000	0.00	2957.43	301.22
507	1124.12	165.33	798.56	542.67	249.57	275.56	0.000	0.00	2990.48	304.59
508	1124.12	165.33	798.56	542.67	282.62	275.56	0.000	0.00	3023.52	307.95
509	1124.12	165.33	798.56	542.67	315.67	275.56	0.000	0.00	3056.57	311.32
510	1124.12	165.33	798.56	542.67	348.71	275.56	0.000	0.00	3089.62	314.68
511	1124.12	165.33	798.56	542.67	51.281	275.56	0.319	52.77	2844.96	289.77
512	1124.12	165.33	798.56	542.67	84.33	275.56	0.319	52.77	2878.00	293.13
513	1124.12	165.33	798.56	542.67	117.38	275.56	0.319	52.77	2911.05	296.50
514	1124.12	165.33	798.56	542.67	150.43	275.56	0.319	52.77	2944.10	299.86
515	1124.12	165.33	798.56	542.67	183.47	275.56	0.319	52.77	2977.15	303.23
516	1124.12	165.33	798.56	542.67	216.52	275.56	0.319	52.77	3010.20	306.60
517	1124.12	165.33	798.56	542.67	249.57	275.56	0.319	52.77	3043.25	309.96
518	1124.12	165.33	798.56	542.67	282.62	275.56	0.319	52.77	3076.29	313.33
519	1124.12	165.33	798.56	542.67	315.67	275.56	0.319	52.77	3109.34	316.69
520	1124.12	165.33	798.56	542.67	348.71	275.56	0.319	52.77	3142.39	320.06
521	1124.12	165.33	798.56	542.67	51.281	275.56	0.704	116.42	2908.60	296.25
522	1124.12	165.33	798.56	542.67	84.33	275.56	0.704	116.42	2941.65	299.61
523	1124.12	165.33	798.56	542.67	117.38	275.56	0.704	116.42	2974.70	302.98
524	1124.12	165.33	798.56	542.67	150.43	275.56	0.704	116.42	3007.75	306.35
525	1124.12	165.33	798.56	542.67	183.47	275.56	0.704	116.42	3040.80	309.71
526	1124.12	165.33	798.56	542.67	216.52	275.56	0.704	116.42	3073.84	313.08
527	1124.12	165.33	798.56	542.67	249.57	275.56	0.704	116.42	3106.89	316.44

#	UV Lamp \$	Duct ft2	Duct Matl, \$	Labor \$	Fan FC \$	Filter FC \$	Reflect Type \$/ft2	Refl Matl, \$	Total FC \$	Annual FC \$
528	1124.12	165.33	798.56	542.67	282.62	275.56	0.704	116.42	3139.94	319.81
529	1124.12	165.33	798.56	542.67	315.67	275.56	0.704	116.42	3172.99	323.18
530	1124.12	165.33	798.56	542.67	348.71	275.56	0.704	116.42	3206.04	326.54
531	1124.12	165.33	798.56	542.67	51.281	275.56	1.089	180.06	2972.25	302.73
532	1124.12	165.33	798.56	542.67	84.33	275.56	1.089	180.06	3005.30	306.10
533	1124.12	165.33	798.56	542.67	117.38	275.56	1.089	180.06	3038.35	309.46
534	1124.12	165.33	798.56	542.67	150.43	275.56	1.089	180.06	3071.40	312.83
535	1124.12	165.33	798.56	542.67	183.47	275.56	1.089	180.06	3104.44	316.19
536	1124.12	165.33	798.56	542.67	216.52	275.56	1.089	180.06	3137.49	319.56
537	1124.12	165.33	798.56	542.67	249.57	275.56	1.089	180.06	3170.54	322.93
538	1124.12	165.33	798.56	542.67	282.62	275.56	1.089	180.06	3203.59	326.29
539	1124.12	165.33	798.56	542.67	315.67	275.56	1.089	180.06	3236.64	329.66
540	1124.12	165.33	798.56	542.67	348.71	275.56	1.089	180.06	3269.68	333.02
541	1124.12	165.33	798.56	542.67	51.281	275.56	1.474	243.71	3035.90	309.21
542	1124.12	165.33	798.56	542.67	84.33	275.56	1.474	243.71	3068.95	312.58
543	1124.12	165.33	798.56	542.67	117.38	275.56	1.474	243.71	3102.00	315.95
544	1124.12	165.33	798.56	542.67	150.43	275.56	1.474	243.71	3135.04	319.31
545	1124.12	165.33	798.56	542.67	183.47	275.56	1.474	243.71	3168.09	322.68
546	1124.12	165.33	798.56	542.67	216.52	275.56	1.474	243.71	3201.14	326.04
547	1124.12	165.33	798.56	542.67	249.57	275.56	1.474	243.71	3234.19	329.41
548	1124.12	165.33	798.56	542.67	282.62	275.56	1.474	243.71	3267.24	332.78
549	1124.12	165.33	798.56	542.67	315.67	275.56	1.474	243.71	3300.28	336.14
550	1124.12	165.33	798.56	542.67	348.71	275.56	1.474	243.71	3333.33	339.51
551	1124.12	165.33	798.56	542.67	51.281	275.56	1.859	307.36	3099.55	315.70
552	1124.12	165.33	798.56	542.67	84.33	275.56	1.859	307.36	3132.59	319.06
553	1124.12	165.33	798.56	542.67	117.38	275.56	1.859	307.36	3165.64	322.43
554	1124.12	165.33	798.56	542.67	150.43	275.56	1.859	307.36	3198.69	325.79
555	1124.12	165.33	798.56	542.67	183.47	275.56	1.859	307.36	3231.74	329.16
556	1124.12	165.33	798.56	542.67	216.52	275.56	1.859	307.36	3264.79	332.53
557	1124.12	165.33	798.56	542.67	249.57	275.56	1.859	307.36	3297.84	335.89
558	1124.12	165.33	798.56	542.67	282.62	275.56	1.859	307.36	3330.88	339.26
559	1124.12	165.33	798.56	542.67	315.67	275.56	1.859	307.36	3363.93	342.62
560	1124.12	165.33	798.56	542.67	348.71	275.56	1.859	307.36	3396.98	345.99
561	1124.12	165.33	798.56	542.67	51.281	275.56	2.244	371.01	3163.19	322.18
562	1124.12	165.33	798.56	542.67	84.33	275.56	2.244	371.01	3196.24	325.54
563	1124.12	165.33	798.56	542.67	117.38	275.56	2.244	371.01	3229.29	328.91
564	1124.12	165.33	798.56	542.67	150.43	275.56	2.244	371.01	3262.34	332.28
565	1124.12	165.33	798.56	542.67	183.47	275.56	2.244	371.01	3295.39	335.64
566	1124.12	165.33	798.56	542.67	216.52	275.56	2.244	371.01	3328.43	339.01
567	1124.12	165.33	798.56	542.67	249.57	275.56	2.244	371.01	3361.48	342.37
568	1124.12	165.33	798.56	542.67	282.62	275.56	2.244	371.01	3394.53	345.74
569	1124.12	165.33	798.56	542.67	315.67	275.56	2.244	371.01	3427.58	349.11
570	1124.12	165.33	798.56	542.67	348.71	275.56	2.244	371.01	3460.63	352.47
571	1124.12	165.33	798.56	542.67	51.281	275.56	2.629	434.65	3226.84	328.66
572	1124.12	165.33	798.56	542.67	84.33	275.56	2.629	434.65	3259.89	332.03
573	1124.12	165.33	798.56	542.67	117.38	275.56	2.629	434.65	3292.94	335.39
574	1124.12	165.33	798.56	542.67	150.43	275.56	2.629	434.65	3325.99	338.76
575	1124.12	165.33	798.56	542.67	183.47	275.56	2.629	434.65	3359.03	342.13

#	UV Lamp \$	Duct ft2	Duct Matl, \$	Labor \$	Fan FC \$	Filter FC \$	Reflect Type \$/ft2	Refl Matl, \$	Total FC \$	Annual FC \$
576	1124.12	165.33	798.56	542.67	216.52	275.56	2.629	434.65	3392.08	345.49
577	1124.12	165.33	798.56	542.67	249.57	275.56	2.629	434.65	3425.13	348.86
578	1124.12	165.33	798.56	542.67	282.62	275.56	2.629	434.65	3458.18	352.22
579	1124.12	165.33	798.56	542.67	315.67	275.56	2.629	434.65	3491.23	355.59
580	1124.12	165.33	798.56	542.67	348.71	275.56	2.629	434.65	3524.27	358.96
581	1124.12	165.33	798.56	542.67	51.281	275.56	3.014	498.30	3290.49	335.14
582	1124.12	165.33	798.56	542.67	84.33	275.56	3.014	498.30	3323.54	338.51
583	1124.12	165.33	798.56	542.67	117.38	275.56	3.014	498.30	3356.59	341.88
584	1124.12	165.33	798.56	542.67	150.43	275.56	3.014	498.30	3389.63	345.24
585	1124.12	165.33	798.56	542.67	183.47	275.56	3.014	498.30	3422.68	348.61
586	1124.12	165.33	798.56	542.67	216.52	275.56	3.014	498.30	3455.73	351.97
587	1124.12	165.33	798.56	542.67	249.57	275.56	3.014	498.30	3488.78	355.34
588	1124.12	165.33	798.56	542.67	282.62	275.56	3.014	498.30	3521.83	358.71
589	1124.12	165.33	798.56	542.67	315.67	275.56	3.014	498.30	3554.87	362.07
590	1124.12	165.33	798.56	542.67	348.71	275.56	3.014	498.30	3587.92	365.44
591	1124.12	165.33	798.56	542.67	51.281	275.56	3.399	561.95	3354.14	341.63
592	1124.12	165.33	798.56	542.67	84.33	275.56	3.399	561.95	3387.18	344.99
593	1124.12	165.33	798.56	542.67	117.38	275.56	3.399	561.95	3420.23	348.36
594	1124.12	165.33	798.56	542.67	150.43	275.56	3.399	561.95	3453.28	351.72
595	1124.12	165.33	798.56	542.67	183.47	275.56	3.399	561.95	3486.33	355.09
596	1124.12	165.33	798.56	542.67	216.52	275.56	3.399	561.95	3519.38	358.46
597	1124.12	165.33	798.56	542.67	249.57	275.56	3.399	561.95	3552.42	361.82
598	1124.12	165.33	798.56	542.67	282.62	275.56	3.399	561.95	3585.47	365.19
599	1124.12	165.33	798.56	542.67	315.67	275.56	3.399	561.95	3618.52	368.55
600	1124.12	165.33	798.56	542.67	348.71	275.56	3.399	561.95	3651.57	371.92

APPENDIX Q: Energy & Maintenance for Cost Optimization

#	Lamp Engy, \$	Cooling Engy, \$	Total dP	Fan Pwr kW	Fan Pwr \$/yr	Mainten \$/yr	Lamp replace.	Filter replace	Total E&M	Life Cycle Cost	CE
1	32.98	23.09	0.5614	1.61	1131.47	50	87.011	112.70	1437.25	1642.18	0.0331
2	43.97	30.78	0.5614	1.61	1131.47	50	116.01	112.70	1484.94	1702.35	0.0381
3	54.96	38.48	0.5614	1.61	1131.47	50	145.02	112.70	1532.63	1762.25	0.0414
4	65.96	46.17	0.5614	1.61	1131.47	50	174.02	112.70	1580.32	1821.86	0.0434
5	76.95	53.87	0.5614	1.61	1131.47	50	203.02	112.70	1628.01	1881.18	0.0446
6	87.94	61.56	0.5614	1.61	1131.47	50	232.03	112.70	1675.71	1940.22	0.0452
7	98.94	69.26	0.5614	1.61	1131.47	50	261.03	112.70	1723.40	1998.97	0.0452
8	109.93	76.95	0.5614	1.61	1131.47	50	290.04	112.70	1771.09	2057.43	0.0450
9	120.92	84.65	0.5614	1.61	1131.47	50	319.04	112.70	1818.78	2115.61	0.0446
10	131.92	92.34	0.5614	1.61	1131.47	50	348.04	112.70	1866.47	2173.51	0.0440
11	32.98	23.09	0.5614	1.61	1131.47	50	87.011	112.70	1437.25	1674.90	0.0412
12	43.97	30.78	0.5614	1.61	1131.47	50	116.01	112.70	1484.94	1735.08	0.0456
13	54.96	38.48	0.5614	1.61	1131.47	50	145.02	112.70	1532.63	1794.98	0.0478
14	65.96	46.17	0.5614	1.61	1131.47	50	174.02	112.70	1580.32	1854.58	0.0487
15	76.95	53.87	0.5614	1.61	1131.47	50	203.02	112.70	1628.01	1913.91	0.0489
16	87.94	61.56	0.5614	1.61	1131.47	50	232.03	112.70	1675.71	1972.94	0.0485
17	98.94	69.26	0.5614	1.61	1131.47	50	261.03	112.70	1723.40	2031.70	0.0478
18	109.93	76.95	0.5614	1.61	1131.47	50	290.04	112.70	1771.09	2090.16	0.0469
19	120.92	84.65	0.5614	1.61	1131.47	50	319.04	112.70	1818.78	2148.34	0.0459
20	131.92	92.34	0.5614	1.61	1131.47	50	348.04	112.70	1866.47	2206.24	0.0449
21	32.98	23.09	0.5614	1.61	1131.47	50	87.011	112.70	1437.25	1707.63	0.0452
22	43.97	30.78	0.5614	1.61	1131.47	50	116.01	112.70	1484.94	1767.81	0.0486
23	54.96	38.48	0.5614	1.61	1131.47	50	145.02	112.70	1532.63	1827.70	0.0500
24	65.96	46.17	0.5614	1.61	1131.47	50	174.02	112.70	1580.32	1887.31	0.0502
25	76.95	53.87	0.5614	1.61	1131.47	50	203.02	112.70	1628.01	1946.63	0.0497
26	87.94	61.56	0.5614	1.61	1131.47	50	232.03	112.70	1675.71	2005.67	0.0489
27	98.94	69.26	0.5614	1.61	1131.47	50	261.03	112.70	1723.40	2064.42	0.0479
28	109.93	76.95	0.5614	1.61	1131.47	50	290.04	112.70	1771.09	2122.89	0.0468
29	120.92	84.65	0.5614	1.61	1131.47	50	319.04	112.70	1818.78	2181.07	0.0456
30	131.92	92.34	0.5614	1.61	1131.47	50	348.04	112.70	1866.47	2238.96	0.0445
31	32.98	23.09	0.5614	1.61	1131.47	50	87.011	112.70	1437.25	1740.36	0.0471
32	43.97	30.78	0.5614	1.61	1131.47	50	116.01	112.70	1484.94	1800.54	0.0499
33	54.96	38.48	0.5614	1.61	1131.47	50	145.02	112.70	1532.63	1860.43	0.0506
34	65.96	46.17	0.5614	1.61	1131.47	50	174.02	112.70	1580.32	1920.04	0.0504
35	76.95	53.87	0.5614	1.61	1131.47	50	203.02	112.70	1628.01	1979.36	0.0496
36	87.94	61.56	0.5614	1.61	1131.47	50	232.03	112.70	1675.71	2038.40	0.0485
37	98.94	69.26	0.5614	1.61	1131.47	50	261.03	112.70	1723.40	2097.15	0.0474
38	109.93	76.95	0.5614	1.61	1131.47	50	290.04	112.70	1771.09	2155.62	0.0462
39	120.92	84.65	0.5614	1.61	1131.47	50	319.04	112.70	1818.78	2213.80	0.0451
40	131.92	92.34	0.5614	1.61	1131.47	50	348.04	112.70	1866.47	2271.69	0.0440
41	32.98	23.09	0.5614	1.61	1131.47	50	87.011	112.70	1437.25	1773.08	0.0479
42	43.97	30.78	0.5614	1.61	1131.47	50	116.01	112.70	1484.94	1833.26	0.0502
43	54.96	38.48	0.5614	1.61	1131.47	50	145.02	112.70	1532.63	1893.16	0.0506
44	65.96	46.17	0.5614	1.61	1131.47	50	174.02	112.70	1580.32	1952.77	0.0501
45	76.95	53.87	0.5614	1.61	1131.47	50	203.02	112.70	1628.01	2012.09	0.0491
46	87.94	61.56	0.5614	1.61	1131.47	50	232.03	112.70	1675.71	2071.13	0.0480
47	98.94	69.26	0.5614	1.61	1131.47	50	261.03	112.70	1723.40	2129.88	0.0468

#	Lamp Engy, \$	Cooling Engy, \$	Total dP	Fan Pwr kW	Fan Pwr \$/yr	Mainten \$/yr	Lamp replace.	Filter replace	Total E&M	Life Cycle Cost	CE
48	109.93	76.95	0.5614	1.61	1131.47	50	290.04	112.70	1771.09	2188.34	0.0456
49	120.92	84.65	0.5614	1.61	1131.47	50	319.04	112.70	1818.78	2246.52	0.0445
50	131.92	92.34	0.5614	1.61	1131.47	50	348.04	112.70	1866.47	2304.42	0.0434
51	32.98	23.09	0.5614	1.61	1131.47	50	87.011	112.70	1437.25	1805.81	0.0482
52	43.97	30.78	0.5614	1.61	1131.47	50	116.01	112.70	1484.94	1865.99	0.0501
53	54.96	38.48	0.5614	1.61	1131.47	50	145.02	112.70	1532.63	1925.89	0.0502
54	65.96	46.17	0.5614	1.61	1131.47	50	174.02	112.70	1580.32	1985.49	0.0495
55	76.95	53.87	0.5614	1.61	1131.47	50	203.02	112.70	1628.01	2044.82	0.0485
56	87.94	61.56	0.5614	1.61	1131.47	50	232.03	112.70	1675.71	2103.85	0.0473
57	98.94	69.26	0.5614	1.61	1131.47	50	261.03	112.70	1723.40	2162.61	0.0461
58	109.93	76.95	0.5614	1.61	1131.47	50	290.04	112.70	1771.09	2221.07	0.0450
59	120.92	84.65	0.5614	1.61	1131.47	50	319.04	112.70	1818.78	2279.25	0.0438
60	131.92	92.34	0.5614	1.61	1131.47	50	348.04	112.70	1866.47	2337.15	0.0428
61	32.98	23.09	0.5614	1.61	1131.47	50	87.011	112.70	1437.25	1838.54	0.0481
62	43.97	30.78	0.5614	1.61	1131.47	50	116.01	112.70	1484.94	1898.72	0.0497
63	54.96	38.48	0.5614	1.61	1131.47	50	145.02	112.70	1532.63	1958.61	0.0497
64	65.96	46.17	0.5614	1.61	1131.47	50	174.02	112.70	1580.32	2018.22	0.0489
65	76.95	53.87	0.5614	1.61	1131.47	50	203.02	112.70	1628.01	2077.54	0.0478
66	87.94	61.56	0.5614	1.61	1131.47	50	232.03	112.70	1675.71	2136.58	0.0467
67	98.94	69.26	0.5614	1.61	1131.47	50	261.03	112.70	1723.40	2195.33	0.0455
68	109.93	76.95	0.5614	1.61	1131.47	50	290.04	112.70	1771.09	2253.80	0.0443
69	120.92	84.65	0.5614	1.61	1131.47	50	319.04	112.70	1818.78	2311.98	0.0432
70	131.92	92.34	0.5614	1.61	1131.47	50	348.04	112.70	1866.47	2369.87	0.0422
71	32.98	23.09	0.5614	1.61	1131.47	50	87.011	112.70	1437.25	1871.27	0.0479
72	43.97	30.78	0.5614	1.61	1131.47	50	116.01	112.70	1484.94	1931.45	0.0492
73	54.96	38.48	0.5614	1.61	1131.47	50	145.02	112.70	1532.63	1991.34	0.0491
74	65.96	46.17	0.5614	1.61	1131.47	50	174.02	112.70	1580.32	2050.95	0.0482
75	76.95	53.87	0.5614	1.61	1131.47	50	203.02	112.70	1628.01	2110.27	0.0471
76	87.94	61.56	0.5614	1.61	1131.47	50	232.03	112.70	1675.71	2169.31	0.0460
77	98.94	69.26	0.5614	1.61	1131.47	50	261.03	112.70	1723.40	2228.06	0.0448
78	109.93	76.95	0.5614	1.61	1131.47	50	290.04	112.70	1771.09	2286.53	0.0437
79	120.92	84.65	0.5614	1.61	1131.47	50	319.04	112.70	1818.78	2344.71	0.0426
80	131.92	92.34	0.5614	1.61	1131.47	50	348.04	112.70	1866.47	2402.60	0.0416
81	32.98	23.09	0.5614	1.61	1131.47	50	87.011	112.70	1437.25	1903.99	0.0475
82	43.97	30.78	0.5614	1.61	1131.47	50	116.01	112.70	1484.94	1964.17	0.0487
83	54.96	38.48	0.5614	1.61	1131.47	50	145.02	112.70	1532.63	2024.07	0.0484
84	65.96	46.17	0.5614	1.61	1131.47	50	174.02	112.70	1580.32	2083.68	0.0475
85	76.95	53.87	0.5614	1.61	1131.47	50	203.02	112.70	1628.01	2143.00	0.0465
86	87.94	61.56	0.5614	1.61	1131.47	50	232.03	112.70	1675.71	2202.04	0.0453
87	98.94	69.26	0.5614	1.61	1131.47	50	261.03	112.70	1723.40	2260.79	0.0442
88	109.93	76.95	0.5614	1.61	1131.47	50	290.04	112.70	1771.09	2319.25	0.0431
89	120.92	84.65	0.5614	1.61	1131.47	50	319.04	112.70	1818.78	2377.43	0.0421
90	131.92	92.34	0.5614	1.61	1131.47	50	348.04	112.70	1866.47	2435.33	0.0411
91	32.98	23.09	0.5614	1.61	1131.47	50	87.011	112.70	1437.25	1936.72	0.0470
92	43.97	30.78	0.5614	1.61	1131.47	50	116.01	112.70	1484.94	1996.90	0.0481
93	54.96	38.48	0.5614	1.61	1131.47	50	145.02	112.70	1532.63	2056.80	0.0477
94	65.96	46.17	0.5614	1.61	1131.47	50	174.02	112.70	1580.32	2116.40	0.0469
95	76.95	53.87	0.5614	1.61	1131.47	50	203.02	112.70	1628.01	2175.73	0.0458

#	Lamp Engy, \$	Cooling Engy, \$	Total dP	Fan Pwr kW	Fan Pwr \$/yr	Mainten \$/yr	Lamp replace.	Filter replace	Total E&M	Life Cycle Cost	CE
96	87.94	61.56	0.5614	1.61	1131.47	50	232.03	112.70	1675.71	2234.76	0.0447
97	98.94	69.26	0.5614	1.61	1131.47	50	261.03	112.70	1723.40	2293.52	0.0436
98	109.93	76.95	0.5614	1.61	1131.47	50	290.04	112.70	1771.09	2351.98	0.0425
99	120.92	84.65	0.5614	1.61	1131.47	50	319.04	112.70	1818.78	2410.16	0.0415
100	131.92	92.34	0.5614	1.61	1131.47	50	348.04	112.70	1866.47	2468.06	0.0405
101	32.98	23.09	0.5614	1.61	1131.47	50	87.011	112.70	1437.25	1682.84	0.0401
102	43.97	30.78	0.5614	1.61	1131.47	50	116.01	112.70	1484.94	1743.02	0.0446
103	54.96	38.48	0.5614	1.61	1131.47	50	145.02	112.70	1532.63	1802.91	0.0470
104	65.96	46.17	0.5614	1.61	1131.47	50	174.02	112.70	1580.32	1862.52	0.0480
105	76.95	53.87	0.5614	1.61	1131.47	50	203.02	112.70	1628.01	1921.84	0.0483
106	87.94	61.56	0.5614	1.61	1131.47	50	232.03	112.70	1675.71	1980.88	0.0480
107	98.94	69.26	0.5614	1.61	1131.47	50	261.03	112.70	1723.40	2039.63	0.0474
108	109.93	76.95	0.5614	1.61	1131.47	50	290.04	112.70	1771.09	2098.10	0.0465
109	120.92	84.65	0.5614	1.61	1131.47	50	319.04	112.70	1818.78	2156.28	0.0456
110	131.92	92.34	0.5614	1.61	1131.47	50	348.04	112.70	1866.47	2214.17	0.0447
111	32.98	23.09	0.5614	1.61	1131.47	50	87.011	112.70	1437.25	1688.21	0.0414
112	43.97	30.78	0.5614	1.61	1131.47	50	116.01	112.70	1484.94	1748.39	0.0456
113	54.96	38.48	0.5614	1.61	1131.47	50	145.02	112.70	1532.63	1808.29	0.0478
114	65.96	46.17	0.5614	1.61	1131.47	50	174.02	112.70	1580.32	1867.90	0.0487
115	76.95	53.87	0.5614	1.61	1131.47	50	203.02	112.70	1628.01	1927.22	0.0487
116	87.94	61.56	0.5614	1.61	1131.47	50	232.03	112.70	1675.71	1986.26	0.0483
117	98.94	69.26	0.5614	1.61	1131.47	50	261.03	112.70	1723.40	2045.01	0.0476
118	109.93	76.95	0.5614	1.61	1131.47	50	290.04	112.70	1771.09	2103.47	0.0467
119	120.92	84.65	0.5614	1.61	1131.47	50	319.04	112.70	1818.78	2161.65	0.0457
120	131.92	92.34	0.5614	1.61	1131.47	50	348.04	112.70	1866.47	2219.55	0.0447
121	32.98	23.09	0.5614	1.61	1131.47	50	87.011	112.70	1437.25	1694.70	0.0425
122	43.97	30.78	0.5614	1.61	1131.47	50	116.01	112.70	1484.94	1754.88	0.0466
123	54.96	38.48	0.5614	1.61	1131.47	50	145.02	112.70	1532.63	1814.77	0.0485
124	65.96	46.17	0.5614	1.61	1131.47	50	174.02	112.70	1580.32	1874.38	0.0492
125	76.95	53.87	0.5614	1.61	1131.47	50	203.02	112.70	1628.01	1933.70	0.0491
126	87.94	61.56	0.5614	1.61	1131.47	50	232.03	112.70	1675.71	1992.74	0.0485
127	98.94	69.26	0.5614	1.61	1131.47	50	261.03	112.70	1723.40	2051.49	0.0477
128	109.93	76.95	0.5614	1.61	1131.47	50	290.04	112.70	1771.09	2109.96	0.0467
129	120.92	84.65	0.5614	1.61	1131.47	50	319.04	112.70	1818.78	2168.14	0.0457
130	131.92	92.34	0.5614	1.61	1131.47	50	348.04	112.70	1866.47	2226.03	0.0447
131	32.98	23.09	0.5614	1.61	1131.47	50	87.011	112.70	1437.25	1701.18	0.0437
132	43.97	30.78	0.5614	1.61	1131.47	50	116.01	112.70	1484.94	1761.36	0.0475
133	54.96	38.48	0.5614	1.61	1131.47	50	145.02	112.70	1532.63	1821.25	0.0492
134	65.96	46.17	0.5614	1.61	1131.47	50	174.02	112.70	1580.32	1880.86	0.0497
135	76.95	53.87	0.5614	1.61	1131.47	50	203.02	112.70	1628.01	1940.18	0.0494
136	87.94	61.56	0.5614	1.61	1131.47	50	232.03	112.70	1675.71	1999.22	0.0487
137	98.94	69.26	0.5614	1.61	1131.47	50	261.03	112.70	1723.40	2057.97	0.0478
138	109.93	76.95	0.5614	1.61	1131.47	50	290.04	112.70	1771.09	2116.44	0.0467
139	120.92	84.65	0.5614	1.61	1131.47	50	319.04	112.70	1818.78	2174.62	0.0457
140	131.92	92.34	0.5614	1.61	1131.47	50	348.04	112.70	1866.47	2232.51	0.0446
141	32.98	23.09	0.5614	1.61	1131.47	50	87.011	112.70	1437.25	1707.66	0.0449
142	43.97	30.78	0.5614	1.61	1131.47	50	116.01	112.70	1484.94	1767.84	0.0484
143	54.96	38.48	0.5614	1.61	1131.47	50	145.02	112.70	1532.63	1827.74	0.0499

#	Lamp Engy, \$	Cooling Engy, \$	Total dP	Fan Pwr kW	Fan Pwr \$/yr	Mainten \$/yr	Lamp replace.	Filter replace	Total E&M	Life Cycle Cost	CE
144	65.96	46.17	0.5614	1.61	1131.47	50	174.02	112.70	1580.32	1887.34	0.0501
145	76.95	53.87	0.5614	1.61	1131.47	50	203.02	112.70	1628.01	1946.67	0.0496
146	87.94	61.56	0.5614	1.61	1131.47	50	232.03	112.70	1675.71	2005.70	0.0488
147	98.94	69.26	0.5614	1.61	1131.47	50	261.03	112.70	1723.40	2064.45	0.0478
148	109.93	76.95	0.5614	1.61	1131.47	50	290.04	112.70	1771.09	2122.92	0.0467
149	120.92	84.65	0.5614	1.61	1131.47	50	319.04	112.70	1818.78	2181.10	0.0456
150	131.92	92.34	0.5614	1.61	1131.47	50	348.04	112.70	1866.47	2238.99	0.0445
151	32.98	23.09	0.5614	1.61	1131.47	50	87.011	112.70	1437.25	1714.14	0.0460
152	43.97	30.78	0.5614	1.61	1131.47	50	116.01	112.70	1484.94	1774.32	0.0492
153	54.96	38.48	0.5614	1.61	1131.47	50	145.02	112.70	1532.63	1834.22	0.0504
154	65.96	46.17	0.5614	1.61	1131.47	50	174.02	112.70	1580.32	1893.83	0.0504
155	76.95	53.87	0.5614	1.61	1131.47	50	203.02	112.70	1628.01	1953.15	0.0498
156	87.94	61.56	0.5614	1.61	1131.47	50	232.03	112.70	1675.71	2012.19	0.0489
157	98.94	69.26	0.5614	1.61	1131.47	50	261.03	112.70	1723.40	2070.94	0.0478
158	109.93	76.95	0.5614	1.61	1131.47	50	290.04	112.70	1771.09	2129.40	0.0467
159	120.92	84.65	0.5614	1.61	1131.47	50	319.04	112.70	1818.78	2187.58	0.0456
160	131.92	92.34	0.5614	1.61	1131.47	50	348.04	112.70	1866.47	2245.48	0.0444
161	32.98	23.09	0.5614	1.61	1131.47	50	87.011	112.70	1437.25	1720.63	0.0471
162	43.97	30.78	0.5614	1.61	1131.47	50	116.01	112.70	1484.94	1780.81	0.0500
163	54.96	38.48	0.5614	1.61	1131.47	50	145.02	112.70	1532.63	1840.70	0.0509
164	65.96	46.17	0.5614	1.61	1131.47	50	174.02	112.70	1580.32	1900.31	0.0507
165	76.95	53.87	0.5614	1.61	1131.47	50	203.02	112.70	1628.01	1959.63	0.0500
166	87.94	61.56	0.5614	1.61	1131.47	50	232.03	112.70	1675.71	2018.67	0.0489
167	98.94	69.26	0.5614	1.61	1131.47	50	261.03	112.70	1723.40	2077.42	0.0478
168	109.93	76.95	0.5614	1.61	1131.47	50	290.04	112.70	1771.09	2135.89	0.0466
169	120.92	84.65	0.5614	1.61	1131.47	50	319.04	112.70	1818.78	2194.07	0.0455
170	131.92	92.34	0.5614	1.61	1131.47	50	348.04	112.70	1866.47	2251.96	0.0443
171	32.98	23.09	0.5614	1.61	1131.47	50	87.011	112.70	1437.25	1727.11	0.0482
172	43.97	30.78	0.5614	1.61	1131.47	50	116.01	112.70	1484.94	1787.29	0.0507
173	54.96	38.48	0.5614	1.61	1131.47	50	145.02	112.70	1532.63	1847.18	0.0514
174	65.96	46.17	0.5614	1.61	1131.47	50	174.02	112.70	1580.32	1906.79	0.0510
175	76.95	53.87	0.5614	1.61	1131.47	50	203.02	112.70	1628.01	1966.11	0.0501
176	87.94	61.56	0.5614	1.61	1131.47	50	232.03	112.70	1675.71	2025.15	0.0490
177	98.94	69.26	0.5614	1.61	1131.47	50	261.03	112.70	1723.40	2083.90	0.0478
178	109.93	76.95	0.5614	1.61	1131.47	50	290.04	112.70	1771.09	2142.37	0.0466
179	120.92	84.65	0.5614	1.61	1131.47	50	319.04	112.70	1818.78	2200.55	0.0454
180	131.92	92.34	0.5614	1.61	1131.47	50	348.04	112.70	1866.47	2258.44	0.0442
181	32.98	23.09	0.5614	1.61	1131.47	50	87.011	112.70	1437.25	1733.59	0.0491
182	43.97	30.78	0.5614	1.61	1131.47	50	116.01	112.70	1484.94	1793.77	0.0514
183	54.96	38.48	0.5614	1.61	1131.47	50	145.02	112.70	1532.63	1853.67	0.0517
184	65.96	46.17	0.5614	1.61	1131.47	50	174.02	112.70	1580.32	1913.27	0.0511
185	76.95	53.87	0.5614	1.61	1131.47	50	203.02	112.70	1628.01	1972.60	0.0501
186	87.94	61.56	0.5614	1.61	1131.47	50	232.03	112.70	1675.71	2031.63	0.0489
187	98.94	69.26	0.5614	1.61	1131.47	50	261.03	112.70	1723.40	2090.39	0.0477
188	109.93	76.95	0.5614	1.61	1131.47	50	290.04	112.70	1771.09	2148.85	0.0465
189	120.92	84.65	0.5614	1.61	1131.47	50	319.04	112.70	1818.78	2207.03	0.0453
190	131.92	92.34	0.5614	1.61	1131.47	50	348.04	112.70	1866.47	2264.93	0.0441
191	32.98	23.09	0.5614	1.61	1131.47	50	87.011	112.70	1437.25	1740.07	0.0501

#	Lamp Engy, \$	Cooling Engy, \$	Total dP	Fan Pwr kW	Fan Pwr \$/yr	Mainten \$/yr	Lamp replace.	Filter replace	Total E&M	Life Cycle Cost	CE
192	43.97	30.78	0.5614	1.61	1131.47	50	116.01	112.70	1484.94	1800.25	0.0520
193	54.96	38.48	0.5614	1.61	1131.47	50	145.02	112.70	1532.63	1860.15	0.0520
194	65.96	46.17	0.5614	1.61	1131.47	50	174.02	112.70	1580.32	1919.76	0.0512
195	76.95	53.87	0.5614	1.61	1131.47	50	203.02	112.70	1628.01	1979.08	0.0501
196	87.94	61.56	0.5614	1.61	1131.47	50	232.03	112.70	1675.71	2038.12	0.0489
197	98.94	69.26	0.5614	1.61	1131.47	50	261.03	112.70	1723.40	2096.87	0.0476
198	109.93	76.95	0.5614	1.61	1131.47	50	290.04	112.70	1771.09	2155.33	0.0463
199	120.92	84.65	0.5614	1.61	1131.47	50	319.04	112.70	1818.78	2213.51	0.0452
200	131.92	92.34	0.5614	1.61	1131.47	50	348.04	112.70	1866.47	2271.41	0.0440
201	82.45	57.71	0.5614	1.61	1131.47	50	217.53	112.70	1651.86	1899.04	0.0417
202	82.45	57.71	0.5614	1.61	1131.47	50	217.53	112.70	1651.86	1923.97	0.0465
203	82.45	57.71	0.5614	1.61	1131.47	50	217.53	112.70	1651.86	1948.90	0.0481
204	82.45	57.71	0.5614	1.61	1131.47	50	217.53	112.70	1651.86	1973.84	0.0485
205	82.45	57.71	0.5614	1.61	1131.47	50	217.53	112.70	1651.86	1998.77	0.0485
206	82.45	57.71	0.5614	1.61	1131.47	50	217.53	112.70	1651.86	2023.70	0.0482
207	82.45	57.71	0.5614	1.61	1131.47	50	217.53	112.70	1651.86	2048.63	0.0478
208	82.45	57.71	0.5614	1.61	1131.47	50	217.53	112.70	1651.86	2073.56	0.0474
209	82.45	57.71	0.5614	1.61	1131.47	50	217.53	112.70	1651.86	2098.50	0.0469
210	82.45	57.71	0.5614	1.61	1131.47	50	217.53	112.70	1651.86	2123.43	0.0464
211	82.45	57.71	0.5614	1.61	1131.47	50	217.53	112.70	1651.86	1901.28	0.0424
212	82.45	57.71	0.5614	1.61	1131.47	50	217.53	112.70	1651.86	1927.71	0.0471
213	82.45	57.71	0.5614	1.61	1131.47	50	217.53	112.70	1651.86	1954.13	0.0485
214	82.45	57.71	0.5614	1.61	1131.47	50	217.53	112.70	1651.86	1980.55	0.0488
215	82.45	57.71	0.5614	1.61	1131.47	50	217.53	112.70	1651.86	2006.98	0.0486
216	82.45	57.71	0.5614	1.61	1131.47	50	217.53	112.70	1651.86	2033.40	0.0483
217	82.45	57.71	0.5614	1.61	1131.47	50	217.53	112.70	1651.86	2059.83	0.0478
218	82.45	57.71	0.5614	1.61	1131.47	50	217.53	112.70	1651.86	2086.25	0.0473
219	82.45	57.71	0.5614	1.61	1131.47	50	217.53	112.70	1651.86	2112.68	0.0468
220	82.45	57.71	0.5614	1.61	1131.47	50	217.53	112.70	1651.86	2139.10	0.0463
221	82.45	57.71	0.5614	1.61	1131.47	50	217.53	112.70	1651.86	1903.98	0.0431
222	82.45	57.71	0.5614	1.61	1131.47	50	217.53	112.70	1651.86	1932.21	0.0476
223	82.45	57.71	0.5614	1.61	1131.47	50	217.53	112.70	1651.86	1960.43	0.0488
224	82.45	57.71	0.5614	1.61	1131.47	50	217.53	112.70	1651.86	1988.66	0.0489
225	82.45	57.71	0.5614	1.61	1131.47	50	217.53	112.70	1651.86	2016.88	0.0487
226	82.45	57.71	0.5614	1.61	1131.47	50	217.53	112.70	1651.86	2045.11	0.0482
227	82.45	57.71	0.5614	1.61	1131.47	50	217.53	112.70	1651.86	2073.34	0.0477
228	82.45	57.71	0.5614	1.61	1131.47	50	217.53	112.70	1651.86	2101.56	0.0471
229	82.45	57.71	0.5614	1.61	1131.47	50	217.53	112.70	1651.86	2129.79	0.0466
230	82.45	57.71	0.5614	1.61	1131.47	50	217.53	112.70	1651.86	2158.01	0.0460
231	82.45	57.71	0.5614	1.61	1131.47	50	217.53	112.70	1651.86	1906.68	0.0439
232	82.45	57.71	0.5614	1.61	1131.47	50	217.53	112.70	1651.86	1936.71	0.0481
233	82.45	57.71	0.5614	1.61	1131.47	50	217.53	112.70	1651.86	1966.74	0.0491
234	82.45	57.71	0.5614	1.61	1131.47	50	217.53	112.70	1651.86	1996.76	0.0490
235	82.45	57.71	0.5614	1.61	1131.47	50	217.53	112.70	1651.86	2026.79	0.0486
236	82.45	57.71	0.5614	1.61	1131.47	50	217.53	112.70	1651.86	2056.81	0.0481
237	82.45	57.71	0.5614	1.61	1131.47	50	217.53	112.70	1651.86	2086.84	0.0475
238	82.45	57.71	0.5614	1.61	1131.47	50	217.53	112.70	1651.86	2116.87	0.0469
239	82.45	57.71	0.5614	1.61	1131.47	50	217.53	112.70	1651.86	2146.89	0.0463

#	Lamp Engy, \$	Cooling Engy, \$	Total dP	Fan Pwr kW	Fan Pwr \$/yr	Mainten \$/yr	Lamp replace.	Filter replace	Total E&M	Life Cycle Cost	CE
240	82.45	57.71	0.5614	1.61	1131.47	50	217.53	112.70	1651.86	2176.92	0.0457
241	82.45	57.71	0.5614	1.61	1131.47	50	217.53	112.70	1651.86	1909.38	0.0446
242	82.45	57.71	0.5614	1.61	1131.47	50	217.53	112.70	1651.86	1941.21	0.0485
243	82.45	57.71	0.5614	1.61	1131.47	50	217.53	112.70	1651.86	1973.04	0.0493
244	82.45	57.71	0.5614	1.61	1131.47	50	217.53	112.70	1651.86	2004.86	0.0491
245	82.45	57.71	0.5614	1.61	1131.47	50	217.53	112.70	1651.86	2036.69	0.0486
246	82.45	57.71	0.5614	1.61	1131.47	50	217.53	112.70	1651.86	2068.52	0.0480
247	82.45	57.71	0.5614	1.61	1131.47	50	217.53	112.70	1651.86	2100.35	0.0474
248	82.45	57.71	0.5614	1.61	1131.47	50	217.53	112.70	1651.86	2132.17	0.0467
249	82.45	57.71	0.5614	1.61	1131.47	50	217.53	112.70	1651.86	2164.00	0.0460
250	82.45	57.71	0.5614	1.61	1131.47	50	217.53	112.70	1651.86	2195.83	0.0454
251	82.45	57.71	0.5614	1.61	1131.47	50	217.53	112.70	1651.86	1912.08	0.0453
252	82.45	57.71	0.5614	1.61	1131.47	50	217.53	112.70	1651.86	1945.71	0.0489
253	82.45	57.71	0.5614	1.61	1131.47	50	217.53	112.70	1651.86	1979.34	0.0494
254	82.45	57.71	0.5614	1.61	1131.47	50	217.53	112.70	1651.86	2012.97	0.0491
255	82.45	57.71	0.5614	1.61	1131.47	50	217.53	112.70	1651.86	2046.60	0.0485
256	82.45	57.71	0.5614	1.61	1131.47	50	217.53	112.70	1651.86	2080.22	0.0478
257	82.45	57.71	0.5614	1.61	1131.47	50	217.53	112.70	1651.86	2113.85	0.0471
258	82.45	57.71	0.5614	1.61	1131.47	50	217.53	112.70	1651.86	2147.48	0.0464
259	82.45	57.71	0.5614	1.61	1131.47	50	217.53	112.70	1651.86	2181.11	0.0457
260	82.45	57.71	0.5614	1.61	1131.47	50	217.53	112.70	1651.86	2214.73	0.0451
261	82.45	57.71	0.5614	1.61	1131.47	50	217.53	112.70	1651.86	1914.79	0.0460
262	82.45	57.71	0.5614	1.61	1131.47	50	217.53	112.70	1651.86	1950.21	0.0492
263	82.45	57.71	0.5614	1.61	1131.47	50	217.53	112.70	1651.86	1985.64	0.0495
264	82.45	57.71	0.5614	1.61	1131.47	50	217.53	112.70	1651.86	2021.07	0.0491
265	82.45	57.71	0.5614	1.61	1131.47	50	217.53	112.70	1651.86	2056.50	0.0484
266	82.45	57.71	0.5614	1.61	1131.47	50	217.53	112.70	1651.86	2091.93	0.0476
267	82.45	57.71	0.5614	1.61	1131.47	50	217.53	112.70	1651.86	2127.36	0.0469
268	82.45	57.71	0.5614	1.61	1131.47	50	217.53	112.70	1651.86	2162.79	0.0462
269	82.45	57.71	0.5614	1.61	1131.47	50	217.53	112.70	1651.86	2198.21	0.0454
270	82.45	57.71	0.5614	1.61	1131.47	50	217.53	112.70	1651.86	2233.64	0.0447
271	82.45	57.71	0.5614	1.61	1131.47	50	217.53	112.70	1651.86	1917.49	0.0467
272	82.45	57.71	0.5614	1.61	1131.47	50	217.53	112.70	1651.86	1954.72	0.0495
273	82.45	57.71	0.5614	1.61	1131.47	50	217.53	112.70	1651.86	1991.95	0.0496
274	82.45	57.71	0.5614	1.61	1131.47	50	217.53	112.70	1651.86	2029.17	0.0490
275	82.45	57.71	0.5614	1.61	1131.47	50	217.53	112.70	1651.86	2066.40	0.0482
276	82.45	57.71	0.5614	1.61	1131.47	50	217.53	112.70	1651.86	2103.63	0.0474
277	82.45	57.71	0.5614	1.61	1131.47	50	217.53	112.70	1651.86	2140.86	0.0466
278	82.45	57.71	0.5614	1.61	1131.47	50	217.53	112.70	1651.86	2178.09	0.0459
279	82.45	57.71	0.5614	1.61	1131.47	50	217.53	112.70	1651.86	2215.32	0.0451
280	82.45	57.71	0.5614	1.61	1131.47	50	217.53	112.70	1651.86	2252.55	0.0444
281	82.45	57.71	0.5614	1.61	1131.47	50	217.53	112.70	1651.86	1920.19	0.0474
282	82.45	57.71	0.5614	1.61	1131.47	50	217.53	112.70	1651.86	1959.22	0.0497
283	82.45	57.71	0.5614	1.61	1131.47	50	217.53	112.70	1651.86	1998.25	0.0496
284	82.45	57.71	0.5614	1.61	1131.47	50	217.53	112.70	1651.86	2037.28	0.0489
285	82.45	57.71	0.5614	1.61	1131.47	50	217.53	112.70	1651.86	2076.31	0.0481
286	82.45	57.71	0.5614	1.61	1131.47	50	217.53	112.70	1651.86	2115.34	0.0472
287	82.45	57.71	0.5614	1.61	1131.47	50	217.53	112.70	1651.86	2154.37	0.0464

#	Lamp Engy, \$	Cooling Engy, \$	Total dP	Fan Pwr kW	Fan Pwr \$/yr	Mainten \$/yr	Lamp replace.	Filter replace	Total E&M	Life Cycle Cost	CE
288	82.45	57.71	0.5614	1.61	1131.47	50	217.53	112.70	1651.86	2193.40	0.0456
289	82.45	57.71	0.5614	1.61	1131.47	50	217.53	112.70	1651.86	2232.43	0.0448
290	82.45	57.71	0.5614	1.61	1131.47	50	217.53	112.70	1651.86	2271.46	0.0440
291	82.45	57.71	0.5614	1.61	1131.47	50	217.53	112.70	1651.86	1922.89	0.0480
292	82.45	57.71	0.5614	1.61	1131.47	50	217.53	112.70	1651.86	1963.72	0.0499
293	82.45	57.71	0.5614	1.61	1131.47	50	217.53	112.70	1651.86	2004.55	0.0496
294	82.45	57.71	0.5614	1.61	1131.47	50	217.53	112.70	1651.86	2045.38	0.0488
295	82.45	57.71	0.5614	1.61	1131.47	50	217.53	112.70	1651.86	2086.21	0.0479
296	82.45	57.71	0.5614	1.61	1131.47	50	217.53	112.70	1651.86	2127.04	0.0470
297	82.45	57.71	0.5614	1.61	1131.47	50	217.53	112.70	1651.86	2167.87	0.0461
298	82.45	57.71	0.5614	1.61	1131.47	50	217.53	112.70	1651.86	2208.70	0.0453
299	82.45	57.71	0.5614	1.61	1131.47	50	217.53	112.70	1651.86	2249.53	0.0444
300	82.45	57.71	0.5614	1.61	1131.47	50	217.53	112.70	1651.86	2290.37	0.0437
301	32.98	23.09	0.0369	0.03	19.07	50	87.011	112.70	324.85	583.36	0.0438
302	32.98	23.09	0.0998	0.12	84.82	50	87.011	112.70	390.60	652.47	0.0628
303	32.98	23.09	0.1934	0.33	228.73	50	87.011	112.70	534.51	799.75	0.0677
304	32.98	23.09	0.3176	0.69	481.43	50	87.011	112.70	787.21	1055.81	0.0616
305	32.98	23.09	0.4725	1.25	873.55	50	87.011	112.70	1179.33	1451.30	0.0509
306	32.98	23.09	0.6580	2.05	1435.73	50	87.011	112.70	1741.51	2016.84	0.0403
307	32.98	23.09	0.8743	3.14	2198.59	50	87.011	112.70	2504.37	2783.07	0.0314
308	32.98	23.09	1.1211	4.56	3192.76	50	87.011	112.70	3498.54	3780.61	0.0245
309	32.98	23.09	1.3986	6.35	4448.88	50	87.011	112.70	4754.66	5040.10	0.0192
310	32.98	23.09	1.7068	8.56	5997.58	50	87.011	112.70	6303.36	6592.16	0.0153
311	43.97	30.78	0.0369	0.03	19.07	50	116.01	112.70	372.54	643.54	0.0398
312	43.97	30.78	0.0998	0.12	84.82	50	116.01	112.70	438.29	712.65	0.0587
313	43.97	30.78	0.1934	0.33	228.73	50	116.01	112.70	582.20	859.93	0.0660
314	43.97	30.78	0.3176	0.69	481.43	50	116.01	112.70	834.90	1115.99	0.0627
315	43.97	30.78	0.4725	1.25	873.55	50	116.01	112.70	1227.02	1511.48	0.0538
316	43.97	30.78	0.6580	2.05	1435.73	50	116.01	112.70	1789.20	2077.02	0.0439
317	43.97	30.78	0.8743	3.14	2198.59	50	116.01	112.70	2552.06	2843.25	0.0350
318	43.97	30.78	1.1211	4.56	3192.76	50	116.01	112.70	3546.23	3840.79	0.0279
319	43.97	30.78	1.3986	6.35	4448.88	50	116.01	112.70	4802.35	5100.28	0.0222
320	43.97	30.78	1.7068	8.56	5997.58	50	116.01	112.70	6351.05	6652.34	0.0179
321	54.96	38.48	0.0369	0.03	19.07	50	145.02	112.70	420.24	703.43	0.0364
322	54.96	38.48	0.0998	0.12	84.82	50	145.02	112.70	485.98	772.55	0.0544
323	54.96	38.48	0.1934	0.33	228.73	50	145.02	112.70	629.89	919.82	0.0629
324	54.96	38.48	0.3176	0.69	481.43	50	145.02	112.70	882.59	1175.89	0.0617
325	54.96	38.48	0.4725	1.25	873.55	50	145.02	112.70	1274.71	1571.38	0.0546
326	54.96	38.48	0.6580	2.05	1435.73	50	145.02	112.70	1836.89	2136.92	0.0456
327	54.96	38.48	0.8743	3.14	2198.59	50	145.02	112.70	2599.75	2903.14	0.0372
328	54.96	38.48	1.1211	4.56	3192.76	50	145.02	112.70	3593.93	3900.69	0.0301
329	54.96	38.48	1.3986	6.35	4448.88	50	145.02	112.70	4850.05	5160.17	0.0243
330	54.96	38.48	1.7068	8.56	5997.58	50	145.02	112.70	6398.74	6712.23	0.0198
331	65.96	46.17	0.0369	0.03	19.07	50	174.02	112.70	467.93	763.04	0.0336
332	65.96	46.17	0.0998	0.12	84.82	50	174.02	112.70	533.67	832.16	0.0506
333	65.96	46.17	0.1934	0.33	228.73	50	174.02	112.70	677.58	979.43	0.0596
334	65.96	46.17	0.3176	0.69	481.43	50	174.02	112.70	930.28	1235.50	0.0598
335	65.96	46.17	0.4725	1.25	873.55	50	174.02	112.70	1322.41	1630.98	0.0541

#	Lamp Engy, \$	Cooling Engy, \$	Total dP	Fan Pwr kW	Fan Pwr \$/yr	Mainten \$/yr	Lamp replace.	Filter replace	Total E&M	Life Cycle Cost	CE
336	65.96	46.17	0.6580	2.05	1435.73	50	174.02	112.70	1884.58	2196.53	0.0462
337	65.96	46.17	0.8743	3.14	2198.59	50	174.02	112.70	2647.44	2962.75	0.0383
338	65.96	46.17	1.1211	4.56	3192.76	50	174.02	112.70	3641.62	3960.29	0.0314
339	65.96	46.17	1.3986	6.35	4448.88	50	174.02	112.70	4897.74	5219.78	0.0257
340	65.96	46.17	1.7068	8.56	5997.58	50	174.02	112.70	6446.43	6771.84	0.0211
341	76.95	53.87	0.0369	0.03	19.07	50	203.02	112.70	515.62	822.36	0.0312
342	76.95	53.87	0.0998	0.12	84.82	50	203.02	112.70	581.37	891.48	0.0473
343	76.95	53.87	0.1934	0.33	228.73	50	203.02	112.70	725.27	1038.75	0.0564
344	76.95	53.87	0.3176	0.69	481.43	50	203.02	112.70	977.97	1294.82	0.0575
345	76.95	53.87	0.4725	1.25	873.55	50	203.02	112.70	1370.10	1690.31	0.0531
346	76.95	53.87	0.6580	2.05	1435.73	50	203.02	112.70	1932.27	2255.85	0.0461
347	76.95	53.87	0.8743	3.14	2198.59	50	203.02	112.70	2695.13	3022.08	0.0388
348	76.95	53.87	1.1211	4.56	3192.76	50	203.02	112.70	3689.31	4019.62	0.0322
349	76.95	53.87	1.3986	6.35	4448.88	50	203.02	112.70	4945.43	5279.10	0.0266
350	76.95	53.87	1.7068	8.56	5997.58	50	203.02	112.70	6494.12	6831.16	0.0221
351	87.94	61.56	0.0369	0.03	19.07	50	232.03	112.70	563.31	881.40	0.0291
352	87.94	61.56	0.0998	0.12	84.82	50	232.03	112.70	629.06	950.51	0.0444
353	87.94	61.56	0.1934	0.33	228.73	50	232.03	112.70	772.97	1097.79	0.0534
354	87.94	61.56	0.3176	0.69	481.43	50	232.03	112.70	1025.67	1353.86	0.0553
355	87.94	61.56	0.4725	1.25	873.55	50	232.03	112.70	1417.79	1749.34	0.0518
356	87.94	61.56	0.6580	2.05	1435.73	50	232.03	112.70	1979.97	2314.89	0.0456
357	87.94	61.56	0.8743	3.14	2198.59	50	232.03	112.70	2742.83	3081.11	0.0389
358	87.94	61.56	1.1211	4.56	3192.76	50	232.03	112.70	3737.00	4078.65	0.0326
359	87.94	61.56	1.3986	6.35	4448.88	50	232.03	112.70	4993.12	5338.14	0.0272
360	87.94	61.56	1.7068	8.56	5997.58	50	232.03	112.70	6541.82	6890.20	0.0228
361	98.94	69.26	0.0369	0.03	19.07	50	261.03	112.70	611.00	940.15	0.0273
362	98.94	69.26	0.0998	0.12	84.82	50	261.03	112.70	676.75	1009.27	0.0418
363	98.94	69.26	0.1934	0.33	228.73	50	261.03	112.70	820.66	1156.54	0.0507
364	98.94	69.26	0.3176	0.69	481.43	50	261.03	112.70	1073.36	1412.61	0.0531
365	98.94	69.26	0.4725	1.25	873.55	50	261.03	112.70	1465.48	1808.10	0.0504
366	98.94	69.26	0.6580	2.05	1435.73	50	261.03	112.70	2027.66	2373.64	0.0449
367	98.94	69.26	0.8743	3.14	2198.59	50	261.03	112.70	2790.52	3139.86	0.0387
368	98.94	69.26	1.1211	4.56	3192.76	50	261.03	112.70	3784.69	4137.40	0.0327
369	98.94	69.26	1.3986	6.35	4448.88	50	261.03	112.70	5040.81	5396.89	0.0276
370	98.94	69.26	1.7068	8.56	5997.58	50	261.03	112.70	6589.51	6948.95	0.0232
371	109.93	76.95	0.0369	0.03	19.07	50	290.04	112.70	658.69	998.62	0.0257
372	109.93	76.95	0.0998	0.12	84.82	50	290.04	112.70	724.44	1067.73	0.0395
373	109.93	76.95	0.1934	0.33	228.73	50	290.04	112.70	868.35	1215.01	0.0483
374	109.93	76.95	0.3176	0.69	481.43	50	290.04	112.70	1121.05	1471.07	0.0511
375	109.93	76.95	0.4725	1.25	873.55	50	290.04	112.70	1513.17	1866.56	0.0489
376	109.93	76.95	0.6580	2.05	1435.73	50	290.04	112.70	2075.35	2432.10	0.0441
377	109.93	76.95	0.8743	3.14	2198.59	50	290.04	112.70	2838.21	3198.33	0.0383
378	109.93	76.95	1.1211	4.56	3192.76	50	290.04	112.70	3832.38	4195.87	0.0327
379	109.93	76.95	1.3986	6.35	4448.88	50	290.04	112.70	5088.50	5455.36	0.0277
380	109.93	76.95	1.7068	8.56	5997.58	50	290.04	112.70	6637.20	7007.42	0.0235
381	120.92	84.65	0.0369	0.03	19.07	50	319.04	112.70	706.38	1056.80	0.0243
382	120.92	84.65	0.0998	0.12	84.82	50	319.04	112.70	772.13	1125.91	0.0374
383	120.92	84.65	0.1934	0.33	228.73	50	319.04	112.70	916.04	1273.19	0.0461

#	Lamp Engy, \$	Cooling Engy, \$	Total dP	Fan Pwr kW	Fan Pwr \$/yr	Mainten \$/yr	Lamp replace.	Filter replace	Total E&M	Life Cycle Cost	CE
384	120.92	84.65	0.3176	0.69	481.43	50	319.04	112.70	1168.74	1529.25	0.0492
385	120.92	84.65	0.4725	1.25	873.55	50	319.04	112.70	1560.86	1924.74	0.0475
386	120.92	84.65	0.6580	2.05	1435.73	50	319.04	112.70	2123.04	2490.28	0.0432
387	120.92	84.65	0.8743	3.14	2198.59	50	319.04	112.70	2885.90	3256.51	0.0379
388	120.92	84.65	1.1211	4.56	3192.76	50	319.04	112.70	3880.07	4254.05	0.0325
389	120.92	84.65	1.3986	6.35	4448.88	50	319.04	112.70	5136.19	5513.54	0.0277
390	120.92	84.65	1.7068	8.56	5997.58	50	319.04	112.70	6684.89	7065.60	0.0236
391	131.92	92.34	0.0369	0.03	19.07	50	348.04	112.70	754.08	1114.69	0.0230
392	131.92	92.34	0.0998	0.12	84.82	50	348.04	112.70	819.82	1183.81	0.0356
393	131.92	92.34	0.1934	0.33	228.73	50	348.04	112.70	963.73	1331.08	0.0441
394	131.92	92.34	0.3176	0.69	481.43	50	348.04	112.70	1216.43	1587.15	0.0474
395	131.92	92.34	0.4725	1.25	873.55	50	348.04	112.70	1608.56	1982.64	0.0462
396	131.92	92.34	0.6580	2.05	1435.73	50	348.04	112.70	2170.73	2548.18	0.0423
397	131.92	92.34	0.8743	3.14	2198.59	50	348.04	112.70	2933.59	3314.40	0.0373
398	131.92	92.34	1.1211	4.56	3192.76	50	348.04	112.70	3927.77	4311.95	0.0323
399	131.92	92.34	1.3986	6.35	4448.88	50	348.04	112.70	5183.89	5571.43	0.0277
400	131.92	92.34	1.7068	8.56	5997.58	50	348.04	112.70	6732.58	7123.49	0.0237
401	82.45	57.71	0.0369	0.03	19.07	50	217.53	112.70	539.46	783.19	0.0327
402	82.45	57.71	0.0998	0.12	84.82	50	217.53	112.70	605.21	852.30	0.0490
403	82.45	57.71	0.1934	0.33	228.73	50	217.53	112.70	749.12	999.58	0.0566
404	82.45	57.71	0.3176	0.69	481.43	50	217.53	112.70	1001.82	1255.65	0.0555
405	82.45	57.71	0.4725	1.25	873.55	50	217.53	112.70	1393.94	1651.13	0.0490
406	82.45	57.71	0.6580	2.05	1435.73	50	217.53	112.70	1956.12	2216.68	0.0408
407	82.45	57.71	0.8743	3.14	2198.59	50	217.53	112.70	2718.98	2982.90	0.0331
408	82.45	57.71	1.1211	4.56	3192.76	50	217.53	112.70	3713.15	3980.44	0.0266
409	82.45	57.71	1.3986	6.35	4448.88	50	217.53	112.70	4969.27	5239.93	0.0214
410	82.45	57.71	1.7068	8.56	5997.58	50	217.53	112.70	6517.97	6791.99	0.0173
411	82.45	57.71	0.0369	0.03	19.07	50	217.53	112.70	539.46	815.92	0.0314
412	82.45	57.71	0.0998	0.12	84.82	50	217.53	112.70	605.21	885.03	0.0476
413	82.45	57.71	0.1934	0.33	228.73	50	217.53	112.70	749.12	1032.31	0.0565
414	82.45	57.71	0.3176	0.69	481.43	50	217.53	112.70	1001.82	1288.37	0.0572
415	82.45	57.71	0.4725	1.25	873.55	50	217.53	112.70	1393.94	1683.86	0.0522
416	82.45	57.71	0.6580	2.05	1435.73	50	217.53	112.70	1956.12	2249.40	0.0449
417	82.45	57.71	0.8743	3.14	2198.59	50	217.53	112.70	2718.98	3015.63	0.0374
418	82.45	57.71	1.1211	4.56	3192.76	50	217.53	112.70	3713.15	4013.17	0.0308
419	82.45	57.71	1.3986	6.35	4448.88	50	217.53	112.70	4969.27	5272.66	0.0253
420	82.45	57.71	1.7068	8.56	5997.58	50	217.53	112.70	6517.97	6824.72	0.0208
421	82.45	57.71	0.0369	0.03	19.07	50	217.53	112.70	539.46	848.65	0.0302
422	82.45	57.71	0.0998	0.12	84.82	50	217.53	112.70	605.21	917.76	0.0459
423	82.45	57.71	0.1934	0.33	228.73	50	217.53	112.70	749.12	1065.03	0.0550
424	82.45	57.71	0.3176	0.69	481.43	50	217.53	112.70	1001.82	1321.10	0.0565
425	82.45	57.71	0.4725	1.25	873.55	50	217.53	112.70	1393.94	1716.59	0.0525
426	82.45	57.71	0.6580	2.05	1435.73	50	217.53	112.70	1956.12	2282.13	0.0459
427	82.45	57.71	0.8743	3.14	2198.59	50	217.53	112.70	2718.98	3048.36	0.0388
428	82.45	57.71	1.1211	4.56	3192.76	50	217.53	112.70	3713.15	4045.90	0.0324
429	82.45	57.71	1.3986	6.35	4448.88	50	217.53	112.70	4969.27	5305.38	0.0269
430	82.45	57.71	1.7068	8.56	5997.58	50	217.53	112.70	6517.97	6857.45	0.0224
431	82.45	57.71	0.0369	0.03	19.07	50	217.53	112.70	539.46	881.37	0.0291

#	Lamp Engy, \$	Cooling Engy, \$	Total dP	Fan Pwr kW	Fan Pwr \$/yr	Mainten \$/yr	Lamp replace.	Filter replace	Total E&M	Life Cycle Cost	CE
432	82.45	57.71	0.0998	0.12	84.82	50	217.53	112.70	605.21	950.49	0.0444
433	82.45	57.71	0.1934	0.33	228.73	50	217.53	112.70	749.12	1097.76	0.0534
434	82.45	57.71	0.3176	0.69	481.43	50	217.53	112.70	1001.82	1353.83	0.0554
435	82.45	57.71	0.4725	1.25	873.55	50	217.53	112.70	1393.94	1749.32	0.0519
436	82.45	57.71	0.6580	2.05	1435.73	50	217.53	112.70	1956.12	2314.86	0.0459
437	82.45	57.71	0.8743	3.14	2198.59	50	217.53	112.70	2718.98	3081.08	0.0392
438	82.45	57.71	1.1211	4.56	3192.76	50	217.53	112.70	3713.15	4078.63	0.0330
439	82.45	57.71	1.3986	6.35	4448.88	50	217.53	112.70	4969.27	5338.11	0.0276
440	82.45	57.71	1.7068	8.56	5997.58	50	217.53	112.70	6517.97	6890.17	0.0231
441	82.45	57.71	0.0369	0.03	19.07	50	217.53	112.70	539.46	914.10	0.0281
442	82.45	57.71	0.0998	0.12	84.82	50	217.53	112.70	605.21	983.21	0.0429
443	82.45	57.71	0.1934	0.33	228.73	50	217.53	112.70	749.12	1130.49	0.0519
444	82.45	57.71	0.3176	0.69	481.43	50	217.53	112.70	1001.82	1386.55	0.0541
445	82.45	57.71	0.4725	1.25	873.55	50	217.53	112.70	1393.94	1782.04	0.0512
446	82.45	57.71	0.6580	2.05	1435.73	50	217.53	112.70	1956.12	2347.59	0.0455
447	82.45	57.71	0.8743	3.14	2198.59	50	217.53	112.70	2718.98	3113.81	0.0392
448	82.45	57.71	1.1211	4.56	3192.76	50	217.53	112.70	3713.15	4111.35	0.0332
449	82.45	57.71	1.3986	6.35	4448.88	50	217.53	112.70	4969.27	5370.84	0.0279
450	82.45	57.71	1.7068	8.56	5997.58	50	217.53	112.70	6517.97	6922.90	0.0235
451	82.45	57.71	0.0369	0.03	19.07	50	217.53	112.70	539.46	946.83	0.0271
452	82.45	57.71	0.0998	0.12	84.82	50	217.53	112.70	605.21	1015.94	0.0415
453	82.45	57.71	0.1934	0.33	228.73	50	217.53	112.70	749.12	1163.22	0.0504
454	82.45	57.71	0.3176	0.69	481.43	50	217.53	112.70	1001.82	1419.28	0.0529
455	82.45	57.71	0.4725	1.25	873.55	50	217.53	112.70	1393.94	1814.77	0.0504
456	82.45	57.71	0.6580	2.05	1435.73	50	217.53	112.70	1956.12	2380.31	0.0451
457	82.45	57.71	0.8743	3.14	2198.59	50	217.53	112.70	2718.98	3146.54	0.0390
458	82.45	57.71	1.1211	4.56	3192.76	50	217.53	112.70	3713.15	4144.08	0.0332
459	82.45	57.71	1.3986	6.35	4448.88	50	217.53	112.70	4969.27	5403.57	0.0281
460	82.45	57.71	1.7068	8.56	5997.58	50	217.53	112.70	6517.97	6955.63	0.0237
461	82.45	57.71	0.0369	0.03	19.07	50	217.53	112.70	539.46	979.56	0.0262
462	82.45	57.71	0.0998	0.12	84.82	50	217.53	112.70	605.21	1048.67	0.0402
463	82.45	57.71	0.1934	0.33	228.73	50	217.53	112.70	749.12	1195.94	0.0491
464	82.45	57.71	0.3176	0.69	481.43	50	217.53	112.70	1001.82	1452.01	0.0518
465	82.45	57.71	0.4725	1.25	873.55	50	217.53	112.70	1393.94	1847.50	0.0495
466	82.45	57.71	0.6580	2.05	1435.73	50	217.53	112.70	1956.12	2413.04	0.0446
467	82.45	57.71	0.8743	3.14	2198.59	50	217.53	112.70	2718.98	3179.27	0.0387
468	82.45	57.71	1.1211	4.56	3192.76	50	217.53	112.70	3713.15	4176.81	0.0331
469	82.45	57.71	1.3986	6.35	4448.88	50	217.53	112.70	4969.27	5436.29	0.0281
470	82.45	57.71	1.7068	8.56	5997.58	50	217.53	112.70	6517.97	6988.36	0.0238
471	82.45	57.71	0.0369	0.03	19.07	50	217.53	112.70	539.46	1012.28	0.0253
472	82.45	57.71	0.0998	0.12	84.82	50	217.53	112.70	605.21	1081.40	0.0390
473	82.45	57.71	0.1934	0.33	228.73	50	217.53	112.70	749.12	1228.67	0.0478
474	82.45	57.71	0.3176	0.69	481.43	50	217.53	112.70	1001.82	1484.74	0.0506
475	82.45	57.71	0.4725	1.25	873.55	50	217.53	112.70	1393.94	1880.23	0.0487
476	82.45	57.71	0.6580	2.05	1435.73	50	217.53	112.70	1956.12	2445.77	0.0440
477	82.45	57.71	0.8743	3.14	2198.59	50	217.53	112.70	2718.98	3211.99	0.0384
478	82.45	57.71	1.1211	4.56	3192.76	50	217.53	112.70	3713.15	4209.54	0.0330
479	82.45	57.71	1.3986	6.35	4448.88	50	217.53	112.70	4969.27	5469.02	0.0281


#	Lamp Engy, \$	Cooling Engy, \$	Total dP	Fan Pwr kW	Fan Pwr \$/yr	Mainten \$/yr	Lamp replace.	Filter replace	Total E&M	Life Cycle Cost	CE
480	82.45	57.71	1.7068	8.56	5997.58	50	217.53	112.70	6517.97	7021.08	0.0239
481	82.45	57.71	0.0369	0.03	19.07	50	217.53	112.70	539.46	1045.01	0.0245
482	82.45	57.71	0.0998	0.12	84.82	50	217.53	112.70	605.21	1114.12	0.0378
483	82.45	57.71	0.1934	0.33	228.73	50	217.53	112.70	749.12	1261.40	0.0465
484	82.45	57.71	0.3176	0.69	481.43	50	217.53	112.70	1001.82	1517.46	0.0495
485	82.45	57.71	0.4725	1.25	873.55	50	217.53	112.70	1393.94	1912.95	0.0479
486	82.45	57.71	0.6580	2.05	1435.73	50	217.53	112.70	1956.12	2478.50	0.0435
487	82.45	57.71	0.8743	3.14	2198.59	50	217.53	112.70	2718.98	3244.72	0.0381
488	82.45	57.71	1.1211	4.56	3192.76	50	217.53	112.70	3713.15	4242.26	0.0328
489	82.45	57.71	1.3986	6.35	4448.88	50	217.53	112.70	4969.27	5501.75	0.0280
490	82.45	57.71	1.7068	8.56	5997.58	50	217.53	112.70	6517.97	7053.81	0.0239
491	82.45	57.71	0.0369	0.03	19.07	50	217.53	112.70	539.46	1077.74	0.0238
492	82.45	57.71	0.0998	0.12	84.82	50	217.53	112.70	605.21	1146.85	0.0368
493	82.45	57.71	0.1934	0.33	228.73	50	217.53	112.70	749.12	1294.13	0.0453
494	82.45	57.71	0.3176	0.69	481.43	50	217.53	112.70	1001.82	1550.19	0.0485
495	82.45	57.71	0.4725	1.25	873.55	50	217.53	112.70	1393.94	1945.68	0.0471
496	82.45	57.71	0.6580	2.05	1435.73	50	217.53	112.70	1956.12	2511.22	0.0429
497	82.45	57.71	0.8743	3.14	2198.59	50	217.53	112.70	2718.98	3277.45	0.0378
498	82.45	57.71	1.1211	4.56	3192.76	50	217.53	112.70	3713.15	4274.99	0.0326
499	82.45	57.71	1.3986	6.35	4448.88	50	217.53	112.70	4969.27	5534.48	0.0279
500	82.45	57.71	1.7068	8.56	5997.58	50	217.53	112.70	6517.97	7086.54	0.0238
501	82.45	57.71	0.0369	0.03	19.07	50	217.53	112.70	539.46	823.85	0.0311
502	82.45	57.71	0.0998	0.12	84.82	50	217.53	112.70	605.21	892.97	0.0472
503	82.45	57.71	0.1934	0.33	228.73	50	217.53	112.70	749.12	1040.24	0.0560
504	82.45	57.71	0.3176	0.69	481.43	50	217.53	112.70	1001.82	1296.31	0.0567
505	82.45	57.71	0.4725	1.25	873.55	50	217.53	112.70	1393.94	1691.80	0.0517
506	82.45	57.71	0.6580	2.05	1435.73	50	217.53	112.70	1956.12	2257.34	0.0444
507	82.45	57.71	0.8743	3.14	2198.59	50	217.53	112.70	2718.98	3023.57	0.0369
508	82.45	57.71	1.1211	4.56	3192.76	50	217.53	112.70	3713.15	4021.11	0.0303
509	82.45	57.71	1.3986	6.35	4448.88	50	217.53	112.70	4969.27	5280.59	0.0249
510	82.45	57.71	1.7068	8.56	5997.58	50	217.53	112.70	6517.97	6832.66	0.0204
511	82.45	57.71	0.0369	0.03	19.07	50	217.53	112.70	539.46	829.23	0.0309
512	82.45	57.71	0.0998	0.12	84.82	50	217.53	112.70	605.21	898.34	0.0469
513	82.45	57.71	0.1934	0.33	228.73	50	217.53	112.70	749.12	1045.62	0.0558
514	82.45	57.71	0.3176	0.69	481.43	50	217.53	112.70	1001.82	1301.68	0.0567
515	82.45	57.71	0.4725	1.25	873.55	50	217.53	112.70	1393.94	1697.17	0.0520
516	82.45	57.71	0.6580	2.05	1435.73	50	217.53	112.70	1956.12	2262.71	0.0448
517	82.45	57.71	0.8743	3.14	2198.59	50	217.53	112.70	2718.98	3028.94	0.0375
518	82.45	57.71	1.1211	4.56	3192.76	50	217.53	112.70	3713.15	4026.48	0.0309
519	82.45	57.71	1.3986	6.35	4448.88	50	217.53	112.70	4969.27	5285.97	0.0254
520	82.45	57.71	1.7068	8.56	5997.58	50	217.53	112.70	6517.97	6838.03	0.0209
521	82.45	57.71	0.0369	0.03	19.07	50	217.53	112.70	539.46	835.71	0.0307
522	82.45	57.71	0.0998	0.12	84.82	50	217.53	112.70	605.21	904.83	0.0466
523	82.45	57.71	0.1934	0.33	228.73	50	217.53	112.70	749.12	1052.10	0.0555
524	82.45	57.71	0.3176	0.69	481.43	50	217.53	112.70	1001.82	1308.17	0.0567
525	82.45	57.71	0.4725	1.25	873.55	50	217.53	112.70	1393.94	1703.66	0.0522
526	82.45	57.71	0.6580	2.05	1435.73	50	217.53	112.70	1956.12	2269.20	0.0452
527	82.45	57.71	0.8743	3.14	2198.59	50	217.53	112.70	2718.98	3035.42	0.0379

#	Lamp Engy, \$	Cooling Engy, \$	Total dP	Fan Pwr kW	Fan Pwr \$/yr	Mainten \$/yr	Lamp replace.	Filter replace	Total E&M	Life Cycle Cost	CE
528	82.45	57.71	1.1211	4.56	3192.76	50	217.53	112.70	3713.15	4032.96	0.0314
529	82.45	57.71	1.3986	6.35	4448.88	50	217.53	112.70	4969.27	5292.45	0.0259
530	82.45	57.71	1.7068	8.56	5997.58	50	217.53	112.70	6517.97	6844.51	0.0214
531	82.45	57.71	0.0369	0.03	19.07	50	217.53	112.70	539.46	842.19	0.0304
532	82.45	57.71	0.0998	0.12	84.82	50	217.53	112.70	605.21	911.31	0.0463
533	82.45	57.71	0.1934	0.33	228.73	50	217.53	112.70	749.12	1058.58	0.0553
534	82.45	57.71	0.3176	0.69	481.43	50	217.53	112.70	1001.82	1314.65	0.0566
535	82.45	57.71	0.4725	1.25	873.55	50	217.53	112.70	1393.94	1710.14	0.0523
536	82.45	57.71	0.6580	2.05	1435.73	50	217.53	112.70	1956.12	2275.68	0.0455
537	82.45	57.71	0.8743	3.14	2198.59	50	217.53	112.70	2718.98	3041.91	0.0383
538	82.45	57.71	1.1211	4.56	3192.76	50	217.53	112.70	3713.15	4039.45	0.0318
539	82.45	57.71	1.3986	6.35	4448.88	50	217.53	112.70	4969.27	5298.93	0.0263
540	82.45	57.71	1.7068	8.56	5997.58	50	217.53	112.70	6517.97	6851.00	0.0218
541	82.45	57.71	0.0369	0.03	19.07	50	217.53	112.70	539.46	848.68	0.0302
542	82.45	57.71	0.0998	0.12	84.82	50	217.53	112.70	605.21	917.79	0.0459
543	82.45	57.71	0.1934	0.33	228.73	50	217.53	112.70	749.12	1065.07	0.0550
544	82.45	57.71	0.3176	0.69	481.43	50	217.53	112.70	1001.82	1321.13	0.0565
545	82.45	57.71	0.4725	1.25	873.55	50	217.53	112.70	1393.94	1716.62	0.0524
546	82.45	57.71	0.6580	2.05	1435.73	50	217.53	112.70	1956.12	2282.16	0.0458
547	82.45	57.71	0.8743	3.14	2198.59	50	217.53	112.70	2718.98	3048.39	0.0387
548	82.45	57.71	1.1211	4.56	3192.76	50	217.53	112.70	3713.15	4045.93	0.0323
549	82.45	57.71	1.3986	6.35	4448.88	50	217.53	112.70	4969.27	5305.42	0.0268
550	82.45	57.71	1.7068	8.56	5997.58	50	217.53	112.70	6517.97	6857.48	0.0223
551	82.45	57.71	0.0369	0.03	19.07	50	217.53	112.70	539.46	855.16	0.0300
552	82.45	57.71	0.0998	0.12	84.82	50	217.53	112.70	605.21	924.27	0.0456
553	82.45	57.71	0.1934	0.33	228.73	50	217.53	112.70	749.12	1071.55	0.0547
554	82.45	57.71	0.3176	0.69	481.43	50	217.53	112.70	1001.82	1327.61	0.0563
555	82.45	57.71	0.4725	1.25	873.55	50	217.53	112.70	1393.94	1723.10	0.0525
556	82.45	57.71	0.6580	2.05	1435.73	50	217.53	112.70	1956.12	2288.65	0.0460
557	82.45	57.71	0.8743	3.14	2198.59	50	217.53	112.70	2718.98	3054.87	0.0390
558	82.45	57.71	1.1211	4.56	3192.76	50	217.53	112.70	3713.15	4052.41	0.0326
559	82.45	57.71	1.3986	6.35	4448.88	50	217.53	112.70	4969.27	5311.90	0.0272
560	82.45	57.71	1.7068	8.56	5997.58	50	217.53	112.70	6517.97	6863.96	0.0227
561	82.45	57.71	0.0369	0.03	19.07	50	217.53	112.70	539.46	861.64	0.0298
562	82.45	57.71	0.0998	0.12	84.82	50	217.53	112.70	605.21	930.76	0.0453
563	82.45	57.71	0.1934	0.33	228.73	50	217.53	112.70	749.12	1078.03	0.0544
564	82.45	57.71	0.3176	0.69	481.43	50	217.53	112.70	1001.82	1334.10	0.0562
565	82.45	57.71	0.4725	1.25	873.55	50	217.53	112.70	1393.94	1729.59	0.0525
566	82.45	57.71	0.6580	2.05	1435.73	50	217.53	112.70	1956.12	2295.13	0.0462
567	82.45	57.71	0.8743	3.14	2198.59	50	217.53	112.70	2718.98	3061.35	0.0393
568	82.45	57.71	1.1211	4.56	3192.76	50	217.53	112.70	3713.15	4058.89	0.0330
569	82.45	57.71	1.3986	6.35	4448.88	50	217.53	112.70	4969.27	5318.38	0.0275
570	82.45	57.71	1.7068	8.56	5997.58	50	217.53	112.70	6517.97	6870.44	0.0230
571	82.45	57.71	0.0369	0.03	19.07	50	217.53	112.70	539.46	868.13	0.0295
572	82.45	57.71	0.0998	0.12	84.82	50	217.53	112.70	605.21	937.24	0.0450
573	82.45	57.71	0.1934	0.33	228.73	50	217.53	112.70	749.12	1084.51	0.0541
574	82.45	57.71	0.3176	0.69	481.43	50	217.53	112.70	1001.82	1340.58	0.0560
575	82.45	57.71	0.4725	1.25	873.55	50	217.53	112.70	1393.94	1736.07	0.0524

#	Lamp Engy, \$	Cooling Engy, \$	Total dP	Fan Pwr kW	Fan Pwr \$/yr	Mainten \$/yr	Lamp replace.	Filter replace	Total E&M	Life Cycle Cost	CE
576	82.45	57.71	0.6580	2.05	1435.73	50	217.53	112.70	1956.12	2301.61	0.0463
577	82.45	57.71	0.8743	3.14	2198.59	50	217.53	112.70	2718.98	3067.84	0.0395
578	82.45	57.71	1.1211	4.56	3192.76	50	217.53	112.70	3713.15	4065.38	0.0333
579	82.45	57.71	1.3986	6.35	4448.88	50	217.53	112.70	4969.27	5324.86	0.0279
580	82.45	57.71	1.7068	8.56	5997.58	50	217.53	112.70	6517.97	6876.93	0.0234
581	82.45	57.71	0.0369	0.03	19.07	50	217.53	112.70	539.46	874.61	0.0293
582	82.45	57.71	0.0998	0.12	84.82	50	217.53	112.70	605.21	943.72	0.0447
583	82.45	57.71	0.1934	0.33	228.73	50	217.53	112.70	749.12	1091.00	0.0538
584	82.45	57.71	0.3176	0.69	481.43	50	217.53	112.70	1001.82	1347.06	0.0557
585	82.45	57.71	0.4725	1.25	873.55	50	217.53	112.70	1393.94	1742.55	0.0524
586	82.45	57.71	0.6580	2.05	1435.73	50	217.53	112.70	1956.12	2308.09	0.0463
587	82.45	57.71	0.8743	3.14	2198.59	50	217.53	112.70	2718.98	3074.32	0.0397
588	82.45	57.71	1.1211	4.56	3192.76	50	217.53	112.70	3713.15	4071.86	0.0335
589	82.45	57.71	1.3986	6.35	4448.88	50	217.53	112.70	4969.27	5331.35	0.0282
590	82.45	57.71	1.7068	8.56	5997.58	50	217.53	112.70	6517.97	6883.41	0.0237
591	82.45	57.71	0.0369	0.03	19.07	50	217.53	112.70	539.46	881.09	0.0291
592	82.45	57.71	0.0998	0.12	84.82	50	217.53	112.70	605.21	950.20	0.0444
593	82.45	57.71	0.1934	0.33	228.73	50	217.53	112.70	749.12	1097.48	0.0535
594	82.45	57.71	0.3176	0.69	481.43	50	217.53	112.70	1001.82	1353.54	0.0555
595	82.45	57.71	0.4725	1.25	873.55	50	217.53	112.70	1393.94	1749.03	0.0523
596	82.45	57.71	0.6580	2.05	1435.73	50	217.53	112.70	1956.12	2314.58	0.0464
597	82.45	57.71	0.8743	3.14	2198.59	50	217.53	112.70	2718.98	3080.80	0.0398
598	82.45	57.71	1.1211	4.56	3192.76	50	217.53	112.70	3713.15	4078.34	0.0337
599	82.45	57.71	1.3986	6.35	4448.88	50	217.53	112.70	4969.27	5337.83	0.0284
600	82.45	57.71	1.7068	8.56	5997.58	50	217.53	112.70	6517.97	6889.89	0.0240

VITA of Wladyslaw Jan Kowalski

<u>wxk116@psu.edu</u>		(814) 867 1478
720 Stratford Drive #13, State College, PA 16801		
Educational Background		
Illinois Institute of Technology		
Location:	Chicago, IL	
Degree:	B.S. Mechanical Engineering, 1978	
The Pennsylvania State University		
Location:	State College, PA	
Degree:	M.S. Architectural Engineering, 1998	



Professional Experience:

1978-1995 Mechanical Engineer/Project Engineer/Senior Engineer for various companies in the Nuclear Power Industry. Specialized in the Design and Testing of Nuclear Air Cleaning Systems, Radioactive Contamination Control Systems, Building Pressurization Systems, HVAC & Cooling Water Systems.

Honors and awards:

Licensed Professional Engineer State of Illinois, ASHRAE Graduate Grant-In-Aid, 1997, UVDI Research Grant 1999, Kissinger Fellowship Award for Scholarship 1999, Laraine and Jack Beiter Excellence Endowment in AE 2001

Bibliography:

- Kowalski, W. J. (1997). **"Technologies for controlling respiratory disease transmission in indoor environments: Theoretical performance and economics."** M.S., The Pennsylvania State University.
- Kowalski, W. J., Bahnfleth, W. P., and Whittam, T. S. (1998). **"Bactericidal effects of high airborne ozone concentrations on *Escherichia coli* and *Staphylococcus aureus*."** *Ozone Science & Engineering*, 20(3), 205-221.
- Kowalski, W., and Bahnfleth, W. P. (1998). **"Airborne respiratory diseases and technologies for control of microbes."** *HPAC Engineering*, 70(6).
- Kowalski, W. J., W. P. Bahnfleth, T. S. Whittam. (1999). **"Filtration of Airborne Microorganisms: Modeling and prediction."** *ASHRAE Transactions*, 105(2), 4-17.
- Kowalski, W. J., and Bahnfleth, W. P. (2000). **"UVGI Design Basics for Air and Surface Disinfection."** *HPAC Engineering*, 72(1), 100-110.
- Kowalski, W. J., and Bahnfleth, W. P. (2000). **"Effective UVGI system design through improved modeling."** *ASHRAE Transactions*, 106v2:4-15.
- Kowalski, W. J. (2000). **"Shedding Light on Moldy Ductwork."** *Home Energy*, 17(3), 6.
- Kowalski, W. J. (2000). **"Indoor mold growth: Health hazards and remediation."** *HPAC Engineering*, September, 2000.
- Kowalski, W. J. (2001). "Air Cleaning Technologies for Animal Research Laboratories." Presented at the ACLAM Annual Conference, April 2, in Pointe Claire, AL.
- Kowalski, W. J., W. P. Bahnfleth, and T. S. Whittam. 2001. Surface disinfection with airborne ozone and catalytic ozone removal. *Ozone Science and Engineering*. (submitted).
- Kowalski, W. J., and W. P. Bahnfleth. (2001). Filtration of Airborne Microorganisms. *HPAC Engineering*. (accepted).
- Kowalski, W. J., Bahnfleth, W. P., Severin, B. F., and Whittam, T. S. (2001). **"Mathematical modeling of UVGI air disinfection."** *Quant. Microb.* (submitted), 26 pages.